Application of gas chromatography-mass spectrometry (GC-MS) in the quantitative analysis of organic analytes generated in gasification/pyrolysis coupled Fischer Tropsch (FT) reactor: syngas clean-up and hydrocarbon production

Sullivan, Geraint L.

Application of gas chromatography-mass spectrometry (GC-MS) in the quantitative analysis of organic analytes generated in gasification/pyrolysis coupled Fischer Tropsch (FT) reactor: syngas clean-up and hydrocarbon production.

A thesis

Submitted in fulfilment

Of the requirements for the Degree of

Doctor of Philosophy in

Chemistry

By

Geraint Sullivan

Swansea University

2018

II. Abstract.

The identification and quantitation of organic tars, often requires specialised sampling techniques, such as gas sampling tubes, headspace vials and thermal desorption kits, which all require additional modules for instrument interfacing and sample introduction. The gold standard analysis techniques for these organic gaseous compounds is gas chromatography coupled to mass spectrometry (GC-MS) as it provides separation of complex samples and high mass selectivity of ions. A solvent trap method using acetone to capture organic tars that originate from thermochemical treatment of different feedstocks; pinewood, brownfield soil (contaminated with oily sludge) and secondary treated sludge cake. It was then possible to analyse tar compounds without the expense of additional instrumentation and user training.

Compounds identified in the solvent traps varied according to the feedstock used. Pine wood was used as an operational standard and generated typical biomass tars from sugar and lignin breakdown. Brownfield soil contaminated with oily sludge generated a wide range of polyaromatic hydrocarbons (PAHs), typical with hydrocarbon waste and secondary sludge cake generated a mixture of biomass breakdown products and nitrogenous compounds.

Acetone provided a dual role, not only as a sample preparation method but for syngas cleaning. Tandem acetone scrubbers removed the majority of tars (>90% efficiency) and also capable of removing troublesome volatile compounds, such as acetylene. Spent acetone scrubbers could easily be recycled using waste heat, with up to >90% of semi-volatile tars being recovered.

Clean syngas was converted to hydrocarbons using the Fischer-Tropsch (FT) reaction where a novel low temperature Cobalt was used. This catalyst was prepared in a different method from conventional cobalt catalysts (energy intensive calcination 12h at 600 ^{o}C in air). The novel catalyst (CAT-1) was prepared using chemical oxidation to generate a cheaper and environmentally friendlier FT catalyst. Initial test experiments, using simulated syngas (bottled

carbon monoxide and hydrogen) showed the generation of hydrocarbon material, suggesting a successful catalytic reaction. Further to this a trial using real scrubbed syngas from a combined gasification/ FT system, generated trace hydrocarbons, with no contamination in the final product from the tars, suggesting progress with acetone scrubbers.

To further the economic feasibility of pyrolysis/gasification-FT process a smaller investigation into possible use of the remaining biochar as a sorbent to treat contaminated water simulating aqueous scrubbers. Biochar derived from pine wood and uncharacterised sludge cake were activated and showed selectivity for volatile polyaromatic compounds and petroleum derived compounds.

Suggested Layout of Declaration/Statements page.

DECLARATION

This work has not previously been accepted in substance for any degree and is not being concurrently submitted in candidature for any degree.

Signed .....  .....(candidate)

Date .....13/08/18.....

STATEMENT 1

This thesis is the result of my own investigations, except where otherwise stated. Where correction services have been used, the extent and nature of the correction is clearly marked in a footnote(s).

Other sources are acknowledged by footnotes giving explicit references. A bibliography is appended.

Signed  ..... (candidate)

Date

.....13/08/18.....

STATEMENT 2

I hereby give consent for my thesis, if accepted, to be available for photocopying and for inter-library loan, and for the title and summary to be made available to outside organisations.

Signed .....  .....(candidate)

Date .....13/08/18.....

NB: *Candidates on whose behalf a bar on access has been approved by the University (see Note 7), should use the following version of Statement 2:*

I hereby give consent for my thesis, if accepted, to be available for photocopying and for inter-library loans **after expiry of a bar on access approved by the Swansea University.**

Signed  ..... (candidate)

Date .....13/08/18.....

Contents List.

V. Common abbreviations.

Symbol/ Abbreviation	Definition/meaning	Units
Avagadros constant	No of atoms in one mole of substance	6.022x10^23.
CH_4	Methane molecule	-
Cn	Alkane series, n is number of carbons in chain	-
CO	Carbon monoxide molecule	-
CO_2	Carbon dioxide molecule	-
Conc	Concentration	mg/L (Liquid) mg/kg (Solid)
CV	Calorific value	MJ/kg or MJ/m^3 (gas)
EI	Electron Ionisation	-
FT	Fischer-Tropsch	-
GC-MS	Gas Chromatography –Mass spectrometry	-
GC-TCD	Gas chromatography- Thermal conductivity detector	-
H_2	Hydrogen molecule	-
HETP	Height equivalence theoretical plate	-
NOx	Nitrous oxide species	-
PAHs	Polyaromatic hydrocarbon	-
PCBs	Polychlorinated biphenyls	-
POPs	Persistent organic pollutant	-
SEM	Scanning electron micrograph/microscopy	-
SIM	Single ion monitoring	-
SOx	Sulfur dioxide species	-
SPE	Solid Phase Extraction	-
SVOT	Semi-volatile organic tars	-
TICC	Total ion current chromatogram	-
TOF	Turn over Frequency	S^{-1}
VOT	Volatile organic tars	-
XRD	X-ray diffraction	-

VI. Acknowledgements.

I would like to dedicate this project to my beloved family, my partner and my children.

I would like to extend my utmost thanks and appreciation to the following people, who without their help the project wouldnot have taken place:

Dr. Robert Prigmore and Hendre holdings Ltd for giving me the oppurtunity and funding me to undertake the project. Mr. Phil Knight for his design and development of the bespoke rigs, which he contributed both his personal time and money. Dr. Ruth Godfrey, for her technical guidance and help with my written work. Dr.Tom Dunlop and Dr. Cecile Charbonneau for their work using XRD at SPECIFIC at the Bay campus, Swansea University. Prof Steven Kelly and Dr. Jersson Placidoescobar for arranging and performing SEM analysis at the Institute of Life sciences at Swansea University

VII. Figures contents list.

<u>VIII. Table content list.</u>

Chapter 1:

Introduction to recycling of carbon waste and the formation of (bio)-fuels.

The ever-growing global need for energy remains to be primarily led by fossil fuel combustion, with the largest consumer being oil (98 %)(1). Energy consumption is expected to increase by additional 50 % by 2030, with 45 % estimated to be contributed to China(1). The demand for fossil fuels is set to increase by 3 % each year putting the predicted reserves to that of below 45 years, with some estimates suggesting that 'peak oil' may have already taken place (1,2). Therefore, alternative energy resources require investigation as a means to substitute for the current global energy demand. It is also imperative to achieve this as environmentally friendly as possible. It was estimated that 23 % of carbon dioxide (CO_2) was emitted between 2007-2008 which originated from transport emission, (crude oil combustion) and it is predicted that 4.1 billion tons of CO_2 will be emitted from 2007-2020 (3). CO_2 is a greenhouse gas that has been linked to climate change (global warming) it is feared that even a rise of 2 °C in global temperature could cause the mass extinction of millions of species (3,4). Current renewable technology is not enough to replace fossil fuels but efforts to tackle the largest consumers could potentially help stabilise greenhouse gases (5). Together with global energy demands, waste production, is another growing environmental concern, which is directly linked to population growth and economical demand (4,5). landfill sites in which majority of waste is disposed has limited space with much of the waste disposed taking decades to decompose (3,6,7). This, in fact, may introduce further problems as a potential source of pollution with the generation of landfill gas (methane and carbon dioxide) and leaching of organic and inorganic pollutants into ground water (8).

Alternative methods to harness the energy potential of MSW could subsidize some of the energy requirements. It is estimated that nearly 80 % of mass sent to landfill has the potential to be

recycled using alternative technologies (7). The common recycling technique adopted today is salvaging materials for re-use and material recovery; this is done on pre-segregated material (recycled bags) whereby it is sorted by mechanical or manual means (8). This material is generally used as a secondary raw material (8) for re-use as a different product or used for composting. With 95 % of municipal solid waste (MSW) is food waste and a large proportion ends up on landfill (25-75 % of MSW) (3), but there is a vast amount of potential energy that can be recovered through alternative routes of recycling, such as bio fermentation, ethanol production (9) and incineration. The calorific value along of MSW can be up to 3-5 MJ/kg,(10) and energy generated from processed MSW in the UK in 2016 generated a total of 5.2 GWh of electricity through combined incineration, equivalent to 1.8 % of the UK electricity generation that year. However, energy recovery through incineration (combustion) is not an ideal method of dealing with harmful greenhouse gases, such as CO_2, nitrous oxide species (NOXs), sulfurous oxide species (SOXs) and often emitted persistent organic pollutants (POPs) (8,11). Strict regulation is required for incinerating waste and violation in emission quality can lead to heavy fines (11). Some alternative recycling routes can utilise the carbon content of this waste material and convert it to either a useful energy source or other products. Pyrolysis and gasification are two alternative methods to recycle waste high in carbon; these use thermal energy in a controlled environment to produce a flammable gas termed syngas, liquid bio-oil and solid biochar (pyrolysis only).

Wood, soil contaminated with petroleum waste, and effluent wastewaters are three feedstocks that are rich sources of carbon. The latter two feedstocks are of particular interest they are known waste streams that are difficult to manage environmentally and thought to contribute to environmental pollution. For example, problems associated with the traditional disposal and treatment of these waste streams are:

1. Oily/ petroleum waste such as oily sludge and brownfield contaminated soil, requires years of remediation to be deemed non-hazardous as they contain high degree of potentially carcinogenic and persistent organic pollutants.

2. Sludge cake derived from treated wastewater effluent is a highly complex matrix, which can still contain a number of harmful components such as viruses, pharmaceuticals, hormones, and persistent pollutants despite treatment (12). A large proportion (52 %) is spread on to agricultural land, with 17 % currently deposited in landfill (13). Research has shown that these pollutants can leach into the environment, exert an ecotoxic impact on aquatic life, and provide a potential route into the food chain through bioaccumulation. Additional adverse effects may include antimicrobial resistance (12).

There is a vast potential in producing hydrocarbon materials from carbonaceous materials such as wood, biomass and natural gas, (14) offering added value as carbon friendly process. Bio-oils derived from the pyrolysis of these feedstocks are an alternative source to crude oil, but work is still required on purification of the target hydrocarbons (15). Fuel production by catalytic processes such as the Fischer-Tropsch process (FT) utilise the syngas generated in thermochemical processes to synthesise hydrocarbons. These combined techniques are referred to as two-stage liquefaction of coal to liquid (CTL), biomass to liquid (BLT) and gas to liquid (GLT) (14) methods. Globally, crude oil the current major source of hydrocarbon fuels (used in combustion engines) (14) and is limited to around 50 years with an increasing demand for replenishing these stocks through biofuel and synthetic hydrocarbon production. In summary, recycling waste carbon materials into a useable product, such as fuel, would enable the potential reclamation of land from heavy industry and an alternative disposal method for waste that is primarily disposed of using landfill at high expense, with the added value of a product that could help with the reduction in fossil fuel as an environmentally friendly energy source.

1.1. Thermal conversion techniques for energy recycling.

1.1.1. Combustion.

Combustion is the main thermal conversion technique used in the treatment of carbon-containing waste (11) where the material is incinerated in oxygen rich atmosphere. It has a high conversion rate with most of the energy contained in the feedstock converted to thermal energy ~80-90 % (11). Hot flue gases are also produced comprising mainly of carbon dioxide, water, non-oxidised carbon particulates and oxides of sulfur and nitrogen (SOx and NOx). Persistent organic pollutants (POPs), such as dioxins and polychlorinated biphenyls (PCBs), have also been identified in flue gases (11) as an environmental concern and emissions from incineration are monitored with strict regulations their production and release. The process of incineration has been developed to reduce the environmental impact; most of the energy generated in this process is produced as heat this is recovered through the production of steam to drive a turbine for electricity generation. Although due to the low efficiency of steam turbines, (15-25 % is converted to electricity) further development of the process is needed to recoup the remaining of the thermal energy (11,16–18).

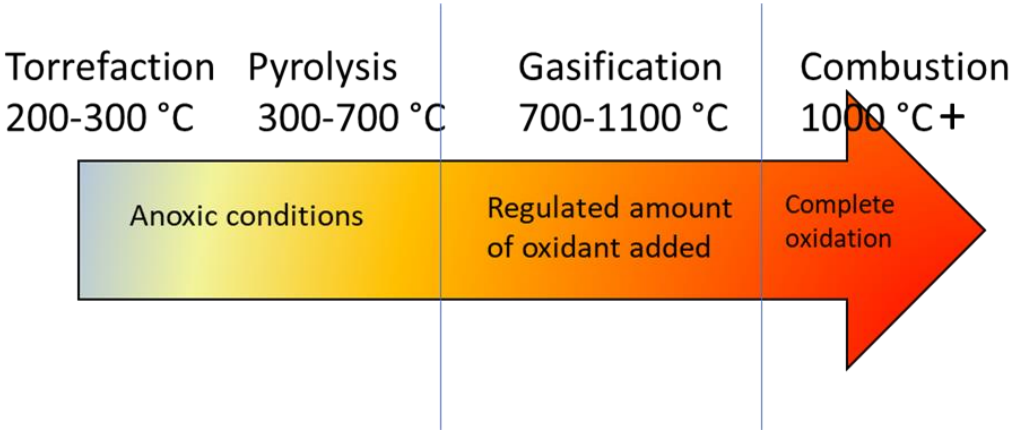

Figure 1 is a diagram illustrating the main differences between the main thermal treatment process. Please note that torrefaction, is included but is often referred to as mild pyrolysis due to the relatively low temperature conditions. Typically, thermal treatment methods are associated with their temperature and environment (inert or oxidative) conditions.

1.1.2. Pyrolysis (Thermal decomposition).

Other thermal conversion techniques for managing carbon waste are pyrolysis and gasification. Unlike combustion, pyrolysis involves heating a feedstock, such as biomass, to 300-650 °C in an oxygen-limited atmosphere (17) generating a flammable syngas, a black solid char (or biochar), and free flowing liquid bio-oil (11,18). Syngas typically consists of volatile substances that are condensable (water, tars and hydrophilic organics) and non-condensable gases (carbon monoxide (CO), hydrogen (H_2), methane (CH_4), carbon dioxide CO_2 and small hydrocarbons (C_2) molecules) (15,19). Commonly, syngas has a high calorific value around 10-20 MJ/m^3 (19–21) and can be used in power generation. Bio-oils however, are often very complex with high water and oxygen content (lower calorific value than hydrocarbon (HC) fuels) and contain the condensable organics derived from breakdown of cellulose, hemicellulose, and lignin. Unlike crude oil distillates, bio-oils are often considered as waste products as they have very different physical and chemical properties which may prevent their use as a fuel without further clean-up (15). However, the lower sulfur and nitrogen content of bio-oil does offer an added benefit as an environmentally friendly alternative to crude oil provided the issues mentioned are resolved (15,22). Biochar or char, is solid material enriched in carbon, (15,23,24) unlike combustion, where carbon is emitted as CO_2, up to 35 % of carbon is locked (sequestered) as a stable product (24). Biochar has a potential use as an alternative soil stabiliser and fertiliser (24). Biochar also possess sorption properties for a range of chemical species (organic and inorganic) and can be applied to contaminated soil and water for remediation (23–27). Biochar is well suited for this application as its structure is highly porous (stacks of randomized graphene layers forming micropores and channels) and contains a number of variable functional groups; polar (hydroxyl (–OH), carbonyl (C=O), ester (–COO-) and carboxylic acid (–COOH) groups) and non polar (aromatic) (23,24,28). These can interact with target pollutants through a number of polar (electrostatic, ion exchange and surface complexation) and non-polar (Van der Waal

dispersion forces, $\pi - \pi$ interactions, and pore filling) mechanisms (23,24,28). It is known that pyrolytic temperature can influence the degree of these functional groups, with higher pyrolysis temperatures producing biochar with lower polar functionality (decreased oxidisable groups) and increased hydrophobicity (increased aromaticity) (23,28,29). Therefore, pyrolytic temperature has a strong influence on biochar selectivity.

The pyrolysis process is categorised according to the length of time material is heated and the temperature range over which it operates. For example:

i. Slow pyrolysis typically operates with slow heating rates (0.1-10 °C/s) with long residence times (minutes) at 400-550 °C; bio-oil is produced around 35 % and (bio)-char is generated around 30 % of the initial mass (30).

ii. Intermediate pyrolysis is also a similar slow technique but takes place in a screw pyrolyser (19) an ablative technique. Typically slow and intermediate pyrolysis generates higher percentage of solid material (char) (31).

iii. Fast pyrolysis, operates at a higher temperature (>500 °C) with a fast heating rate (10-200 °C/s) and short residence time (0.5-10 s). Typically, fast pyrolysis is favoured for bio-oil production as yield is higher (up to 50-85 %) than slower techniques (30,31).

iv. Finally, flash pyrolysis (very fast uses gravity or gas flows to move material through a hot region. It is characterised by high temperatures (up to 1000 °C) and very short residence times (<0.5 s) and high heating rates (>1000 °C/s) (30).

There are several pyrolysis reactor designs, the main types are fixed bed, ablative, and fluidised bed reactors. Fixed bed reactors are not ideal for rapid manufacture as they are used in conventional slow pyrolysis. This is a contact driven process and heat transfer is achieved

through contact of feedstock with the reactor vessel (30) Ablative reactors are another contact driven reactor, where mechanical movement of the feedstock through a heated vessel results in the ablation of the char layers of the biomass. This technique has good heat transfer rates and the residency time of the material can be controlled. This method also allows the use of relatively large feedstock particles <20 mm and an inert carrier gas is optional to minimise any oxidation. However, the main disadvantages of this reactor is that it requires external heating with the reaction dependent on the heat transfer to the reactor, and the associated with difficulties to scale up to commercial use (30). Issues of low heating rate, thermal and mass transfer may be overcome by using fluidised bed reactors; these use heated particles of larger surface area, such as inert sand or a catalyst, to act as a heat transfer source. The solid bed of particles is fluidised by passing an inert gas through the particle bed, and there are several approaches to achieve this, with the most common being bubbling fluidised bed (BFB) and circulating fluidised bed (CFB) designs. In BFB reactors inert gas can pass through the bed of heated particles causing it to bubble aggressively. When the feedstock is introduced it reacts with the hot, abrasive material reducing the size of the feedstock. Once the particles are of a certain size they are expelled and recirculated and captured using a separator known as a cyclone (30). However, in CFB high gas flows mix the hot solid particles with the feedstock into a cyclonic mixture which is fed into a burner. Some of the feedstock is oxidised and the heat produced is transferred to the solid inert material, which is then recirculated back to the reactor (30). The advantage of fluidised bed reactors over other designs are the improved heat transfer from to the feedstock, making the process faster and more efficient and higher throughput as gases are generated and removed quickly. However, separation of products from bed particles can be difficult and the use of inert gases can dilute the target product syngas, lowering its calorific value (30).

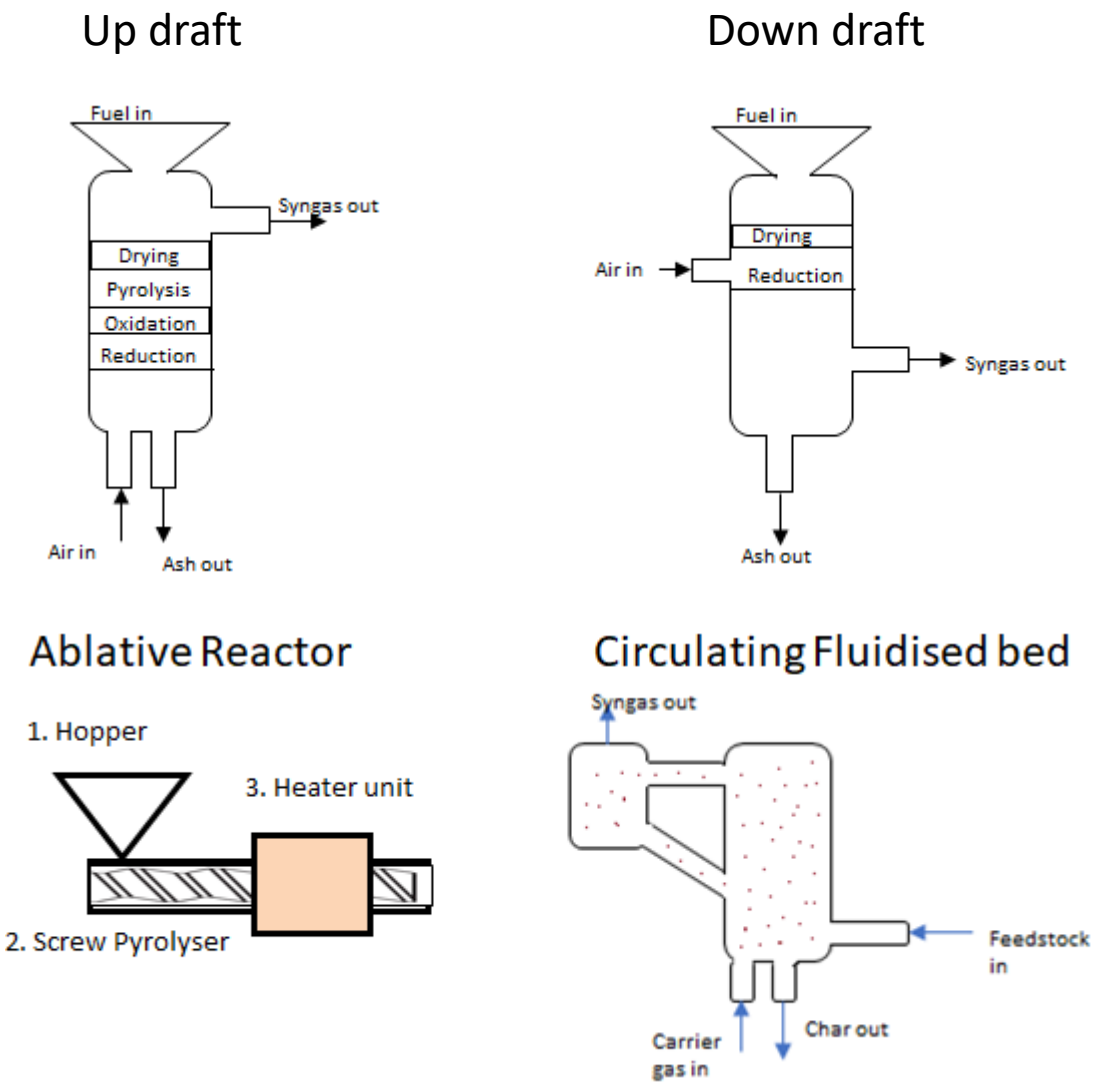

Figure 1.1 A schematic of the typical thermochemical reactors. Top the left: an updraft gasifier, feedstock is introduced in at the top and air the bottom of the reactor syngas is collected at the top of the tower. Top right: shows a downdraft gasifier. Feedstock is inserted at the top of the gasifier and air is fed in at the side; syngas is collected at the bottom of the tower. Bottom right: a circulating (cyclone) fluidised bed reactor; material is suspended in an air stream, fine particles may be returned in a gas stream to the hot region, syngas is collected at the top. Bottom left is a screw fed ablative reactor: feedstock moves through a heated vessel and decreases in size. Gas is collected at opposing end of the hopper.

1.1.3. Gasification.

Gasification involves intensive heating of carbonaceous material to 700-900 °C in the presence of a limited source of an oxidant such as pure oxygen, air or steam. Initially, the feedstock breaks down *via* pyrolysis between 300-600 °C and forms pyrolytic liquids (tars) and gases (17), with the remaining solid (char) and some tars reacting with the oxidant at higher temperatures (>900 ^{o}C) to produce syngas. The oxidising agent used in gasification has a direct impact on the calorific value of the syngas. Syngas from air gasification (5-6 MJ/m^3) is considerably lower than that produced in oxygen-limited pyrolysis (11,17,32) due to high nitrogen content of air having a dilution effect. When steam or pure oxygen is used in gasification, the calorific value of syngas increases to 9-19 MJ/m^3, (17,18) with steam used to boost the hydrogen (H_2) levels in the syngas, and oxygen the carbon monoxide (CO) levels. The ensure the amount of carbon dioxide is kept to a minimum, the amount of steam or oxygen is tightly regulated.

Inside the gasification reactor, the material will progress through several steps or zones with a range of chemical reactions as shown in figure 1 and table 1:

1. Drying zone: liquid water and steam migrate through the feedstock (200-400 ^{o}C) (7,32).

2. Pyrolysis zone: as temperatures increases, the solid material starts to vaporise decomposing in temperatures in excess of 600 ^{o}C and the final gas mixture containing organic tars, hydrocarbon residues, carbon monoxide, methane (CH_4), and water (H_2O) vapour (20).

3. Combustion/oxidation zone: at higher temperatures of above 900 ^{o}C, the pyrolysis products undergo further decomposition forming simple tars (organic compounds), CO_2, CO, CH_4 and H_2 (20). Unreacted residue will fall to the bottom of the gasifier and be removed as char or ash. This latter waste differs in colour to biochar (char) and

typically contains a high percentage of alkali metals, such as potassium (K), sodium (Na), magnesium (Mg) and calcium (Ca) (33,34) and carbonates, sulfates, phosphates and silica (34). Gasification occurs in this combustion zone with typical reactions involving carbon (C), carbon dioxide (CO_2) and tars with steam, H_2 and/or oxygen (O_2). However, careful monitoring to ensure target gas proportions for downstream processes/products are met is necessary as the product gases CO and CH_4 may also react with steam in the water-gas shift reaction; this can alter the balance of CO_2 and CO.

Oxidation Reactions	Reaction Type
$C+O_2 \rightarrow CO_2$ (-394 MJ/kmol)	Carbon oxidation
$2H_2 + O_2 \rightarrow 2H_2O$ (-242 MJ/kmol)	Hydrogen oxidation
$C+½\ O_2 \rightarrow CO$ (-111 MJ/kmol)	Carbon partial oxidation
$CO + ½\ O_2 \rightarrow CO_2$ (-283 MJ/kmol)	Carbon monoxide oxidation
Gasification Reactions	
$C+ H_2O \rightarrow CO+ H_2$ (+131 MJ/kmol)	Water-gas reaction
$CO+ H_2O \rightarrow CO_2 + H_2$ (+131MJ/kmol)	Water-gas shift reaction
$CH_4+ H_2O \rightarrow CO +3\ H_2$ (+206MJ/kmol)	Steam methane reforming
$C+2H_2 \rightarrow CH_4$ (-75MJ/kmol)	Hydrogasification
$CO+3H_2 \rightarrow CH_4 + H_2O$ (-277 MJ/kmol)	Methanation
$C+CO_2 \rightarrow 2CO$ (+172 MJ/kmol)	Boudourad reaction
$C_nH_m + nCO_2 \rightarrow 2nCO + m/2\ H_2$ (endothermic)	Dry reforming
Decomposition reaction	
$pC_nH_y \rightarrow qCnHy + rH_2$ (endothermic)	Dehydrogenation
$C_nH_m \rightarrow nC+ M/2\ H_2$ (endothermic)	Carbonisation

Table 1. A table Illustrating typical reactions within the gasifier. These are typically endothermic (indicated by the positive enthalpy sign) requiring energy (i.e. heat) to occur (7).

When characterised the overall gasification process is endothermic (see table 1.0) and is unlikely to proceed without the addition of heat (energy). The energy required may be generated from the partial oxidation feedstock (combustion) in the reactor (20,33) or alternatively, through the redirection of some of the combustible syngas to burners that heat the system as a feedback loop, thereby reducing the carbon needs of the process. In addition to this potential gain in efficiency, gasification has the advantage of converting a greater proportion of feedstock to

syngas *versus* pyrolysis and so, not only is there a greater yield of product, the solid (waste) material or 'ash' remaining is typically considerably less. The main disadvantage of gasification is the high start-up and operational costs, it is therefore, considered more efficient (feasible) to build larger plants (11,18) and requires skilled operators to monitor and react to the constant changes in process conditions such as oxidant feed, temperature fluctuations, pressure readbacks and catalyst condition, which all require constant surveillance.

1.1.3.1 Gasification equipment.

Several types of gasifiers have been developed with most designed to produce heat and power from syngas rather than liquid fuel (20). Gasifiers are typically classified according to how feedstock is introduced into the gasifier, the oxidising agent used (air, oxygen or steam), the operating temperature and pressure range and the directional flow of the oxidant, syngas or feedstock. Given these criteria the main types of gasifier are as follows:

i. <u>Updraft Fixed Bed Gasifier.</u>

Here the feedstock is fed into the top of the gasifier and air is drawn in from the bottom of the rig. Methane and hydrocarbon-rich gases are sourced from the top of the gasifier, whilst the waste ash is collected and separated using a grate at the bottom of the gasifier (7,20). The main advantages of using updraft gasifiers are the good thermal efficiency with small pressure fluctuations giving rise to less variable syngas composition and low slag (glassy waste product containing metal oxides and silicon dioxide) formation (32). However, they are prone to tar formation with increased moisture content of the fuel, a relatively long start-up time and poor reaction capability of heavy gas loads (32). This leads to reduced quality of syngas with a high percentage of tars and methane (7).

ii. Downdraft Fixed Bed.

This gasifier operates under gravity with the feedstock and gases (oxygen and steam) fed in through the top of the rig. The design of the vessel narrows restricting the passage of hot feedstock forming a hot zone of charcoal. Gases pass through this hot zone whereby they react with the charcoal producing a high-quality syngas with relatively low tar content (7,20). In addition to the syngas quality downdraft gasifiers have the benefits of low susceptibility to dust and tar but are not suitable for small particle size of feedstock (32).

iii. Entrained Flow.

In this rig, the feedstock is used as a fine powder mixed with pressurised steam and oxygen and typically operates at high temperatures (1200-1500 °C) achieved by burning a proportion of the feedstock (7,20). This gasifier is capable of a very rapid conversion of feedstock to gas producing a high-quality syngas and molten ash is removed as a solid slag material (7,20).

iv. Bubbling Fluidised Bed (BFB).

This technology typically operates at a lower temperature (<900 °C) and the feedstock is fed in through the sides of the gasifier where it is mixed with an inert (20) granular solid ranging from 1-3 mm in size, such as sand or gravel (for biomass feedstock) or limestone or ash (for coal feedstock) (35) on a metal grate. During operation gas and steam are fed upwards through the material at around 1-3 m/s, where the feedstock combusts to form syngas, leaving the top of the reactor (20). This reactor is particularly useful for high conversion efficiency of feedstock to syngas, with efficiencies within 90-98 % (35).

v. Circulating Fluidised Bed (CFB).

Unlike the BFB rig the feedstock is introduced at the side of the gasifier, whereby it is suspended on the inert 'bed' material, the operational temperatures are also below 900 °C (20). Air, oxygen or steam is directed up through the material at an increased rate of 5-10 m/s. This results in the combustion of the feedstock generating heat and syngas, (20) with the energy from the fast-moving gases sufficient enough to drive solids out of the furnace (35) through the formation of a cyclone and is returned to the bottom of the gasifier (35) by use of a capture gas (35). During operation, target syngas is separated from solid waste material and removed from the top of the rig with conversion efficiency between 97-99.5 % (7,35).

Of these designs the fluidised bed reactors are often the gasification rig of choice as, unlike the other systems described, they are capable of gasifying a wide range of feedstocks without having a detrimental effect on performance of the system (20). They are characterised by high combustion efficiency and high thermal transfer due to intense mixing. They also generally produce cleaner gases, and can use limestone particulates to remove sulfur impurities (35) by reacting with SO_2 to form solid CaS, lowering potential SO_2 emissions (35). Also, as fluidised bed reactors operate at lower temperatures (<900 °C), the temperature is not sufficient to oxidise nitrogen to NO_2 reducing the likelihood of these unwanted, polluting gases from forming during the process (35).

1.2. Catalytic conversion techniques for energy recycling: the Fischer-Tropsch process.

Syngas generated from thermal conversion process may be used as a starting material for other target products. For example, CO and H_2 from syngas may be converted to a synthetic fuel *via* the catalytic Fischer-Tropsch process whereby CO is hydrogenated using a Group VIII transition metal catalyst, such as iron, cobalt or ruthenium, to form the desired hydrocarbons and

oxygenates (36). In 1938, Franz Fischer and Hans Tropsch used alkalised iron (Fe) catalysts (36) to generate a mixture of oxygenates and hydrocarbons using CO and H_2 from coal gas. The reaction required operating temperatures and pressures of 150 to 300 °C and 10-100 bar, respectively (37). To ensure an efficient and high yield of the desired saturated hydrocarbons for fuel use it is important to obtain a clean gas supply with a higher partial pressure of H_2 to CO before the gas mixture enters the Fischer-Tropsch reactor. To produce saturated hydrocarbons (alkanes) for diesel, the FT process will require a ratio of H_2: CO of >2:1 to ensure appropriate saturation (38), (ideally slightly higher in practice) (14,20) to produce distillates above C5 range. Therefore, appropriate clean-up and control of the gaseous mixture entering the reactor are key to the success of the technique and remains a challenge for interfacing the process as the final fuel production stage. The latter factor may be achieved by supplementing with the appropriate gas prior catalytic conversion. For example, during gasification, oxygen and steam may be added or methane (CH_4) may be oxidised to generate a higher H_2: CO (7). These processes are described by the following equations (1.1 and 1.2)

$2C + ½\ O_2 + 2H_2O \rightarrow 4H_2 + 2CO$ Equation 1.1

2 : 1

$CH_4 + ½\ O_2 \rightarrow 2H_2 + CO$ Equation 1.2

2 : 1

The production of target materials may be influenced by adjusting the equilibrium reaction of the FT process. For example, to generate the optimum yield of product the reactor may be operated at increased pressure of 10-100 bar, increasing the partial pressure of the reactants

(H_2 and CO), to shift the equilibrium in favour of the formation of the reaction products (i.e. straight-chain alkanes or paraffins, $C_nH(2_n+2)$) to address the imbalance of the chemical system:

$(2_n+1)\ H_2 + nCO \rightleftharpoons C_nH(2_n+2) + {}_nH_2O$ -145 KJ Equation 1.3

However, due to the broad selectivity of the FT catalyst the process is not 100 % efficient producing alkane fuels for diesel; resulting a wide distribution of products (20) from light synthetic fuels to heavy waxes. In addition to straight-chain alkanes, there are also minor amounts of other undesirable materials formed, such as branched-saturated and unsaturated hydrocarbons (i.e. methyl paraffins and olefins) (20) and primary alcohols.

$nCO + (2n+1)\ H_2 \rightleftharpoons C_nH_{2n+2} + nH_2O$ (alkanes) or Equation 1.4

$nCO + (2n)\ H_2 \rightleftharpoons C_nH_{2n} + nH_2O$ (alkenes) Equation 1.5

$nCO + (2n + 1)\ H_2 \rightleftharpoons C_nH_{2n} + nROH + nH2O$ (production of alcohols) Equation 1.6

$CO + 3H_2 \rightleftharpoons CH_4 + H_2O$ (Hydrogenation of CO) Equation 1.7

Typical catalysts used in the FT process are heterogeneous (different physical state to the reactants) and contain iron (Fe) or cobalt (Co) (20,36,39). Of these, Co catalysts generally produce a greater percentage of saturated hydrocarbons that are liquid distillates of C5+ (20,39) and tend to have a longer lifespan. However, they are considerably more expensive than Fe catalysts (20,39) but Fe catalysts are known to form higher levels of undesirable side products including unsaturated hydrocarbons (olefins) and oxygen containing products, such as alcohol. These oxygen containing products may also include aldehydes, organic acids and esters, and are by-products of all FT catalysts formed when the hydrocarbon chain is terminated at the site of the oxygen atom or from the condensation of two alcohols at site of the FT process (14). Some oxygenated species are considered beneficial to the process and have been re-used, for example fatty alcohols have been used to improve the heating value, increase lubrication and ignition

value of synthetic diesel (14). However, it is the undesirable oxygenated substances that are prevalent when using Fe-based catalysts (with yields observed up to 30 %) but, with a greater tolerance to sulfur impurities and lower operating costs, these catalysts are often chosen as a compromise for the FT process (20).

In addition to catalyst material, the temperature of the reactor also determines the distribution of chain length; higher temperatures (330-350 °C) favour the production of light olefins and gasoline fractions, while lower temperatures lead to the production of heavier chains such as diesel and waxes (220-250 °C) (20). However, at higher temperatures the yield of gasoline materials is often compromised; the addition of thermal energy to generate these materials can cause the equilibrium of this exothermic process to favour the reverse reaction to remove excess heat, leading to an undesirable low yield.

1.2.1 Mechanism of FT synthesis.

In 1926, Fischer proposed the carbide mechanism for FT synthesis using Fe-based catalysts. He postulated several mechanisms, including the formation of oxygenated species, such as alcohols and ketones (40). However, the mechanisms were revised after discovering alkanes as a main product of the reaction (40). This early work suggested that carbides were generated from the adsorption of CO to the metal catalyst surface where it is hydrogenated forming methylene (CH_2) groups that polymerise to form a hydrocarbon (14,38,40). Following this work, a more detailed mechanism was introduced by Croxford proposing that adsorbed CO dissociates in the presence of H_2 forming chemisorbed carbon (C*) on the surface of the catalyst, followed by the release of water and CO_2 (40,41). The adsorbed carbon is hydrogenated to form chemisorbed methylene which initiates chain growth through oligomerisation to produce a hydrocarbon chain (40–42) (see figure 1.1).

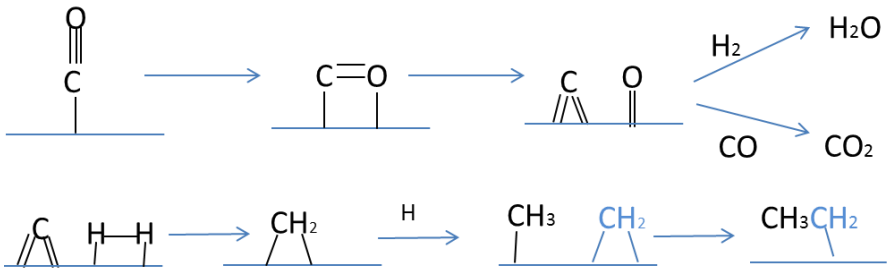

Figure 1.2 A reaction mechanism adapted from (Davis, 2009)(40) *shows the proposed carbide mechanism for hydrocarbon alkane formation. CO and Hydrogen are dissociated on the surface of the catalyst, the formed carbide is hydrogenated to form methylene groups, which are then oligomerised.*

However, this carbide mechanism does not explain the formation of oxygen containing compounds. Starch and co-workers suggested that oxygen containing intermediates (formyl or oxymethylene radical) on the surface of the catalyst go through poly-condensation with the elimination of H_2O *via* an enol reaction. For example, oxygen reacts with Lewis acid sites of the metal complex, resulting in a condensation reaction forming carbon-carbon bonds, thereby initiating chain propagation (40,41). It is the termination of this chain containing oxygen and the elimination of H_2O that leads to the formation of hydrocarbons and can occur with or without reacting with hydrogen generating alkanes or alkenes, respectively (14).

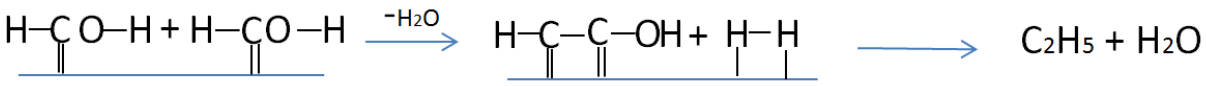

Figure 1.3: A reaction mechanism adapted from (Krylova, 2014)(14)*, shows the formation alkyl chain through an oxygen intermediate.*

However, if chain termination occurs without the elimination of water, undesirable oxygen containing compounds, such as aldehydes, alcohols, and acids (14), and unsaturated compounds can form through the reaction of the alcohol intermediate with H_2 or water (14) and thus, the control of the reaction conditions are key to generating the target alkane species.

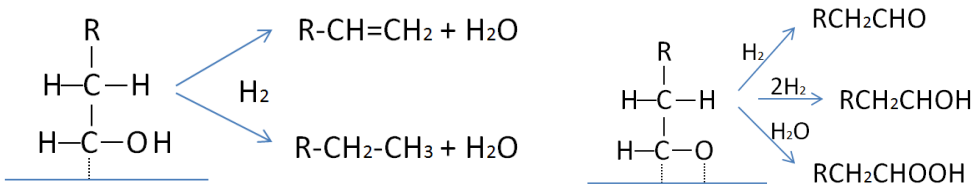

Figure 1.4 A mechanisms adapted from (Krylova, 2014)(14)*, left shows the formation saturated and unsaturated hydrocarbons chain through reaction of oxygen intermediate with hydrogen. Right shows the proposed mechanism for the formation of different oxygenates.*

1.2.2 Optimisation of catalytic processes.

Catalysts were first defined in 1895 by Ostwald as a substance that accelerates a reaction but is not consumed by the reaction (14). This is achieved by providing an alternative reaction pathway of lower activation energy (energy barrier of a process, which reactants need to exceed to form products) than that of the non-catalysed reaction (43,44). Although catalysts increase the rate of both the forward and reverse reactions of a system, they have no effect on the equilibrium or the thermodynamics of the process (43,44) . Catalysts operate by forming a complex with the reactants (45) enabling an alternative reaction pathway to be taken, which has a lower activation energy. These complexes are unstable intermediates formed between the catalyst surface, reactant(s) and at least one ligand (46). According to Sabatier's principle, states that interactions between the reactants and catalyst so neither be to strong or two weak and these intermediates must be stable enough to be formed in sufficient quantities and react to form a final product (45,46). Following the transformation of the reactant(s), the product(s) are released from the catalyst which is then free to react again (46). The kinetics of this process maybe influenced by several parameters including the thermodynamics of the reaction, the frequency of collisions between catalyst and reactant(s), the number of active sites on the catalyst and its activity and selectivity for the reactant(s). Manipulation of these conditions enables the optimisation of the catalytic process for improved efficiency and efficacy.

1.2.2.1 Thermodynamic considerations of catalytic reactions.

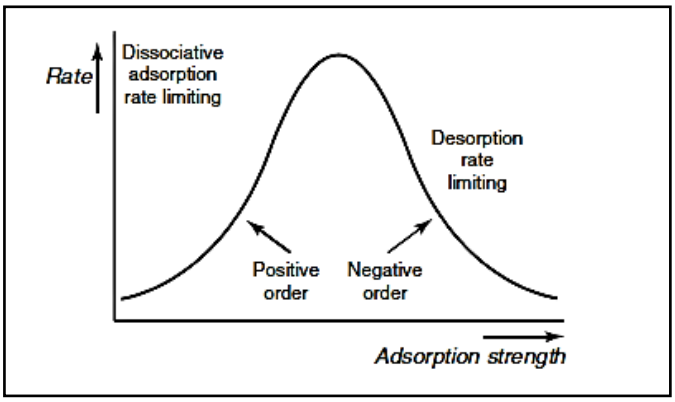

Figure 1.5 Figure showing Sabatier's principle graphically, the rate of the catalytic reaction reaches the optimum point at which the catalyst is most effective (45).

There is a direct correlation between thermodynamic quantities (heat, Δq) and activation energy (ΔE) of a reaction; when Δq increases, ΔE decreases, lowering the activation energy of a reaction (46) as shown by equation 1.8.

$$\Delta E = a\Delta q \qquad \text{Equation 1.8}$$

The relationship between temperature of the catalysed reaction and the formation of the intermediate product (46) are represented by volcano plots, see Figure 1.5. It is a plot of adsorption strength of an intermediate over the rate of reaction, this is essentially a measure the intermediate stability. The rate of reaction can be measure of heat of adsorption of reactants or heat of desorption of surface compound; therefore, if the heat of formation of the intermediate (ΔHf) is low, the reaction rate is low, resulting in low-rate of adsorption to the surface of the catalyst. At high values of ΔHf, the reaction rate is also low and relates to a low desorption rate (46). Therefore, an optimum is observed at intermediate values of ΔHf (45,46).

1.2.2.2 Catalyst surface area and number of active sites

Traditionally, it has been thought that metal catalysis occurs in a planar fashion whereby, reactants interact on the flat surface of a catalyst (46). However, recent work has shown that metals or metal oxide catalysts have a rather complex crystal structure with reactions dependent on the surface of the material and what is available to the reactants. Therefore, the surface area of the catalyst will directly impact on the reaction conditions with a high surface area increasing the potential frequency of collisions (45) with the reactant(s). These reactions occur at specific areas of the catalyst, known as active sites, containing atoms of particular coordination properties (46), where atoms of different coordination numbers result in different sites (46). It is believed that these active sites form on edges or corners of crystal lattices (46) to expose active site for maximum opportunity of coordination with the reactant(s), therefore, metal catalysts can have multiple active sites where several reactions can occur (46). Adsorption of the reactant to the catalyst surface can occur by a physical process or 'physisorption' (involving relatively weak Van der Waal forces), or by chemical means or 'chemisorption'; where reactants adsorb through strong valence forces of attraction (covalent bonding) (46). Once the reactant adsorbs to the surface of the catalyst it may stay intact (molecular adsorption) or its bonds may break (dissociation adsorption), with the product able to diffuse away, following the reaction (44) leaving the catalyst free to react again.

1.2.2.3 Catalyst activity and selectivity.

The measure of activity is best described as the catalytic turnover rate and is expressed in units of product made per unit of time (44,46). The selectivity of the catalyst, however, is defined as the amount of desired product obtained per amount of consumed reactant. Selectivity can be thought as the yield of desired product multiplied by the conversion rate, or the ratio of desired product compared to the rate of consumption of starting material (46). The selectivity of catalysts may originate from the shape of the active site and coordination chemistry at the

active site, where only those reactants of correct electronic configuration will bind. For example, zeolites are crystalline aluminium oxide catalyst containing regular pore sizes through their structure (45) and can enhance the selectivity of the catalyst based on shape. This may be achieved by:

1. Selectively enabling the correct isomer and its spatial configuration of the reactants to only enter the pore.

2. Maintaining the position and transition state of the functional groups in the active site of the catalyst is crucial for adsorption.

3. Selectively releasing the correct product of appropriate configuration from the active site, however, this can be a barrier to reaction optimisation with some isomers becoming trapped within the pore, having an inhibitory effect of the catalyst.

1.2.3 Fischer-Tropsch Catalysts.

Fischer-Tropsch catalysts are heterogeneous catalysts containing a transition metal on a solid silica or alumina support, over which reactant gases can diffuse and react to form target intermediates. Common FT catalysts utilize the metals Fe or Co depending on the process requirements for example, typically Fe catalysts have lower activity than Co based catalysts but are considerably cheaper (250 x cheaper). Fe catalysts are often preferred for interfacing with gasification as they are more suitable for low H_2/CO feedstock, due to their high water-gas shift activity (36). They usually consist of Fe oxide with reduction and chemical promoter such as copper (Cu), an alkali metal such as potassium (K) respectively. Silicon dioxide (SiO_2) is a common support medium providing structural integrity and a large surface area for the catalyst to promote higher reaction rates (36). Within this mixture, the Cu promoters enable the reduction of Fe(ll) to Fe (lll) or metallic Fe, while K facilitates longer hydrocarbon chain formation. Studies have shown that the performance of FT catalysts maybe enhanced by using combinations of

transition metals. For example, the addition of chromium (Cr) to Fe based catalysts produced longer chain products while manganese (Mn) promoted the formation of light C2-C4 species (36). Research by Lohitharn *et al.* 2008 also showed that by adding a third transition metal (Cr, molybdenum (Mo), Mn, tantalum (Ta), vanadium (V) or zirconium (Zr)) to Fe-based catalysts enhanced the catalytic activity further, particularly for the hydrogenation of CO and water-gas shift activity, making Fe catalysts ideal for conversion of low-quality syngas, (low H2/CO ratios) to fuels.

However, for low temperature FT process alternative Co catalysts are more typical, especially for generating mid-range distillates and waxes using slurry bubble or multi-tabular fixed bed reactors, (39) as they requires a high ratio of H_2/CO. Like Fe catalysts, these tend to be supported using inorganic oxides with high surface areas, such as alumina or SiO_2, and have increased catalytic activity (39). They are typically 15-30% by weight of Co (39), and often have small amounts noble metals, such as ruthenium (Ru), rhodium (Rh), platinum (Pt) or palladium (Pd), as metal promoters (0.05-1%) and oxide promoters that may include zirconia, lantania or cerium oxide at ≈1 to 10 % (39). These noble metals are key to the catalysts performance by increasing selectivity and activity of the Co catalyst unfortunately this can make the catalyst expensive, especially when prepared with rare noble metal promoters, and are typically prepared using long energy intensive calcination reactions by heating in air at > 600 °C, to modify cobalt oxide to active pre-active state on the support.

Using a support such as carbon, or silica, can enhance the activity of the catalyst (47), but with an increased cost. Cheaper supports such as aluminium oxide are available although a reduction in activity is observed due to a high adsorption strength of the support for the catalyst, reducing its efficiency (47). However, for a more energy efficient low temperature production of the catalyst, aluminium oxide may be an advantage over supports such as silica. The normally undesirable high binding strength of aluminium oxide with cobalt may enable this process to

occur successfully at reduced preparation temperature, reducing the energy resource required for the process (47). The cost efficiency of this process can be further improved by using cheaper promoters such as manganese and could enable the production of cheaper cobalt catalyst, by combining these approaches. This with a lower calcination stage to modify the cobalt; may offer a potentially cheaper and more energy friendly catalytic synthesis.

1.2.4 Fischer-Tropsch (FT) reactors.

Once the catalyst is synthesised it is used within the FT reactor, these may be classified according to those that operate at low temperature (to produce heavy hydrocarbons and waxes), and at high temperature (to produce light unsaturated hydrocarbons). Given the exothermic nature of the process, with approximately 145 KJ per $-CH_2-$ formed, temperature monitoring and the removal of excess heat are key to the design of the FT reactor. There are three designs currently in use:

1. Tubular fixed bed reactors.

   These operate at low temperatures (180-250 ^{o}C) and pressures of (10-45 bar). Based on fixed bed reactors these are multi-tubular, resembling heat exchangers, where small amount of catalyst is packed into narrow tubes, surrounded by water (48). This is important as rapid heat exchange through the water enables near 'real-time' monitoring of axial and radial temperature profiles (49,50). High conversion rates take place within the first few metres of the reactor (37,49). The main advantage of this type of reactor is that the product is clearly separated from catalyst and recovery is relatively simple, however, this type of reactor is associated with high start-up costs and problems with the catalyst replacement during operation (37).

2. Slurry phase reactor.

This is also operates at low temperature, whereby the catalyst is supported in a wax through which the syngas is bubbled (48,49). The heat generated is passed from this slurry to cooling coils inside the reactor which remove excess heat as steam. The main disadvantage of this reactor is that the target liquid hydrocarbons require separation from the solid wax; achieved by an appropriate preparation method to ensure product cleanliness (49).

3. Circulating fluidised bed reactor (bubbling or circulating).

This reactor operates at higher temperatures (330-350 °C) and a pressures of 25 bar (37). For hydrocarbon production, fast flowing syngas is mixed with fine powdered catalyst which swept up to the reaction zone and recirculated back to the reactor. This circulating reactor produces lighter hydrocarbons suitable for fuel production (47) and offers several advantages over other reactor designs including good temperature control, lower fluctuations (reduced compression costs) and lower start-up costs.

1.3 Pyrolysis, gasification and Fischer-Tropsch as a combined recycling method for fuel production.

Gasification and pyrolysis are both endothermic reactions with 55-75 % of the thermal energy supplied converted to chemical energy. Therefore, the products of the reactions are elevated to a higher heating value than the original feedstock and, unlike combustion, syngas, bio-oil, and biochar can be easily transported (11) and utilised in several energy recovery routes, boosting the overall efficiency of the process (18). Typical approaches of energy recovery may include:

1. Combustion of syngas using additional technologies, such as steam cycles (efficiency 14-27 %), combined cycle gas turbines (up to 60 % efficiency, lowered to 40 % after gas

cleaning), co- firing with fossil fuels (~40 % efficient), gas engines (efficiency 25 %) and used in fuel cells (efficiency >50 %) (11,17,18,50).

2. Synthesis of products such as methanol and Fischer-Tropsch fuels from syngas (50-90 % conversion of CO to hydrocarbons) (20).

3. Direct use of pyrolysis bio-oils as a fuel or processed to obtain high value products, such as phenolic compounds, used in resins and adhesives and flavouring compounds (15).

This flexibility in energy recovery benefiting from lower emissions from the lower operating temperatures of gasification and pyrolysis provide, these processes with significant advantages as a cleaner, environmentally friendlier potential recycling process than incineration (11,17).

Regarding different waste streams, pyrolysis may offer a potential recovery method for useful hydrocarbons in brown field soils contaminated with oily sludge as in similar study using waste hydrocarbon material as a feedstock (51) was successful in producing high valued products. Pyrolysis could also be used to convert wastewater sludge into syngas, bio-oil and biochar (52,53) and gasification could potentially generate quality syngas due to its similarity to biomass possessing a high carbon and oxygen content (54). These processes are typically thought of as carbon and environmentally friendly alternatives to incineration and landfill disposal. For example, carbon is sequestered in pyrolysis (19,23) and through the replenishment of biomass, such as wood and agricultural plants, it is deemed as carbon neutral process. Pyrolysis and gasification are considered primary routes of synthesis as they are involved in the initial production of syngas while, gas to liquid technology or the FT process is secondary as it focuses on conversion of the syngas into liquid fuels such as methanol and diesel (20). Fuels generated by the FT process, involve the catalysed reaction of hydrogen and CO derived from the syngas into useful distillates. These fuels are considered more environmentally friendly than those generated from crude oil with lower amounts of sulfur and nitrogen, along with heavy metals

and aromatics that contribute to the emission of greenhouse gas and persistent organic pollutants (POPs), respectively (14). Although pyrolysis and gasification are widely considered a cleaner alternative to waste disposal than incineration or landfill, both methods involve intense heating of organic material and will ultimately lead to the generation of unwanted impurities such as tars and volatilised metals (16,21,55). These impurities are problematic as they can cause fouling and sintering of downstream processes such as FT and this leads to regular plant shut downs to remove blockages from slagging and replenished fouled catalysts, ultimately lowering the productivity of the system. These impurities need to be treated in a cost-effective and environmentally friendly manner to avoid introducing new undesirable waste streams.

Some of the pollution and impurity concerns of pyrolysis and gasification may be overcome by adequate engineering and gas cleaning with the risks of hazardous emissions greatly reduced through the use of filters and scrubbers post process (16,55,56). There remains a need for appropriate clean-up of these processes which must be economically and environmentally friendly to offer a greener solution to the current energy demand, particularly for diesel alternatives, containing linear alkanes of C10-C24, to be used as a fuel for engines.

1.3.1 Current approaches to syngas cleaning prior FT process.

Thermochemical processes that involve heating material, such as pyrolysis or gasification, generate unwanted by-products in addition to syngas; these include tars, un-burnt particulates, inorganic gases and volatised heavy metals (7,16,57). Tars are organic compounds that may be classified as non-condensable (within C2-C5 hydrocarbon range) and condensable (C6+, compounds typically larger than benzene). Heavy and non-condensable tars can be problematic causing mechanical fouling, blocking downstream processes and can be corrosive to mechanical surfaces. Condensable tars are mixtures of light aromatic, heterocyclic, phenolic and polyaromatic hydrocarbons (15,16,21). Non-condensable components comprise of small

organic tars such as acetylene, ethylene, benzene and small unsaturated hydrocarbons. The composition of tar can vary dramatically according to the feedstock used. Some of the more volatile species within the tars, can also migrate to secondary processes that have catalysts, such as FT, if they are not effectively removed resulting in fouling and inactivation of the catalysts employed (16,56) increasing maintenance costs for the process. Other problematic volatile species in syngas include inorganic gases such as sulfur-oxides (SOx), nitrous oxides (NOx), ammonia (NH_4), hydrogen sulfide (HS) along with volatilised heavy metals (in temperatures above 700 ^oC) (7,20,54,58). These can also foul downstream catalysts, shortening their lifespan and contaminate the target product (20,33,56). Other substances that can contribute to catalyst fouling include large particulates and alkali metals (56,58,59), often requiring filtration using hot gas filters or cyclone separators. These, with other more volatile impurities described above, must be removed for syngas to be used in a cost-effective and efficient manner with downstream processes, that could include gas turbines, methanation, and the FT process. Unlike heavy tars, lighter, more volatile tars remain cannot be removed easily by condensation. Several methods have been attempted remove these species however, their success is not guaranteed and can be variable depending on the impurity levels, primarily governed by differences between feedstock materials. Common methods include: (53).

1. Solvent traps or scrubbers
2. activated carbon or membrane filters,
3. catalytically reforming the tars and,
4. altering the conditions of the gasifier to reform tars (21,53,56).

One of the most common approaches is using a solvent trap (scrubber) such as methanol or water, through which the syngas is bubbled, and soluble impurities of lower volatility remain in the scrubber,based on the solvation interaction between the solvent and impurity. During

solvation, the solvent molecules interact with the impurity (solute) by complexation mediated through interactions of hydrogen bonding (δH), dipole effects (δP) and polarizability (δD) of the solvent towards the impurity (60). The contribution of these effects determines whether the solvent is polar protic (solvated negatively charged solutes), polar aprotic (large dipole moments) and non-polar (dispersion forces) (60). Water and methanol are polar protic solvent and effective at removing organic tars containing polarisable groups and inorganic compounds (61). The lack of waters non-polar character means its less effective at removal of hydrocarbon and heterocyclic compounds (non-polar compounds) which causes these scrubbers tend to saturated quickly, separating in to two distinct phases (61). Aprotic polar organic solvents such as methanol, dimethyl ether of polyethylene glycol (DEPG), N-methyl-2-pyrrolidone (NMP) and propylene carbonate (PC) (62,63) are typically used in syngas processing to remove acidic gases such as H_2S and CO_2 (62,63). Although more polar organic compounds are soluble in these solvents, their main focus is the removal H_2S and CO_2 (62). Further to this, trapping of tars in organic solvent scrubbers can be highly effective method of syngas cleaning. A low temperature scrubber containing the methanol (maintained at around -40 °C) has been shown to be an effective technique for removing small organic compounds greater than C6+ such as benzene. To enhance the systems efficiency, once the scrubber is saturated, it can be used as a feedstock fuel to heat the thermal processes (16) reducing the waste generated and reducing its carbon footprint. Oil based (non-polar) scrubbers are another form of wet scrubber and have proven very effective at removing non-polar semi volatile tars, but similarly to other wet techniques are ineffective at capturing volatile impurities such as acetylene and ethylene (16,53,59). Given that these traps are dependent on solubility, it is likely that alternative solvents scrubbers may be more effective at trapping the volatile organic compounds generated during pyrolysis and gasification. Isopropanol (IPA) a protic solvent and has been used in impinger based solvent trap methods (lab-scale) as it has a wide solubility range and high saturation capacity (64–66). Isopropanol has good polar (δP) and non-polar functionality (δD) (Hansen solubility parameter

index see table 1.1) (60) and capable of interaction with impurities through hydrogen bonding and dispersion forces. A structurally similar solvent to IPA is acetone. Although under used as a solvent trap, acetone has a similar range of solvent miscibility to IPA and therefore capable of dissolving a variety of organic compounds. Acetone however, is considered an aprotic polar solvent due to large dipole moment of the ketone functional group (>=O). Although possessing a similar value of (δD) to IPA, the hydrogen bonding ability (δH) is considerably lower than that of IPA (-OH) and methanol. However, it has been found practically that acetone is a better extraction solvent for PAHs in sludge (67) and phenolic compounds in plant matrices, compared to IPA and methanol (68). This increase in extraction efficiency could possibly linked to the higher dipole moment of acetone (67)(see table 1.1) which may influence extraction of aromatic compounds through polarizing effects. Since it is anticipated that tars generated in recycling of waste material such as biomass and contaminated soil will contain polyaromatic hydrocarbons and phenolic compounds, then acetone may be a better suited scrubber solvent. An additional advantage of using acetone over common scrubbers such as methanol, is that ketones offer better adsorption of troublesome alkynes over alcohol solvents. (69).

	dispersion bonds δD	polar bonds δP	H bonds δH	Dielectric constant	Debye dipole moment
Water	6.0	15.3	16.7	80.4	1.9
Acetone	7.58	5.1	3.4	20.7	2.7
Methanol	7.42	6.0	10.9	32.6	1.6
Isopropanol	7.75	3.3	8.5	19.9	1.7
Hexane	7.24	0	0	1.89	0
DCM	8.91	3.1	3.0	8.39	0
Toluene	8.70	0.7	1.0	2.38	0

Table 1.1 showing some of the solubility parameters of common laboratory solvents.

Due to the lower volatility of acetone over solvents such as DEPG, IPA, methanol, could possibly suited to more complete recycling process, where waste heat from the process could be used to evaporate the acetone, to be condensed as a clean solvent. This may offer a potential reduction in solvent cost of scrubbing syngas using cryo cooled methanol particularly due to the

lower cost of acetone solvent. In addition to organic substances, scrubber systems can also remove alkali metal impurities by using water and chlorine (as hydrochloric acid, HCl) additive which reacts with the metal to form solid salts that can be removed by filtration (16,53).

The second clean-up approach using activated carbon is also limited to the range of compounds and is not suited to removal of volatiles below C2 in size and is typically used for substances with a maximum carbon size (C20) range. The main advantage of activated carbon is that it can be re-used by desorbing the captured organic tars from its structure using heat after use, reducing the carbon footprint of the process. This principle of re-use can be extended further whereby, benzene captured from the tar may be recovered after desorption by distillation or liquid capture and then re-used as a fuel (16). For the small organic volatiles not suited to activated carbon, these require cryogenic separation based on their boiling points (16). Unfortunately, this requires expensive equipment and the undesirable handling of extremely cold liquids.

Alternatively, these C2 gases may be reformed rather than captured by the using steam, hydrogen or a reforming catalyst. These reforming catalysts typically contain noble metals and minerals such as limestone, dolomites, olivines and zeolites (56,70,71) and promote the hydrogenation of tars to reform these volatile organics to CO and H_2 (70,71). Other catalysts may also be used with activated filters to remove tars. For example, catalytically activated filters using silicon carbide (SiC) catalysts with magnesium and aluminium oxide ($MgO\text{-}Al_2O_3$) supports removed 99% of tars in a simulated gas containing naphthalene, benzene, and hydrogen sulfide (H_2S) (72). However, as with FT catalysts, these are prone to coking and have limited lifespan (70) potentially increasing the costs of the clean-up process. It also is possible to reform tars simply by altering the parameters of the gasifier, with the addition of steam or hydrogen, however, the energy required to heat water in this process resulting a lower efficiency of the system and a poorer carbon footprint (16).

In summary, impurity removal and reformation are key to reducing the energy needs and waste associated with a pyrolysis/gasification- diesel fuel production process while ensuring the maintenance and operational costs (in terms of catalyst use) are kept as low as possible. It is clear the clean-up method(s) for syngas from different carbon feedstocks is an important stage that requires further development and characterisation if these two techniques are to be combined as a carbon waste recycling process.

1.4 Carbon waste feedstock.

Feedstocks used in thermochemical treatment processes should ideally have a high carbon content. There are a vast number of potential feedstocks available that can be suitable for gasification and pyrolysis. These can include; biomass which typically covers plant material such as wood, agricultural and grassy plants, household (municipal) waste, these usually contain high degree of paper, plastic and food waste, and industrial wastes such oily waste, coal and process waste. It is essential that the feedstock has a low water content (typically <30 %) as drying the material is energy consuming and lowers the efficiency of the process, typically feedstocks have (20). Ideally material should also have a low sulfur content (53) to minimise SOx production. Another oxide species of environmental concern is NOx, this is rarely an issue as the vast amount of fixed nitrogen is converted to molecular nitrogen or ammonia; with the latter being removed by wet scrubbing (53,57). In any thermochemical process there are always generation of impurities, these can be inorganic and organic. Limiting the production of impurities would enable better interfacing of a pyrolysis/gasification and diesel fuel production process (such as FT), however, this would require a feedstock that would generate fewer organic and inorganic compounds and better clean-up process at the interface with the aim to produce a syngas that contains an appropriate ratio of H_2: CO. To ensure the process is sustainable, the syngas would also need to be generated in a large enough quantity and biomass plant material is considered a very good feedstock partly for these reasons (they generate good quality syngas in sufficient

quantity (32,53), with low NOx and SOx levels). However, biomass still has many challenges with tar removal and high alkali content causes problems with slag production and fouling of equipment (53,58,70). This feedstock is often grown and sold purposely for this process, replenishment of crops for this purpose is considered carbon neutral as the net growth of atmospheric carbon is not altered, in fact carbon may be sequestered (biochar generation in pyrolysis) and therefore considered more environmentally friendly. The recycling of problematic waste streams which include contaminated land with petroleum waste and secondary treated municipal sludge cake could in fact be a friendlier alternative to conventional deposition. To understand the potential differences in impurities from each sample type, it is prudent to understand the chemical makeup of the feedstock.

Energy source	Calorific value	Power output
Wood	18-20 MJ/kg	5 kWh/kg
Wood gas (syngas)	5.4 MJ/m^3	1.5 kWh/m^3
LPG	24.55 MJ/kg	6.82 kWh/kg
Natural gas	36 MJ/kg	10 kWh/kg
Coal	27.6 MJ/kg	7.67 kWh/kg
Kerosene	38.6 MJ/L	10.7 kWh/L
FT fuels	10-43 MJ/L	2.8-12 kWh/L
Methanol	19.93 MJ/L	5.54 MJ/L

Table 1.2 A table showing typical calorific values and power output of common fuels adapted from Krajnc (2015)(73).

1.4.1 Biomass (wood).

Biomass is an organic (plant) material, such as wood or grass, which can be used as a renewable fuel in the generation of electricity. Energy is derived from solar energy, captured and stored as chemical energy by photosynthesis at around 4000 EJ/year (53). Biomass is comprised of three major components; lignin, cellulose, and hemicellulose (15,19,53). Cellulose is a high molecular weight (≥10^6) linear polymer of D-glucose (β-(1-4)-glucopyranose) molecules of 200-400 residues, which form long chains that interact through hydrogen bonding and twist to make ribbon like microfibrils that are resistant to hydrolysis (15,74). This provides structural support

to the plant (15,74) and constitutes about 40-50 % of the mass of wood. Hemicellulose however, is a branched amorphous polymer of different sugar molecules, typically containing 5 and 6 carbon rings (53,55,75) such as glucose, galactose, xylose, mannose, and arabinose (15). Hemicellulose has lower molecular weight than cellulose and is comprised of approximately ~150 repeating units (15). Like cellulose, hemicellulose aids in providing support to the cell wall (15,55,75) and is the second major component of biomass, accounting for 28 % weight (wt.) of soft wood and up to 35 % wt. of hardwood (15). Lignin accounts for 10-30 % wt. of wood (15,76,77) although unlike cellulose and hemicellulose, it is not comprised of sugar molecules but is a large highly aromatic macromolecule, that is highly cross-linked and amorphous (15,76,77). Lignin is generally associated with the vascular parts of the plant, acting as a binder for cellulose and assisting in the protection against microbial and fungal destruction (15). The chemical composition of lignin is varied but mainly consists of three monomers of phenylpropane; p-coumaryl alcohol, coniferyl alcohol, and sinapyl alcohol (15,34,76,77). For example, guaiacyl lignin, found in softwood, is comprised of mainly of polymers of coniferyl phenylpropane (15) while guaiacyl-syringyl lignin, in hardwood, is comprised of co-polymers of coniferyl and sinapyl phenylpropane (15,76). A minor component if biomass includes the extractives comprised of a mixture of volatile alkaloids (terpenoid compounds) (78). They have varied chemical structures and are generated by plants as natural defence against micro-organisms. There are three classes of terpenes extractives; mono-terpenes, sesquiterpenes and diterpenes (34,78). The table 1.3 below shows some of the common terpenoids found in extractives:

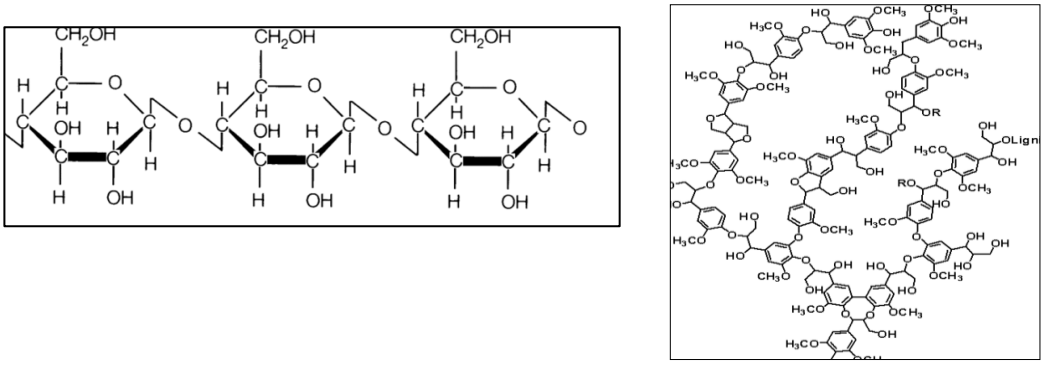

Figure. 1.6 Figure demonstrating the main polymers within biomass. Left is the chemical structure of cellulose, and to the right is lignin. Both structures have a high carbon and oxygen content; cellulose is made from repeating D-Glucose molecules bonded while lignin is composed of methoxylated phenol groups.

Class	**Examples of Terpenoid compounds**
Mono- Terpenes	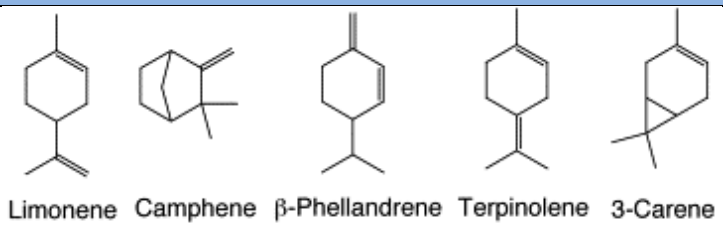
Sesquiterpenes	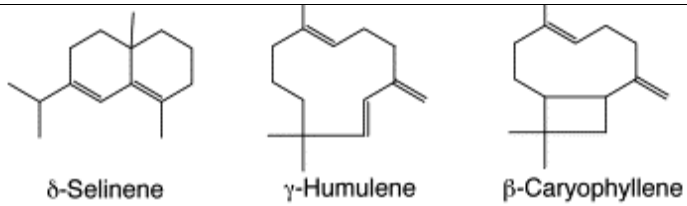
Diterpenes	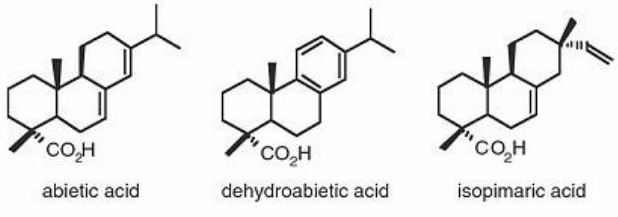

Table 1.3 Examples of common class of terpenes and their structure usually found in extractives.

The high oxygen and carbon content of cellulose, hemicellulose, lignin and the extractives result in biomass being an ideal feedstock for pyrolysis and gasification, generating the appropriate gases (CO and hydrogen) needed for diesel production.

Despite a lower calorific value (CV) to other common fuels (coal and other petroleum derived fuels), 5.4 MJ/$m^3$of syngas, this is deemed a viable feedstock due to the relatively high amount of syngas generated from 1 kg of wood, which typically produces 2.5 m^3 of syngas, this elevates the CV to 13.5 MJ/m^3 (32) making wood a sustainable feedstock. During the thermal degradation of biomass, several thermochemical reactions take place, such as depolymerisation, fragmentation, rearrangements, and carbonisation. Given that many of the large polymeric structures within biomass (cellulose, lignin and hemicellulose) breakdown to produce a wide range of organic impurities (tars) (34), that consist of heterocyclic, light aromatic, light polyaromatic and heavy polyaromatic substances of molecular masses typically greater than 78 Da (i.e. benzene). Their formation follows a temperature dependent pathway, with oxygenated species and heavy aromatics observed at low and high temperatures, respectively (see figure 1.8) (34). It is thought that at lower temperatures of between 300-500 ^oC, oxygen functional groups are cleaved as C-O bonds are thermally less stable than C-C bond, resulting in primary oxygenated compounds such ketones and furfurals (34,74). Higher temperatures between 700-850 ^oC can cause primary reaction products to undergo further, secondary reactions (34); giving rise to the lighter PAHs, heterocyclic ethers, and aromatics (15,34). Of the components of biomass, it is understood that thermal degradation of cellulose occurs at temperatures above 300 ^oC and contributes to furfurals (an aldehydic furan), hydroxyacetaldehydes, ketones and oligo-sugars (34,74) (see figure 1.8)

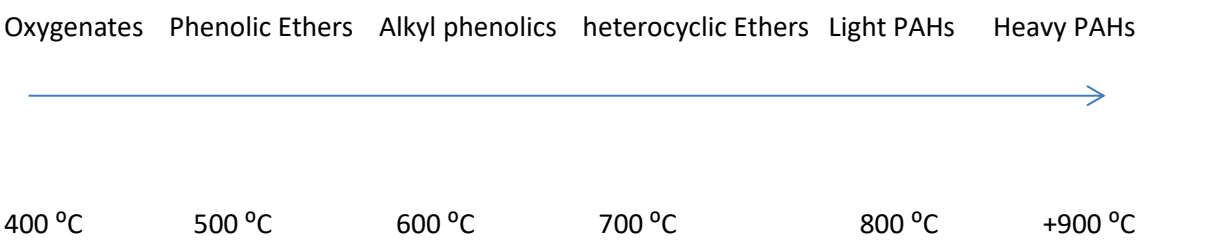

Figure 1.7 A diagram illustrating the generation of various classes of tars with temperature.

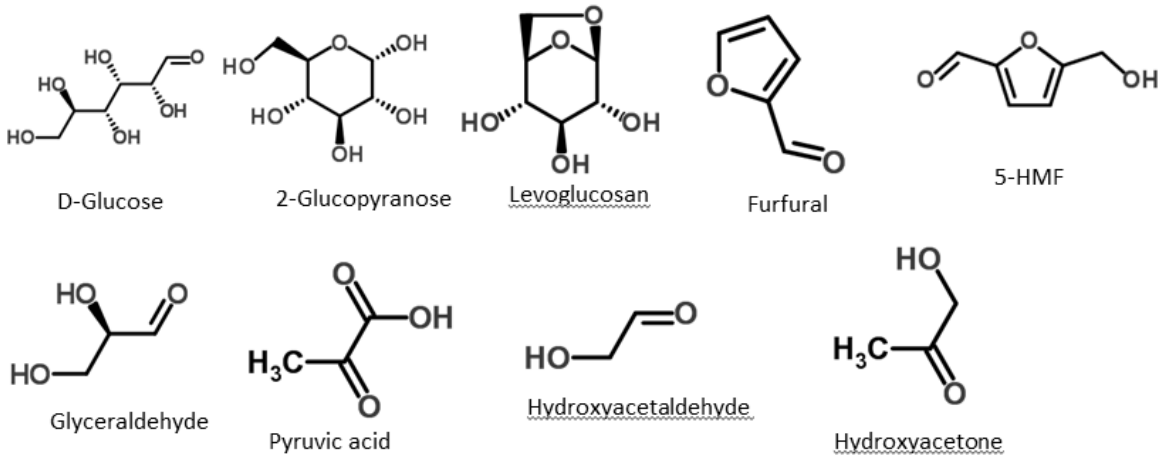

Figure 1.8 Chemical structure of glucose, glucopyranose, and common compounds found in bio-oils.

At lower temperatures (200-300 °C) Shen and Gul 2009, proposed that dehydrogenation of the cross-links of cellulose occurs producing anhydrocellulose or active cellulose. From this there are two possible decomposition pathways for anhydrocellulose, forming char and gases, and secondly, tars and condensable organics. The lower temperature is also thought to generate higher amounts of char, through the carbonisation of cellulose by the rearrangement, dehydrogenation and cross-linking reactions to form a highly irregular aromatic structure. Tars and condensable oils are likely to occur at higher temperatures 300 °C+ through the cleavage of the β 1, 4 glycosidic bond by acetal reaction at position C1 and C6 of the cellulose unit, producing a hydroxyl radical at position C6. The free radical disrupts the C4 bond to form levoglucosan, the main component of bio-oil, and may also undergo further rearrangements forming other

degradation products such as furfural, glyceraldehyde, pyruvic acid and hydroxyl acetone. Other compounds resulting from cellulose degradation include isomers of levoglucosan, anhydro-D-mannose and 1,6 anhydrofuranos, although these are of relatively low abundance verses the primary products described earlier.

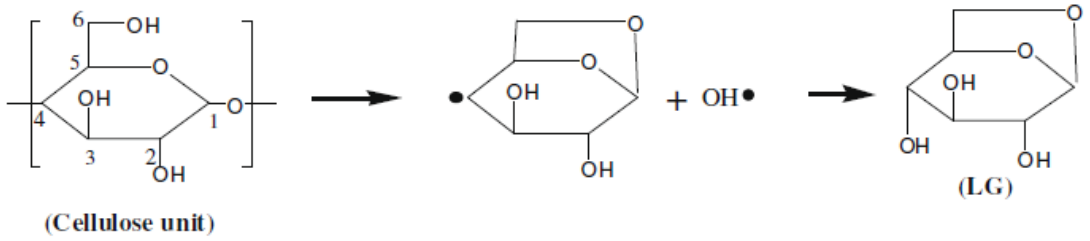

Figure 1.9: This illustrates the proposed mechanism for the formation of Levoglucosan from acetal reaction at position C1 on cellulose monomer; this produces hydroxyl radical which reacts at position C4. This was adapted from Shen and Gu 2009.

Hemicellulose is another abundant component of biomass and is comprised of linear polysaccharides of hexose (D-glucose, galactose, mannose) and pentose (arabinose and D-xylose) (55,75), where the combinations of these monomers determine the density of the wood. For example, soft wood has mannose as the primary monomer and xylose dominates the structure in hard wood (75). Above 200 °C hemicellulose starts to decompose generating acetic acid, furans and pentose and hexose monomers (34). In hardwood, the formation of sugars such as xylosan (1,4 anhydro-D xylopyranose, dehydrated product of xylose) is attributed to the cleavage of glycosidic linkage of xylan (polysaccharide of xylose linked to arabinose). Other substances such as acetic acid and furfurals are generated formed through the elimination of active O-acetyl groups linked to xylan on the C2 position (75) and from the cleavage of the bond between oxygen and C5 position on xylan, followed by the closing of the ring between position C2 +C5 (75), respectively.

The final major component of biomass is lignin; it is a polymer of phenylpropane linked by an ether or C-C bonds (34,76,77). Thermal decomposition of lignin takes place between 200-500 ^{o}C

where at low temperatures, the loss of oxygen functional groups occurs, giving rise to low molecular weight volatiles (76,77). At higher temperatures (> 700 °C), the polymer backbone can rearrange (76) with the thermal scission of α and β alkyl-aryl bonds, resulting in depolymerisation (76,77). These breakdown products include monomeric phenols, guaiacols (o-methoxy phenol), syringol (2,6-dimethoxyphenol) and catechol (1,2 benzenediol) (76). At high temperatures, it is believed that most PAHs, benzene, and toluene arise following reactions with secondary products *via* tertiary reactions (34). However, some aromatic and polyaromatic compounds have been identified at lower temperatures and these are thought to evolve from part of the charring process. For example, at temperatures of 400 ^{o}C, alkyl and methoxy (O-CH_3) functional groups are cleaved producing aromatic radicals and this may provide an initial reaction step for the formation of PAH ring systems, typically associated with carbonisation (34).

1.4.2 Sewage Sludge Cake.

Wastewater in the UK is estimated to be generated at over 11 billion litres per day (13), treated by 9000 sewage treatment sites and generating over 1 million tons of dry solid per year (13). During treatment, the (semi-)solid material is concentrated and dewatered to form sewage sludge cake (13) and is a highly energy consuming process owing to 40 % of the operational costs (79) . Imported sludge is screened and centrifuged to form solids with a dry mass of 19%. This is heated as a disinfection stage before it is thermally hydrolysed to solubilise the majority of the solid material. The sludge is then fed into mesophilic anaerobic digesters, where the majority of the volatile material is converted into biogas (80–82) which can have a methane content up to 80 % (calorific value of 27 MJ/m^3) which and can be used to process the system (83).The remaining undigested material is then dewatered producing secondary sludge (13,80,82) which has calorific values ranging from 8-14 MJ/kg similar to low grade coal (84,85). This largely comprises of protein, lipids and carbohydrates and has a high carbon content (54,80) making up ~60 % dry mass (80) and the remaining proportion consisting of inorganic species

such as silicates, aluminates, phosphorus, and nitrates, and heavy metals that include zinc, cadmium, mercury, arsenic and copper. The composition of sludge cake is likely to vary based on location, due to differences dietary intake of the region and differences in treatment stage. To investigate this, a comparison study between a Ghanaian sample, whose diet is largely comprised of starchy foods such as maze corn and other vegetables and UK sludge cake, whose diet contains a higher fat content derived from processed foods, will be analysed. Both sludge samples have been through similar treatment stages to generate secondary sludge, but the inferior technology of Ghanaian will ultimately generate a sludge cake of different quality and composition to UK (13,86) .

1. Disposal of sludge cake is an environmental concern, with evidence to show it may contain toxic persistent organic pollutants (POPs) that can exert potential mutagenic, endocrine disrupting and genotoxic effects. These pollutants may include polyaromatic hydrocarbons (PAHs), polychlorinated biphenyls (PCBs), linear alkyl surfactants, dioxins, furans, pharmaceuticals, and pesticides (12,54,80). Recent research concerning disposal has shown that incineration can still lead to the release of harmful compounds to the environment and that sludge cake distributed on agricultural can also leach pollutants into the environment and waterways with detrimental effects on the environment and human health (12,54,80). Removal of these compounds from sludge cake prior to distribution *via* membrane treatment is not 100 % effective and is expensive. These difficulties of disposal and the high carbon and oxygen content of sludge cake make it an attractive feedstock for energy recovery such as: Advanced digestion; generates biogas from microbial (mesophilic) digestion of sludge. Used to generate electricity from combustion of the biogas. Unfortunately, only

20-30 % of the material is converted to methane. The rest of the sludge is disposed in a conventional manner (80).

2. Biofuels from microbial fermentation; methanol, ethanol and various organic solvents can be generated from microbial fermentation of sludge. The sludge requires preparation, such as microwave digestion, and hydrolysis to solubilise the solid material. The extraction of solvents is very complicated and is not a promising means of generating fuels (13,80).

3. Microbial fuel cells; organic compounds are oxidised at an anode using microbes, the oxidation reactions cause the transfer of electrons to a cathode, generating electricity. The downside is the electricity generated is low, in the millivolts and bacteria are susceptible to environmental changes, i.e. pH, nutrient level etc. (80).

4. Incineration; nearly all solid material is converted to gas with oxidation of the sludge at high temperatures. This is typically used to generate electricity; however, strict emission guidance is required due to the potential release of pollutants. The ash generated will require proper disposal as it potentially contains high amounts of inorganic metals (80).

5. Pyrolysis and Gasification; an attractive alternative as it generates more useful products such as syngas (CV 5.12 MJ/m^3 in gasification)(84) biochar (CV ranges between 5-10 MJ/kg) and bio-oils (CV ranges between 23-28 MJ/kg) (85,87). Good electrical efficiencies generated from syngas combustion, biochar can be used as fertiliser and source of energy. However, there are still issue with generation of toxic tars and how these are dealt with.

Dried sewage sludge has a similar heating value to that of low-grade coal as it is comprised of many volatiles. However, unlike wood biomass, sludge cake contains a higher percentage of nitrogenous compounds derived from proteins and nucleic acids, primarily from microbes within wastewater and their thermochemical breakdown generates nitrogen containing tars (88,89). Therefore it is expected that many of the compounds will correlate with wood pyrolysis but with the addition of several nitrogen analogues (80,88); for example, light aromatics (benzene and toluene), light polyaromatics (naphthalene, phenanthrene and biphenyls), heavy polyaromatics (fluoranthene and pyrene), sulfur containing compounds (benzo(b)thiophene), and oxygen/nitrogen aromatics (benzofurane, pyrazine, phenol, pyridine, carbazole, quinoline and cyano-naphthalene) (89) The latter are thought to be formed by either by dehydrogenation of amino groups of proteins or through hydrogen cyanide addition to light aromatics, and that larger molecular weight species form at higher temperatures (89), thereby increasing the potential complexity of impurities further.

1.4.3 Hydrocarbon waste.

This is derived from industrial processes, such as crude oil refining, containing high amounts of heavy chain hydrocarbons and polyaromatic hydrocarbons (PAHs), and can exist as simple oils, emulsions or sludges and all three contain crude oil components and are differentiated by the amounts of water, oil and solid materials (90). Simple oils have low viscosity and water content, while sludges have high solid content and are more viscous due to the presence of heavy molecular weight hydrocarbons and PAHs (90–92). Emulsions can also occur with oils following high water contamination where water droplets coalesce and rise to the top of the oil, separating into two layers over time (90). Typical composition of crude oil by weight is 80% carbon, 11 % hydrogen and 1-6 % sulfur (90,92) and waste oils can therefore contain variable amounts of sulfides, phenols, heavy metals, aliphatic (i.e. saturated alkanes or paraffins), aromatic (saturated aromatic or naphthenic compounds) and unsaturated aromatic compounds

(90) and aromatic and polyaromatic hydrocarbons are known to exert ecological and human toxicity (90). These have been linked to sub chronic, reproductive and developmental effects in humans (90). The high moisture and sediment content of hydrocarbon waste make these samples no longer cost effective to refine and are currently disposed in landfill. Disposal in landfill or on brownfield sites also require years of monitoring and land remediation increasing the cost involved and is becoming increasingly untenable with limited number of sites available (92). Other methods of treating oily waste are chemical extraction and incineration however, these are only partially effective with high costs, incineration known to generate secondary pollutants such as heavy metals, NOx and SOx. Therefore, there remains a need to develop alternative methods of dealing with this waste stream that are of low cost to the environment, public health and monetary value (93).

Pyrolysis of oily sludge may offer this with low operating temperatures (460-650 °C) capable of generating lower emissions, and the recovery of 70-84 % of oil for re-use (92). Pyrolysis products from hydrocarbon waste consist of solid (56-67 %), liquid (25-32 %) and gas (7-12 %) with each product having a relatively high calorific value of 13-34 MJ/kg, 44.4-46 MJ/kg and 23.94-48.23 MJ/m^3, respectively, indicating potential as a viable secondary feedstock and energy source via this recycling approach. For example, Qin *et al. 2015* (91) demonstrated the feasibility of oil pyrolysis for recycling; 1kg of oily sludge required 2.4-2.9 MJ of energy consumption and the solid, liquid and gas products subsequently, generated 20.8 MJ, 6.32 MJ and 0.83 MJ of energy. This is significantly greater than the energy added to the process making this a potential recycling feedstock. This successful approach may be used to separate oily sludge from contaminated soil (brownfield soil), a complex waste material that is difficult to deal with. Therefore, it seems possible to separate oily sludge or hydrocarbon waste from contaminated land and recovering potentially energy rich (useful) products.

In fact, it is thought that up to 80 % of waste oil (oily sludge) may be suited to conversion into usable hydrocarbons as it contains mainly, large aliphatic alkane, alkene and branched hydrocarbons, with aromatic and polyaromatic compounds. Pyrolysis offers an approach to thermal cracking (>525 ^{o}C) these large hydrocarbons to smaller, more useful hydrocarbon materials for re-use or further recycling. (91).

1.5 Methods for analysis of products derived from pyrolysis/gasification and Fischer-Tropsch synthesis.

Given the complexities of feedstocks used in recycling processes involved in pyrolysis, gasification and FT recycling technologies, appropriate sample clean-up and analytical characterisation both in-process and of the final product are necessary to ensure the integrity of the materials. Analysis of complex samples typically require the following stages; pre-treatment, sample preparation, sample introduction into analytical instrumentation, separation (chromatography), detection and data processing.

1.5.1 Sample pre-treatment and preparation.

Pre-treatment and sample preparation is usually a physical process, involving homogenising, drying (94) or chemically altering the sample by adjusting the pH. Homogenisation achieved through stirring and sieving (similar particle size distribution) ensures sample is representative and helps release target substances physically trapped within a complex solid material. Similarly, pH adjustment of aqueous samples may also be used to help release target substances that may be chemically bound within a complex matrix. Drying can be key to analysing solid matrices; as it is often important to remove water from these samples, to reduce the water soluble interaction that may affect the efficiency of other sample preparation methods (95). Following pre-treatment, samples may undergo further preparation in the form of extraction to isolate analytes of interest or interferences (impurities). Samples can be solid, liquid or gas; for syngas,

solvent scrubbers may be used as a clean-up procedure whereby syngas is bubbled through the solvent which captures substances of a similar in polarity, extracting them from the syngas. This is based on the principle of partitioning and may also be carried out on two immiscible liquid phases, known as liquid-liquid extraction.

There are, however, a broad range of extraction methods, grouped according to matrix type:

1. Thermal desorption: gaseous analytes are retained on a sorbent tailored to the chemistry of the analytes. The analytes are desorbed on to a gas chromatography (GC) column using a desorption module (96).
2. Gas sampling devices (Tedlar ® bags or Gresham™ tubes) are containers used to collect gaseous sample under pressure and can be analysed using a gas chromatography mass spectrometer (GC-MS) with a modified autosampler using a gas sampling valve (96).
3. Ultrasonic extraction uses mechanical energy to generate a low frequency sound to disrupt the solid samples such as soil ensuring faster contact time between solvent and sample reducing extraction time considerably (96,97).
4. Soxhlet extraction can be a lengthy sample preparation process, it uses continuous flow of clean solvent set up in reflux apparatus to remove analytes from solid material. This maintains a high partitioning distribution to ensure high recoveries of analyte. (96,97).
5. Solid phase extraction (SPE) is a more common approach for liquid samples where analytes may be extracted on to a solid sorbent bed contained within a cartridge, which is conditioned prior to sample application. Analytes are retained through various interactions depending on sorbent chemistry, such as electrostatic, $\pi - \pi$ interaction or through ion exchange (94–97). The advantage over solvent (liquid-liquid) extraction is less organic solvent is required and samples are pre-concentrate in the extract (using a smaller volume of elution solvent) allowing enhanced detection limits to be achieved (95–97).

6. Headspace sampling technique enables the analysis of gaseous analytes from liquid or solid samples. The sample is placed in a sealed glass vial, whereby volatile analytes enter the gas phase or headspace above the liquid or solid surface and may be increased by heating or agitating the sample (96–99).
7. Solid phase micro-extraction (SPME) is another sampling technique used for gas or liquid analysis but uses a micro fibre with a liquid polymeric coating of similar chemistry to SPE sorbents to extract analytes from the gas (headspace) or the liquid sample directly (96,97). For analysis the SPME fibre is withdrawn into the device and then inserted into a specialist injection port of a GC or liquid chromatography (LC) inlet where retained compounds are desorbed by temperature or through elution with an appropriate solvent (96,97,99) respectively.

1.5.2 Sample analysis.

Once the sample has been prepared it needs to be introduced into the analytical detector. This is typically an automated process and often requires interfacing with a separation method for complex samples. Volatile and semi-volatile analytes such as those discussed in previous section of this chapter are separated by gas chromatography (GC) with detection by mass spectrometry (MS) or thermal conductivity (TCD). These detection methods analyse samples in real-time however, complex samples can be difficult to interpret with prior separation therefore, methods like GC, enable 'simpler' measurements to be acquired without interference, increasing the selectivity and sensitivity of the analysis.

1.5.2.1 Chromatography

Chromatography is a technique used to separated components of a mixture into discrete bands based on their distribution between a stationary and mobile (carrier) phase. Separation is successful when analytes in a mixture migrate at through the column at different rates. This is

strongly influenced by the differences in analytes interactions with the stationary phase. The longer the analyte resides in the stationary phase then the longer it takes for it to reach the end of the column and be detected. Retention time (t_R) can be described as the time it takes for an analyte to elute from a chromatographic column (100–102).

The mobile phase is typically an inert gas (helium or hydrogen) used in gas chromatography (GC) or high-pressure liquid used in liquid chromatography (LC). The mobile phase aids the motion of the components through a column containing the stationary phase where the analytes interact, either adsorbing (dissolve in) or absorbing (surface affinity) to the stationary phase (100–102). Separation is achieved according to differences in analyte chemistry, vapour pressures (GC) or affinities to the stationary and mobile phase (LC) (100–102). Both processes are reliant on the partitioning of analytes between the two phases. This is an equilibrium process of mass transfer and variations in the physiochemical properties of the analytes results in differing degrees of interaction with the stationary phase and elution rates through the column, leading to separation (100–102). This may be described using a distribution constant, K_D, and the retention time of the analyte. The distribution constant represents the partitioning behaviour of the analyte between the mobile and stationary phases whereby those that have a higher K_D value reside in the stationary phase for longer, resulting in greater retention time or retention time factor (100–102).

$$K_D = \frac{Concentration\ of\ analyte\ on\ stationary\ phase}{Concentration\ of\ analyte\ in\ mobile\ phase} \qquad \text{Equation 1.9}$$

This distribution can be represented graphically (See Figure 1.10) using an isotherm plot of concentration of analyte in mobile phase against analyte concentration in the stationary phase. Non-linear isotherms are generated if the K_D values changes with concentration to produce asymmetric peaks. For a convex isotherm, then K_D decreases with increasing concentration on the stationary phase, producing tailing peaks. If the value of K_D increases with increasing

concentration in the mobile phase, the generated isotherm is concaved, producing fronting peaks (100,103). Symmetrical peaks are generated when K_D values are independent of concentration changes and graphically shown by linear isotherm plots (100).

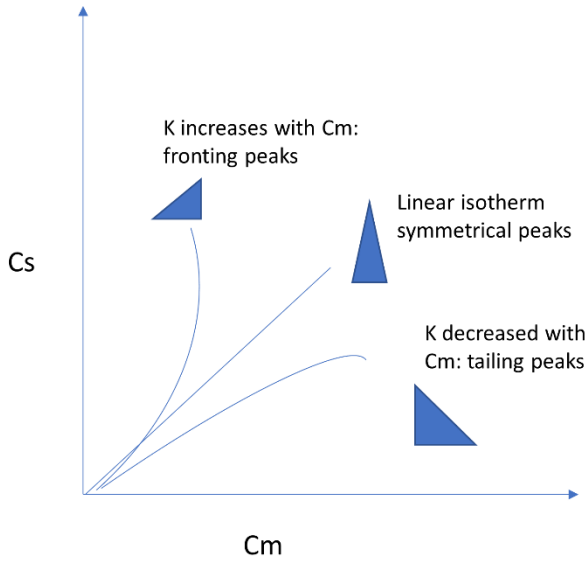

Figure 1.10 A graphical illustration of isotherm plots resulting in development of different peak shapes.

For separations by GC, analytes will elute from the stationary phase, held within a very narrow bore silica column, according to vapour pressure; where those of lower volatility (and vapour pressure) and affinity towards the stationary phase elute first. Components that have high vapour pressure and stronger affinity towards the stationary phase, requiring a greater temperature to elute from the column (100–102). Therefore, for complex mixtures a temperature gradient and choice of stationary phase are major factors influencing the selective elution of analytes. Together with stationary phase chemistry, other factors such as column length can also have an impact on the separation of analytes by GC, with longer columns typically resulting in longer retention times and greater separation capacity as shown by equation 1.13

As mentioned previously, chromatography is the separation of components of a mixture into discrete bands, with components remaining longer in the stationary phase having greater retention times (t_R). Calculation of (t_R) consists of time spent in the stationary phase ($t_{R'}$) and time spent in the mobile phase often referred to as the dead time (t_M) (see equation 1.11) (100,102). The dead time is the time taken for the analyte to transmit through the column, this value is the same for all analytes. The dead time is determined by injecting an inert component (Argon gas in GC) and measuring the time it takes to emerge. A more reproducible way to characterise retention time is to use relative retention times. This expression is termed retention factor (k) (equation 1.10) (100,102). Assuming that distribution isotherm is linear the k is equal to mass of analyte in the stationary phase and mobile phase. Therefore, higher k values mean greater retention as more solute resides in the stationary phase. Therefore, k is a measure of retention.

$$k = \frac{t_S}{t_m} \qquad \text{Equation 1.10}$$

$$t_R = t_M + t_{R'} \qquad \text{Equation 1.11}$$

$$t_R = t_M\,(1 + k) \qquad \text{Equation 1.12}$$

$$t_R = \frac{L}{u}(1 + k) \qquad \text{Equation 1.13}$$

L = column length

U = average linear velocity

K = retention time factor.

Analytes that possess the same retention time (factor) as each other, often lead to problems with compound identification and quantitation as they are detected at co-eluted peaks. The ability of a column to resolve two closely eluting peaks can be expressed by the separation factor

(α) often referred to as column selectivity (equation 1.14). This is the ratio of retention times (factors) of two adjacent peaks and the value for (α) is always greater than 1 (101,102,104).

$$\alpha = {}^{t_{R2}}/_{t_{R1}} \qquad \text{Equation 1.14}$$

The degree of separation can be calculated using resolution values (R_s) with values approaching 1.0 referring to completely resolved peaks (equation 1.15). There are two ways that resolution can be increased, one by increasing the distance between the peaks (selectivity) usually by altering oven temperature parameters or stationary phase composition secondly, by narrowing the peak widths, achieved by increasing the column efficiency (101–103). Efficiency of a column refers to the number of physical sites (plates) analytes can interact with on the column. Increasing the number of physical sites (N) increases the efficiency of the column. Efficiency is often referred Hight Equivalence Theoretical Plate (HETP) value and in chromatography, is also determined by the length (L) of column and number of plates (N) (see equation 1.16). The higher the number of plates (N) per meter is considered more efficient (lower plate height) to aid with the partitioning of the analytes (101,102). Therefore, longer columns have more sites of interaction and are deemed more efficiency and have better resolving power.

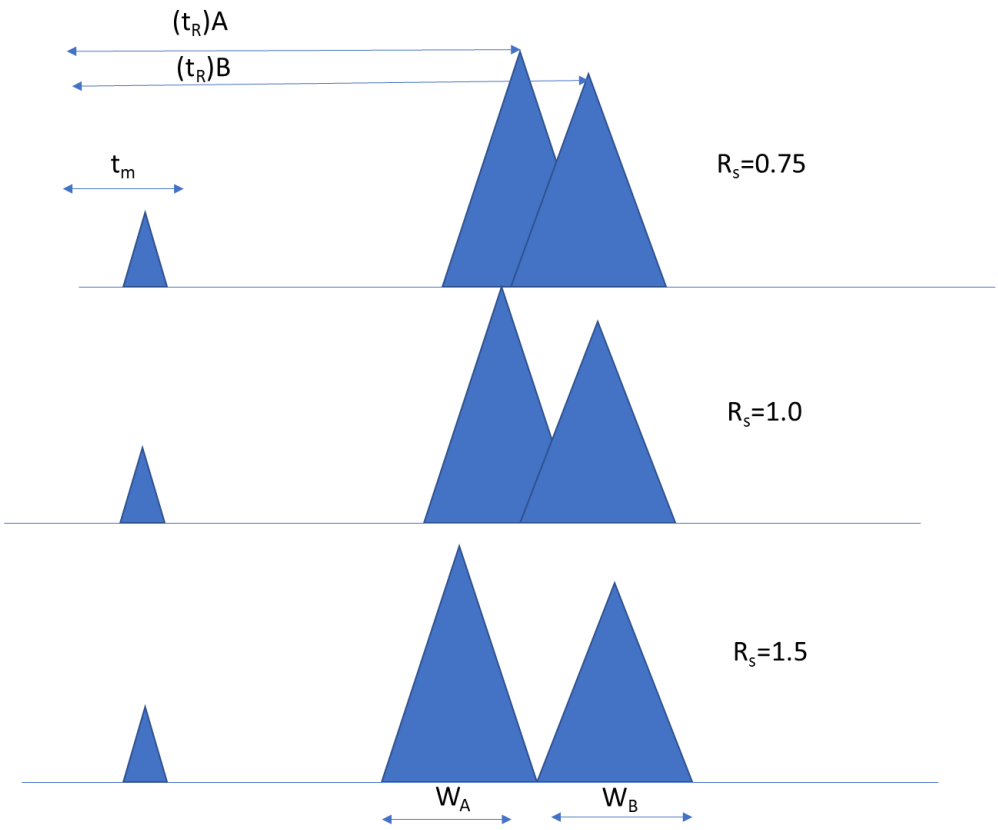

Figure 1.11. Figure shows chromatograms of unresolved sample components (R_s 0.75), those that are resolved peaks (R_s1.0) and fully resolved peaks (R_s 1.5). Equation 1.11 is used to determine resolution factor R_s. (t_R)A is retention time of first eluting component and W_A is the peak width of the first eluting component. (t_R)B is retention time of second eluting peak and W_B is the peak width of the second eluting peak.

$$R_S = \frac{(t_R)B-(t_R)A}{W_A+W_B/2} \qquad \text{Equation 1.15}$$

$$HETP = \frac{L}{N} \qquad \text{Equation 1.16}$$

The number of theoretical plates (N) may be calculated from chromatographic elution and is described using the following equation:

$$\mathrm{N} = 5.545(\mathrm{t_R}/\mathrm{W_h})^2 \qquad \text{Equation 1.17}$$

Where, w_h is the peak width at half-height and t_R is the retention time.

Additional factors that can affect the migration of an analyte down a chromatographic column have been expressed by the Van Deemter equation and describes the relationship between analyte behaviour on column, to column length and mobile phase linear velocity. Gas flow (mobile phase) can also affect chromatography, as retention time is inversely proportional to average linear velocity (100–102). A slower flow rate increases the retention time on column affecting the resolving power (resolution) of the separation by affecting the peak shape (broader peaks). Equally a flow rate that is to high is also a problem as analytes do not interact sufficiently with the stationary phase resulting in limited or no separation is achieved and therefore, a balance needs to be struck between these and other parameters to achieve separation (100–102). The Van Deemter equation describes efficiency as a relationship in terms of Height Equivalence to a Theoretical Plate (HETP). This takes into consideration of a number of parameters, termed A, B, C and U (see equation 1.18). Thus, an optimum average linear velocity of the mobile phase exists for each column. Therefore, column flow and carrier gas type can be selected to give the greatest column efficiency producing the narrowest peaks therefore increasing resolution.

Van Deemter Equation:

$$HETP = A + \frac{B}{U} + (Cs + Cm).u. \qquad \text{Equation 1.18}$$

HETP: Height equivalence theoretical plate

A: Eddy diffusion coefficient

B: Diffusion coefficient in longitudinal direction

C: resistance to mass transfer coefficient between stationary and mobile phase

U: Linear velocity of mobile phase

$$R_s = \frac{\sqrt{N^2}}{4} \times \left[\frac{\alpha-1}{\alpha}\right] \times \frac{K_D^2}{(K_D^2+1)}$$ Equation 1.19

Resolution can be expressed by combining the terms for column efficiency (N), selectivity (α) and retention factor (K) to produce the resolution equation (equation 1.19).

1.5.2.2 Practical considerations of GC.

For GC separations columns can be diverse and chosen to suit the needs of the analysis, varying in length, width, stationary phase composition and film thickness. For example, as GC-MS is often used for more complex samples typical dimensions of a capillary columns are 15-60 m in length with diameters of 0.15-0.32 µm (102,105) for increased efficiency and resolving power. However when coupled to thermal conductivity detectors (TCD) these tend to be shorter packed columns, 8-15 m in length, to separate relatively simple gas mixtures (105,106). Packed columns are diverse and packed with an adsorbent material (stationary phase) which can vary from diatomaceous earth (silicate), graphitized carbon, liquid deposited support or molecular sieves. The finer the particles size of the adsorbent the more efficient the column is as it increases the number of pathways for eddy diffusion currents (term A) thus slowing the internal flow rate of the column for better resolution (105). The introduction of capillary columns in the late 70s saw a decline in the use of packed columns. The development of immobilized and crosslinked supported columns soon replaced majority of packed polymeric and liquid phase columns, as crosslinked capillary columns possessed higher efficiencies (more N per meter of length), increased thermal stability and better chromatographic reproducibility (100,105). However, packed columns are still main column for applications using small molecules. For this, the stationary phased is comprised of molecular sieves (zeolites) used for separation of simple gases such as H_2, CO and O_2 (101,105). Again, fine particle sizes of the adsorbent influences efficiency by increasing the diffusion pathway of the analytes, while pore size (5-10 Å) affects column

selectivity by filtering out analytes of a certain cross-sectional area. Carbon molecular sieves are adsorbents used for separation of permanent gases (hydrocarbons with carbon numbers between C1-C3), they behave in a similar manner to zeolite molecular sieves, reliant on the selectivity based on molecular diameter of the analyte(105). However, selectivity is also governed by analyte interaction via intermolecular forces with various functional groups.

In capillary columns analyte affinity towards the stationary phase dictates the selectivity of separation intermolecular forces, such as hydrogen bonding, dispersion, induction and dipole-dipole forces, influencing the interaction between the analyte and stationary phase (102) and dependent on conformation of structure (stearic hindrance) and polarisable groups. Traditionally, the stationary phase of capillary columns was comprised of derivatised polysiloxanes however, more modern columns have changed the column chemistry by modifying the composition of the stationary phase with additional bonding and functionality such as non-polar (100 % dimethylpolysiloxane) to more polar (90 % cyanopropyl-phenyl polysiloxane) stationary phases (100,101,105). Therefore, columns can cover a polarity range to cater for different analyte chemistries, enabling greater selectivity in separation with more polar analytes (containing heteroatoms) having a stronger interaction with polar stationary phases, and non-polar analytes (e.g. hydrocarbons), showing greater retention with non-polar columns, resulting in a longer retention time (100,101). Some applications may even adopt two columns of very different polarity, to give even greater resolution. The sample is injected and separated in 2 dimensions (polar and non-polar), this technique referred to as 2D chromatography. This is a powerful technique and is used to maximise resolving power (107,108) and is used on complex samples which has the ability to separate out many co eluting compounds (107). 2D chromatography requires a specialised GC oven that can accommodate two columns, a modulator and is greatly enhanced by coupling to a pulsed mass spectrometer such as a TOF with fast acquisition rates (107,108).

In addition to column chemistry, the stationary phase 'film' thickness and column diameter can also be used to optimise the separation (109). Generally, smaller diameter columns require lower mobile phase flow rates to achieve the desired linear velocity and this decreases the phase ratio (mobile phase volume/stationary phase volume) or β term of the Van Deemeter relationship. The combination of a reduction in both flow rate and diameter gives rise to improved efficiency (providing column length remains constant) of separation with higher K_D values. However, this can lead to increased retention times (102) and a reduction in diameter also lowers the column loading capacity resulting in limited tolerance for uncharacterised samples whereby the concentration is unknown and greater risk of column overloading, leading to peak broadening and co-elution. However, this may be overcome by choosing an appropriate stationary phase 'film' thickness with a thicker stationary phase (of greater volume) enabling higher loading capacities (102). However, this can lead to increased retention times due to a greater volume of stationary phase for the analyte to desorb from for elution and so (102) thicker films are typically used for more volatile compounds to increase their retention on column.

1.5.2.3 Gas chromatography-thermal conductivity detection (GC-TCD).

Gas chromatography-thermal conductivity detection (GC-TCD) is a non-selective and non-destructive analytical method, suitable for a range of inorganic gases such as hydrogen, carbon monoxide, sulfur dioxide. It can be used to monitor small organic compounds but typical sensitivity is less than alternative techniques, including flame ionisation detectors (FID) and GC-MS (106,110,111). Simple gases, such as CO, H_2, CH_4, acetylene and ethylene, can be analyse on GC-MS but the instrument would require modification for the introduction of specialised sampling valves due to poor portability (samples would need to be collected and later injected on to the instrument) of instrumentation and a column that is selective for separation of permanent gases such as a fused silica CP-PoraPLOT Q-HT column (112). While GC-FID is

incompatible with inorganic gases, such as $H_{2,}O_2$ CO_2 and CO. FID relies on detection of ions generated from the combustion of the analyte in a hydrogen flame (111). The ions are detected by ions striking a negative electrode which generates a current and is plotted as a peak (picoamps), the area under the peak is directly proportional to the concentration of analyte, and typically works well with organic species with little or no heteroatoms (111).

To ensure separation and detection of simple gases, columns tightly packed with particles of aluminium silicate to increase their retentive character allowing suitable time for detection. These particles increase the number of flow paths that the mobile phase (argon or nitrogen) and analytes must follow (106), increasing the retention time and peak width so that it may be captured by the detector. As the analysis is primarily concerning simple gases packed columns typically use an isothermal (constant temperature) separation determined by the particle size and shape (106,109). Therefore, for the analysis of simple gases in syngas, a packed column using GC-TCD is preferred as the sample will contain mainly CO, H_2 and CH_4.

Thermal conductivity detection operates by measuring the difference in thermal conductivity of a reference channel (mobile phase carrier gas) and effluent flow (mobile phase carrier gas and analyte) using a heated resistance wire commonly consisting of four tungsten filaments incorporated in a Wheatstone bridge. The difference in conductivity produces a voltage signal proportional to the concentration of analytes in the mobile phase enabling, TCD to be used as a concentration dependant detector (106). As this signal does not discriminate between different gases within a mixture, separation, in the form of gas chromatography, is necessary to selectively measure each component. Therefore, reference gases representing those expected in the mixture (syngas) must be analysed prior to an uncharacterised mixture to identify the individual gases according to retention time. The proportions (or concentration) of these individual gases can then be determined using a calibration standard approach and the chromatographic peak area for each component.

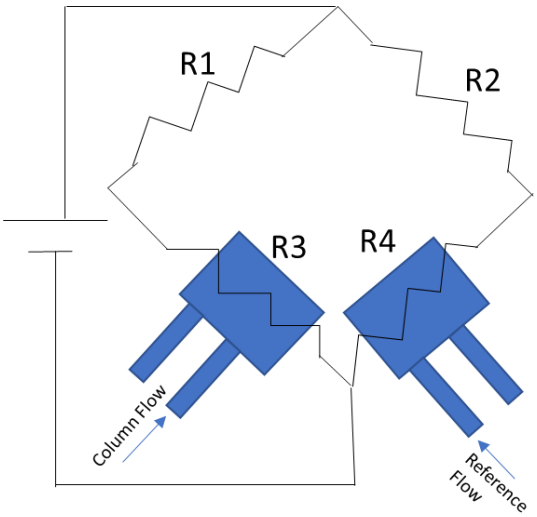

Figure 1.12 diagramatic representation of TCD detector.

1.5.3 Gas chromatography-mass spectrometry (GC-MS).

This approach involves coupling gas chromatography with a mass selective detector or mass spectrometer. Like GC-TCD, GC-MS is capable of analysing gaseous mixtures however, due to the enhanced selectivity of detection by mass it is often used for more complex mixtures and larger volatile organic species. However, like TCD, mass spectrometry also requires separation to enhance this selectivity enabling the analysis of highly complex mixtures such as fuels. This method is therefore operated using a column temperature gradient (60-300 °C) to elute analytes from the column, offering greater selectivity of separation for a broader range of analyte volatilities. Given this, GC-MS systems may analyse both gaseous and volatile liquid samples where samples may be introduced using a gas-tight syringe into a heated inlet by piercing a septum. The sample is then vaporised before being swept on to the GC capillary column using the carrier gas (102). Following separation, analytes are introduced into the mass spectrometer using a heated transfer line to maintain the analyte separation and vaporisation states where they are ionised and detected according to their mass to charge ratio (*m/z*) (113,114) and represented as a mass spectrum.

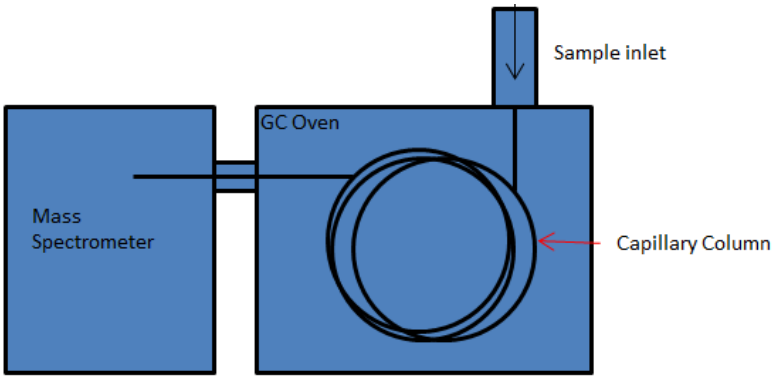

Figure 1.13. A typical GC-MS.

The sample inlet comprises of narrow heated stainless-steel tube, which houses a glass liner of fixed volume (split/ spitless). On column flow is directed over the glass liner and some is diverted to septum purge or split vent. The septum purge ensures a constant flow of carrier gas below the septum removes any analyte that may be adsorbed reducing potential carry over. The split valve can adjust via the software reduce the amount of sample that goes on to column, by diverting some to the split vent Once the sample is injected, the inlet is either maintained at a high temperature or the temperature is ramped rapidly using a heating element to vaporise the sample. Sample injection is typically carried out using an autosampler for qualitative work to ensure reproducibility of sample injections. Within this system, injection modes may include full sample volume ('splitless') or a partial volume ('split') being introduced on column. Typical injection volumes are 1-10 µL and the injection mode chosen according to the vapour pressure of the sample, size of the liner and concentration of analytes/interferences (102,113). For example 'split' injection mode are often used for concentrated or uncharacterised samples where the concentration is unknown to limit overloading the column that may lead to carryover on successive injections thereby, aiming to prolong the lifetime of the column, mass spectrometer filament and detector (102). Once the sample is vaporised, it is mixed with flow gases such as helium or hydrogen and enters the capillary column for separation prior ionisation and analysis within the mass spectrometer.

1.5.3.1 Sample ionisation: Electron ionisation.

The emerging gaseous analytes from the GC column, enter the mass spectrometer through an orifice known at the transfer line and are ionised in a region known as the source, before being transmitted into the mass analyser (113,115). In GC-MS the standard ionisation technique is electron ionisation which operates under vacuum pressure and is suited to volatile gas phase molecules. In the source the analytes are bombardment with a high energy electron (70 eV), emitted from a heated filament of tungsten or ruthenium (113,115). The emitted electrons are directed at the analytes through an attraction to a metal plate of opposing (positive) electrical potential, known as the positive lens plate (113,114,116), with the space between the filament and positive lens plate the site of analyte introduction from the GC column (114).

The emitted electron has a corresponding wavelength ʎ and is described by equation 1.20.

$$ʎ = \frac{h}{mv} \qquad \text{Equation 1.20}$$

Where *m* is the mass, *v* is velocity and *h* is Planks constant (113). If the electron frequency *hv* corresponds to a transition state within a molecule, then energy transfer can lead to electronic excitation. When the energy supplied is greater than the ionisation energy (Ei) (7-15 eV), an electron can be expelled from the molecule forming a positively charged radical molecular ion ($M^{\bullet+}$). The probability of an electron interacting with a molecule is significantly reduced at low ionisation energies. To increase the efficiency of ionisation the electron energy is increased (113,115) by applying a greater voltage across the filament. Plotting ionisation efficiency for a given analyte with electron energy, generally produces a curve that reaches a general plateau region between ~50 and 70 eV (see figure 1.13 right curve) used as any drift in this value will still mean on the plateau region. The emitted electron at 70 eV covers a wide range of bond lengths ensuring ionisation for multitude of compounds. For organic molecules the maximum bond length is wide so even small changes to electron energy does not significantly alter the

pattern of the mass spectrum (113,115). Typically, a value of electron energy between 60-80 eV produces highly reproducible spectra (113,115). For this reason, 70 eV was adopted as the standard ionisation energy allowing spectra to be accurately compared against data bases. At 70 eV the energy transfer leads to ionisation and approximately 1 in every 1000 molecules entering the source is ionised (113,114)

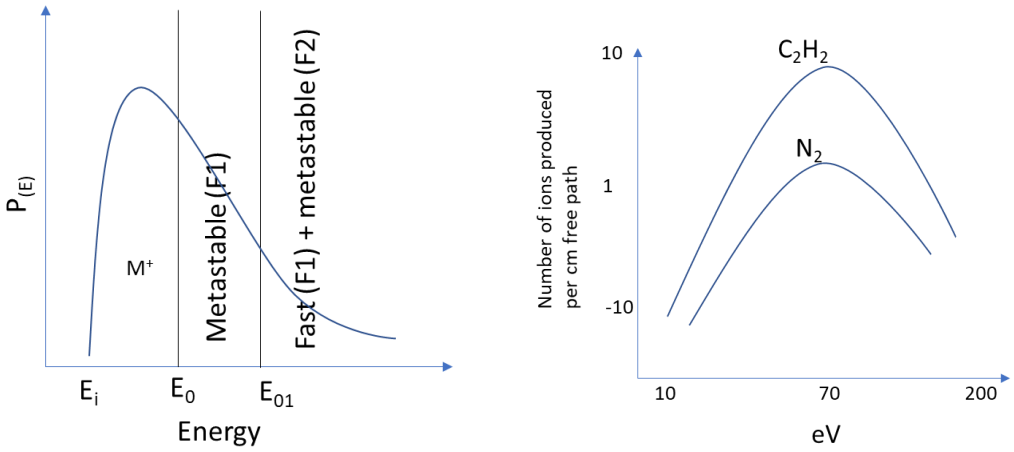

Figure 1.14 shows an energy curve associate with ionisation (left) and plot of number of ions produced with kinetic energy of the emitted electron (right)

As mentioned previously, for ionisation to occur, the accelerated electron needs to interact with the molecule with enough energy to overcome the ionisation energy (Ei) barrier (appearance of the molecular ion) (115). For fragmentation to proceed, enough electronic energy must be converted to vibrational energy. Increasing the electron energy above the dissociate energy activation barrier (E_0) raises the probability of vertical transition states and favours the formation of ions possessing higher internal energy (113). Generally, these ions fragment on return to ground state but are often undetectable as their rates of formation is comparably slow. To observe these fragments excess energy is used (70 eV) to overcome the energy barrier E_{01} (113). These fragment ions as generated kinetically faster and are more likely to be observed. The overall timescale from ion generation to detection occurs between 10-50 µS (see figure

1.14) (115). The initial electron ionisation occurs extremely fast ($2x10^{-16}$S), and typically ion resides in the source for enough time for fragmentation to occur (1 µS), before the ions are ejected by the action of the accelerating potential.

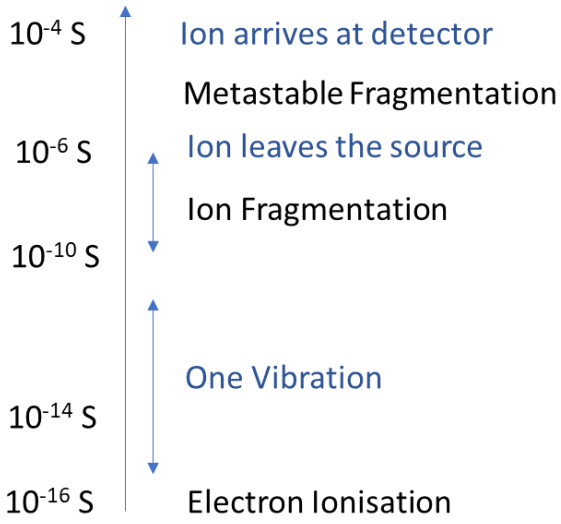

Figure 1.15 is a diagrammatic representation of the events and timescale of EI.

To overcome this fragmentation, the EI source can be modified introducing a reagent gas, such as ammonia, methane or isobutane (113). The high abundance of reagent gas versus the sample analyte molecules, will preferentially be ionised resulting in a reagent gas mixture comprising mainly of primary ions and radicals. These primary ions react with the analyte through secondary ionisation to produce intact precursor and adduct ions; through addition of a proton $[M+H]^+$, adduct formation with cations $[M+CH_3]^+$, or through loss of a proton $[M-H]^-$ or hydride ion via abstraction $[M-H]^+$. Electron capture of low energy thermal electrons generated in the reagent gas can also generate negative molecular ions $M^{-\bullet}$ (113). Chemical ionisation (CI) process generates fewer fragment ions due to the lowered energy of secondary ionisation (fewer ions excited above the dissociative level) and its common for the precursor/adduct ion to be the dominant species. CI is therefore, considered a softer ionisation technique (113,116). If methane was introduced into the source as the reagent gas, the primary reactions will be

identical to standard EI. The generation of methane cation from the expulsion of a molecular electron will generate an odd electron precursor (molecular) ion, $CH_4^{\bullet+}$ (113,115). The ion will fragment through two pathways generating an odd electron and eleven electron fragment ions ($CH_2^{+\bullet}$ and CH_3^+). These will most likely collide with other methane molecules to generate CH_5^+ (113,115) .

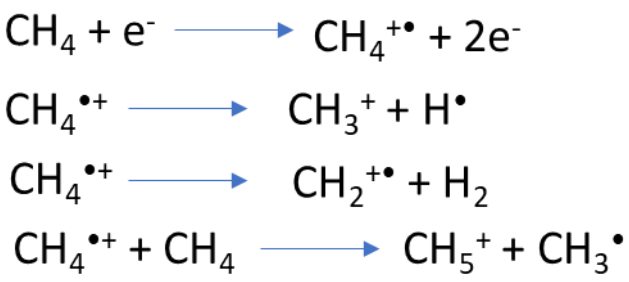

Figure 1.16 shows the reactions associated with primary ionisation of methane reagent gas.

There are other successive gas phase reactions, but for simplification, the following will focus in the reaction of CH_5^+ with the analyte molecule. Most analytes containing heteroatoms will gain a proton in an acid-base reaction generating $[M+H]^+$ (113). For polar molecules adduct formation is observed $[M+CH_3]^+$, but for molecules with no heteroatoms such as unsaturated hydrocarbons, these experience hydride extraction generating an even electron ion (M^+) and a molecule (H_2) (113).

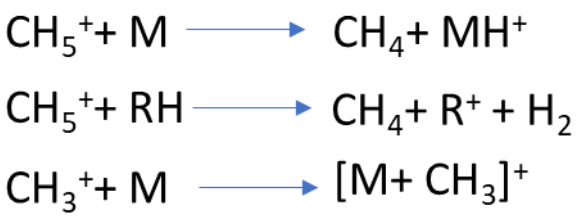

Figure 1.17 shows the typical secondary ionisation reaction during CI with analyte molecule.

1.5.3.2 Mass analysis and ion detection: the single quadrupole mass analyser and electron multiplier detector

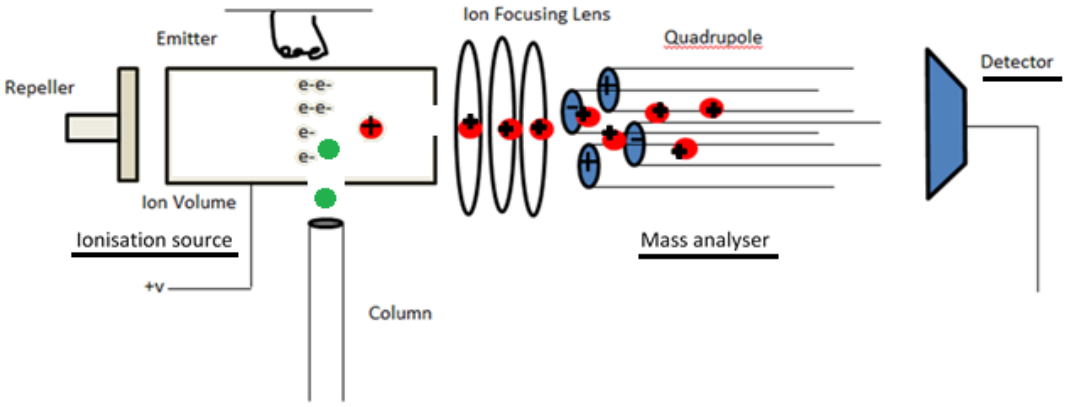

Figure 1.18: A typical single quadrupole mass spectrometer with EI source.

Once ions are formed (in EI and CI) in the electron free region they are directed into the mass analyser using a repeller plate (held at opposing potential) and ion focusing lens. The focused ions are then separated according to their mass/ charge ratio in the analyser which are recorded using specialised detectors.

The majority of bench-top GC-MS instrumentation used in rapid trace quantitative work incorporates a quadrupole mass analyser as it can scan different masses quickly, necessary for GC data recording, and it is robust. This consists of a set of four hyperbolic metallic rods, with each pair of rods having an opposing electrical polarity from a (113,115) radio frequency (RF)/direct current (DC) voltage applied the pair of rods. This voltage is oscillated between the pair of rods and specific voltage corresponds to the stable trajectory of an ion of particular mass: charge ratio (*m/z)*. Those with a stable trajectory successfully travel through the analyser to the detector while those ions of different *m/z* escape through the sides of the quadrupole or discharged on the quadrupole surface and are undetected (113). To generate a mass spectrum containing multiple *m/z,* the Rf/dc voltage is ramped or 'scanned' sequentially directing ions of

specific *m/z* to the detector. There are several classes of detectors and can be differentiated as to how they collect data; ion bombardment to generate electrons (electron multiplier), ion collection (Faraday cup) or by monitoring the frequency of ion motion (Fourier transform methods using ion detection plates recording an image current) (113,115). These detectors are suited to different types of mass analyser and their application. Quadrupole analysers are commonly used with an electron multiplier where ions from the mass analyser strike the surface of the detector, emitting secondary electrons which are amplified through successive collisions with the detector surface in a cascade effect producing a current which is then converted to a signal recorded as a mass spectrum. Typically, the mass analyser is calibrated against a known compound such as perfluorotributyl-amine using an automated tuning programme. This programme adjusts the source and analyser settings to optimise for the best response of ions spanning the mass range (*m/z* 69, 219, 502).

1.5.3.3 Typical GC-MS operation modes and data handling for quantitation.

When combined with chromatography, mass spectra (full mass scan) of precursor (and fragment) species for a relatively wide *m/z* range may be recorded with time and represented as a mass spectrum. These mass spectra can show the increase in relative abundance of ion(s) observed by the mass spectrometer with time and represented as a chromatogram for an individual *m/z* if required, known as an extracted total ion current chromatogram (EICC). However, sensitivity of data for an individual *m/z* may be enhanced by removing excess noise recorded with this full mass scan and focusing the main analyser to a particular *m/z*. This mode of operation is known as single ion monitoring (SIM), this provides data with improved signal to noise (S/N) due to greater data acquisition times, enabling lower amounts of ion signal to be detected and therefore, achieving greater sensitivity for trace quantitation.

To process data for analyte quantitation, the sum of the signal attributed by the analyte (all mass spectra of relevant *m/z)* may be used. This is typically represented by the integrated peak area of the ion chromatogram of the applicable *m/z* and will correlate to the amount of analyte introduced into the mass spectrometer providing the detector is not saturated. This relationship may be used to determine the quantity of an analyte by calibrating the signal response using standard samples containing known amounts of analyte. For example, reference calibration standards of known concentration, representing the relationship between response and concentration, are analysed and the integrated peak areas plotted versus concentration as a calibration graph (curve). Using regression statistics, the linearity of the relationship between response and concentration may then be used to determine concentrations of unknowns. To understand how suitable the calibration graph is for quantitation, performance of the calibration graph maybe evaluated using samples of known concentrations or quality control (QCs) samples. This evaluation enables the accuracy (closeness of the result to the expected value) and precision (how repeatable is the result) of quantified values to be determined (113). However, this accuracy and precision can often be poor with increasing sample complexity due to co-eluting analytes that can 'interfere' with the signal response generated by the mass spectrometer. A method of mitigating this is to normalise the analyte response by comparing with an analyte of known and constant concentration (internal standard). This internal standard should be an analyte of similar chemistry to ensure fluctuations observed in the signal response are closely replicated and monitored. The gold standard approach is to use a stable isotope labelled analogue of the analyte, with those most common being deuterium (^{2}H), carbon (^{13}C) and nitrogen (^{15}N), that differ in *m/z* to provide sufficient mass selectivity for detection but very similar chromatographic behaviour. The internal standard should therefore be added to all standards used in the calibration graph, quality controls and unknown samples, and at the same concentration. To plot the calibration graph, the normalised response or peak area ratio to

internal standard is plotted against concentration and regression statistics determined as before.

1.5.3.4 Electron ionisation spectral interpretation: ion fragmentation.

During EI, radical cations with an odd number of electrons are generated as precursor ion species (113,114). Excess energy from the high energy electron (used to ensure greater ionisation efficiency) usually induces fragmentation of the precursor ion through randomization of excess internal energy (113–115). Ionisation at 70 eV, is considered highly reproducible and little to no differences in peak ratios can be seen around 60-80 eV (115). Fragmentation of the molecular ion results in the formation of ions with an even number electrons or a radical fragment ion of an odd number of electrons (see figure 1.20) (113,114).

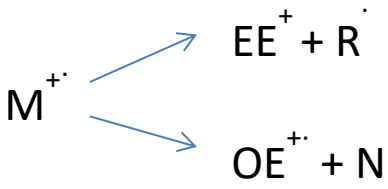

Figure 1.19 Figure shows two potential fragmentation pathways a molecular ion can undertake, either to produce an even electron species and radical or odd electron species with a neutral molecule.

Fragmentation of a molecular ion can take place by single bond cleavages, such as a homolytic or heterolytic cleavage, or through rearrangement of bonds (113–115). Understanding these fragmentation mechanisms can aid in the identification and explanation of the data observed in EI for organic molecules amenable by GC-MS. The location of cleavage is driven by a principle of charge site localisation; the charge resides on the fragment with the lowest internal (ionisation) energy, favouring the formation of stable ions. In EI the charge site is most likely to reside on the heteroatom as they have a pair of non-bonding electrons, capable of losing an electron during EI with lower ionisation energy (113).

A homolytic cleavage, sometimes referred as alpha (α) cleavage involves the cleavage of the C-C bond adjacent to the heteroatom. The carbon directly attached to the heteroatom is referred to as the alpha atom (114). Homolytic cleavage always forms an ion and a radical. Loss of a single electron from the non-bonding pair of the heteroatom or pi (π) bond forms a radical site with an odd number of electrons (114). The radical site initiates the transfer of a single electron (represented by a single fishhook on diagrams) from the C-C bond adjacent to the radical site (α atom) causing the formation of an additional bond with the heteroatom. Consequently, the alpha bond is cleaved (113,114) and the charge remains associated with the heteroatom (113,114).

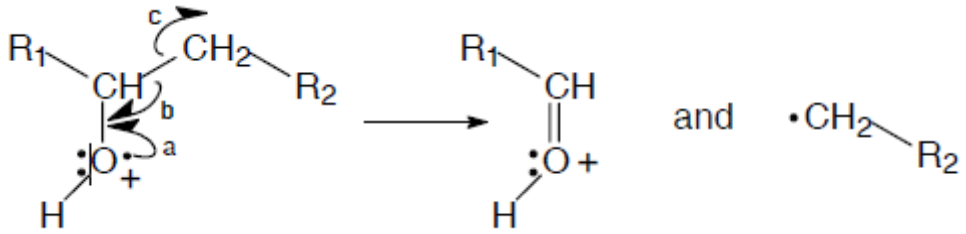

Figure 1.20. A diagrammatic representation of homolytic cleavage. Movement of single electron is shown by a half hook arrow (Watson and Sparkman 2007)(114).

Heterolytic cleavage, also referred to as charge site induced cleavage involves the movement of a pair of electrons from the bond to the charge site (113,114). The charge site is stimulated by a loss of an electron from a heteroatom (or π bond) with the highest energy level (electron furthest away from the nucleus). The positive charge on an ion creates an inductive effect that drawing both electrons from an adjacent bond causing dissociation of the bond and neutralisation of the original charge site, forming a radical and an even electron ion (see Figure 1.22) (113,114).

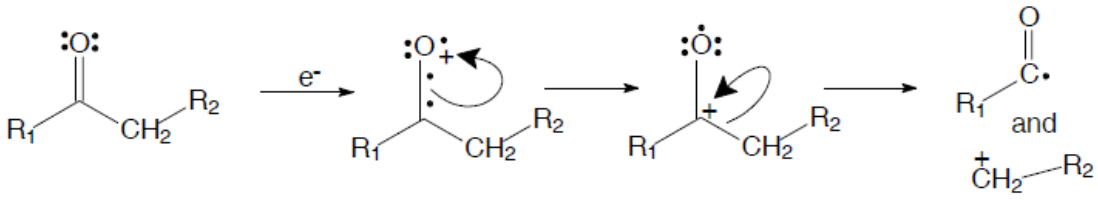

Figure 1.21. Figure showing a diagrammatic representation of charge site driven cleavage. Movement of a pair of electrons is shown with a double headed fishhook (Watson and Sparkman, 2007).

A sigma (σ) bond cleavage involves the loss of an electron from a σ bond such as a C-H or C-C and is typical in EI fragmentation of saturated hydrocarbons (114). Unlike charge sites associated with heteroatoms or π bonds, those in saturated hydrocarbons resulting from a σ bond can migrate throughout the molecular ion $M^{+\bullet}$, making the charge site highly mobile and difficult to predict leading to cleavage at any point along the C-C backbone (114). For saturated hydrocarbons this results in EI mass spectra dominated by primary carbenium ions (in particular C2, C3, C4 and C5) separated by 14 *m/z* units (113,114), and is described by Stevenson's rule; 'in competing fragmentations the product ion formed from its neutral species counterpart with the lower ionisation energy will usually be the more abundant.' Therefore, for saturated hydrocarbons the loss of the largest alkyl radical is often observed and the spectrum is dominated by low molecular fragment ions which are more stable (114,115).

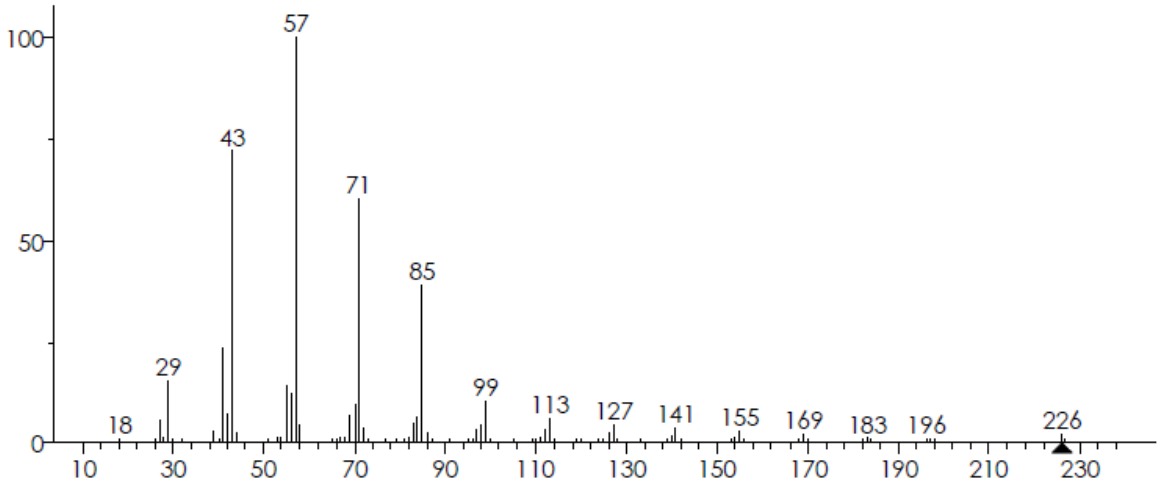

Figure 1.22 A mass spectrum of hexadecane (Watson and Sparkman, 2007).

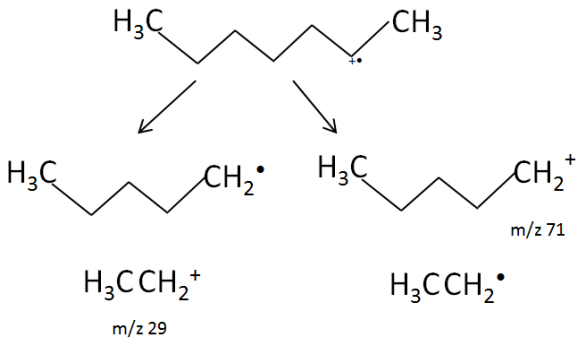

Figure 1.23. Sigma bond cleavage of heptane.

In addition to the simple cleavages described above, fragmentation can involve the rearrangement of the structure, involving the transfer of atoms and bonding electrons, to stabilise the structure, with eventual bond cleavage. For example, McLaffety rearrangements consist of a transfer of an H atom to a radical site using a six-atom ring intermediate (113,114). The rearrangement is followed by either a radical or charge site induced fragmentation, yielding a neutral molecule and radical cation (113,114).

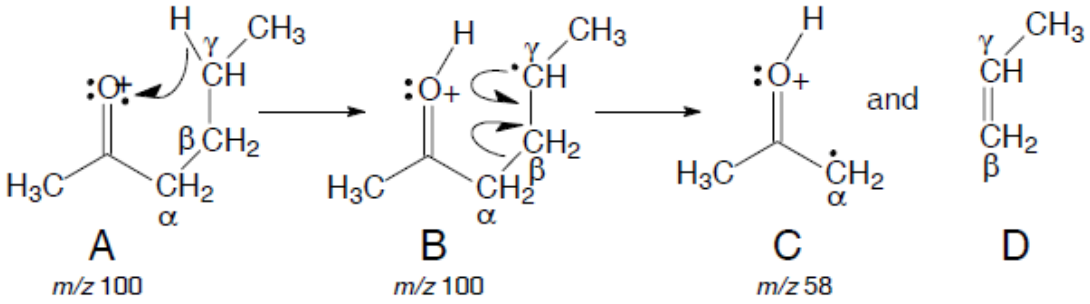

Figure 1.24. A diagrammatic representation of McLaffety rearrangements.

1.6. Research aims and hypothesis.

Pyrolysis and gasification are two alternative ways to recycle high carbon waste, and these methods use thermal energy in a controlled environment to produce a flammable gas termed syngas, bio-oil and solid biochar (pyrolysis only). However, the recycling process is not 100% efficient and generation of organic impurities known as tars are an additional potential source of chemical waste that may vary with uncharactised feedstocks. Tars can be a mixture of light aromatic, polyaromatic, heterocyclic organic compounds.These require removal as they can present potential health problems if they enter the environment and can foul downstream processes including catalytic secondary routes such as the Fischer-Tropsch process, leading to increased operational costs. Identification of these gaseous compounds requires specific sampling techniques that involves trapping into a vessel or onto a sorbent which is then typically analysed GC-MS. However, introduction of gases to GC-MS requires instrument modification, additional modules to accommodate gas sampling valves and desorption tubes, which can expensive (96). Alternative impurity capture methods may include solvent traps (scrubbers), such as methanol and water, however, these have shown limited recoveries for the compounds mentioned above. It is proposed that an acetone scrubber, will be an effective means of capturing these organic tars (including small volatile tars such as acetylene) as it is capable of

dissolving a wide range of polar and non-polar compounds, it is cheap, has low toxciity and volatility offering good compatiblity with GC-MS (117). A further upshot of this is that standard automated liquid sampling (ALS) may be used to analyse tar compounds, saving on the expense of additional GC modules and user training. The aim of this investigation will therefore be; to set up and evaluate acetone as an extraction method versus existing scrubber solvents and GC-MS methods for the identification of tars in uncharacterised feedstocks; brownfield soil contaminated with oily sludge and sludge cake. The sludge cake from human waste will be sampled from two locations UK and Ghana to see if location and composition will have an affect on the products generated by thermal treatment. Pine wood will be used as a standardised feedstock for biomass to confirm the successful operation of the pyrolysis / gasification process. For problematic wastes such as uncharacterised brownfield soil and municipal sludge, pyrolysis and gasification may provide a potential solution to removing these problematic wastes to generate usefull products such as syngas, bio-oils and biochar. Characterisation of these secondary pollutants derived from the pyrolysis and gasification process is therefore vital to evaluate the cleanliness of the recyling process.

The processed syngas will then be analysed using an in-line GC-TCD method for its suitability for conversion into hydrocarbons using a Fischer-Tropsch reaction. The GC-TCD will analyse small molecules such as hydrogen, carbon monoxide, methane and acetylene. Carbon monoxide and hydrogen with be converted to hydrocarbons using a novel low cost FT catalyst. Generally the FT process uses cobalt catalysts to generate linear alkanes, cobalt catalysts are expensive (350 x greater than iron catalyst) (39,40) and requires an energy intensive calcination (12h at 600 ^{o}C) stage to prepare the catalyst (47). This latter stage is fundamentally an oxidation process and it is proposed that a cheaper catalyst preparation method could be envisaged using chemical oxidation to generate a suitable precursor catalyst for the FT process, thus lowering operational

costs of the FT process. To characterise the catalyst a number of parameters will be studied to ensure the catalyst is likely to function these include surface area, porosity and crystallinity.

Finally, in order to maximise the economic feasibility of the process, waste biochar derived from pyrolysis of the biomass feedstocks (pine wood and sludge cake), will be activated and trialled as a sorbent to clean up contaminated water (industrial waste water or contaminated water scrubbers) before it is returned to the enviroment. The ability of this activated biochar to remove potential hazardous compounds such as phenols, polyaromatics hydrocarbons and petroleum derived compounds from water will be investigated for application within the FT process. It is documented that the activation of biochar can alter the surface area and chemistry of biochar increasing its ability as a sorbent (118). Together with activation, temperature in which the biochar is produced can have an effect on its selectivity to different compounds with high temperature biochars having higher hydrophobicity than lower temperature biochars (23,24). A further investigation will be carried out and to evaluate activated biochars (pine wood and sludge cake) in removing non-polar organic pollutants such as polyaromatic hydrocarbons (PAHs). The main research problems and aims are listed below:

1.6.1 Research problems.

1. There is a requirement to characterise potential feedstocks for thermochemical processes, for their suitablity to generate useful products such as syngas (that may have the potential energy source or used in FT reaction) and biochar (used as a sorbtive medium or a fuel). Products from the feedstocks pine wood (process standard), brownfield contaminated with oily sludge, and secondary sludge filter cake (uncharcaterised) will be characterised using a number of techniques. Syngas will be analysed using GC-TCD to determine its quality (calorific value and gas ratio), whilst biochar will be analysed for its suitability as a sorbant

(recovery experiment of target analytes from aqueous samples) and as a fuel (calorific value).

2. Tars that are generated for thermochemical processes of uncharacterised feedstocks require classification (to determine human and enviromental fate) and removal (prevention of contamination of downstream processes). Often classification tars involve alternative sample preparation methods and modification to standard analytical GC-MS equipment (gas- sampling valves, headspace, SPEME and thermal desorption) which can be expensive. Tar removal from the process can be complicated (hot gas filters and catalyst reforming) and sometimes removal is specific to compound class (water and methanol scrubbers are selective to removal of polar compounds). The tar generated from the thermal-chemical processes will be captured in a suitable solvent trap. Acetone will be selected because its cheap, has low toxcity and capable of dissolving a wide range of organic compounds (polar and non polar). Acetone solubility towards acetylene may also prove to be cheaper method for capturing small problematic unsaturated tars. Due to acetones low volatility it can be used as a solvent for GC-MS, and therfore double up as a sample preparation method, for analysing tars derived from uncharacterised feedstocks. Aliquots of the scrubbers can then be analysed by direct injection with no requirement for additional sampling techniques (SPEME, HS) and instrumentation.
3. The clean syngas may be used in FT to synthesis hydrocarbons. The generation of hydrocarbon material will require idenitfication and classification (GC-MS) to determine whether the process is optimized to generate the desired product. Assesment of biochar at adsorbing organic compounds will be evaluated using a recovery experiment, using a spike before and spike after comparison. Two temperature ranges will be assesed (high and low) to determine whether temperature is significant factor in biochar selectivity

4. Waste material remaining from recycling (pyrolysis) requires evaluating as a potential method to remove organic contaminates from aqueous solutions. The preparation temperature of the biochar also requires investigation as it may exhibit selectivity towards different classes of compounds. The clean syngas (if deemed suitable) will be converted to hydrocarbons using FT reaction. Products generated by this synthesis will be placed in a suitable solvent and passed through a clean up technique (SPE) to remove possible contaminates from the catalyst. These products will then be analysed to determine whether the process was successful.
5. FT process can occur considerable cost, especially in catalyst development; these include the raw materials (Co and rare earth promoters) and catalyst synthesis conditions (calcination at >600 °C for up to 12 h). A cheaper alternative approach is required to generate a more economical process. Due to the expense in generating a FT catalyst; a novel low energy approach will be used to synthesis a Co/ Al_2O_3 (alkane generation). This will involve chemically oxidsing cobalt (II) chloride to produce the desired Co (III) transition state on a Al_2O_3 support to generate a precursor catalyst (before activation). Therefore, the energy intensive calcination stage will not be required; the addition or manganese instead of rare earth metal promoters, will lower the production cost of the catalyst.

Chapter 2:

Materials and Methods.

2.1 Materials and reagents.

2.1.1 Standard reference materials.

Acetone (ACS grade), methanol (ACS grade), pentane (GC grade), nitric acid (68 %) and the internal standard, triphenylethylene (1g powder), were purchased from Sigma Aldrich (Suffolk, UK). The EPA 8040a phenol calibration mixture (500 µg/mL in isopropyl alcohol), QTM PAH mixture 1 (PAH aromatic mixture 2000 µg/mL in dichloromethane) were obtained from Supelco (Suffolk, UK). While the aromatic mixture 1 (PAHs, 2000 µg/mL in dichloromethane), phenol mixture 1 and 2 8040a (2000 µg/mL in isopropyl alcohol), volatile aromatic mixture CLP VOA (2000 µg/mL in methanol) and naphthalene-d8 (Internal standard 500 mg powder) were sourced from Restek (Wycombe, UK). TPH mix 861421-u (alkanes C10-C28) (2000 µg/mL in methylene chloride), were obtained from Supelco (Suffolk, UK). Diesel range organic mix 31064 (alkanes C10-C28) 1 (2000 µg/mL in methylene chloride) was sourced from Restek (Wycombe, UK).

The carrier gases for GC-MS and GC-TCD were, ultra-pure helium and Argon gas were purchased from Air Products (Swansea, UK) with high purity nitrogen from the British oxygen company (BOC) used for the purge gas for the pyrolysis rig. The TG-5MS (5 % diphenyl 95 % dimethyl polysiloxane) gas chromatography column (length 30 m, I.D 0.25 mm film thickness 0.25 µm) was purchased from Fisher Scientific (Leicestershire, UK). The Molsieve MSA BF 9 (10 m) and CP-SIL 5CB (8 m) columns used in the GC-TCD came as standard for analysis of simple industrial gases.

2.2 Instrumentation.

Analysis were undertaken using a Trace 1300 and ISQ GC-MS system (Thermo Scientific, Hemel Hempstead, UK) operating with Tracefinder Xcalibur™ software and the GC-TCD was a Varian CP-4900 using galaxy Saturn software (varian now owned by Agilent). The laboratory scale gasifier was constructed based on an in-house commercial design.

2.2.1 Method parameters for VOT analytes.

The analytical protocol was optimised for the detection of light aromatic compounds using a mixture of standards. Samples were analysed by injecting 2.5 µL into the GC-MS system using split-less injection with constant helium flow (1.5 mL/minute) on a 30 m TG-5MS (same phase as DB5) 0.25 µm bore column with 0.25 µm film i.d., at an inlet temperature of 300 °C. A stepped GC oven temperature programme was used; 40 to 150 °C at 15 °C per minute, which was held for one minutes, followed by an increase to 300 °C at 25 °C per minute, totalling a run time of 16.33 minutes. To introduce the analytes into the mass spectrometer the transfer line was held at 300 °C and the ion source at 250 °C. Data was acquired scan (*m/z* 50-350) and single ion monitoring (SIM) conditions approach recording *m/z* 78, 91 at 2.0-3.80 minutes, *m/z* 91, 112 at 3.80 to 4.55 minutes, *m/z* 104, 91 at 4.55 to 4.80 minutes, *m/z* 105 at 4.80 to 5.70 minutes, *m/z* 146, 5.70 to 6.50 minutes and *m/z 136, 179* from 6.50 to 16.33 minutes.

2.2.2 Method parameters for SVOT analytes.

For semi- volatile organic tar analysis, the protocol was optomised for target analystes such as phenols and poly aromatic hydrocarbons (PAHs). Standard samples were analysed by introducing 2.5 µL of mix into the GC-MS system using split-less injection, with constant helium flow (1.5 mL/minute) on a 30 m TG-5MS 0.25 µm bore column with 0.25 µm film i.d., at an inlet temperature of 300 °C. Again stepped GC oven temperature programme was used; 40 to 250 °C at 20 °C per minute, which was held for five minutes, followed by a further ramp from 250-

300 °C at 20 °C per minute, totalling a run time of 24 minutes. To introduce the analytes into the mass spectrometer the transfer line was held at 300 °C and the hot ion source at 310 °C for optimum sensitivity of PAHs (119). Data was acquired under full scan (*m/z* 50-450) and single ion monitoring (SIM) conditions with the latter operated as a segmented approach recording *m/z* 228 at 14-20 minutes and *m/z* 276 and 278 from 20-24 minutes.

2.2.3 Method parameters for Fischer-Tropsch monitoring method.

The analytical protocol was optimised for the detection of even number alkanes within C10-C28 (diesel range) by comparing with a mixture of standards. Samples were analysed whereby 1.0 µL of sample was introduced into the GC-MS system using split-less injection, with constant helium flow (1.5 mL/minute) on a 30 m TG-5MS 0.25 µm bore column with 0.1 µm film i.d., at an inlet temperature of 250 °C. A GC oven temperature programme was used; 65 to 300 °C at 15 °C per minute, which was held for five minutes, totaling a run time of 24.33 minutes. To introduce the analytes into the mass spectrometer the transfer line was held at 300 °C and the ion source at 300 °C, the high temperature of the source and transfer line prevents condensation of the less volatile analytes. Data was acquired under full scan (*m/z* 50-450) and SIM conditions recording *m/z* 71 at 3-6.50 minutes and *m/z* 98 and 85 from 6.50-24.33 minutes.

2.2.4 Gas chromatography-thermal conductivity detection (GC-TCD) method for syngas monitoring.

A GC-TCD method was developed to monitor the ratio of simple gases, such as CO, H_2, CH_4 and acetylene, within the syngas. The GC-TCD method was developed on a Varian micro GC-TCD comprising of two columns; channel 1 operating with a 8 m column containing a 100 % dimethyl-polysiloxane stationary phase (CP-SIL 5CB), for separating small organics such as acetylene, and channel 2 operating with a 10 m molecular sieve column containing aluminosilicate stationary phase (Molsieve MSA BF) for separating simple gases, CO, H_2, CH_4. The carrier gas used for both

columns was ultra-pure Argon and the parameters of the method are listed in Table 5. The column parameters were set as follows: channel 1 injector was and held at 40 °C, with a constant pressure of argon at 20 psi, channel 2 injector was held at 60 °C with a constant pressure of 20 psi. Both channels had a injection time of 50 ms and sampling frequency of 100 Hz. Both columns, 1 and 2, were held at constant temperature of 50 °C and the detector sensitivity was set at medium with acquisition/ run time of 240 seconds.

2.3 Standard solutions

The standard 10 mg/L working solution containing volatile analytes was prepared by adding 125 µL of the CPL volatile mega mix™ (batch A0111166) into 25 mL of acetone. Likewise, a 10 mg/L quality control working solution for the quantitation of volatile analytes was prepared using a separate batch of CPL volatile mega mix™ (batch A0112573), again 125 µL was introduced into 25 mL of acetone.

The standard 10 mg/L working solution containing semivolatile analytes was prepared by spiking 125 µL of the QTM PAH mixture 1 and 500 µL EPA 8040a phenol calibration mixture into 25 mL acetone. Similarly, a 10 mg/L quality control working solution for the quantitation of semi-volatile analytes was prepared by spiking 125 µL PAH mixture 1 and 125 µL of phenol mixture 1 and 2 8040a into 25 mL of acetone. The internal standard solution was prepared as 100 mg/L concentration by weighing 0.01 g of triphenylethylene powder and naphthalene-d8 into 25 mL of acetone.

The standard 10 mg/L working solution containing even linear alkanes ranging from C10-C28 was prepared by spiking 125 µL of the TPH mix 861421-u into 25 mL acetone. Likewise, a 10 mg/L quality control working solution for their quantitation was prepared using a separate batch Diesel range organic mix 31064 , again 125 µL was spiked into 25 ml acetone. The internal standard solution was prepared as 100 mg/L concentration by weighing 0.01 g of tetracosane

d50 powder and spiking 100 µL of dodecane d26 98 % and hexadecane d34 98 % into naphthalene-d8 into 100 mL of acetone.

2.3.1 Calibration standards used to quantify syngas impurities.

To quantify the target SVOT and VOT impurities expected from the gasification process, a set of calibration standards of known concentration were prepared to create a calibration graph for the relevant target analytes using the spiking protocols in Table 2 and 2.1. As mentioned above, d8 naphthalene was used as a quantitative internal standard (IS) for the VOT and SVOT analytes, and triphenylethylene as a volumetric IS (surrogate) for SVOT determination.

Cal level	Volume of solvent (Acetone)	Volatile working solution (10 mg/L)	Internal standard spike (100 mg/L) d8 napthalene	Final concentration
Cal 1	995 µL	5 µL	10 µL	50 µg/L
Cal 2	990 µL	10 µL	10 µL	100 µg/L
Cal 3	975 µL	25 µL	10 µL	250 µg/L
Cal 4	950 µL	50 µL	10 µL	500 µg/L
Cal 5	900 µL	100 µL	10 µL	1000 µg/L

Table 2. The spiking protocol for the analysis of small volatile aromatic impurities (VOT) within in the solvent.

Cal level	Volume of solvent (Acetone)	Semivolatile working solution (10 mg/L)	Internal standard spike (100 mg/L)	Final concentration
Cal 1	975 µL	25 µL	10 µL	250 µg/L
Cal 2	950 µL	50 µL	10 µL	500 µg/L
Cal 3	900 µL	100 µL	10 µL	1000 µg/L
Cal 4	850 µL	150 µL	10 µL	1500 µg/L
Cal 5	800 µL	200 µL	10 µL	2000 µg/L

Table 2.1. The spiking protocol for the analysis of semi-volatile organic tars (SVOT, phenols and PAHs impurities) within in the solvent.

2.3.2 Calibration standards used to quantify hydrocarbons for fuel use.

In order to quantify the target hydrocarbons expected from the Fischer-Tropsch (FT) process the following calibration standards (2.2):

Cal level	Volume of solvent (Pentane)	Standard spike (10 mg/L)	Internal standard spike (100 mg/L)	Final concentration
Cal 1	975 µL	25 µL	10 µL	250 µg/L
Cal 2	950 µL	50 µL	10 µL	500 µg/L
Cal 3	900 µL	100 µL	10 µL	1000 µg/L
Cal 4	850 µL	150 µL	100µL	1500 µg/L
Cal 5	800 µL	200 µL	10 µL	2000 µg/L

Table 2.2. The spiking protocol for a non-extracted calibration procedure.

2.4 Sample preparation.

2.4.1 Assessing solvent scrubbers performance using analyte recovery.

A comparison of acetone, water, and methanol in recovering impurities within the SVOT and VOT methods was performed using an impinger/trap containing 100 mL of solvent (acetone/ methanol/ water), connected to a round bottom glass reaction vessel containg 100 mg of PAH, phenol and volatile analyte mix. For example, 50 µL of 2000 mg/L standard was spiked into the vessel and was heated heated to 450 °C ± 10 °C to simulate pyrolysis and vapourise the target analytes to the impinger by a constant flow of nitrogen carrier gas at 100 mL/per minute. For recovery, this was 'spike before' sample and 1 mL aliquot was placed in a vial with 10 µL (100 mg/L) internal standard mixture (naphthalene-d8 and triphenylethylene) for analysis. For water extracts, solvent transfer is required for GC-MS anlysis; 0.5 mL of nitric acid was added to the solvent sample and analytes (PAHs and phenololic compounds) extracted into pentane, with 1 mL of pentane aliquoted and spiked with internal standard for analysis.

To assess the performance of the extraction for the target classes of compounds, additional QCs were prepared as discussed below.

For QC *'spike after'* extraction sample; 50 µL of each analyte standard mixture (PAH mixture, phenol mixture and light aromatic each 2000 mg/L) was added to 100 mL of solvent derived

from the solvent blank (water, methanol or acetone). A 1 mL aliquot of methanol or acetone were transferred to GC vials and internal standard added as above. For water, 0.5 mL nitric acid was again added and extracted using 10 mL of pentane with 1 mL transferred to GC vial with addition of internal standard.

Recovery was assessed using the following method:

$$\frac{Spike\ before\ conc}{Spike\ after\ conc\ (Quality\ control\ spike)} \times 100 = \%\ Recovery \qquad \text{Equation 2.1}$$

To compare the absolute amounts of analyte recoverd by the acetone and methanol scrubber, were run in triplicate. Relevant target analytes were quantified using a calibration curve from appropriate standards (semi-volatile analytes over the concentration range 250-2000 µg/L and volatile analytes covering 50-1500 µg/L). Blank samples were also analysed to test for chromatographic and mass selectivity; these included a double blank consisting of solvent with no internal standard analysed after the highest standard to assess for carryover. Quality control samples (QCs) containing a known amount of the volatile (single ring aromatics) and semi-volatile analyte mixture (PAHs and phenols) were also used test the continued quantitative performance of the calibration curve following method validation.

Figure 2. A photo showing the set up for activated biochar recovery experiment

2.5 Design and operation of pyrolysis and gasification rig.

10 g of pine wood, sludge filter cake and 20 g of brown field soil was submitted to temperatures in excess of 700 °C in an inert atmosphere, using a lab scale rig. The lab scale rig designed in house by Phil Knight and Geraint Sullivan, is comprised of a cylindrical stainless steel tube with dimensions of 4.7 cm^2 by 70 cm, at one end is an end cap that can be opened to introduce the feedstock material, the opposing end contains a gas port. The entire rig is at a constant purge with nitrogen; this maintains a low oxygen environment and allows for the flow of syngas gases. Nitrogen feed into an inlet valve while the emerging syngas comes out of the output value. This can then be connected in-line to the scrubber system, which comprises of glass impingers containing acetone; for tar monitoring, and connected to the GC-TCD; for simple gas analysis. Nitrogen can be exchanged for to compressed air if gasification reactions are required. When in an inert atmosphere the feedstock undergoes pyrolysis (low oxygen environment) a slow heating rate of 20 °C per minute, mimics slow pyrolysis.

A sample of pine wood, contaminated soil (10 % contamination with petrochemical oily waste) and sludge cake derived from human effluent was sieved to below 2 mm. Each feedstock was individually heated to >700 °C. Each run was connected to a scrubber system, comprised of three impingers, containing 150 mL acetone; the final output of the impinger was connected to the GC-TCD to analyse composition of simple gases in the syngas. A thermocouple is housed at the centre of the rig and monitors the temperature output (can monitor up to a 1000 °C); this is relayed to a thermostat for accurate temperature control. Heat is supplied to the rig by an outer kiln jacket that can reach temperatures in excess of 900 °C.

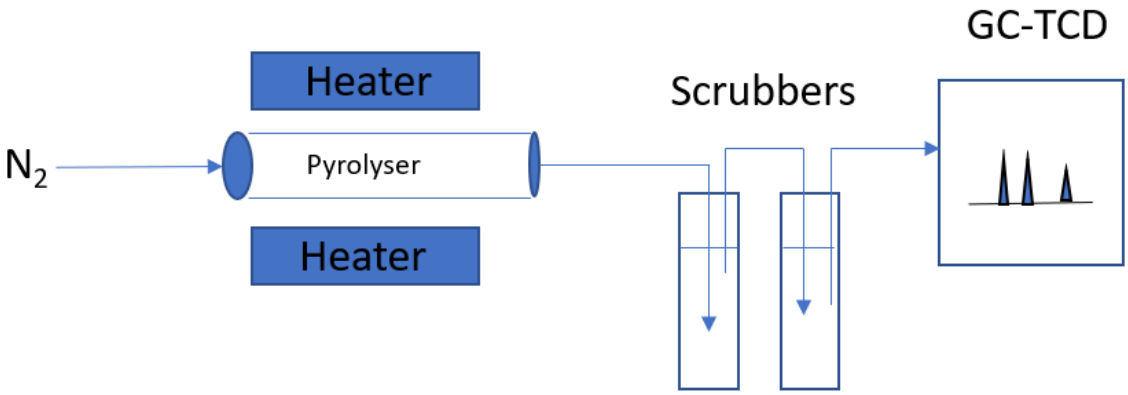

Figure 2.1 Shows a diagramatic representation of the labscale pyrolyser/gasification set up, including scrubber and GC-TCD. Nitrogen gas can be exchanged for compressed air to change oxidative state of the environment.

2.5.1 Preparation and analysis of organic syngas impurities.

The identification of tars from the thermochemical processes used to generate syngas is important in determining the performance of the clean-up procedure required combing with downstream processes, such as the Fischer-Tropsch catalysis reaction for biodiesel production. Two GC-MS methods were developed to analyse syngas impurities differentiated according to volatile organic tars and semi-volatile tars (SVOT). For the VOT method, target analytes are small aromatic analytes, such as benzene and toluene, while the SVOT method was developed for less volatile polyaromatic hydrocarbons (PAHs) and phenols). Aliquots of scrubbers containing captured tars were removed and 1 mL placed into GC-MS vials, spiked with a known quantity of internal standard (1 mg/L) and analysed on GC-MS using the appropriate method . These were run under full scan and single ion monitoring (SIM) conditions and any unknown analytes determined by their spectral characteristics and semi-quantified next to the nearest standard peak; while target analytes are quantified using their SIM ions.

2.5.2 Preparation and analysis of Fischer- Tropsch fuels.

The aim of generating hydrocarbons from the hydrogenation of carbon monoxide over a cobalt catalyst will require verification through the development of an analytical technique (GC-MS). The product generated through the FT reaction will firstly undergo sample preparation to make sure it is suitable for analysis via this technique. The sample will be passed through strong cation exchange solid phase extraction (SCX-SPE) to remove any potential inclusion of metallic catalyst that may damage the GC column and mass spectrometer. The extract with then be anaysed and quantified under full scan and SIM conditions using an isotopic internal standard calibration curve. The standards will cover even range alkanes from C10 to C28, with the anticipated fuel to fall with in this distrubution; hydrocarbons identified out of this range with be semi-quantified by camparison to the nearest standard.

2.5.3 Removal of (organo)metallic interferences for Fischer-Tropsch monitoring method.

The FT process may result in contamination of final product with metallic species derived from the catalyst if the support is not stable and could potentally be significant (>10-100 ppm). These are detrimental to the GC-MS system, potentially causing damage to the column and therefore a clean-up procedure is essential before analysis. Due to the high concentration of FT product any liquid samples taken from the FT reactor must be diluted by a factor of 1000, using pentane and passed through strong cation exchange solid phase extraction cartridge (SPE), such as LC-SCX (Supelco). This SPE cartridge has propylsulphonic acid functional group within the sorbent and has a strong affinity to positive cations with the sulphonic acid group being negatively charged during sample application. Samples were extracted using SPE cartridges held within a vacuum manifold as follows:

1. The sorbent was solvated (conditioned) 2 x 2 mL deionised water, 2 x 2 mL LC grade methanol and 2 x 2 mL pentane or acetone.

2. The cartridge was kept solvated and the sample added at a flow rate of approximatedly 0.5 mL/minute.
3. The extract was collected after passing through the cartridge and 1 mL placed into GC vial with the addition of 100 µL of internal standard mix.
4. The sample was analysed using the appropriate GC-MS method with an extracted analytical quality control (AQC) and a external calibration .

The AQC was prepared by making a 1 mg/L spiking solution in pentane from materials of a different batch to the standards and passing the through the sample clean-up procedure. Similarly to the test samples, 1 mL of the collected AQC was placed into a GC vial and 100 µL of internal standard added. A blank was also extracted following this protocol to detect potential contamination during the extraction process and carryover from the autosampler.

2.6 Feedstock and char preparation

2.6.1 Activation of biochar:

50 g of biochar was mixed into a paste using concentrated phosphoric acid (85 %) and left to react for 60 minutes (120). The biochar was then filter washed with deionised water. This process was repeated for a minimum of three times to ensure the phosphoric acid and polar impurities were removed. The biochar contents were then collected and dried in a muffler oven at 100 °C for 30 minutes and then raised to 350 °C for 2-3 hours to form activated biochar (120).

2.6.2 Method for determining the effectiveness of bio char in the removal of organics pollutants in aqueous solutions.

Contaminated water was directed over a bed of biochar in a one pass experiment to mimic a treatment bed. All samples were prepared and extracted using 0.5 g of activated biochar placed

into an empty solid phase extraction (SPE) cartridge. The sorbent was monitored for the uptake of various contaminants by eluting the sorbent using acetone and analysing using GC-MS. Biochars generated different temperatures were tested for their recovery efficiency towards selected compounds; polyaromatic hydrocarbons and phenolic compounds. Standard mixtures representing PAHs, and phenols were prepared as quality control samples, 'spike before' (SBE) and 'spike after' (SAE) to determine the recovery of the specific analytes to the sorbent. The SBE was prepared by adding 100 µL of 10 mg/L mixture of PAH or phenol working solution (in acetone) to 100 mL of deionised water, and this was then passed over the biochar at a steady flow of approximately 5 mL/minute using a vacuum manifold. The cartridge was washed with 2 mL of methanol and then left to dry on the manifold under vacuum for 1 hour. Analytes were eluted using 1.5 mL of acetone, with approximately 1 mL of extract transferred to a GC autosampler vial along with 10 µL of 100 mg/L internal standard mixture (naphthalene-d8 and triphenylethylene) to measure absolute amounts recovered by the biochar and account for any fluctuations in extract volume. For SAE quality control samples, blank deionised water (no analytes) was passed over the biochar at approximately 5 mL/minute. The biochar was then eluted with 1.5 mL acetone and 100 µL of analyte standard mixture (10 mg/L) was added to the extract. The samples were run in triplicate and quantified against a internal standard calibration curve containing analytes present in the standard mixture. The calibration concentration range covered from 250-2000 µg/L. Blank samples to test for chromatographic and mass selectivity, and carryover were included as a biochar, solvent and double blank. The biochar blank consisted of a deionised water sample (without standards) that underwent the biochar extraction. While the solvent blank (containing internal standard) was not extracted and was used to ensure there was no detectable contamination of the analyte within the solvent used to prepare the standards. A double blank however, consisted of solvent with no internal standard and was run after the highest standard to assess carryover between samples. To test the quantitative performance of the calibration curve additional non-extracted QCs containing a known amount

of the semi-volatile analyte mixture in solvent were used. The calibration was deemed acceptable, providing a good linear regression statistics, $R^2 > 0.980$ was generated and if the QC determined concentration was within ± 15 % of the expect value. This calibration relationship was then used calculate the concentration of the target analytes to determine recovery.

To assess the viability of biochar for use with complex samples indicative of industrial contamination, these were investigated for the clean-up of a gasoline and diesel standards. Mixtures of diesel and gasoline were used to prepare QCs spiked before and after extraction to give a 2 mg/L solution. The SBE was prepared using 100 mL deionised water spiked with 10 µL of the diesel and gasoline standards (20 mg/mL) and passed through biochar extraction cartridge. The SAE was prepared as an extracted 100 mL deionised water sample, collected, and spiked with 10 µL of diesel or gasoline standards. Due to the high hydrophobicity of these samples they would typically be eluted using pentane to ensure solubility. However, preliminary work involving direct elution using pentane showed the co-extraction of other highly abundant organic species from the biochar which compromised the selectivity of the analytical method. Therefore, the water collected after passing over the biochar was extracted using 10 mL of pentane of which 1 mL was analysed using GC-MS under full scan conditions as a survey scan.

To determine the recovery of diesel and gasoline, the extracted ion chromatograms (XICs) were integrated to generate a signal response as peak area (see equation 1) and compared to the area count of the QC SAE. For quantitation of PAHs and phenolic compounds the single ion monitoring (SIM) chromatogram for the relevant target ion was integrated to generate the signal response.

$$\frac{concentration\ spike\ before\ extraction}{concentration\ after\ extraction} \times 100 = \%\ Recovery\ (adsorption) \qquad \text{Equation 2.2}$$

2.7 Fischer- Tropsch catalyst preparation.

To prepare the FT catalyst, 40 g of cobalt chloride was dissolved in 100 mL deionised water with 10 g of manganese sulphate (promoter) and stirred. For the catalyst support, 100 g of anhydrous activated alumina beads (2.0-5.0 mm) were used, onto which the cobalt and manganese solution was precipitated by incipient wetness. This support was dried at 250 °C for 3 hours and treated chemically to oxidize the cobalt chloride (CoCl) to the desired cobalt (III) oxide (Co_3O_4) by titrating 30 mL of 15 % sodium hypochlorite solution onto the support. Following oxidation, the support was dried again at 250 °C for 2 hours before it was washed using deionised water and filtered, to remove any soluble sodium chloride that may have formed. The collected support was again heated at 250 °C in air for 2 hours, forming the precursor (inactive) catalyst, termed CAT-1. To activate the catalyst, the cobalt (III) oxide was reduced to metallic cobalt (sites of catalytic activity), in a hydrogen atmosphere for 4-8 hours at 400 °C. The catalyst was then tested using a laboratory scale Fischer-Tropsch reactor fabricted in-house.

2.7.1 Catalyst Characterisation methods.

ICP-OES: The elemental composition of the catalyst was determined using a PerkinElmer optima 7300, inductively coupled plasma optical emission spectroscopy (ICP-OES). This method uses an argon plasma to atomise the sample and detects the photon emission of excited elements as they return to ground state (121). Prior analysis the catalyst was digested in aqua regia solution and diluted to a suitable concentration (within methods dynamic range) using deionised water. The catalyst digest was introduced to analyser whereby the solution was atomised and the spectral intensity compared to a standard calibration (acidifyed solutions with known concentration of metal additives) to determine the elemental concentration (composition). ICP-OES operates on the principal that different elements upon atomisation generate unique wavelength photons and the concentration is directly proportional to the intensity of the emitted photons.

XRD: The surface composition and crystalline structure of the catalyst was characterised using X-ray diffraction (XRD) using a Bruker XRD D8 instrument with Da Vinci, and Cu Kα radiation with a λ of 1.5418 Å. For all scans an applied voltage of 40kV and a current of 40mA was used. The scanning range varied between 20 and 80^{o} using a Göbel Mirror set-up with 0.02^{o} step size with a time of 0.5 seconds per step.

SEM: Scanning electron microscopy (SEM) was carried out using Hitachi S4800, this uses focused electron beams, which interact surface of the catalyst sample, to generate secondary electrons which were detected and produced an image of the surface topography.The voltage was set at 10 kV for secondary electron imaging, with a working distance of 10 mm.

BET analysis : Brunauer- Emmett-Teller (BET) analysis using a Tristar 3020 by micrometrics for determining catalyst pore size and surface area. 0.1 g of catalyst was degased using helium at temperature of 250 °C over night prior analysis. Samples were prepared in a pre-calibrated tube and immersed into a liquid nitrogen bath while the instrument commenced with adsorption and desorption tests (122). This is achieved by the introduction of set amounts of nitrogen gas to calculate *P/Po*, (where p is the equilibrium pressure of nitrogen and *Po* is the saturation pressure of nitrogen gas)(122). The value of *P/Po* is plotted to generate an isotherm used to determine surface area and pore volume (122).

2.7.2 FT reactor design and operation

FT reactor developed in-house by Phil Knight and Geraint Sullivan, consisted of a high-grade stainless steel (8 mm thick) heated reaction vessel of dimensions 80 cm x 2.5 cm. The rig contained two pressure regulated valves to allow the entry of the reactant gases, carbon monoxide (CO) and hydrogen (H_2), with the pressure monitored using a pressure probe. A safety dump valve was situated near the gas regulators to mitigate sudden increases in pressure. The temperature of the rig was controlled using a thermocouple connected to a relay and

temperature controller. Prior to hydrocarbon synthesis, the catalyst was activitated using of 100 mL per minute flow of pure hydrogen at 400 °C for 4 h. This causes reduction of cobalt oxide (Co_3O_4) to metallic cobalt (Co) and Co/Al_2O_3.

Chapter 3.

Results: Method development and validation for syngas analysis and hydrocarbon identification.

3.1 Analytical selectivity.

3.1.1 MS identification of target analytes.

3.1.1.1 Volatile organic tar method .

A standard volatile organic analyte mixture (CLP mega mix) containing benzene, xylene isomers, ethylbenzene, styrene, and chlorinated benzene compounds was diluted to 2 mg/L and injected into the GC-MS using 30 m TG-5MS column with diameter of 0.25 µm and film thickness of 0.1 µm, and data was aquired using a full mass scan method described in 2.2.1 and target analytes identified by interrogating their characteristic EI mass spectra versus an EI mass spectral database (NIST version 2.2). Analyte retention times (T_R) were noted along with the most abundant fragment ion for developing the quantitative method (see Table 3). To ensure sufficient data points were captured within the chromatographic peak for accurate and precise quantitation, the MS method was segmented according to average analyte retention times and operated as a single ion monitoring mass scan to enhance sensitivity. Typically the aromatic components gave excellent reverse and forward match scores using the EI mass spectral database and were greater than 950 scoring factor (reverse and forward scoring is deemed good with a factor value above 800) (123) which gave confidence in compound identification. For compounds such as xylene it was difficult to distinguish between isomers because they generated very silmilar spectra. Generally, the volatile aromatic components produced a characteristic spectra; with the $M^{\cdot+}$ peak of significant intensity with few fragment ions and common ions *m/z* 77 (phenyl ion) and *m/z* 91 (tropylium ion) being present. Cleavage of side groups in benzyl derivatives (toluene, xylene, ethyl benzene etc.) usually result from homolytic

cleavage with loss of the radical and the charge site localised around the ring, this is sometimes reffered to as benzylic cleavage (114).

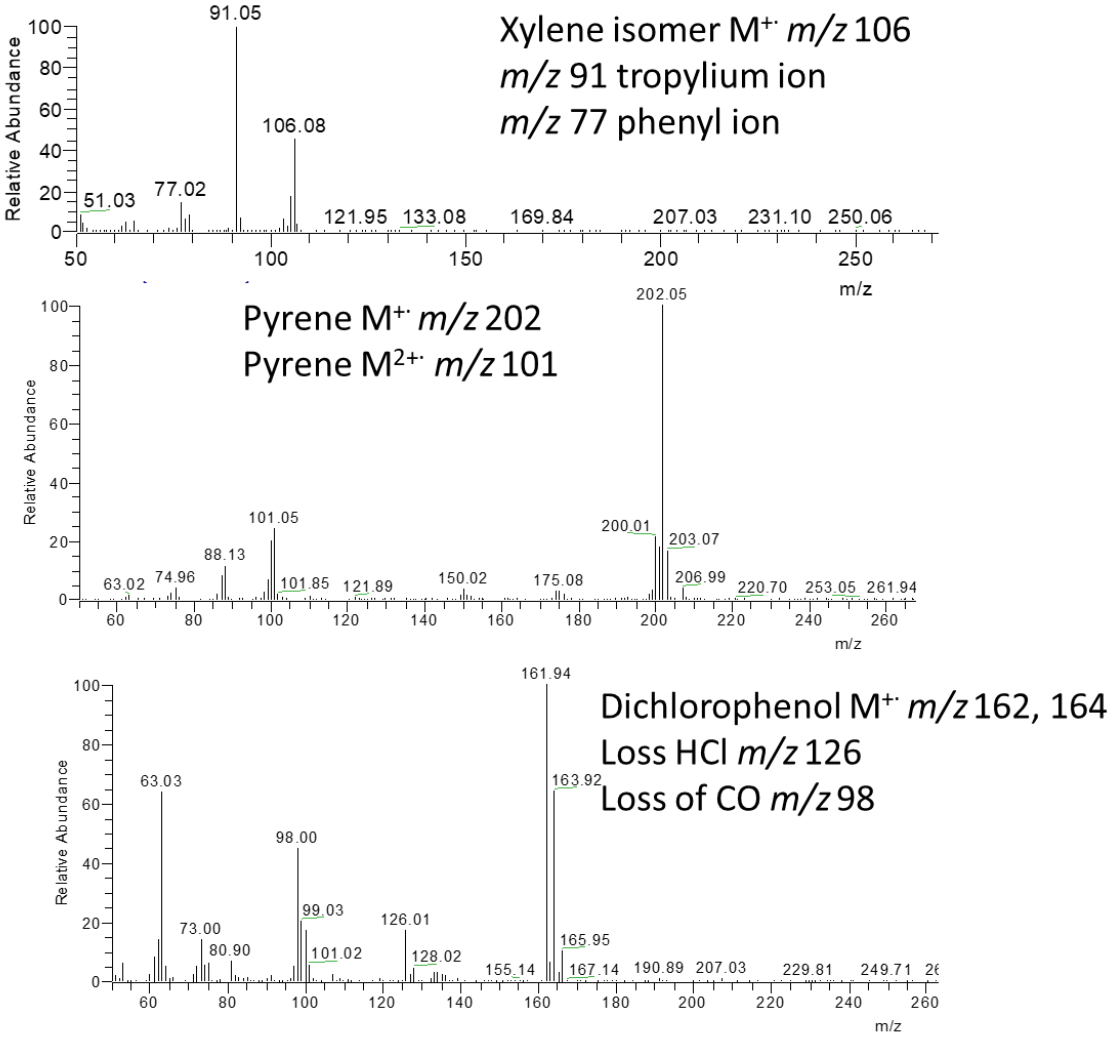

Figure 3 mass spectrum of xylene isomer (top), pyrene (middle) and dichlorophenol (bottom).

3.1.1.2 Semi-volatile aromatic and polyaromatic hydrocarbon (PAH) impurities

Two standard mixtures containing 16 PAHs and phenolic analytes were analysed using the method described in section 2.2.2. A 2 mg/L standard solution containing QTM PAH mixture and EPA8040a phenol mixture was directly injected into the GC-MS under full scan conditions. Again, target analytes were identified by their characteristic EI mass spectra and compared to the NIST version 2.2 EI mass spectral database for confirmation. The compounds produced good match scoring (reverse and forward), typically greater than 950, which gave confidence in their identification. PAHs produced characteristic EI spectra, with the predominate ion being $M^{+\cdot}$ from the loss of an electron of a π bond. This does not result in cleavage due to stabilization of the resonance structure of the delocalized electrons, and a peak at half the observed *m/z* of the molecular ion is usually seen which is infact a $M^{2+\cdot}$ due to loses of two electons from the resonance ring. For phenolic compounds, the spectra will show and intense molecular ion peak with less intense fragment peaks, representing the loss of CO (heterolytic cleavage) and ethene. For substituted phenols such as dichloro phenol, the intense molecular ion (*m/z 162)* and isotope patterns for Cl are identifiable around the molecular and fragment ions in which Cl resides. Dichlorophenol shows a loss of a HCL group (*m/z 126)*, and CO (*m/z 98)*. After injection the identified compounds were noted for their retention times, with care taken to ensure that analytes did not co elute, and the most abundant fragment ion selected for the quantitative method. In the interest of minimising the amount and number of samples required for analysis, the two standards were combined with d8-naphthalene and the additional volumetric internal standard triphenylethylene. These were analysed and assessed as a quantitative method using D8-naphthalene and triphenylethylene as internal standards (see Table 3.1).

3.1.1.3 Fischer-Tropsch monitoring method: Detection of target hydrocarbons (alkanes) by GC-MS.

A standard containing 10 aliphatic alkanes, ranging from C10 to C28 was diluted to 2 mg/L and injected on to DB5 column and analysed using full mass scan method as per section 2.2.3. All aliphatic hydrocarbons were identified showed characteristic EI mass spectra predominated with low *m/z* fragment ions separated by 14 *m/z* units (*m/z* 43, 57, 71, 85), and compared to the NIST version 2.2 EI mass spectral database. However, due to the similarity of the EI spectra using the database would often give misleading alkane results. It was therefore imperative to use the information on volatility to identify the hydrocarbons. After their retention times were determined, the fragment ion *m/z* of the highest abundance was choosen for quantitation. However, due to the extensive fragmentation of hydrocarbons, the 'highest' fragmentation was relatively low in comparison to the molecular weight of the compounds, typically *m/z* 71 (for C10 and C12) and *m/z* 85 (C14 +) was used. Due to the low *m/z* of the quantitation ion, retention time was equally if not more important for alkane confirmation.

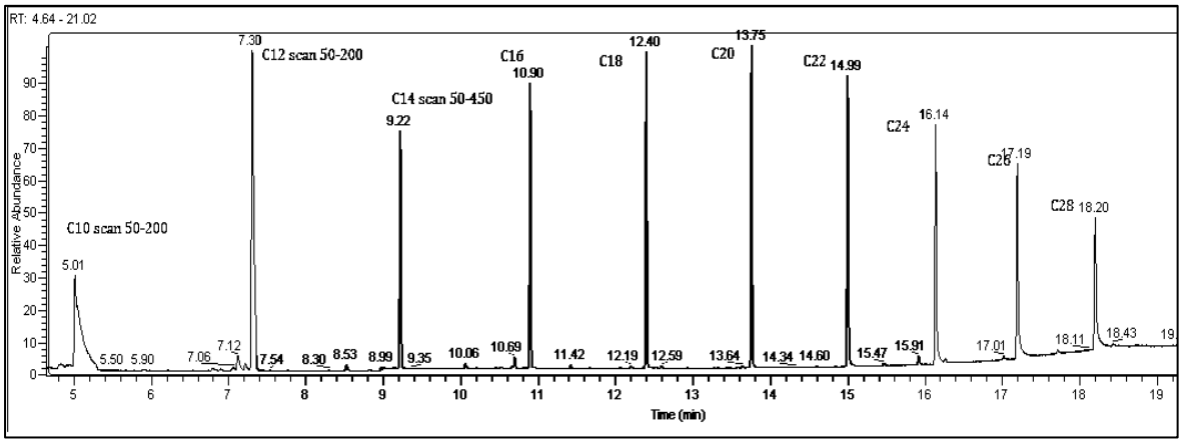

Figure 3.1 A total ion chromatogram of the target hydrocarbon in the analysis method. Each peak represent a hydrocarbon, the area of the peak is proportional to its concentration and is the sum of the total ions detected.

The same process was performed on the deuterated internal standard; dodecane D26, hexadecane D34, and tetracosane D50. Once all were identified, both internal standards and standards were mixed to limit the amount of instrument time required and run on the above method. Each compound was assigned to the nearest eluting internal standard and a quantitation method was developed based on the components individual retention times and quantitation ions.

3.2 Chromatographic characterisation of GC-MS methods.

To ensure sufficient separation of the target analytes, the oven temperature programme and carrier gas flow were optimised. The inlet temperature was set to account for the analyte with the highest boiling point to ensure sufficient vapourisation within the inlet. To prevent peak broadening, the transfer line into the mass spectrometer was kept at the maximum temperature of the GC oven ramp with the oven starting temperature set above the boiling point of the solvent but lower than the boiling point of the first eluting analyte; this allowed the solvent front to elute early in the chromatographic run and prevented column solvent interaction through condensation. For each method, chromatographic repeatability and reproducibility was assessed as a % relative standard deviation (% RSD) of repeat injections of a standard within one batch and an F- test of injections over two separate days, respectively.

Compound	Average Retention Time (minutes)	F-test n=9	% RSD of Rt Day 1	% RSD of Rt Day 2	Regression coefficient	Quantitation ion *(m/z)*	Internal std
Benzene	2.49	2.713	0.51	0.31	0.9965	78	d8-napthalene
Toluene	3.32	2.374	0.20	0.13	0.9973	91	d8-napthalene
Chlorobenzene	4.13	1.881	0.05	0.07	0.9991	112	d8-napthalene
Ethylbenzene	4.29	1.621	0.06	0.05	0.9978	91	d8-napthalene
Benzene 1,3, dimethyl	4.38	1.428	0.05	0.06	0.9984	91	d8-napthalene
Styrene	4.61	1.298	0.06	0.05	0.9983	104	d8-napthalene
P-Xylene	4.64	1.283	0.05	0.04	0.9989	91	d8-napthalene
Benzene, 1,methyl	4.99	1.734	0.05	0.06	0.9989	105	d8-napthalene
Benzene 1,3 dichloro	5.91	1.034	0.04	0.0004	0.9998	146	d8-napthalene
Benzene 1,4 dichloro	5.98	2.542	0.03	0.05	0.9998	146	d8-napthalene
Benzene 1,2 dichloro	6.24	1.464	0.04	0.04	0.9998	146	d8-napthalene
d8-napthalene	7.82	-	-	-	-	136	d8-napthalene

Table 3: Summary table for the VOT syngas impurity analysis method illustrating the retention time (in minutes) and fragment ion selected for quantitation for each target analyte with the associated internal standard. F-test was used to determine retention time stability, by comparing % RSD of analytes over two days.

Compound	Average Retention time	F-test value n=9	% RSD Rt day 1	% RSD Rt Day 2	Regression Coefficient	Quantitation ion *(m/z)*	Internal std
Phenol	4.74	1.56	0.032	0.040	0.9967	94	D8- naphthalene
2, chloro phenol	4.89	2.21	0.033	0.049	0.9975	128	D8- naphthalene
2-methyl phenol	5.38	1.49	0.043	0.035	0.9950	108	D8- naphthalene
4-methyl phenol	5.53	2.12	0.038	0.026	0.9969	107	D8- naphthalene
2-nitro phenol	6.08	1.37	0.025	0.030	0.9949	139	D8- naphthalene
2,3 dimethyl phenol	6.13	1.42	0.025	0.030	0.9982	122	D8- naphthalene
D8- naphthalene	6.48	-	-	-	-	136	D8- naphthalene
2,5,dichloro phenol	6.46	100	0.028	0.003	0.9973	162	D8- naphthalene
Napthalene	6.51	1.21	0.032	0.029	0.9992	128	D8- naphthalene
2,6 dichloro phenol	6.61	2.01	0.030	0.022	0.9997	162	D8- naphthalene
4, chloro 3 methyl phenol	7.19	116	0.027	0.003	0.9930	142	D8- naphthalene
2,3,6 trichloro phenol	7.58	1.37	0.020	0.023	0.9977	196	Triphenylethylene
2,3,5 trichlorophenol	7.93	1.21	0.023	0.021	0.9993	196	Triphenylethylene
Acenapthylene	8.42	1.00	0.021	0.021	0.9994	152	Triphenylethylene
Acenaphthene	8.65	1.02	0.019	0.019	0.9983	153	Triphenylethylene
4, nitrophenol	8.80	2.07	0.024	0.017	0.9921	139	Triphenylethylene
Fluorene	9.35	5.14	0.027	0.012	0.9992	165	Triphenylethylene
Pentachlorophenol	10.3	3.38	0.026	0.014	0.9871	266	Triphenylethylene
Phenanthrene	10.4	2.40	0.027	0.017	0.9994	178	Triphenylethylene
Anthracene	10.5	116	0.019	0.002	0.9981	178	Triphenylethylene
Fluoranthene	11.9	1.99	0.021	0.015	0.9997	202	Triphenylethylene
Pyrene	12.2	3.06	0.020	0.012	0.9963	202	Triphenylethylene
Triphenylethylene	12.4	1.93	0.025	0.018	-	256	Triphenylethylene
Benza(a)anthracene	14.7	4.08	0.031	0.016	0.9990	228	Triphenylethylene
Chrysene	14.8	4.56	0.033	0.016	0.9963	228	Triphenylethylene
Benza(b)fluoranthene	18.2	1.79	0.021	0.015	0.9913	252	Triphenylethylene
Benzo(a)pyrene	18.9	2.58	0.018	0.011	0.9932	252	Triphenylethylene
Indeno(123-cd)pyrene	21.3	1.87	0.019	0.014	0.9904	276	Triphenylethylene
Dibenza(ah)anthracene	21.4	4.15	0.024	0.012	0.9920	278	Triphenylethylene
Benzo(ghi)perylene	21.9	1.74	0.023	0.017	0.9981	276	Triphenylethylene

Table 3.1: A table summarising the target analyte retention time (minutes), retention time stability and fragment ion used for quantitation (with internal standard) for the SVOT syngas impurity analysis method. F-test was used to determine retention time stability, by comparing % RSD of analytes over two days.

The syngas impurty monitoring methods (VOT and SVOT) also showed stable chromatographic retention times when analysed on one day with the % RSD for coefficent of variance for both days was below 1 %. However, despite the majority of target analytes showing similar chromatography (F-statistic calculated below 5.39 for 9 degrees of freedom), phenol, 2,5-dichloro, 4-chloro 3- methyl phenol and phenanthrene showed significantly different retention times between the two days of analysis with F-statistics greater than 5.39. However, on closer inspection the data shows a 10 fold improvement of variance on day 2 for 2,5 dichloro phenol

(0.03 to 0.003), 4-chloro 3- methyl phenol (0.03 to 0.02) and phenanthrene (0.02 to 0.002) indicating improved chromatographic stability (better precision). This data was used to inform the programmed retention time window for the analyte data acqusition with the segmented method and relevant data processing conditions.

Compound	Average Time (minutes)	% RSD Rt Day 1	% RSD Rt day 2	F-Rest Value	Quantitation ion (*m/z*)	Internal standard	Regression Coefficient
Decane C10	5.09	0.095	0.162	2.55	71.1	Dodecane D26	0.9963
Dodecane D26	6.92	0.056	0.061	1.15	82.2	NA	1.0000
Dodecane C12	7.33	0.052	0.037	2.00	71.1	Dodecane D26	0.9983
Tetradecane C14	9.23	0.036	0.040	1.13	85.1	Dodecane D26	0.9986
Hexadecane D34	10.47	0.023	0.032	1.92	98.2	NA	1.0000
Hexadecane C16	10.90	0.019	0.030	2.36	85.1	Hexadecane D34	0.9944
Octadecane C18	12.40	0.018	0.021	1.47	85.1	Hexadecane D34	0.9932
Eicosane C20	13.75	0.015	0.022	2.07	85.1	Hexadecane D34	0.9970
Docosane C22	14.99	0.014	0.015	1.02	85.1	Hexadecane D34	0.9932
Tetracosane D50	15.67	0.012	0.018	2.26	98.2	NA	1.0000
Tetracosane C24	16.31	0.014	0.019	1.89	85.1	Tetracosane D50	0.9963
Hexacosane C26	17.182	0.013	0.016	1.49	85.1	Tetracosane D50	0.9990
Octacosane C28	18.185	0.012	0.014	1.53	85.1	Tetracosane D50	0.9983

Table 3.2 Table showing the target compounds in the calibration standard with their associated internal standards used in the quantitation of hydrocarbons. Also stated is their typical retention times and quantitation ion used. F-test was used to determine retention time stability over two days. Calabrition regression statistics were deemed acceptable if R^2 was above 0.980.

For the FT method for hydrocarbon identification all standard compounds showed good retention time reproducibility and repeatability over two days, with F-test values below the critical value 5.39 for 9 degrees of freedom, and % RSD below 1 % for both days.

3.3 Method establishment for quantifying target analytes via GC-MS

It anticipated that the impurities derived from waste pyrolysis and gasification will be in great abundance and therefore not a problem to identify and quantify. For this reason, any unknows determined by full scan have anticipated LOD of 100 µg/L for SVOT and VOT methods, providing the unknown has S/N > 3 at a lower concentration.

3.3.1 VOT validation (linearity, accuracy and precision).

Following confirmation of selectivity, each analyte was assigned an internal standard that eluted with a similar retention time to assess the quantitative performance of the method. Using a segmented method utilising both a survey full scan and a quantitative SIM scan, a minimum of 10 data points (spectra) across the chromatographic peak, necessary for reliable quantitation, were achieved. This should allow for full scan spectra to be used for identification while operating in SIM scan, boosting acquisition speed and sensitivity for quantitation. The ISQ is capable of fast quadrupole scanning of 20,000 u/S with a mass range of 1.2-1100 u at unit mass resolution. It can preform 240 scans/S in SIM and 97 in scan (over 125 u)(124).

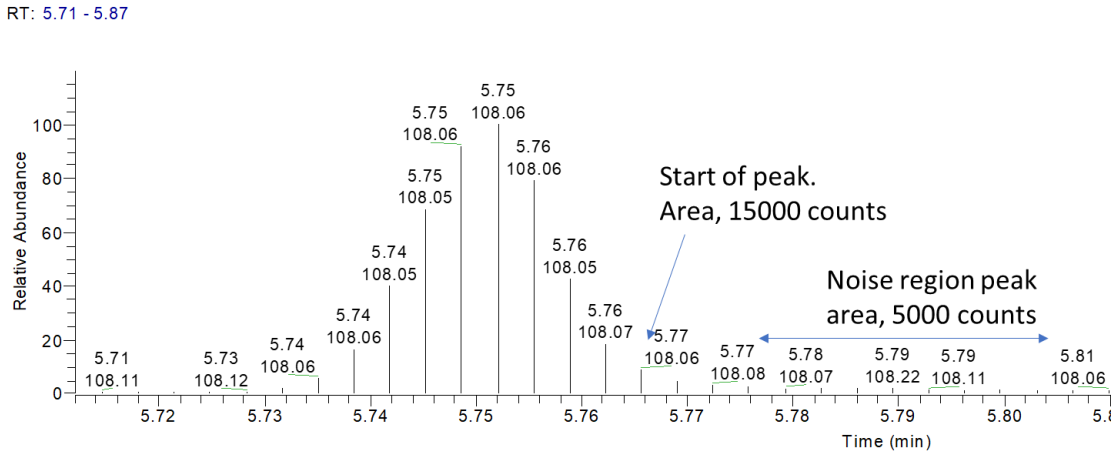

Figure 3.2: A typical extracted ion current chromatogram (for m/z 108) for 2-methyl phenol showing the number of mass spectra (n = 10) observed across the peak. Typically, at least 10 mass spectra are required for accurate quantitation suggesting that this method is suitable for reliable quantitation.

Calibration graphs covering the concentration range of 50-1000 ug/L using the internal standard d8-naphthalene were generated for each of the volatile organic impurities contained within the mixture. Due to the volatility of the analytes repeat injections from the same vial was not possible without a variation of the peak areas. Two calibration sets were run at the beginning and end of the run. Data was processed using equal weighted regression statistics and under these conditions each impurity showed excellent linearity, with all coefficient of determination >0.99 (see Table 3), ranging from 0.9965-0.9998. Generally, the regression statistics appear improved with higher retention time due to increased stability of retentative sites on column and higher volatile compounds exhibit less variation during perparation of standards and equate to this apparent improvement in R^2 value.

To test the method performance for quantitation these were validated using the following protocols. For VOT analytes two batches, each containing a full range of calibration standards, five blanks and five analytical quality control samples (AQCs) spiked at second highest standard level (500 µg/L), were used for assessment. Additional AQCs at low (250 µg/L) and high concentrations (1000 µg/L) were used for determining the lower level of quantitation (LOQ) and upper limit of quantitation. The lower limit of quantitation (LLOQ) was determined by spiking multiple AQCs below near the lowest standard that met accuracy and precision <20 %.

3.3.2 SVOT validation (linearity, accuracy and precision).

The syngas impurity mass spectrometry (MS) method, termed SVOT which focuses on the identification of semi-volatile tars, has been divided into two parts; a full scan from 3.00 to 14.00 minutes for phenols and mid-volatile PAHs and those that eluted early showed good sensitivity however, this gradually diminished. To ensure sufficient sensitivity it was established that the detection of the less volatile PAHs required a combination of selective ion monitoring and full scan (SIM/scan). This heightened sensitivity and allowed for good quantitation and still allowed for analyte identification using the full mass spectrum. However, this proved difficult for earlier

eluting compounds (volatile phenols and PAH), for this time segment was rather crowded and SIM/ scan would have impacted on the instruments duty cycle (increased scans) and inter scan delay (reset of quadrupoles) and therefore lowering sensitivity.

Calibration graphs covering the concentration range of 250-2000 µg/L using the internal standard d8-nahpthalene were generated for each of the volatile organic impurities contained within the mixture (see figure 3.3 for an example calibration graph). Two calibration sets were run, at the beginning and end of the batch, to acertain retention time and concentration drift. Data was processed using equal weighted regression statistics with each impurity showing excellent linearity with coefficient of determination >0.985 (see Table 3.2), ranging from 0.9871-1.000. From a closer inspection it appears that polyaromatic compounds exhibit overall better regression statistics with analytes having R^2 ranging from 0.9920 to 0.9997, when compared to the phenolic compounds with R^2 values with analytes ranging from 0.9871 to 0.9997. The polar functionality from hydroxyl (–OH) and chlorine (Cl) groups on the phenol derivatives interact through hydrogen bonding to glass liners and column stationary phase, whereas PAH do not have any polar characteristics; this difference could be the reason why there is variation in phenol analyte linearality.

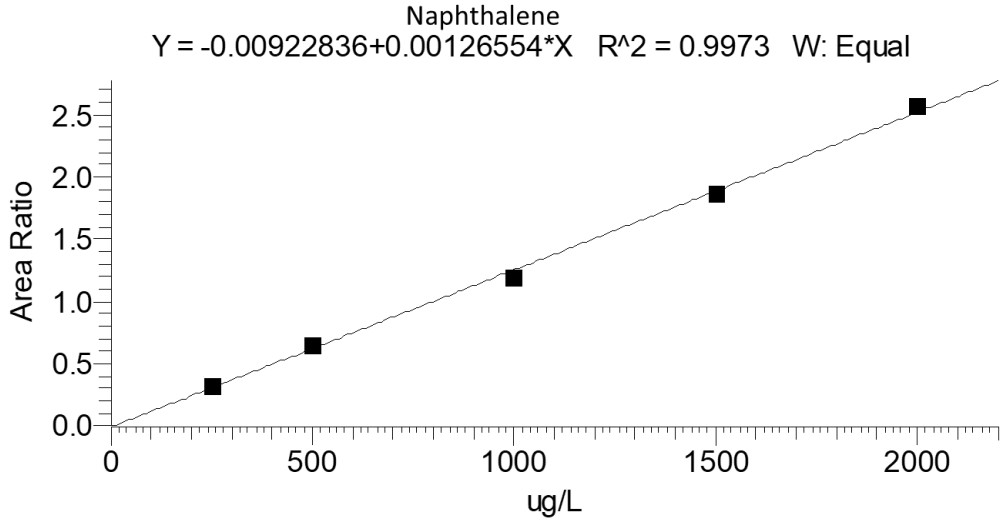

Figure 3.3 Calibration curve for naphthalene, a target analyte in the syngas impurity method, with a coefficient of determination was >0.99. d8-naphthalene, a deuterated version of the target analyte, is used as the internal standard.

For syngas impurity method SVOT, two batches, each with a full range of calibration standards, five blanks and five high AQCs, (second highest standard, 1500 µg/L) and five low (spiked at the lowest standard level, 250 µg/L) were used for assessing quantitation. Consequently, the result for the low AQC was used for determining the low level of quantitation (LLOQ). Two batches were run on two occasions. Within the two batches, multiple standard spikes of 100 % of the dynamic range were used to determine upper limit of quantitation (ULOQ). The lower limit of quantitation (LLOQ) was determined by spiking multiple AQCs near the lowest standard that met accuracy and precision <20 %. The accuracy of the quantitative method will describe how close the calculated concentrations of the AQCs are to the theoretical (expected) value as a percentage, while precision will describe the spread of calculated concentrations, with higher precision represented by % RSD.

3.3.3 FT monitoring method validation (linearity, accuracy and precision).

For the FT monitoring method, calibration graphs covering of 250-2000 µg/L using the deturated alkanes (tetracosane D50, hexacosane D34 and dodecane D26) were generated for each of the target alkanes contained within the mixture (C10-C28). As in the previous methods; calibrations run at beginning and end of the batch and data was processed using equal weighted regression statistics. Each target hydrocarbon expressed excellent linearity with coefficient of determination >0.99 (see table 3.2), ranging from 0.9932-0.9990. Generally, there is no obvious trend in regression statistics with retention time of analyte. However, the peak shape of decane (C10) see figure 3.1, is less symmetrical compared to the other higher alkanes in this series, on closer reflection, this is a likely cause of the starting oven temperature being to high, lowering the tendancy of decane to partition into the stationary phase, therefore causing poorer chromatographic efficiency and peak shape. However, all other parameters did pass validation criteria and therefore peak shape was not detrimental to the overall quantification of decane.

For the FT monitoring method, two validation batches each with a full set of calibration standards, five blanks and five analytical quality controls, at mid-level (50 % of dynamic range) and low level (lowest standard range) were run on two separate days. As with the previous methods, the batches also contained spikes to assess limit of detection, the lower limit of quantitation and the upper limit of quantification. The LLOQ was determined from the AQCs spiked at lowest standard (0.25 mg/L) while the LLOQ was determined by spiking a standard near the lowest calibration point that met < 20 % accuracy and precision. The ULOQ was determined by spiking replicate samples at the highest calibration standard (2.0 mg/L).

3.3.4 Validation assesment criteria for GC-MS methods.

The method validation data was established using the following figures of merit; accuracy, precision, standard error and limit of detection, upper limit of quantitation, limit of quantitation and lower limit of quantitation. The acceptance criteria for the method was based on UKAS requirements (125) and an approved company standard operating procedure (SOP). Successful validation required a pass of 20 % and below for accuracy and precision of the method to quantify the target analyte for ULOQ and LOQ QCs.

The LOD for the GC-MS methods was initially calculated using 3* standard deviation of the blank results, however, this can be missleading as differences in software and manual intergration of the baseline can give discrepancies and increase variation, without identifying the compound of interest. Therefore an experimental approach was performed to calculate the LOD, by spiking the lowest standard which can be seen with a signal to noise ratio (S/N) >3.

3.4.1 Validation summary: volatile organic tars (VOT) by GC-MS

All of the analytes within the VOT method showed very good accuracy with values of AQCs ranging from -0.36-5.53 % and those showing improved accuracy with a more linear coefficient of determination (nearer 1). In addition to accuracy, very good precision was observed with values between 5.4-12.39 % RSD. However, for the LLOQ, accuracy had negative bias, with analytes approaching -20 % and chlorobenzene marginally failing at -21 %. This may be mitigated by analysing more replicates. This method also shows good precision at LLOQ with values ≤ 10 %. For the ULOQ, accuracy and precision were both satisfactory but greater compared to the mid-range AQC (500 µg/L). With benzene showing poorest precision at both concentrations. A potential cause could be lowered stability for benzene on the column, early elution suggests fewer retention sites and poorer coefficients are due to variability with. A second explanation could be due to sample evaporation from GC vial during the analysis, which could cause variation in analyte concentration and again could account for poorer regression coefficient. Typical S/N at the LOQ spike (50 µg/L) ranges from 282 to 5019, significantly higher than the 1 1 µg/L spike, which ranges from 20 to 296. Therefore, sensitivity and quantification is not an issue at the lower end of the calibration range. A summary of validation data can be found in the Table 3.3.

Compound	ULOQ 1000 µg/L		LOQ 50 µg/L		S/N of LOQ	S/N of LOD spike (1 µg/L)	Linearity R2	AQC 500 µg/L	
	Accuracy	Precision	Accuracy	Precisi-on				Accuracy	Precision
Benzene	3.18	18.36	3.72	7.61	282	39	0.9965	2.24	12.39
Toluene	1.07	6.01	-6.58	16.27	2285	79	0.9973	5.53	10.02
Chlorobenzene	4.27	9.48	-21.82	4.14	9820	69	0.9991	2.53	5.86
Ethyl benzene	3.03	8.43	-18.60	4.25	2900	82	0.9978	2.89	6.52
Benzene-1,3, dimethyl	3.54	8.76	-18.25	4.08	4325	205	0.9984	1.71	6.11
P-xylene	4.09	9.11	-15.18	4.52	3231	296	0.9983	2.33	6.12
Styrene	0.47	10.74	-17.38	4.11	3802	193	0.9989	-0.36	7.30
Benzene(1-methyl)	2.77	7.60	-17.79	6.30	5019	36	0.9989	2.34	6.75
Benzene1,3 dichloro	3.55	8.71	-12.66	7.67	4733	27	0.9998	0.73	5.90
Benzen 1, 4 dichloro	3.70	8.75	-11.65	6.95	4516	24	0.9998	0.44	5.40
Benzne 1,2 dichloro	4.12	8.45	-10.61	10.03	4020	20	0.9998	1.18	5.89

*Table 3.3 A summary of validation data for the VOT method which include precision, accuracy and limit of detection (LOD). The LOD was deduced by dilution of a low spike that produced a S/N >3. The precision and accuracy are deemed acceptable as the values of both are below 20%. Accuracy was calculated by the (mean –expected)*100/expected and precision was calculated by the standard deviation of the batch divided by the expected result. The limit of quantitation was determined by spiking AQCs at the low calibration level, which met < 20% precision and accuracy.*

3.4.2 Validation summary: semi-volatile organic tars (SVOT) by GC-MS.

All of the analytes validated for SVOT method (phenol and PAH standards) passed validation (see Table 3.4). Precision at AQC (1500 µg/L) level ranged between 4.35-10.32 and accuracy between -5.98 to 4.70 %, largely with a negative bias. For ULOQ accuracy shows mainly a negative bias with a range -2.24 to 5.48 %, similar to the AQC level. Poorer accuracy and precision was observed for LLOQ to higher concentrations, but all concentration levels were acceptable ranging from -9.27 to 19.8 %. Satisfactory precision was observed at the LLOQ but

this was poorer than the higher concentration levels with ranges between 3.38 and 15.95 %. Those analytes showing improved accuracy with more linear coefficent approaching 1. As mentioned earlier, acquisition for this method was divided into two segments; full scan for the volatile phenols and PAHs and SIM/scan for less volatile PAHs (eluting after 14 minutes). Sensitivity was not compromised by running in full scan with the majority of the volatile compounds between phenol to pyrene showing good sensitivity with high S/N (1481- 12660) at LLOQ spike (100 µg/L), except pentarchlorphenol (S/N 6) and 4-nitro phenol (33). These LLOQ values were observed at approximately an order of magnitude greater than the LOD for the majority of analytes, apart from 2,3,5 trichlorophenol, 2,3,6 trichlorophenol and pentachlorophenol. While 4-nitro phenol has the poorest sensitivity of all the analytes with its LOD equivalent to the LOQ spike (250 µg/L).

Compound	LOD spike		LLOQ Spike 100 µg/L	Linearity	UL OQ (2000 µg/L)		AQC (1500 µg/L)		LOQ (250 µg/L)	
	µg/L	S/N	S/N	R^2	Accuracy	Precision	Accuracy	Precision	Accuracy	Precision
Phenol	10	525	4038	0.9967	3.09	10.93	-1.74	10.32	12.33	4.62
2-chlorophenol	10	275	3331	0.9975	0.44	9.45	-3.71	9.12	11.76	4.97
2-methyl phenol	10	368	4613	0.9950	0.81	9.24	-1.51	8.31	15.77	3.24
4-methyl phenol	10	445	7110	0.9969	0.97	9.31	-2.58	7.73	12.70	6.45
2-nitro phenol	25	178	1799	0.9949	-0.94	6.85	-2.75	10.86	7.29	5.40
2,3-dimethyl phenol	10	307	4969	0.9982	-2.00	6.76	-1.32	8.84	6.33	6.44
2,5-dichlorophenol	10	132	2614	0.9973	-0.46	8.23	-2.01	7.66	13.82	6.08
napthalene	10	63	12721	0.9992	0.14	7.78	-4.70	6.91	18.00	5.42
2,6-dichlorophenol	10	7	2489	0.9997	0.07	8.39	-1.62	7.72	8.21	6.84
4-chloro-3-methyl phenol	10	136	3741	0.9930	1.28	9.71	-0.77	7.67	14.44	3.38
2,3,6 trichloro phenol	100	1481	1481	0.9977	-1.70	6.34	-4.18	7.16	8.60	7.67
2,3,5 trichlorophenol	100	1562	1562	0.9993	5.48	9.91	4.70	10.17	5.01	7.76
Acenaphthylene	10	3280	12660	0.9994	0.28	6.38	-3.26	6.65	15.03	9.93
Acenaphthene	10	3020	11284	0.9983	1.27	6.95	-3.13	5.66	12.64	7.58
4, nitrophenol	250	33	33	1.000	-2.42	7.20	-2.80	8.58	-9.27	14.74
Fluorene	10	327	7051	0.9992	-0.25	6.71	-3.83	4.50	14.16	8.52
Pentachlorophenol	100	6	6	0.9871	1.74	8.27	0.75	8.33	4.96	14.35
Phenanthrene	10	781	9951	0.9994	0.32	5.38	-3.10	4.35	15.25	7.46
Anthracene	10	570	9025	0.9981	-2.05	7.69	-5.98	4.94	19.81	5.58
Fluoranthene	10	1403	12820	0.9997	-1.29	7.06	-3.21	4.59	8.91	9.81
Pyrene	10	1648	11476	0.9963	-0.74	6.36	-3.48	4.60	10.11	6.64
Benza(a)anthracene	10	699	11987	0.9990	-0.73	4.01	-2.15	5.67	10.98	15.93
Chrysene	10	866	12917	0.9963	-0.71	3.95	-1.45	5.17	16.12	9.09
Benza(b)fluoranthene	10	261	7697	0.9913	-0.22	4.40	-2.64	6.00	3.18	14.30
Benzo(a)pyrene	10	183	600	0.9932	-0.19	3.93	-2.00	6.35	16.47	10.19
Indeno(123-cd)pyrene	10	404	3502	0.9904	-0.24	5.11	-2.63	6.87	15.65	9.98
Dibenza(ah)anthracene	10	465	3222	0.9920	0.37	3.98	-1.87	7.32	14.25	9.53
Benzo (ghi) perylene	10	534	3456	0.9981	-1.02	5.27	-2.18	6.46	11.15	10.42

*Table 3.4. Table summarising validation data for the SVOT method. Listed in first column are the analyte believed to be most likely found 'tars' derived from gasification which include precision, accuracy and limit of detection (LOD). The LOD was deduced by dilution of a low spike that produced a S/N >3. The precision and accuracy are deemed acceptable as the values of both are below 20 %. Accuracy was calculated by the (mean –expected)*100/expected and precision was calculated by the standard deviation of the batch divided by the expected result. The limit of quantitation was determined by spiking AQCs at the low calibration level, which met <20 % precision and accuracy.*

3.4.3 Fischer-Tropsch monitoring method: validation summary.

The validation process used in section 3.3.3 was also carried out on the hydrocarbon analysis method and results summarised in table 3.5

Compound Alkane	RT minute	Precision			Accuracy			S/N LLOQ spike 100 µg/L	LOD ug/L	S/N LOD spike	Linearity R^2
		uLOQ 2000 µg/L	LOQ 250 µg/L	1000 µg/L <20 %	1000 µg/L <20 %	LOQ 250 µg/L	uLOQ 2000 µg/L				
C10	5.10	4.47	7.56	4.53	-2.83	3.58	-5.43	296	10	98	0.9963
C12	7.35	3.64	3.78	5.90	-4.34	0.77	-2.76	714	10	231	0.9990
C14	9.26	1.04	2.97	2.78	-3.40	3.93	-3.60	2389	10	802	0.9983
C16	10.92	1.77	3.51	2.73	-4.96	5.71	-5.31	2916	10	1073	0.9986
C18	12.42	1.57	3.25	3.00	-5.02	7.76	-4.00	2100	10	699	0.9982
C20	13.77	1.61	2.76	3.50	-5.79	11.25	-2.25	2020	10	38	0.9944
C22	15.00	1.42	2.50	2.24	-5.62	16.02	-5.99	1304	10	14	0.9932
C24	16.15	1.39	2.91	4.97	-5.16	14.47	-2.28	884	10	9	0.9970
C26	17.20	1.88	1.95	4.11	-5.83	17.35	0.02	539	10	121	0.9932
C28	18.21	2.16	2.35	4.96	-5.38	17.10	1.50	414	10	88	0.9913

*Table 3.5 Table showing the summary of validation data for the hydrocarbon identification method which includes precision, accuracy and limit of detection (LOD). The LOD was deduced by dilution of a low spike that produced a S/N >3. The precision and accuracy are deemed acceptable as the values of both are below 20 %. Accuracy was calculated by the (mean – expected)*100/expected and precision was calcul ated by the standard deviation of the batch divided by the expected result. The limit of quantitation was determined by spiking AQCs at the low calibration level, which met < 20 % precision and accuracy.*

The accuracy and precision for AQC spike (1000 µg/L) pass the acceptance criteria of <20 %, with precision of the AQC spike showing small variation for analytes C10 to C28, ranging from 2.24 to 5.90 % while demonstrating a slight negative bias for accuracy ranging from -5.83 to -2.83. The parameters for accuracy and precision are well within the acceptance criteria of <20 %. All analytes passed validation for the LOQ spike (250 µg/L) and ULOQ (2000 µg/L) with accuracy and precision meeting the acceptance criteria. However, in comparison to the remaining QCs, the LOQ spike shows reduced accuracy with values ranging from 0.77 to 17.35 % and precision from 1.95 to 7.56 %, indicating a good degree of confidence in the quantitative values across

the validation batches. A cause for poor accuracy maybe the weighting of the curve towards the higher concentration range, therefore affecting the accuracy of lower calibration ranges. The ULOQ shows similar accuracy (-5.43 to 1.50 %) and precision (1.04 to 4.47 %) to the AQC spike (1000 µg/L), also suggestive that accuracy is better at high calibration range.

The limit of detection (LOD) (determined by 3 times standard deviation of the blank), was below 100 µg/L for all components, C10-C28, with the highest (decane) at 82.9 µg/L and lowest (octasane) at 1.43 µg/L respectfully. However, after experimentally spiking a low concentration standard mix of 10 µg/L in the GC-MS, all target hydrocarbon peaks were still visible with a S/N>3, in fact it ranged from 9 to 1073, with lowest being tetracosane (C24) and highest being hexadecane (C18). Therefore the method could comfortably detect as low as 10 µg/L (although could be lower for some compounds) with the anticipated level of hydrocarbon material from the FT process being considerably higher than this, 10 µg/L was deemed an acceptable LOD for this method. By comparing the S/N of the LLOQ spike at 100 µg/L, it can be seen that the highest S/N ranges from tetradecane to tetracosane (C14-C24), 884- 2916, while analytes either side of this carbon distribution have reduced S/N. However, all S/N at the LLOQ are well above the LOD threshold of S/N > 3 suggesting this method is capable of detecting low ug/L levels of target alkanes.

The lower limit of quantitation (LLOQ) was determined to be 250 µg/L with an initial LLOQ concentration of 100 µg/L failing to achieve accuracy and precision <20 %. For example, despite good accuracy being observed for C10 and C12 (7.5 and 14.5 %), poor accuracy was observed for the remaining alkanes (31.5 to 92.9 %). However, precision was suitable for C12 to C28 alkane (1.76 to 9.3 %) with analyte decane (C10) showing poor precision at 24.16 %. This suggests that the reliablity and reproducibility of the method for low level quantitation is not as good for alkanes compared to volatile or semi-volatile organic compounds.

3.4.4 Recovery for FT process clean-up.

3.4.4.1 Removal of metallic interferences from the FT process.

In order to determine the effectiveness of the strong cation exchange (SCX) SPE cartridges for removing potential metallic impurities from the FT hydrocarbon material. A standard reference (Trace cert transition metal mix 1, 100 mg/L) containing transition metals was diluted using methanol that had been passed through the SPE cartridge to generate spike after extraction QCs (10 mg/L), these were then compared with QCs (10 mg/L of transition mix) that had been passed through the SPE process (spike before), to determine recovery. The extracted QCs were run on ICP-OES using an existing UKAS accredited method. Results of analysis found that SCX cartridges are effective at removing chromium, copper, lead, iron, and tin (recovery > 80 %), while less effective at recovering cobalt (40.35 %). Providing the catalyst is stable under pressures and temperatures of the FT reactor, then metallic contamination should be at a minimum. However, if suspected contamination for cobalt is high, then multiple SCX clean-up on the same sample should be used to maximize cobalt removal.

Element	Blank S0	Blank SB1	Spike after sample ug/L				Spike after Average conc µg/L	Spike before sample ug/L				Spike after Average conc µg/L	% decrease
			1	2	3	4		1	2	3	4		
Chromium	0.22	0.43	178.7	177.2	177.1	179.3	178.08	4.61	9.58	8.13	9.52	7.96	95.53
Copper	0.26	0.18	153.3	150.6	150.9	152.9	151.93	0.95	1.00	0.81	0.65	0.85	99.44
Nickle	0.00	0.00	171.1	169.8	170.3	170.2	170.35	103.2	114.8	110.2	103.10	107.86	36.70
Lead	0.00	4.35	170.3	157.5	167.0	163.5	164.58	8.09	11.34	16.27	10.44	11.54	92.99
Iron	1.33	0.37	219.2	217.6	219.0	219.3	218.78	41.88	43.29	46.51	43.32	43.75	80.00
Cobalt	0.03	0.08	103.2	102.8	103.1	103.8	103.23	62.74	61.46	60.16	62.15	61.58	40.35
Yttrium	0.00	0.04	94.86	93.94	94.32	93.73	94.21	0.17	0.01	0.05	0.02	0.06	99.93
Zirconium	0.00	0.00	82.37	86.51	88.12	88.69	86.40	15.28	21.73	17.91	19.32	18.56	78.52

Table 3.6. A table demonstrating recovery of metals in spike passed through stroong cation exchange. Appears to have high recovery (78.5 -99.4 %) for chromium, copper, iron, lead, and yttrium and zirconium.

A second experiment was performed using QCs spiked with target hydrocarbons % loss (recovery) during the SCX-SPE procedure. This was achieved by comparing a sample (QC) spike before extraction (SBE) and a sample that was spiked after extraction (SAE). The SBE was prepared as a 1 mg/L sample (analyte + internal standard) that was extracted using SPE and eluent collected. The SAE however, was a blank sample taken through the extraction process, with the eluent collected and spiked with 1 mg/L of analyte and internal standard. Each extract was placed in a GC vial and analysed using the FT hydrocarbon monitoring method. Recovery was determined by a comparison of the area counts ratio of SBE and SAE.

$$\%Recovery = \frac{Area\ count\ of\ standard\ in\ SBE}{Area\ count\ of\ standard\ in\ SAE} x100 \qquad \text{Equation 3.1}$$

Below are the results of the recovery for the SPE clean-up procedure for the Fischer-Tropsch monitoring method.

Compound	Average area count SBE (AU)	Average Area count SAE (AU)	% Recovery
Decane	4523342	4054866	111.6
Dodecane-D26	3151933	2632711	119.7
Dodecane	5586369	4847397	115.2
Tetradecane	7329661	6396343	114.6
Hexadecane-D34	5441185	4542787	119.8
Hexadecane	8339935	7077021	117.8
Octadecane	8834142	7838540	112.7
Eicosane	8894969	7961376	111.7
Docosane	7585069	7249652	104.6
Tetracosane-D50	2494083	2199218	113.4
Tetracosane	6885430	6539872	105.3
Hexacosane	6342535	6430930	98.6
Octacosane	5841008	5207223	112.2

Table 3.7 A table showing the losses (recovery) of hydrocarbon material using the SPE clean-up method. Generally there is some over recovery, possible due to solvent evaporation in the final extract.

The results in table 3.7 suggest that there was no apparent loss during SPE clean-up process, for hydrocarbon material, with recoveries >98.6 %, with a high degree of confidence. However, the

positive bias associated is likely to be due to solvent (pentane) loss through evaporation and would explain for the over recovery of hydrocarbon material.

3.5 GC-TCD method: Validation summary for the detection of combustible gases in syngas.

Two batches of pure carbon monoxide, hydrogen and methane were run over two separate days with 10 repeat injections to evaluate retention time stability. This was deemed repeatable if the % RSD was below 1 % and reproducible if no adverse change in the repeatability was observed and if the value of the two batches were below the F-test calculated critical value (5.35).

The percentage area of the chromatogram was taken over two days. As the gases were pure, the expected value would be 100 % and therefore, the acceptance criteria for this was tighter than the GC-MS methods with necessary accuracy and precision >10 %.

Gas	Expected %Area count	Mean % Area count	Rt minutes	% RSD Batch Rt 1	% RSD Batch Rt 2	F-test value	Accuracy	Precision
H_2	100.0	97.14	0.49	0.72	0.95	1.66	-2.86	2.27
CO	100.0	96.3	0.91	0.53	0.83	2.00	-3.72	2.80
CH_4	100.0	97.4	1.01	0.73	0.47	2.63	-2.68	1.60

Table 3.8 A table showing validation preformed on simple gases on the GC-TCD by injecting 100 % gas standards 10 times on two separate days, to determine retention time stability, accuracy and precision.

The three gases assessed show good retention time stability with repeatable data observed shown by % RSD below 1 %. This method was also reproducible passing the F-test, with calculated values below the critical value of 5.35. Each gas showed good accuracy and precision with values below 10 %. These results indicate this GC-TCD method is suitable method for identifying small gases by retention time and universal detector with signal is proportional to analyte concentration, the gas composition can be determined accurately and precisely as molar %.

3.6 Conclusion.

Three GC-MS and a GC-TCD methods were successfully validated by meeting the figures of merit according to laboratory and UKAS procedure, they exhibited good precision and accuracy. For the GC-MS methods (SVOT, VOT and FT monitoring method) each demonstrated good linearity and accuracy of QC data furthering the confidence in quantifying targeted compounds within samples. The low sensitivity of the GC-MS methods demonstrated by LOQ and LOD data means that we can accurately quantitate and identify down to low µg/L levels, respectively. This will aid research if levels of targeted analytes (tars) are low. However, from previous experience, it is anticipated that samples are to be complex and concentrated, which will require dilution to bring them into a sensible working range.

For analysis of syngas using the GC-TCD because it uses a non selective detector, retention time stability is crucial determinant analyte identification. As with the other GC methods, retention time repeatability and reproducibility all passed acceptance criteria and showed good stability. This is also particularly useful for FT monitoring methods, whereby the similar spectra and low quantitation ions generated by alkanes, makes it often difficult to identify closely related hydrocarbon chain lengths. Retention time is a useful parameter to discriminate these hydrocarbons by using the reference standards as markers.

Chapter 4.

An initial investigation in enhancing the cleanliness of the pyrolysis/gasification process.

4.1 Sample preparation development for the removal of syngas impurities generated during pyrolysis/gasification.

There are several published methods (16,52,53,59), reported to remove impurities from the syngas. A common approach is the use of solvent (wet) 'scrubbers', typically involving methanol and water solvents. Solvent scrubbers remove impurities based on the solubility of impurities in the solvent with polar inorganic species, such as ammonia, chlorine, favouring polar solvents by interacting through hydrogen bonding, while non-polar organic tars, will favour non-polar solvents such as the oil-based scrubber, OLGA, governed by non-polar interactions such as Van der Waal forces (59). As detailed in chapter 1, methanol is often used to remove acidic gases such as hydrogen sulfide (H_2S) and carbon dioxide (126) along with light aromatics such as benzene, toluene, and light polyaromatics (16) when used under cryogenic conditions. Water scrubbers however, are useful for removing metallic and non-volatile organic analytes such as heterocyclic compounds (16,21,33). As described here, a combination of scrubber is often required for more complete syngas cleaning and an alternative solvent covering this range would offer reductions in cost and solvent waste. Based on the literature acetone been uninvestigated as a scrubber solvent and is a good candidate given that it can dissolve a wide range of organic compounds including polar and non-polar compounds. Other advantages; include a low toxicity, cost and volatility making it compatible with gas chromatography mass spectrometry (127). It is therefore is anticipated acetone be an effective solvent for removal of the broad class of organic impurities expected from pyrolysis and gasification. This chapter will look at the evaluation of acetone as a potential scrubber to

remove organic tars for the laboratory scale pyrolyser, particularly problematic volatile tars such as acetylene and benzene.

4.2 Results and discussion of solvent recovery.

Solvents acetone, methanol and water were compared to evaluate their effectivness at removing potential tar compounds (as described in methods section 2.4.1). Generally, all solvents showed good precision of recovery with a relative standard deviation (RSD) for compounds analysed on the volatile organic tar (VOT) and semi-volatile organic tar (SVOT) methods below 20 %. All solvents showed an RSD below 10 % for volatile and semi-volatile PAHs and below 20 % for light aromatic compounds, showing good method repeatability. However, the precision range for phenolic compounds was higher in methanol (RSD < 15 %) compared to that of water and acetone (RSD < 10 %).

Generally, as expected, water shows poor recovery for non-polar compounds (with a high log P or lipophilicity constant) and is particularly ineffective at removing volatile aromatic and PAHs with a boiling point greater than 340 °C showing recoveries between 1-14 % (see figure 4.1). However, smaller, more volatile PAHs (218-295 °C) showed improved recovery 24–43 %. Water can interact through π- H-O, non-covalent bonding which allows for a certain degree of solubility of smaller aromatic compounds however, aqueous solubility tends to be greater with smaller ring structures, and typically solubility decreases with addition of more rings (128,129). Water does however, show a marked improvement for the recovery for phenolic compounds, with recovery typically decreasing with increasing lipophilicity and trichloro compounds showing the lowest recovery of 49 and 45 %. This behaviour offers the potential to estimate the degree of recovery for uninvestigated compounds.

Compound class: volatile aromatic	Boiling point	Log P	Scrubber					
			Acetone		Water		Methanol	
			Mean %Recovery	% RSD	Mean %Recovery	% RSD	Mean %Recovery	% RSD
Benzene	80 °C	2.1	126.24	8.79	1.78	9.94	117.29	14.49
Toluene	111 °C	2.7	84.23	11.93	13.83	7.87	90.00	7.62
Chlorobenzene	131 °C	2.9	69.90	19.03	4.10	8.98	72.78	2.80
Ethylbenzene	136 °C	3.1	94.32	12.59	3.27	12.44	79.16	5.36
Xylene isomers	140 °C	3.2	94.90	13.24	5.84	11.41	79.45	5.72
Styrene	145 °C	2.9	99.13	14.27	5.05	14.55	75.65	10.66
1-Methyl-2-ethylbenzene	165 °C	3.5	117.90	16.16	1.48	9.32	63.16	3.37

Table 4 A table showing the comparison of recoveries of the volatile aromatic compounds with boiling point range between 80 to 165 °C, likely to be found in tars using different solvents scrubbers. Acetone has similar recovery for benzene and toluene to methanol. But overall acetone has better recovery for volatile aromatics than methanol and water.

Compound class: volatile PAHs	Boiling point	Log P	Scrubber					
			Acetone		Water		Methanol	
			Mean % Recovery	% RSD	Mean % Recovery	% RSD	Mean %Recovery	% RSD
Naphthalene	218 °C	3.3	93.41	3.98	42.68	5.24	44.90	5.98
Acenaphthylene	280 °C	3.7	68.84	9.44	36.14	4.77	66.35	3.82
Acenaphthene	279 °C	3.9	67.25	4.51	32.48	4.57	64.01	8.89
Fluorene	294 °C	4.2	63.58	6.15	23.51	6.47	64.82	3.34
Phenanthrene	339 °C	4.5	56.41	3.45	9.74	4.87	62.45	8.12
Anthracene	340 °C	4.4	60.70	3.48	8.81	4.77	59.90	5.27
Fluoranthene	375 °C	4.6	54.52	4.67	4.68	5.77	47.32	0.96
Pyrene	404 °C	4.9	54.52	5.50	4.59	3.91	46.71	5.72

Table 4.1 A table comparing the recovery of polyaromatic hydrocarbons between the boiling point range 218-404 ^{o}C using different solvent scrubbers. Acetone has similar recovery for the majority of PAHs in this range to methanol. Generally water has poor recovery PAHs within this range. Acetone typically has higher recoveries with good precision

Compound class: semi-volatile PAH	Boiling point	Log P	Scrubber					
			Acetone		Water		Methanol	
			Mean %Recovery	% RSD	Mean %Recovery	% RSD	Mean %Recovery	% RSD
Benz (a) anthracene	438 °C	5.8	56.07	5.73	3.67	4.99	29.23	3.20
Chrysene	448 °C	5.7	54.87	5.21	4.10	4.79	34.53	2.12
Benzo (a) pyrene	481 °C	6.0	55.00	5.48	4.12	7.67	33.21	2.81
Benzo (b) fluoranthene	496 °C	6.4	52.80	5.90	3.42	5.74	31.67	4.24
Indeno (1,2,3-cd) pyrene	524 °C	7.0	49.18	2.74	4.31	8.20	29.80	2.71
Dibenzo (a h) anthracene	536 °C	6.5	49.63	4.59	2.99	7.21	32.16	1.73
Benzo (ghi) perylene	550 °C	6.6	47.66	3.85	3.28	8.14	28.13	2.85

Table 4.2 A table representing a comparison of recovery of polyaromatic hydrocarbons between the boiling point range 438- 550 ^{o}C using different solvent scrubbers. Water is not effective at recovering PAHs within this range, while acetone shows overall better recovery for PAHs within this range, compared to methanol and water

Compound class: phenolic compounds	Log P	Boiling point	Scrubber					
			Acetone		Water		Methanol	
			Mean %Recovery	% RSD	Mean %Recovery	% RSD	Mean %Recovery	% RSD
Phenol	1.5	182 °C	82.47	0.79	86.66	9.84	68.35	5.04
2-Nitrophenol	1.8	175 °C	86.52	6.84	86.37	8.06	73.82	8.41
4-Methylphenol	1.9	191 °C	77.14	3.76	81.55	2.02	67.30	4.48
2-Methylphenol	2.0	202 °C	81.86	2.62	79.87	1.58	69.22	5.94
2-Chlorophenol	2.1	216 °C	84.31	6.23	85.86	2.53	68.19	1.92
2, 3 Dimethylphenol	2.6	218 °C	79.33	3.31	75.27	3.44	74.00	3.50
2, 6 Dichlorophenol	2.7	211 °C	84.90	5.89	72.42	5.00	70.67	4.05
2, 5 Dichlorophenol	3.1	220 °C	80.33	3.21	73.91	4.42	69.46	4.36
4-Chloro-3 methylphenol	3.1	235 °C	72.20	5.09	60.59	4.37	71.75	8.84
2,3,6 trichlorophenol	3.6	248-253 °C	73.76	4.17	44.54	3.21	76.39	1.37
2,3,5 trichlorophenol	3.8	272 °C	72.92	1.77	49.04	4.64	76.57	13.45

Table 4.3 A table detailing the recovery of phenolic compounds using different solvent scrubbers. Water and acetone show similar recovery for phenols. However, acetone has better recovery for the trichlorophenols compare to water. Methanol shows slightly poorer recovery for phenols, but comparable recoveries for the trichloro phenols to acetone.

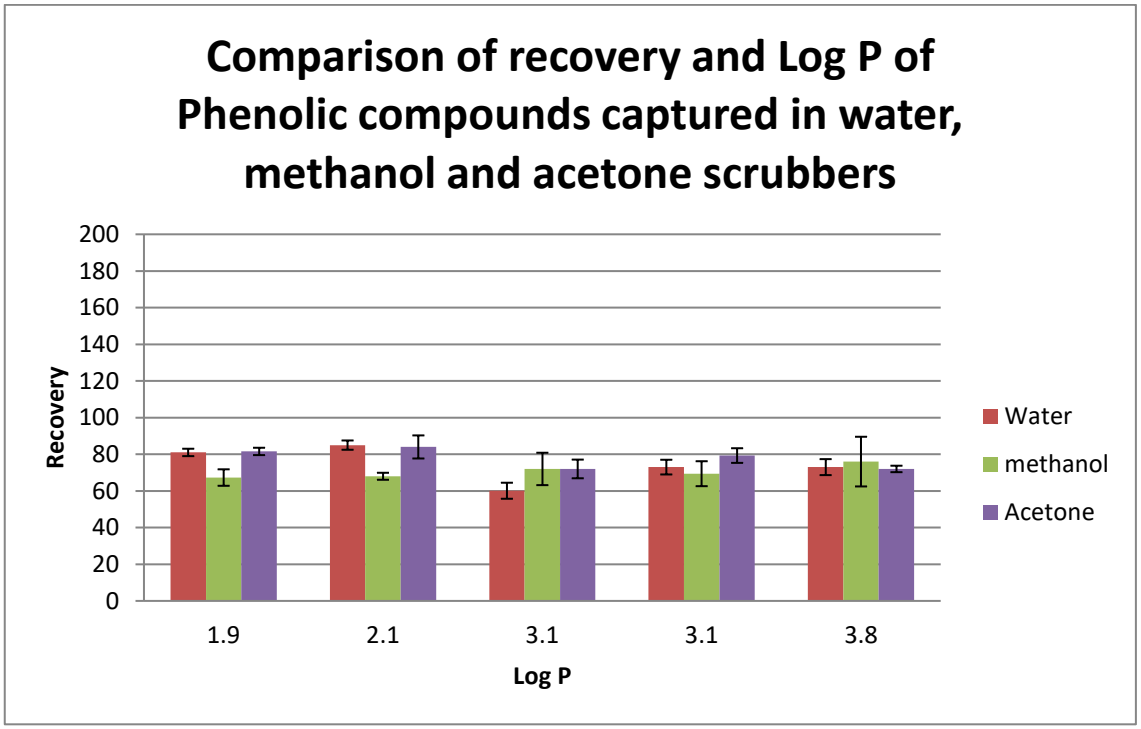

Figure 4 Figure showing the recovery of phenolic compounds using different solvent scrubbers; water, methanol and acetone, plotted against Log P (lipophilicity constant): 4-methylphenol (LogP 1.9), 2-chlorophenol (LogP 2.1), 4 chloro 3 methylphenol (LogP 3.1), 2, 5-dichlorophenol (LogP 3.1) and 2, 3, 5-trichlorophenol.

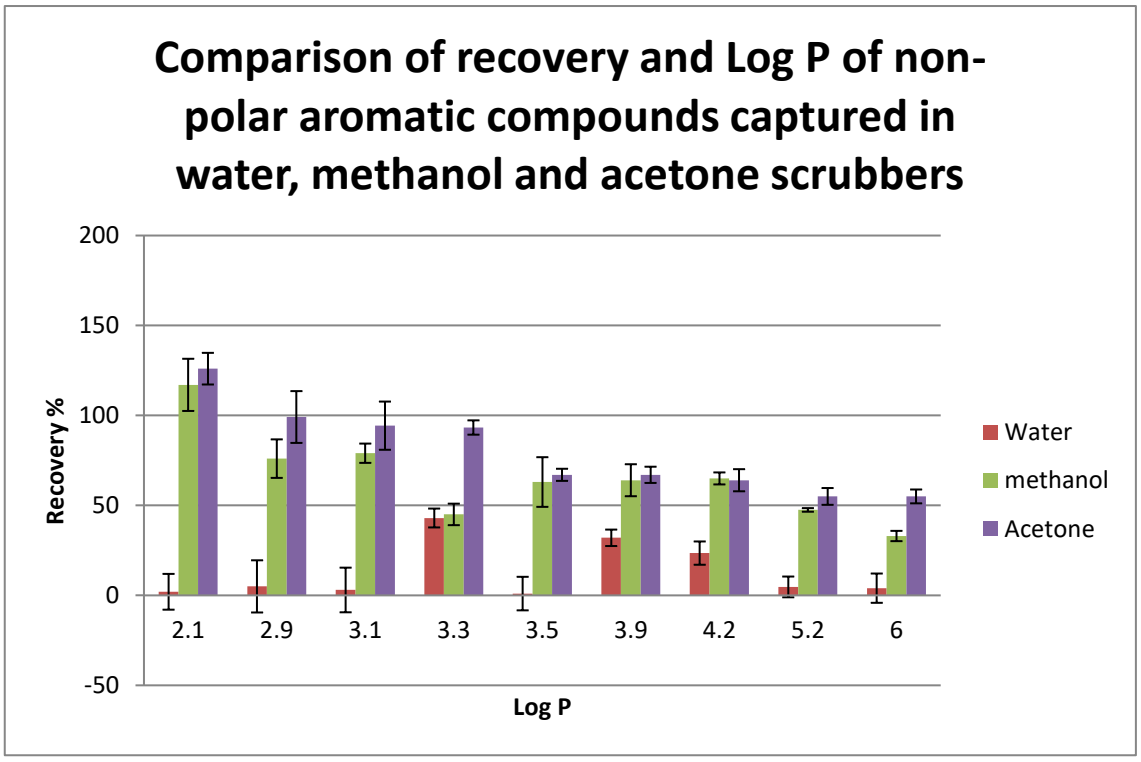

Figure. 4.1. A figure showing the recovery of non-polar aromatic compounds using different solvent scrubbers; water, methanol and acetone, plotted against Log P (lipophilicity constant):

b*enzene (LogP 2.1), styrene (LogP 2.9), ethyl benzene (LogP 3.1), naphthalene (LogP 3.3), benzene -1 methyl-2 ethyl (LogP 3.5), acenapthene (LogP 3.9), fluorene (LogP 4.2), fluoranthene (LogP 4.6) and benzo (a) pyrene (LogP 6.0). Generally as Log P increases so does the molecular mass of compound and therefore there is a trend between larger Lop P/ mw of compound and recovery. The larger compounds have larger Log P and reduced recovery. Acetone has greatest recovery compared to water and methanol within this compound class.*

Methanol and acetone also show good recoveries for phenolic compounds; acetone recovers between 72-86.58 % of phenols, and methanol 68-76.57 %. A comparison of the mean recovery of phenolic compounds between different solvent scrubbers was statistically evaluated using a t-test with the critical value determined as 2.78 at 3 degrees of freedom (see appendix 3). The results showed phenol, 2-chlorophenol, 2-methylphenol and 4-methylphenol were significantly different between acetone and methanol, with a greater recovery in acetone, while phenolic compounds, 2-nitrophenol, 3-methyl-4-chlorophenol, 2, 3-dimethylphenol and 2, 3, 5- and 2, 3, 6-trichlorophenol showed no statistical difference between acetone and methanol. This indicates that acetone is a preferred solvent for extracting small phenolic compounds versus methanol with a similar extraction performance to water solvent scrubbers (appendix 5.1.1). This apparent increase in extraction efficiency was in agreement with Wlóka and Smol, 2014 paper (67), and is likely that the larger dipole moment of acetone (2.7) over methanol (1.6) is one contributing factor for the increase in efficiency. Acetone is therefore, capable of interaction through stronger polarizing effects on -OH groups and π delocalised electrons of phenolic compounds. A second contributing factor is that acetone is also capable of increased dispersion forces due to the additional methyl group (CH_3COCH_3) whereas methanol can only has one methyl group (CH_3OH).

Acetone is particularly good at recovering non-polar compounds with recoveries from 48 to 118 %. However, as with methanol, recovery does appear to decrease with increasing log P (see figure 4) particularly for PAHs indicating that both hydrophobicity and molecular weight contribute to volatility. Generally, acetone has greater recovery for compounds with low to mid

log P values (and low to mid volatility) such as volatile aromatics and volatile PAHs, demonstrated by figures 4 and 4.1. For example, the semi-volatile polyaromatic hydrocarbons showed significantly higher recoveries using acetone (48 to 56 %) compared to methanol (28 to 35 %) indicating a more suitable solvent capture for these highly toxic and carcinogenic species. For single aromatic compounds, acetone appears to have the highest recovery ranging from 68.9 to 126.2 % while methanol recovery ranges from 63.16-117.3 %. However, this trend is less clear; specifically, observed recoveries using methanol and acetone solvents were not significantly different for single aromatic compounds with the exception for 1-methyl-2-ethyl-benzene, 117.9 % for acetone and 63.2 % in methanol. For the volatile polyaromatic hydrocarbons (218-404 °C) no significant difference in recoveries using acetone and methanol solvent was observed for acenaphylene to anthracene however, acetone showed significantly greater recovery of naphthalene (93 %), fluoranthene (55 %) and pyrene (55 %) compared to methanol (45, 47 and 46 %, respectively). Again, it is likely the larger dipole moment of acetone (2.7) over methanol (1.6) and the additional methyl group are both contributing factors for the increase in efficiency. These mechanisms interact with the PAHs through increased polarizability and dispersion forces. In Wlóka and Smol, 2014 paper (67), acetone had higher recoveries for PAHs than methanol (and IPA), and all solvents tested exhit a similar trend in PAH recovery, with increase in size (MW), there is an decrease in extraction efficiency, as the PAHs become more insoluble (higher log P).

In summary, acetone appears more effective than water and methanol in capturing non-polar aromatics and PAHs, with a likely cause being improved solubility of these compounds within acetone, and more similar hydrophobicity (Log P). Acetone also shows improved recovery of non-polar phenolic compounds again with solubility/volatility appearing key given the decrease in recovery with increasing hydrophobicity and mass. The apparent trends for acetone with physiochemical properties for PAH and phenolic compounds may offer an estimation/ predictor

of solvent scrubber efficacy for targetting the removal of these chemistries that have not ben characterised here.

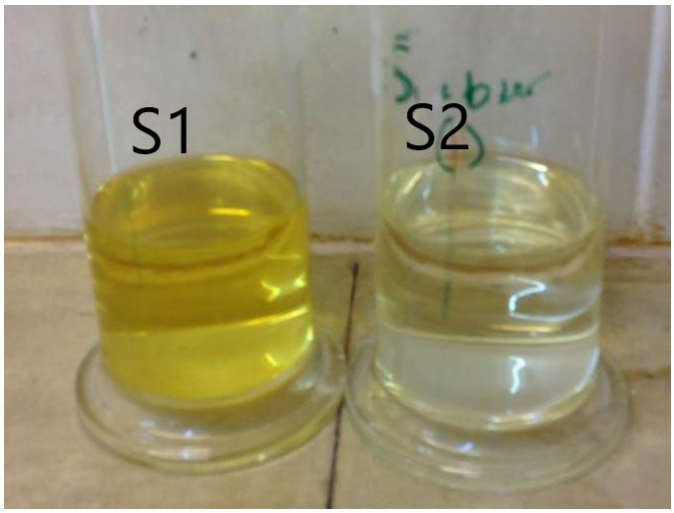

Figure 4.2 shows a photo of the typical impingers used in the experiment. S1 being exposed directly to the outflow gas and S2 placed sequentially to S1. Although there is some evaporation during the experiment the solvent reduction was not significant.

4.3 Comparison of methanol and acetone scrubbers for biomass feedstock.

Although acetone has been shown to recover a broader selection of chemistries used in the initial testing, there are many other breakdown products found in tars. To assess the performance of methanol or acetone for a complex sample containing a range of tar compounds, the rig was tested by pyrolysing 10 g of dried pine wood. This was placed in the reaction vessel and connected to an impinger containing either methanol or acetone. The reaction vessel was heated to 450 ± 10 °C and purged with nitrogen at 50 mL per minute to ensure an anoxic environment that could allow the movement of the gaseous compounds to the impinger. Following the reaction, the impinger scrubber solvent was tested for volatile and semi-volatile chemistries using the methods described in chapter 2 (VOT and SVOT). From initial observations both solvents dissolve the same range of tar compounds as seen in the overlaid the chromatograms of methanol and acetone, revealing a similar profile of tar compounds (see

figure 4.3). However, as expected from the preliminary experiment, the amounts (signal intensity) did appear to be different for each solvent.

To assess the recovery of specific chemical classes, extracted ion chromatograms of target *m/z* were used of representative compounds. For semi-volatile species the *m/z* of phenol, 2-methylphenol, 4-methylphenol, 2, 3-dimethylphenol, 4-chloro-3-methylphenol and naphthalene were used to generate the extracted ion chromatogram. This initially appeared similar between acetone and methanol however, upon closer inspection, it is clear that increased signal intensity is observed with the acetone extraction and is confirmed by the tabulated data with an approximate 200+ % fold increase in recovery.

Semi-volatile organic tars (SVOT)	Methanol scrubber pine wood tar conc^{n} mg/L	Acetone scrubber pine wood tar conc^{n} mg/L	% difference
Phenol	5.84	15.38	263.4
2-methyl phenol	3.43	10.69	311.7
4- methyl phenol	3.25	10.24	315.1
2, 3 dimethyl phenol	3.13	11.53	189.8
4 chloro 3 methyl phenol	0.79	2.53	368.4
Naphthalene	0.10	0.30	300.0

Table 4.4 A table showing the comparison of semi-volatile organic tars (SVOT) identified in the impingers from pyrolysis of pine wood at 450 °C. There is approximately 3 x higher concentrations for semi-volatile tars captured using acetone as a solvent scrubber.

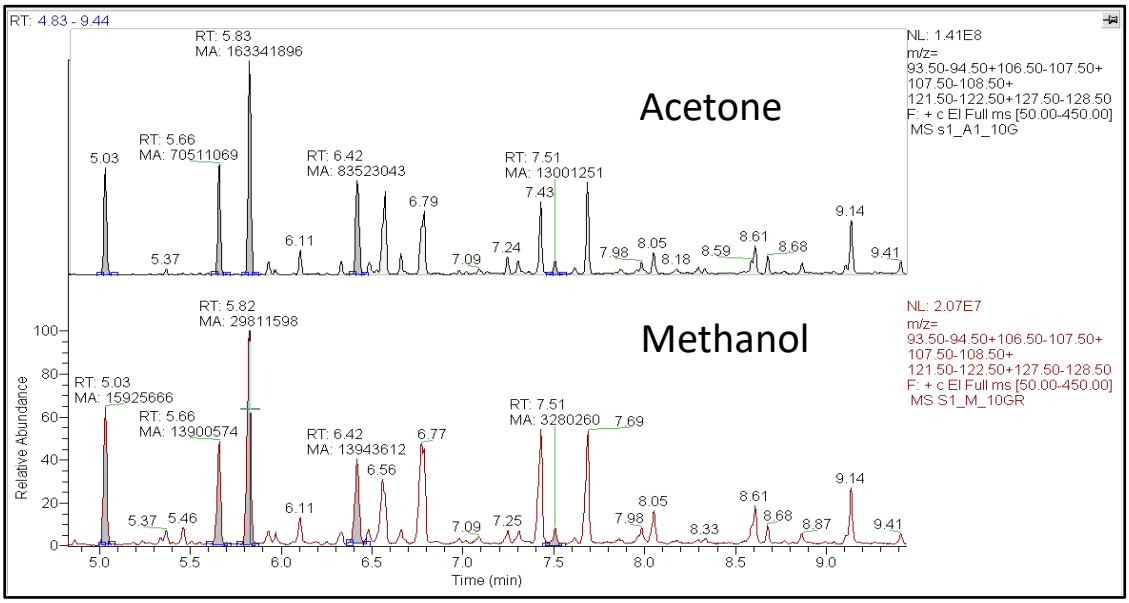

Figure 4.3. Figure showing an extracted ion chromatogram (XIC) of pyrolysis attempt at 460 °C using pine wood as a standard using the glassware setup. This was done to compare acetone and methanol as a solvent scrubber. This initial trial shows acetone (top black XIC) recovering more targeted semi-volatile compounds, phenol, 2-methyl phenol, 4-methyl phenol, phenol 2,3 dimethyl and phenol 4, chloro, 3 methyl due to increase in peak area count.

Volatile organic tars (VOT)	Methanol scrubber pine wood tar conc mg/L	Acetone scrubber pine wood tar conc mg/L	% difference
Benzene	2.10	4.50	214.3
Toluene	10.2	17.3	169.6
Benzene 1, 3 dimethyl	1.62	2.64	162.9
Ethyl benzene	0.98	1.86	189.8
Styrene	1.98	2.04	103.0
P-xylene	0.85	1.21	142.4

Table 4.5 A table demonstrating the comparison of volatile organic tars identified in the impinger from pyrolysis of pine wood at 450 ^{o}C. There is higher concentrations for volatile aromatic tars captured using acetone as a solvent scrubber, with benzene having double the concentration in acetone.

For volatile species, a similar pattern was observed with the ion chromatogram for acetone and methanol scrubbers. However, these showed significantly different signal intensities, with a >100 % increase in signal intensity for volatile species. It is apparent that acetone and methanol

dissolve the same range of tar compounds as seen in the overlaid chromatograms, suggesting similar tar compounds are extracted, however, further investigation shows that acetone recovers nearly double the amount of volatile organic tars (determined by VOT method) and triple the amount of semi-volatile organic tars (determined by SVOT method), correlating with our previous data using standard solutions. In summary, even for complex samples, acetone appears more effective in the removal of organic tars. Also noted was the apparent change in retention time drift for the very volatile organic compounds benzene to chlorobenzene using the different solvents (figure 4.4, with highlighted peaks) with compounds extracted using methanol eluting slightly early (0.06 minutes). However, statistical analysis of repeat injections, determined by an F-test, (at confidence level P 0.05 and critical value of 19.00) suggest that these were not significantly different.

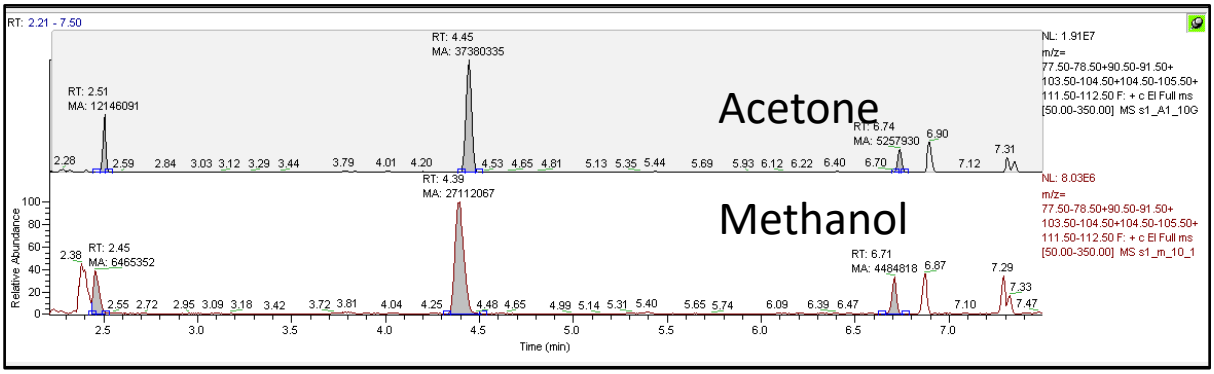

Figure 4.4. Figure of a XIC of pyrolysis attempt at 460 °C using pine wood as a standard using the glassware setup. This was done to compare acetone and methanol solvent to see which would be more effective solvent 'scrubber'. This initial trial shows acetone (top black XIC) recovering more targeted compounds, benzene, toluene, and benzene 1,3 dimethyl shown by an increase in area count of the integrated peaks. There is also a shift in retention of the volatile compounds time using methanol (red).

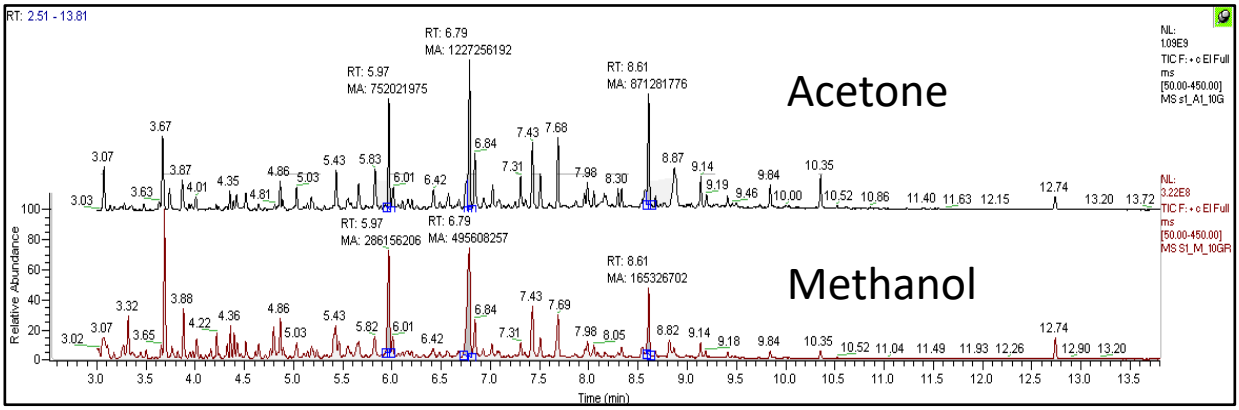

Figure 4.5 shows overlaid total ion chromatogram of pine wood pyrolysis at 460 °C comparing methanol (red) and acetone (black). The same compounds are detected in both solvents, except that the recovery is on average 5 times greater with acetone.

4.4. Recycling potential materials of the pyrolysis process.

4.4.1 Efficacy and re-use of acetone scrubber solvent for various applications.

In order to test determine the capacity of the acetone scrubber was tested using 3 different feedstocks was pyrolysed at 10 g increments and three scrubbers were run in parallel to capture tars following scrubber saturation. Once scrubber 1 was reaching its critical point, tar would then appear in scrubber two. It was at this point the scrubber was deemed to be 'saturated'. It was calculated in table 4.6 that 30 g of feedstock saturated 150 mL of acetone, by scaling this to a litre, (multiplying the mass of feedstock used by 6.67) that it would require 200 g of each feedstock before the acetone reached its critical value. For brown soil, the level of contamination was 25 % mass of oily sludge in the soil. Acetone had comparable capacities for all feedstocks tested, indicating a critical value of 6-10 g/L of tars. Although saturation values may be considerably larger as this method does not take account of compounds that are not compatible with GC-MS (highly polar and/or large >600 Da).

	Sample mass (g)	Volume of scrubber solvent (mL)	Concentration of tars (mg/L) (%total tars)			Saturation point of scrubber/ mg/L	Max mass of feedstock (g/L)
			Scrubber 1	Scrubber 2	Scrubber 3		
Pine (Acetone)	30	150	1219 (94 %)	73.8 (6%)	Blank	8,124.0	~200
Sludge (Acetone)	30	150	928 (96.6 %)	31.6 (3.4%)	Blank	6,186.0	~200
Brown Field soil (25% contaminated) Acetone	30	150	1584 (99.6 %)	6.10 (0.4%)	Blank	10,559.0	~200
Brown Field soil (25% contaminated) Acetone	60	300	1499 (99.2 %)	11.9 (0.8%)	Blank	9,990.0	~200

Table 4.6. Table illustrating the results of the scrubber capacity study performed using acetone and different feedstocks. Methanol was also investigated using pine wood as a comparison to benchmark the performance of acetone.

To investigate potential improvements of the waste management of acetone scrubbers through recycling, these were tested by pooling 100 mL waste acetone (brown in colour), containing tars from all feedstocks. These were placed within a round bottom flask and tested by GC-MS prior to recycling to determine the amount of volatile and semi-volatile analytes within the original scrubber. To test the remediation of the pooled scrubber, the sample was heated to 60 °C±5 °C with the vapour condensed as a clear liquid using a Leigberg condenser, leaving a brown residue behind in the round bottom flask; the liquid was then analysed by GC-MS for both volatile and semi-volatile organic analytes. From the data, recycling acetone in this manner proved effective in removing semi-volatile organics, reducing these levels from 36.35 mg/L to below the detection limits of our analytical methods (0.01 mg/L for SVOT and 0.1 mg/L for full scan of unknowns). The LOD for unknowns is speculated based upon $1/10^{th}$ the area count of the internal standard (spiked at 1 mg/L), peaks below deemed to difficult to distinguish from noise of coelutions. For the volatile compounds benzene and toluene, there was no significant reduction in their level; these two compounds have similar volatility/vapour pressure to acetone and may have been condensed during the recycling process. Other volatile compounds, ethylbenzene, p-xylene and styrene, showed a reduction of 67 %, 65.4 % and 82.4 %,

respectively, further supporting the suggestion. An added advantage of this approach is that the efficiency of remediation has the potential of being extended, using waste heat from pyrolysis to evaporate the solvent in the scrubber and recycle the acetone, further enabling the realisation of a greener process.

	Compounds identified	Concentration (mg/L)	
		Pooled scrubber pre-recycling	Recycled scrubber
VOT Target	Benzene Toluene Ethylbenzene P-Xylene Styrene	10.84 9.86 1.37 0.78 2.56	9.17 8.19 0.46 0.27 0.45
Total VOT		**25.41**	**18.54**
SVOT Targeted	Phenol 2-Methylphenol 4-Methylphenol 2,3-Dimethylphenol Napthalene 4-Chlorophenol Phenanthrene	3.89 2.00 2.62 2.23 0.60 0.70 0.35	ND ND ND ND ND ND ND
Total SVOT		**12.39**	**<0.01**
Non-targeted	2-Propyl-1-pentanol methyl ether N-Cyclohexyl propanamide 2,2,6,6-Tetramethy-4-piperidinone Cresol 2, 5-Dimethoxytoluene Isoegenol Andro-D-mannosan	1.09 6.21 2.41 8.69 1.19 1.37 3.00	ND ND ND ND ND ND ND
Total Non-targeted		**23.96**	**<0.100**

Table 4.7. A table describing the main compounds identified in the acetone pooled scrubber before and after recycling through distillation. For full list of compounds identified during pyrolysis of the different feedstocks please see chapter 5

Acetylene is a small unsaturated organic molecule generated as a minor product in pyrolysis and gasification. Although it has a significant heating value, it can become problematic if systems are connected to secondary processes that contain catalysts such as Fischer-Tropsch as acetylene can foul catalysts rendering them ineffective (16,53). Acetone is used to stabilise acetylene in its transportation due to its high solubility (130) and may be possible to use acetone as a scrubber to reduce acetylene concentration of syngas. To test this theory acetylene (60 mol

%) was bubbled through impinger(s) containing acetone and analysed in-line using GC-TCD. A reduction in acetylene was assessed by a reduction in peak area and molar fraction (% fraction) of the GC-TCD chromatogram. A trial using methanol was also included for a comparison as a common scrubber solvent. The data from these experiments (see table 4.8) indicate that acetone is a more effective solvent at reducing acetylene than methanol scrubbers. It is also apparent from Table 4.8 that sequential scrubbers containing acetone can provide the best means of recovering acetylene and effective the overall concentration by up to >90 %. This suggests acetone may be used as a cheap means of removing acetylene from syngas potentially extending the lifetime of catalysts used in down stream processes such as the Ficsher-Tropsch process.

Method of removal	Mean molar fraction		% Reduction of acetylene
	Before bubbling through acetone	After bubbling through acetone	
Acetone S1	63.00 %	43.95 %	30.2 %
Acetone S1+S2	60.00 %	27.10 %	54.84 %
Acetone S1+S2+S3	65.71 %	5.11 %	92.16 %
Methanol S1	60.03 %	60.20 %	Not effective

Table 4.8. Table illustrating the reduction of acetylene with alternative solvent scrubbers (methanol and acetone) and the number of impingers within the scrubber set-up (S1,S2,S3).

4.5 Tar generation with system temperature.

The presence of the different class of tars can be a useful indicator of system performance such as system operating temperatures. Aliquots of scrubber 1 were removed at different temperatures and analysed using the VOT and SVOT method to determine the emergence of various volatile and semi-volatile tar compounds fom different feedstocks. The results of the experiment, shown in Table 4.9, evidences the diversity of compound class detected in acetone that are consistent with its solubility range (volatile aromatics to less volatile polyaromatics and

polar compounds, such as sugar molecules and n-heterocyclic structures). These all have different volatilities and therefore, their generation in the process (and presence within the scrubber) depend on temperature.

Compound class	Pine wood	Sludge cake	Brown Field soil
Volatile aromatics	Emerge at 400 °C increasing in conc as temperature increases	Emerge at 300 °C increasing in conc temperature increases	Benzene increases throughout. Most volatile aromatics increase between 600-700 °C
Phenolic compounds	Emerge at 300 °C Continue to increase throughtout	Emerge at 300 °C Increases throughout	Not detected
Heterocyclic aromatics	Not detected	Emerge between 400-600 °C	Not detected
Light PAHs naphthalene to phenanthrene	Emerge between 400-600 °C	Emerge between 400-600 °C	Emerge between 400-600 °C.
Heavy PAHs above Pyrene	Not detected	Not detected	Emerge between 600-700 °C
Carbohydrates	Identified at 300 °C increasing in conc throughout temp profile	Not detected	Not detected
Furan Carboxyaldehyde	Present from 300 °C	Not detected	Not detected
Furan methanol and furanone	Above 700 °C	Not detected	Not detected
Light hydrocarbon (alkane and alkenes)	Not detected	Not detected	Not detected
Heavy Hydrocarbon	Not detected	Not detected	Not detected

Table 4.9. A summary of emergence of different compound classes during the slow pyrolysis of Pinewood, sludge filter cake and brown field soil. For full list of compounds identified during pyrolysis of the different feedstocks please see chapter 5.

For example aromatics generated in pinewood and sludge start at 300-400 °C, which indicates the evolution from the material as part of the charring process. In brown field soil, aromatics are generated at higher temperatures 600+ °C which indicates their generation requires an alternative pathway to pinewood and sludge, and therefore likely to be observed due to tertiary reactions (34). During sludge cake and pine wood pyrolysis, phenols were observed from 400 °C and continued to increase in concentration with increasing temperature. This is consistent with the thermal decomposistion of lignin (200-500 °C) (76,77) which is thought to be the main source of phenolic substances within feedstocks. Another compound class observed at relatively

low temperatures (<300 °C) in pinewood are carbohydrates (sugar molecules). In particular, degradation products of hemicellulose (found in pinewood) are observed. These include a pentose sugar anhydro-d-mannosan (75) and arabinose (55,75). As described in the introduction, sludge cake is more complex sample with additional substances expected. For example N-heterocyclic aromatics are observed around 400 °C. These may arise from secondary reactions of the tars, however, certain heterocyclic compounds such as heterocyclic ethers only form at high temperatures (above 700 °C) (34,89). Specifically these are observed to increase with temperature and therefore, it is likely that these compounds may arise from decomposition of proteins and nitrogen containing compounds, potentially from the digestive microbes used in the waste water treatment process.

4.5.1 Tar recycling for bio-oil generation.

A large proportion of tars generated in pyrolysis have the potential to be condensed to form bio-oils. This maybe possible through the recovery of tars or simply by adding a drop out condenser before the scrubbers to convert the tars into bio-oil, thereby further increasing the lifespan of the scrubber. To test this approach 20 g of pine wood sample (as it produced a wide variety of organic tar compounds) and a blank impinger 1 was used to collect and condense the tars to form brown bio- oil. A second impinger containing 150 mL acetone was used as the first scrubber to monitor any tars that were not condensed in impinger 1.

Bio-oil collected in impinger 1 was diluted by a factor of 100 in acetone and analysed using the SVOT method for the quantitation of semi-volatile organic compounds within the bio-oil. The compostion of the bio-oil contained typical breakdown products associated with biomass as discussed in the introduction chapter. These included; furfurals, furanone and furncarboxaldehyde, derived from decomposition of cellulose and hemicellulose, and phenolic compounds, such as p-ethylguaicol and 2-methoxyphenol from the decomposition of lignin. The

compounds identified in this bio-oil are typical and have 45-50 % oxygen content (15). This results in bio-oils having a low heating value due the high oxygen and water content. Further to this, as the bio-oil ages over time aldehylic compounds may react to form more non-volatile species, forming waxes also contributing to lower heating value of bio-oils (15).

Bio-oil	Compounds identified	Concentration mg/L	Corrected value mg/L
Targeted SVOT	Phenol 2-Methylphenol 4-Methylphenol 2,3-Dimethylphenol Naphthalene	6.95 1.75 1.79 0.74 0.025	695.00 175.00 179.00 74.10 2.50
Non targeted	Furfural 2-Furanone 2-Furancarboxaldehyde Cyclotene 2-Methoxyphenol 4-Methoxy-3-methylphenol Methenamine P-Ethylguaicol	4.49 1.24 1.30 0.66 2.40 2.51 0.79 0.38	449.02 123.89 130.33 65.97 240.26 251.31 79.47 37.62
Total		25.03 mg/L	2502.50 mg/L
Total per gram of wood			125.15 mg

Table 4.10. Table showing the concentration of the major compounds found in the bio-oil derived from pine wood pyrolysis. For full list of tars identified in pine wood, please see chapter 5.

The condenser experiment was repeated and the total amount of tars generated was found to be 72.34 mg. Of this 55.18 mg was condensed in the bio-oil in impinger 1 (condenser) this equating to roughly 76.3 % of the tars generated in this process, showing the potential of condensing in removing these substances. An upshot of this finding is that the amount of solvent required for the scrubber should be would be significantly less (76.3 % less).

	Condenser1	Scrubber 1	Scrubber 2
Targeted VOT	10.206 mg	7.59 mg	<0.001 mg
Targeted SVOT	9.03 mg	0.98 mg	<0.01 mg
Unknown	35.94 mg	8.59 mg	<0.1 mg
Total	55.18 mg	17.16 mg	
%	76.28 %	23.72 %	

Table 4.11. Table listing the total mass and percentage of tars found in condenser 1, scrubber 1 and 2. A large proportion of tars especially SVOT reside in the condenser.

4.6 Conclusion.

Acetone has proved to be a more suitable solvent for recovering organic tars in comparison with water and methanol. Generally, all solvents exhibit low % RSD (< 15 %) over all compound classes, suggesting that extraction and preparation of the solvents was repeatable, suggesting both preparation and analytical methods are robust which allows for confidence in the results. As expected, water proved to be ineffective at removing hydrophobic and volatile compounds such as single ring aromatics and polyaromatics. However improved recoveries were observed for polar phenols (log P <3.1 with recovery >61 %). Similarly methanol and acetone showed good recovery for phenolic compounds including the more non-polar chlorinated phenols (log P 3.1-3.8) with recovery ranging between 72-133 % for water, and 68 -117 % for methanol. Methanol and water have both polar and non polar moeities and interaction is likely influenced through both functionalities. However, acetone proved more effective at the removal of semi volatile PAHs (438 to 550 °C) over methanol capable of dissolving more hydrophobic compounds. The low % RSD generated by acetone in this investigation, suggests that acetone is is a more reliable extraction method compared to water and methanol as it is more reproducible. Acetone scrubbers work most effectively when placed in series and has shown the ability to remove >90 % of organic tars Where three acetone scrubbers were placed in tandem, over 90 % of the tars were identified in the first scrubber and the third scrubber remained blank, ensuring effective tar removal. Similar results were identified in the investigation of acetylene removal. Acetylene has proven to be a difficut compound to remove using conventional means of syngas cleaning due to its high volatily and low molecular mass. In this investigation, acetylene was shown to have some solubility in acetone at ambient temperastures and pressures with recovery of acetylene > 90 % using three scrubbers in series. Finally, remediating acetone using evaporation and condensation has proved that >99 % of semi-volatile tars can be

recovered as a bio-oil, conversley, condensing the tars directly in the first place can also improve the lifespan of the acetone up to >75 %.

Chapter 5:

Pyrolysis/gasification of pine wood, brownfield contaminated soil and sludge filter cake.

The analytical and sample preparation methods developed in chapters 3 and 4, were used to investigate tar production on three feedstocks. This involved thermochemically heating waste material above >700 °C and connecting the outflow gas to impingers (scrubbers) containing acetone with the final output flow connected to GC-TCD for syngas characterisation. Analysis of the acetone scrubbers for the identification of tars was undertaken by GC-MS and pinewood was used as a biomass standard to ensure the method was functioning analysing the acetone for typical biomass tars. Two uncharacterised feedstocks, municipal sludge cake and brownfield soil (10 % contamination with petrochemical oily waste), were also analysed using this setup. The final output gas flow after the impingers was connected to GC-TCD for syngas characterisation of each feedstock. Prior to thermochemical treatment, the feedstocks were characterised for semi-volatile content using solvent extraction along with any remaining char after thermal and analysed using GC-MS (see figure 5.1).

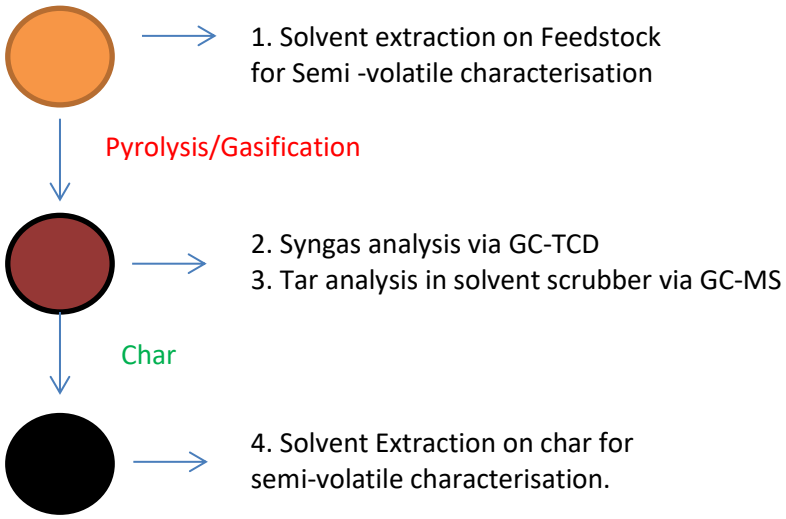

Figure.5 A flow diagram illustrating the typical analysis carried out on each feedstock. At point one a sample of virgin feedstock is solvent extracted for analysis of semi-volatiles. At point 2 and 3, the material is pyrolysed or gasified, the syngas is analyses for simple gases using GC-TCD, while solvent scrubbers are analysed for organic tars. Point 4. Is solvent extraction of the char, to analyse the semi-volatiles associated with char.

5.1 Feedstock characterisation.

Pine wood, municipal sludge cake and a sandy loam contaminated with oily sludge were subjected to slow pyrolysis and gasification. The pyrolysis conditions followed a temperature ramp to 700 °C at 20 °C/min with nitrogen as a carrier gas (at 100 mL per minute), to remove any products and keep the system under anoxic conditions. Gasification, was performed using the same parameters but using compressed air (50 mL per minute) as the carrier gas (and oxidant). The feed stocks used in the pyrolysis and gasification experiment were characterised using a number of parameters:

- Moisture content: 20 g of feedstock was dried at 100 °C for 6 hours, the mass loss was determined gravimetrically and converted into a percentage
- Calorific value (CV): 0.1-0.9 g of dried material was combusted in a bomb calorimeter to determine the calorie content of the feedstock in MJ/kg
- Solvent extraction of feedstock: This was done to characterise the semi-volatile content of the feedstock which can be used to explain the origins of the organic tars formed in the thermochemical process
- Nitrogen content of sludge cake; This was determined by Kjeldahl method (see appendix 2)
- Total extractable lipophilic compounds on sludge filter cake (see appendix 2)

5.1.1 Pine wood characterisation: pre-pyrolysis.

Off cuts of planed pine wood plankswere rasped by to produce saw dust and sieved to below 2 mm. The moisture content was determined gravimetrically, measuring the mass of 10 g of pine wood before and after heating at 105 °C for 2 hours and moisture content was found to 11.3 %. The calorific value (CV) was performed using a bomb calorimeter; and measured to be 18.67 MJ/kg, this is typical of wood (18-20 MJ/kg (73)). To characterise the semi-volatile constituents

of pine wood (prior pyrolysis), two extracts were performed, using two different solvents, pentane and acetone. A 0.5 g amount of solid material was extracted with 10 mL of each solvent and d8 naphthalene and triphenylethylene added as internal standard prior analysis via SVOT GC-MS method.

The compounds were identified by their spectrum and compared to NIST data base and annotated total ion chromatograms for each feedstock are located in appendix 1. As some chromatograms are complex, selected compounds have been classed into groups based of chemical similarity, for ease of data handling.

The semi-volatile species within the pentane extract consisted of two identifiable compounds only: labd-8-(20)-14-dien-13-ol (13S) and dehydroabietic acid. These are both common diterpenes found in wood extractives as discussed in chapter 1. The main constituent of wood are lignin, cellulose and hemicellulose, however it is likely that the extracts contain substances from other components of biomass. For example, large macromolecules would not be sufficiently volatile to be analysed *via* GC-MS or extracted with these solvent. In addition to pentanes, an acetone extraction was performed to see if more extractives could be identified as this solvent would be more suitable in removing more polar compounds due to its solubility range. This proved correct with a greater breadth of compounds extracted and in particular a range of terpenoids expected within soft wood (see table 5)

Class	Compound	Concentration mg/kg
Mono-terpenes	Methylcyclooctane α-Pinene β-Pinene D-Limonene α-Terpineol	2.11 0.40 0.36 0.70 1.74
Sesquiterpenes	Germacrene D Cembrene Geranyllinalool Dihydro-β-ionone	1.88 5.93 4.45 5.99
Diterpenes	Hyodeoxycholic acid Dehydroabietal Dehydroabietic acid	6.17 1.70 9.22
Other compounds	1-Decanol 2,4-Bis(1,1-dimethyl)-phenol 2-Undecanol n-Hexadecanoic acid Phalic acid	14.10 4.20 5.26 3.43 1.20
Total		68.84

Table 5 A table illustrating the extractive compounds and their approximate concentration determined by area count comparison to nearest intenal standard in the acetone extraction of pine wood.

It is anticipated that some of the tars generated in the pyrolysis of pine wood may arise from the volatising or degradation of the terpenoids and will be identified in the solvent scrubber.

5.1.2 Brownfield soil characterisation: Pre-pyrolysis.

A sandy loam contaminated with 10 % mass of oily sludge aquired from a site in South Wales was used for the following investigation and the CV measured to be 7.02 MJ/kg. Due to the likely hydrophobic nature of oily sludge, the sample was extracted in equally non-polar solvent, whereby 0.5 g of brown field soil was solvent extracted using 10 mL pentane and run on GC-MS spiked with d8 naphthalene and triphenylethylene (internal standards) and analysed on SVOT GC-MS method.

Annotated total ion chromatograms for are found in appendix 1.0. The compounds were identified according to their EI spectra and compared to NIST database (see table 5.1).

Retention time (min)	Extracted compound identified	Concentration mg/kg
8.81-13.63	Volatile PAHs (bp < 400 ° C)	2000.0
15.74	Benz(a)anthracene	106.0
15.88	Chrysene	112.0
19.52	Benz(b)fluoranthene	114.0
19.62	Benz(a)pyrene	98.0
22.39	Indeno (123)-cd pyrene	45.2
22.41	Dibenz(ah)anthracene	14.00
23.12	Benzo(ghi)perylene	43.6
	Total PAHs	**2528.0**
	Total mass PAHs	**$1.26*10^6$ mg/kg**

Table 5.1: A table showing the compounds and their approximate concentrations identified in the pentane extraction of 10 % brown field contaminated soil. After calculation the concentration of oil appears to be 12.6 % by mass which analogous to the contamination level of 10 %.

The overal contamination level of brownfield soil is particulary high with polyaromatic hydrocarbons (PAHs) consistent with petroleum waste oily sludge. These compounds have known harmful, environmental and human effects and are very stable as they are typically generated through high temperature processes (129). It is anticipated that pyrolysis temperatures may not be sufficient to degrade these PAHs, but could be used to remediate the contaminated soil and capture these harmful compounds so they can be disposed in a safe manner (or reused as a fuel).

5.1.3 Sludge cake characterisation: Pre-pyrolysis.

Secondary treated sludge cake was obtained from a UK wastewater treatment works and a plant from Ghana. The UK material had a similar texture to soil with 36 % moisture content. Calorimetry of the dry material gave a CV of 12.15 MJ/kg, similar to values of digested sludge 10.5 MJ/kg (80). The nitrogen content was determined to be 2.5 mg/kg and total extractable lipophilic compounds were 1160 mg/kg. Due to the high lipophilic content, the sample was extracted in a non-polar solvent. Again, the semi-volatile constituents of this sample was characterised by taking 0.5 g of sludge cake and solvent extracted using 10 mL of pentane and spiked with internal standards d8 naphthalene and triphenylethylene and run on SVOT GC-MS

method. The chromatograms for UK sludge cake are rather complex, some compounds have been classed into groups and annotated total ion chromatograms are included appendix 1.0. The results showed that it contained a high percentage of mixed hydrocarbons (including alcohols) possibly derived from fatty acids, and sterol compounds likely to have a dietary origin.

Retention time (min)	Extracted compound identified	Concentration mg/kg
8-11.20	Mixed hydrocarbons	143.17
11.6-13.45	Long chained aromatics	24.00
18.98	Squalene	11.02
21.15	Cholestan-3-ol	30.24
21.53	Cholestan-3-one	21.70
	Total Semi-volatiles	**230.13**

Table 5.2 A table listing the compounds and their concentrations identified in the pentane extraction of UK sludge cake. The semi volatile composition of UK sludge cake mainly consists of long chain fatty acids and other lipid soluble molecules such as cholesterol and unsaturated hydrocarbons. These are typical biological fats derived from dietary excretion.

The Ghana sludge cake was consistent with grassy biomass material and a moisture content of 13-20 %, with a CV between 13 and 18 MJ/kg. This is similar to untreated raw sludge (17.5 MJ/kg) (80) and had a higher CV *versus* UK sludge cake (12.15 MJ/kg). The nitrogen content also significantly higher at 3.5 mg/kg (UK sludge cake, 2.5 mg/kg) and with a lower extractable lipid content of 800 mg/kg (see appendix 2.0).

Simlarly to the UK sludge cake, 0.5 g of Ghana material was solvent extraction using 10 mL of pentane internal standard added and analysed on SVOT GC-MS method. The chemical composition of Ghana sludge cake contained a high amount of sterols; coprosterol and hyodeoxycholic acid. These may originate from the dehydrogenation of cholesterol or found in intestines of higher animals and is directly excreted in faeces (131,132), respectively. Stimansol, is a common plant phytosterol indicative of a high amount of dietary vegetables (133). The minor amounts of fatty acids and phenols are again likely to originate from the plant material

extractives or biological origin. The physical and chemical differences between Ghana and UK sludge cake may indicate either a difference in dietary composition or variation of treatment process procedure between countries, with Ghana having a shorter microbial residency time (or lower content) in the digesters (13,86).

Retention time (min)	Extracted compound identified	Concentration mg/kg
5.79	P-Cresol	2.15
11.45	Undodecanoic acid	13.25
21.08	Coprsterol	2228.0
21.47	Hyodeoxycholic acid	408.0
23.13	Stigmastanol	836.0
	Total Semi-volatiles	**3487.4**

Table 5.3 A table demonstrating the main constituents found in the solvent extraction of sludge filter cake from Ghana.

5.1.4 Summary of Feedstock extracts: semi-volatile characterisation.

- Pine wood extracted contained typical compounds associated with the 'extractable' compounds which were various alkaloids.
- Brown field soil contaminated with oily sludge extract contained large amounts of polyaromatic hydrocarbons (approximately 12.5 % by mass) which are typical class of compounds associated with petroleum waste (134).
- Sludge cake from the UK comprised of mainly long chain hydrocarbons and some cholesterol likely to be derived from dietary and microbial origin but have become modified from the anaerobic digestion process (decarboxylation of fatty acids to HC).
- Sludge cake from Ghana comprised of fatty acid and sterols likely from a dietary origin. The difference in chemical finger print may indicate differences in the treatment parameters between the two countries.

5.2 Characterisation of biochar generated following pyrolysis of feedstocks.

The solid material produced by thermochemical treatment was solvent extracted in the same manner as the 5.1. It was anticipated that the majority of the char is carbon with some carbonate compounds (34) however, ash from gasification should contain little or no organic compounds as these are oxidised in the process but are typically abundant in metallic and inorganic carbonates (34). This important in order to understand the viability and usability of the waste materials for potential re-use with other applications.

5.2.1 Characterisation of pine wood char.

0.5 g of the char, was solvent extracted using 10 mL pentane and and analysed using the SVOT GC-MS method. To quantify the chemistries, d8 naphthalene and triphenylethylene were again spiked as internal standards and added to the extract.

Retention time (min)	Extracted compound identified	Concentration mg/kg
7.5-8.0	Phytols (Branched unsaturated alcohol)	15.33
8.65-10.66	Branched long chained alcohols	33.50
12.84	Pyrene	4.00
	Total	**52.83**

Table 5.4 A table showing the main compounds associated with the biochar after pyrolysis of pine wood. The composition is different from the original extract on virgin pine wood.

Of the chemistries observed it was apparent that the original terpene compounds were no longer detected but branched alcohols and pyrene were prominent constituents of the sample. A likely cause of this is the original macromolcules of pinewood have degraded from the feedstock forming alternative smaller semivolatile compounds.

This conversion results in minimal change in the overall total semi-volatile content of the biochar 57.1 mg/kg to 52.83 mg/kg. The biochar from pine wood was also tested for its calorific value (CV) indicating that this material has maintained the calorific content with 90.8 % (16.89 MJ/kg) of the original feedstock (18.60 MJ/kg) and could offer potential as a feedstock for an alternative thermal process. Unlike pyrolysis, gasification of pine wood produced an ash sample and this

was solvent extracted for characterisation using the SVOT method. Interestingly this sample did generate any semi-volatile compounds that were detectable, suggesting oxidation of the organic material. This data indicates that we can tailor the thermochemical process to target the recycling of organic material and produce a high CV (material) if required.

$C+½\,O_2 \rightarrow CO$ (-111 MJ/kmol) oxidation of char

$C_xH_y + \left(\frac{x}{2}+\frac{y}{4}\right)O_2 \rightarrow xCO + \frac{Y}{2}\,H_2O$ oxidation of tar

5.2.2 Characterisation of brown field 'char'.

Similary to pine wood, 0.5 grams of the remaining brown field soil was characterised to understand the further useability of this waste sample. To do this, again 0.5 g of 'char' was solvent extracted using 10 mL pentane and analytes quantified using d8 naphthalene and triphenylethylene as internal standards.

The residue remaining from brown field soil pyrolysis showed primarily PAH compounds similar to the pre-pyrolysed soil. However, the overall content has shown a significant decrease of 80.5 % from the original feedstock (2528 mg/kg) to the 'char' residue (493.03 mg/kg) suggesting that pyrolysis may be a means of remediating contaminated soil of carcinogenic compounds. The residue was also tested for CV however there was no successful ignition of the material, suggesting a very low CV. This indicated that the remaining material from pyrolysis of brown field soil had a low carbon content potentially containing high levels of inert silicates resulting in a low CV. This is important in understanding the useability of this sample as data suggests that the remaining material from brown field may offer little or no calorific value as a feedstock, but pyrolysis could be used to minimise health risks involved in the disposal of contaminated soil.

Retention time (min)	Extracted compound identified	Concentration mg/kg
8.2-14.0	Mixed PAHs	291.70
15.90	Benz(a)anthracene	43.0
16.04	Chrysene	25.4
19.63	Benz(b)fluoranthene	45.0
19.74	Benz(a)pyrene	54.5
22.56	Indeno (123)-cd pyrene	18.0
22.65	Dibenz(ah)anthracene	5.20
23.32	Benzo(ghi)perylene	10.23
	Total PAHs	**493.03**

Table 5.5. A table showing the main compounds identified in the remaining soil after pyrolysis of brown field soil. The composition similar to the extract preformed on the virgin soil, however, the amount of PAHs has significantly reduced.

5.2.3 Sludge cake biochar characterisation.

The content of sludge cake contained high amount ofs mixed hydrocarbons from the analysis completed on the pre-pyrolysis feedstocks. The results indicated varying amount of long chain alcohols, branched and linear hydrocarbonss with phytosterols, indicative of differing degrees of microbial treatment or dietary content. It was therefore anticipated that these feedstocks would result in quite different char profiles. As before, these were solvent extraction (0.5 g of sludge cake biochar and ash) after pyrolysis and gasification. The extracts were analysed on SVOT GC-MS method and spiked with internal standard to quantify semi-volatile compounds.

Retention time (min)	Extracted compound identified	Concentration mg/kg
5.15-9.62	Mixed linear and branched alkanes	22.27

Table 5.6 A table of compounds identified in the solvent extraction of UK sludge cake after pyrolysis. Char contains a selection of hydrocarbons, likely to be derived from the fatty acids found in the extract on pre-pyrolysed sample.

After pyrolysis of UK sludge 90.3 % of the semi-volatiles present were decomposed, leaving behind 9.7 % in the char (22.27 mg/kg). The remaining semi-volatiles were identified as a mixure of linear and branched hydrocarbons similar to the pre-pyrolysed feedstock, but at reduced levels. The CV of the biochar was determined to be 63.8 % (7.75 MJ/kg) of the original value of

the feedstock (12.15 MJ/kg) suggesting that the char still has considerable value as a feedstock for alternative thermal processes.

However, following air gasification of UK sludge, ash formed (Grey colour) rather than char (black) and this was found to have a very low level of semi-volatile content below the detection limit of the full scan method (SVOT). This again indicates that during gasification, oxidation of the organic material of the feedstock commences leaving behind the inert inorganic material.

In addition to sludge cake from the UK plant, a sample was tested from a treatment works in Ghana which was prepared in a similar manner. The extraction of the initial material showed significant differences from the UK material and therefore it was considered important to characterise the biochar generated from the Ghana sludge cake. The biochar again was solvent extracted in the same manner as the UK sludge cake biochar and analysed accordingly. Unlike the UK sludge cake biochar, Ghana biochar was was high in phenols (118.8 mg/kg), volatile aromatics (89.05 mg/kg) with lower amounts of naphthalene (21.94 mg/kg) and isoeugenol (16.67 mg/kg). The phenolic compounds are typical breakdown products of lignin (76) and indicative of leaner treatment of the sludge cake. The presence of volatile aromatics and naphthalene arise from secondary reactions and within the biochar (34). The Ghana sludge cake biochar was also tested for calorific content and the CV was determined to be 12.24 MJ/kg. This is higher than the biochar derived from UK sludge (7.72 MJ/kg) potentially due to the suggested higher plant biomass and semi-volatile content. Therefore Ghana biochar has considerable calorific value and could potentially be used as an alternative feedstock for thermal processes.

Retention time (min)	Extracted compound identified	Concentration mg/kg
3.94-4.22	Volatile aromatics	89.05
4.97-7.67	Phenol and methylated phenols	118.8
8.60	Isoegeuol	16.67
7.53	Benzyl nitrile	17.65
8.20	7-Methyl-Indolizine	13.73
6.77	Naphthalene	21.94
	TOTAL	277.84

Table 5.7 A table of compound identified in the solvent extraction of Ghana sludge cake after pyrolysis. Char contains large proportion of mixed phenols, similar to the ones identified in pine wood pyrolysis. It is likely that these arise from breakdown of lignin found in dietary plants.

5.2.4 Summary of char characterisation: extractable compounds.

- The extract of the pine-wood biochar contained branched alcohols (unsaturated and saturated) and pyrene (four ring PAH). The original alkaloids found in the feedstocks were no longer detectable suggesting that they have decomposed or vaporised and are no longer present on the material. Ash from pine wood gasification contained no detectable organic compounds.
- Brown field contaminated soil 'char' was consistent with PAHs of the original feedstock, but at reduced concentration (80.5 % less). This suggests majority of the PAHs were vaporised during the thermal treatment of the soil.
- UK sludge biochar contained a mixture of hydrocarbons consistent with the original sample, but fewer oxygen containing hydrocarbons (alcohols) suggesting the cleavage of C-O bonds during heating. The ash generated in gasification contained no detectable organic compounds suggesting oxidation of the biochar.
- Extraction of sludge cake biochar from Ghana contained a wide range of organic compounds; volatile aromatics, phenolics, nitrogenous compounds and naphthalene. This suggests that the variety of compounds generated between the two sludge cakes

are directly linked to the differences in the initial feedstock composition and may be the result of the differences of sludge cake preparation between Ghana and the UK.

Sample type	Lipid/ semi-volatile composition	Nitrogen content	CV feedstock	CV biochar	CV-syngas
Brown field	PAH 2.5 g/kg (solvent extraction)	N/A (Kahjel)	7.02 MJ/Kg	N/A	0.725 MJ/ m^3
Pine wood	Extractives terpenoids such as dehydroalbeitic acid (solvent extraction) 195.84 mg/Kg	N/A	18.67 MJ/kg	**16.89**	6.34 MJ/m^3
UK sludge	Lipids soluble compounds 230.13 mg/Kg	2.5 mg/kg	**12.15**	**7.75**	3.04 MJ/m^3
Ghana sludge	Sterols 3.5 g/Kg	3.5 mg/kg	18 MJ/kg	**12.24**	**6.4**

Table 5.8 A summary table of the typical chemical composition and energy content of the feedstocks that were pyrolysed, also listed is the energy values of the products generated.

5.3 Syngas analysis of the feedstocks.

5.3.1 Thermochemical conversion of pine wood.

To measure the syngas composition from pinewood *via* pyrolysis, 10 g of material was heated in an inert atmosphere of nitrogen to above 700 °C using the laboratory rig. The gas produced was then passed through two solvent scrubbers before analysis using the GC-TCD, previously calibrated using gas standards. The high reproduciblity (precision < 2 %) of retention time of analytes provided added confidence in analyte identification. To characterise the pyrolysis and gasification products evolved gases were sampled and analysed with temperature thereby measuring the optimum conditions for production of carbon monoxide and hydrogen production.

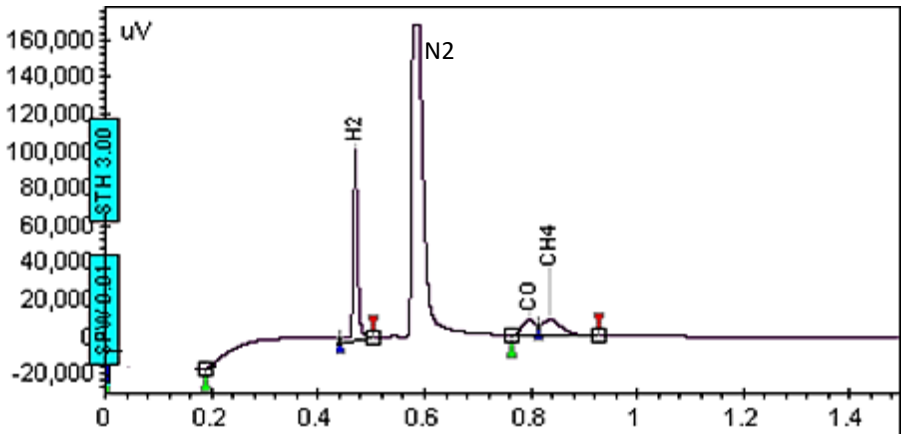

Figure 5.1. A GC-TCD chromatogram for the pyrolysis of pine wood. The main peaks of interest are labelled accordingly; the major peak at 0.6 min is nitrogen carrier gas.

From the initial data it is clear that both hydrogen and carbon monoxide are successfully generated from the pyrolysis of this feedstock. However, following an increase in temperature the pyrolysis of pine wood shows a steady increase in hydrogen up to 730 °C. For example at 575 °C hydrogen (H_2) and carbon monoxide (CO) have a ratio of 3.6:1 but this increases to 8:1 H_2:CO by 645 °C suggesting that lower pyrolysis temperatures are more suited to the FT process. A potential cause of this decline in CO is that CO is liberated earlier (at lower temperatures) from the decomposition of side groups of carbon-oxygen containing molecules, such as lignin and cellulose (34), with increasing temperature, these side groups are less prevalent in the material thus lowering the CO ratio. The heating value of the syngas was also determined to understand the calorific value of the syngas. This was calculated based on the molar percentage of the gas mixture was found to be 6.34 MJ/m^3, comparable if not slightly higher than the value stated in introduction (5.4 MJ/m^3 for wood gas table 1.2).

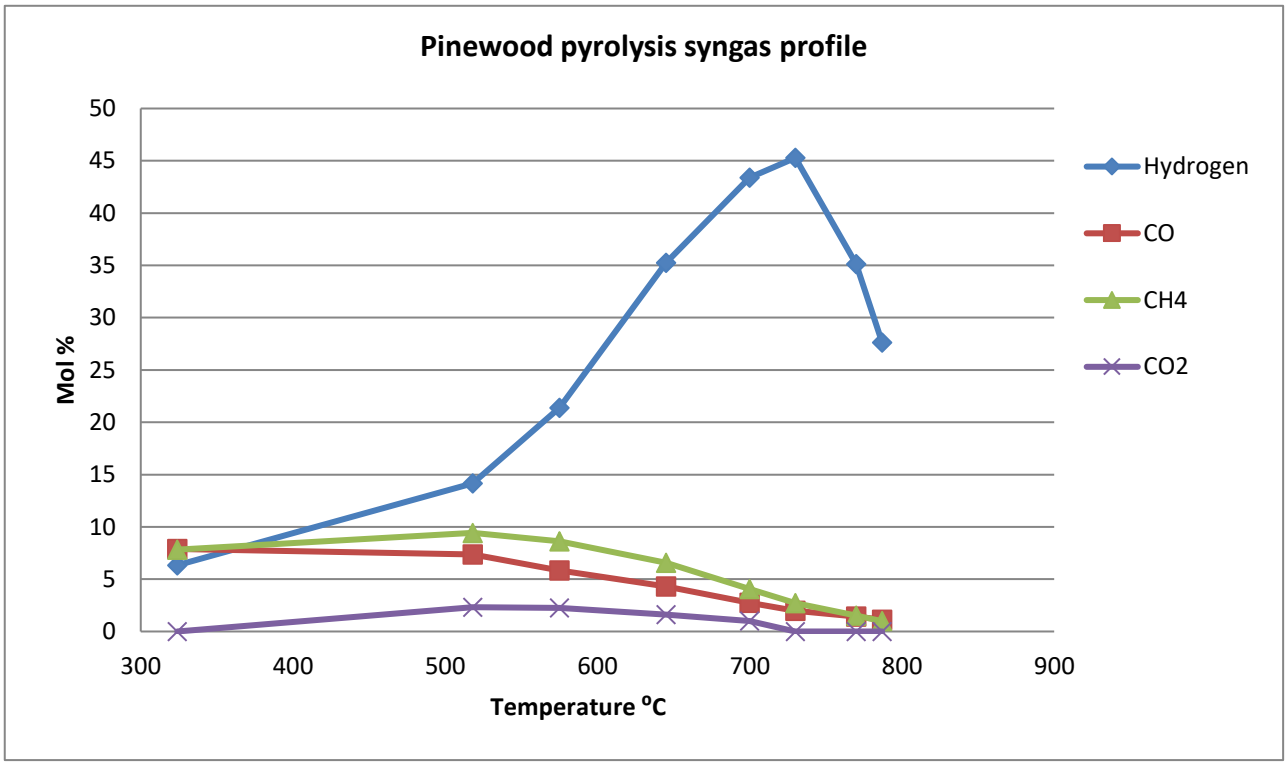

Figure 5.2. A temperature profile of the major constituent of syngas generated by pine wood pyrolysis. As temperature increases (20 °C per minute) so does the amount of hydrogen produced, carbon monoxide and methane steadily declines.

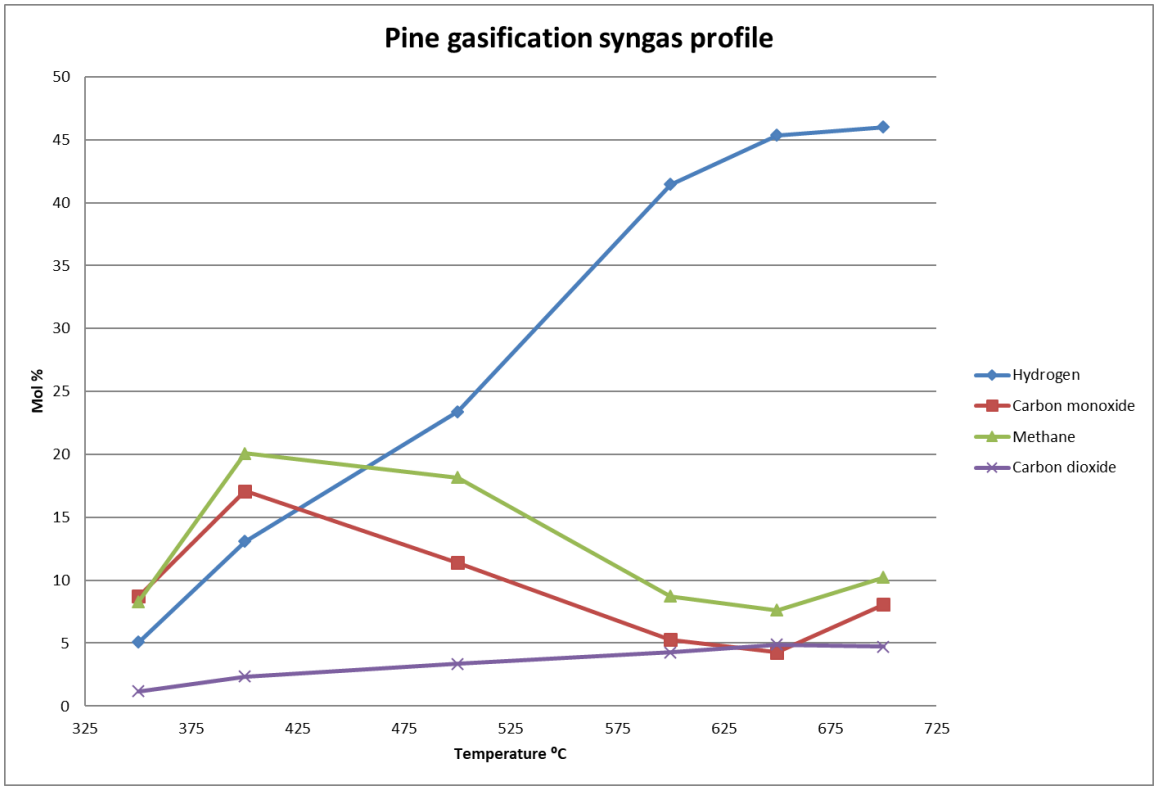

Figure 5.3. A temperature profile (20 °C per minute) of the Major constituents of syngas generated by pine wood Gasification. Hydrogen increases throughout the run. Gasification occurs around 650 °C with the step increase in carbon monoxide and methane.

Conditions for gasification were also tested with syngas profiles for pyrolysis and gasification similarities, a steady increase in hydrogen with temperature, with a drop in CO and methane production over the course of the experiment however, unlike pyrolysis these appear to rise again at 700 °C. A potential cause for this increase is that at this temperature oxidation reactions may occur, in addition to CO, minor components of carbon dioxide (CO_2), were detected. These were typically lower than CO except at 650 °C, where CO reaches a low of 4.3 % and exceeded by CO_2 4.89 %. At 700 °C CO levels increase signficiantly to 8.1 % counts (CO_2 4.71 %). If CO_2 was the predominant species throughout the syngas profile, then this would suggest that complete oxidation is taking place, however, by having CO at a higher level than CO_2 signifies that incomplete combustion is occuring which is synonymous with gasification. The heating value of the syngas from gasification of pine wood was determined by calculation similary to pyrolysis with the gross calorific value found to be 10.46 MJ/m^3 higher value than pyrolysis (6.34 MJ/m^3)

at 700 °C. This value corresponds to the literature, where gasification has been suggested to produce a higher calorific gas, with wood gas is typically around 9-19 MJ/m^3 from gasification (see table 1.2)

5.3.2 Pyrolysis of brown field soil.

To understand the syngas profile generated from the recycling of brownfield soil a 10 g sample was pyrolysed at 700 °C in an inert atmosphere using the laboratory rig. The gas produced was passed through two solvent scrubbers, containing 150 mL acetone and analysed on GC-TCD. Interestingly, unlike pinewood, this sample did not appear to generate carbon based gases such as CO and CH_4 with only hydrogen measured above detectable levels. However, similarly to pine wood, showed a pyrolysis that increases in hydrogen content throughout the course of the experiment however, the amount of hydrogen is low (3.5 % max) in comparison to pine wood (45 % max). The oily sludge contaminating the soil was found to mainly comprise of polyaromatic hydrocarbons. These do not contain oxygen functional groups and are very stable due to their high aromaticity. This data suggests that the majority of carbon remains with the material (possibly as volatile tars) and hydrogen is the main simple gas liberated. It is possible that this is released from cleavage of C-H bonds of the PAHs resulting in smaller unsaturated carbon-based molecules. The gross calorific value of the gas generated from brown field contaminated soil also supports this suggestion with a CV of 0.725 MJ/ m^3. This is approximately 1/10^{th} of the original CV of the oily sludge (7.02 MJ/kg) indicating the majority of calorific value has potentially been emitted as volatile organics due to the drop in the observed char. It is therefore, unlikely that pyrolysis of contaminated land would be a source of renewable energy with such a low CV, but it still could be used as a successive means of remediating the soil.

After discusions with collegues who have worked using hydrocarbon waste gasification; they warned that dangerous and potentially explosive amounts of gas are generated using this method, and for this reason, gasification was not trialed using the laboratory scale rig.

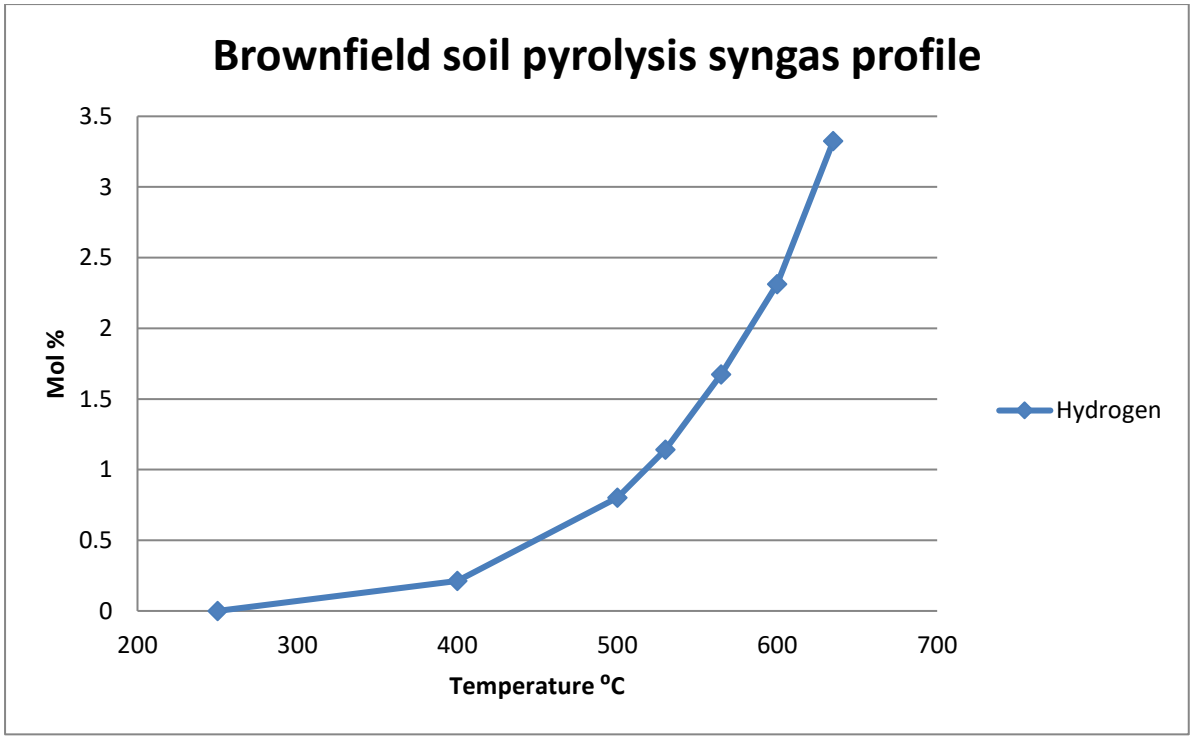

Figure 5.4 is a temperature profile (20 °C per minute) of the typical syngas generated by brownfield soil pyrolysis in an inert atmosphere. As temperature increases so does the amount of hydrogen produced, carbon monoxide and methane are undetectable. It also appears that hydrogen does not reach saturation, but with increased temperature range the level may return. The lab scale rig was only safety tested to 700 ° C.

5.3.3 Pyrolysis and gasification of sludge cake.

Sludge cake from two sources (UK and Ghana plants) were investigated in terms of syngas production as a recycling process by pyrolysis and gasification. For pyrolysis 10 g of each sample was dried and heated in an inert atmosphere of nitrogen to above 700 °C. Similarily to other samples tested the gas produced was passed through two solvent scrubbers, containing 150 mL acetone for cleaning and analysed using GC-TCD for simple molecular gases.

For UK sludge cake pyrolysis the profile of hydrogen shows a similar increase with a temperature as pine wood however, akin to contaminated soil this lower CO and methane production throughout the temperature ramp. Of the CO that is generated, it appears to be at the temperature of 560 °C, whereby the ratio of CO: H_2 is 1:9. This suggests that the formation of

CO occurs at a 'optimum' temperature range, and may arise from the cleavage of C-O bonds of oxygenated functional groups of oxygenates (identified in the extracts of the pre-pyrolysed feedstocks) or oxygen functional groups of dietary lignin and undigested cellulose (34,74,76,80). Interestingly low amounts of ethylene was also detected and may be further evidence of long chain hydrocarbon degradation; through thermal scission of the alkyl chain. The presence of hydrogen is likely to arise from C-H cleavage of organic molecules or the dissociation of bound water (34,74)

The gross calorific value was determined by calculation based on the molar percentage of the gas mixture was found to be 3.04 MJ/m^3, this is lower than the pine wood but unsurprising as the amounts of CO was comparatively less.

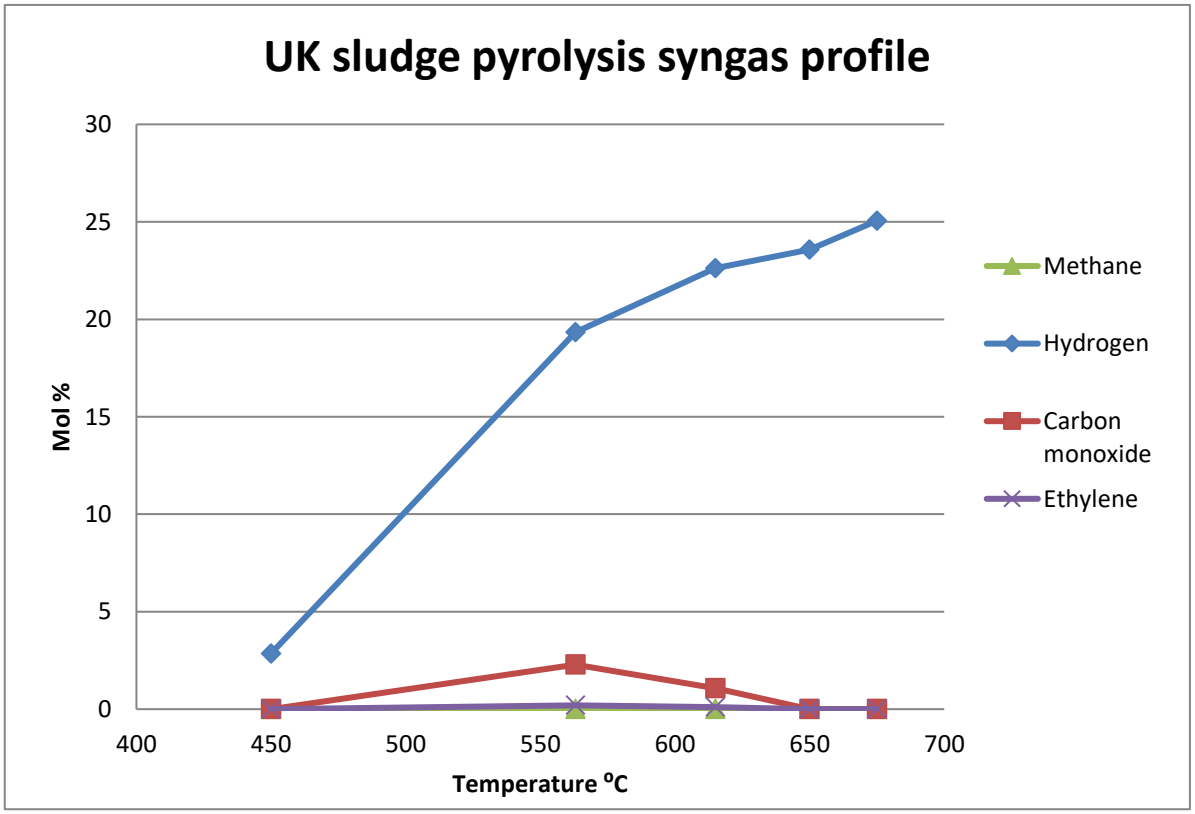

Figure 5.5 A temperature profile (20 °C per minute) of the typical syngas generated by sludge pyrolysis in an inert atmosphere. As temperature increases so does the amount of hydrogen produced, there is little carbon monoxide and methane production, suggesting the composition of sludge.

The syngas composition of Ghana sludge cake appears very similar to the UK sample although the hydrogen and carbon monoxide levels are higher in Ghana sludge cake (48 % and 9 %) is higher than UK sludge cake (25 % and 2.2 %). This increase in carbon monoxide and hydrogen gives Ghana sludge cake syngas a significantly higher CV (12.24 MJ/m^3) and is unsurprising given that the high CV of the original feedstock (13-18 MJ/kg)(syngas density ~1 kg/m^3 (0.95 kg/m^3)) (53) and likely due to the significantly higher semi-volatile content (9727 mg/kg) compared to UK sludge cake (230.13 mg/kg). This may decompose to contribute to the carbon monoxide and hydrogen in the syngas and as a result give rise to higher tar generation.

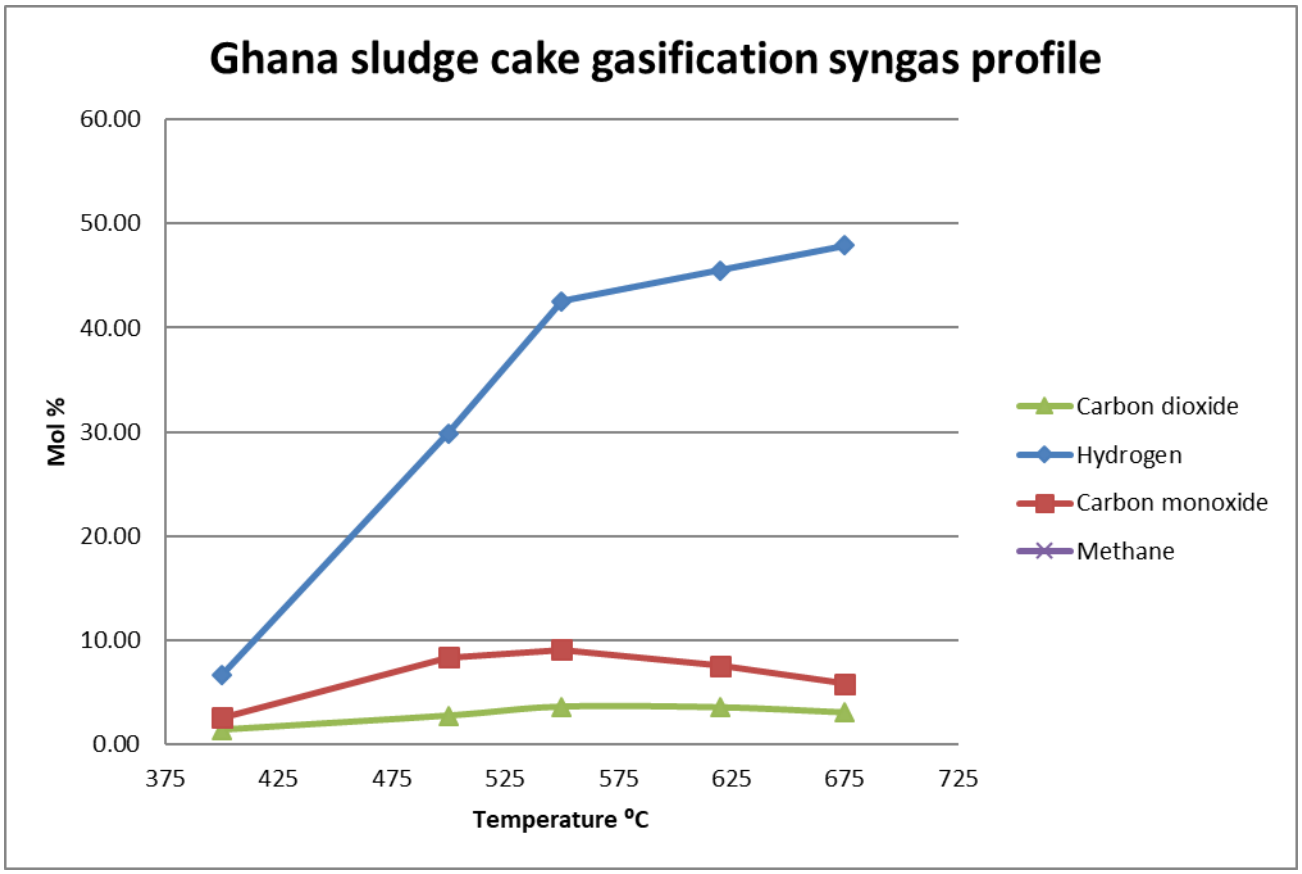

Figure 5.6 A temperature profile (20 °C per minute) of the typical syngas generated by Ghana sludge cake pyrolysis in an inert atmosphere. As temperature increases so does the amount of hydrogen produced, carbon monoxide and methane rise until 550 °C suggesting derives from the cleavage of functional groups.

The addition of oxygen to generate gasification conditions appeared to increase the CV of the syngas for pine wood therefore, the addition of air to sludge was also investigated to evaluate any observed increase the CV of the syngas. Again 10 g of UK sludge cake was heated to 700 °C, but in the presence of compressed air at 50 mL per minute to mimic air gasification. The gas generated from the process was sampled at different temperatures to monitor simple gas evolution and plotted as a profile. The results indicate that both CO and CO_2 were generated,with levels of CO increasing from 630 °C and plateauing at temperatures above this. It is likely that oxygen reacts with carbon in the char or tar compounds to generate CO and CO_2. In fact the H_2: CO ratio is above at 6:1 at all sampling intervals. The increased CO levels (~6 %) compared to pyrolysis (2.2 % max) should add more calorific value to the syngas and will benefit processes such as FT ensuring more hydrocarbon production (through hydrogenation of CO). The minor levels of CO_2 observed suggest combustion is occuring albeit at low amounts. The heating value of the syngas was also determined and compared to pyrolysis. The gross calorific value syngas of sludge cake in air gasification was found to be 5.50 MJ/ m^3, greater than that of pyrolysis (3.04 MJ/ m^3) further supporting the necessary addition of air to increase the CV of the syngas.

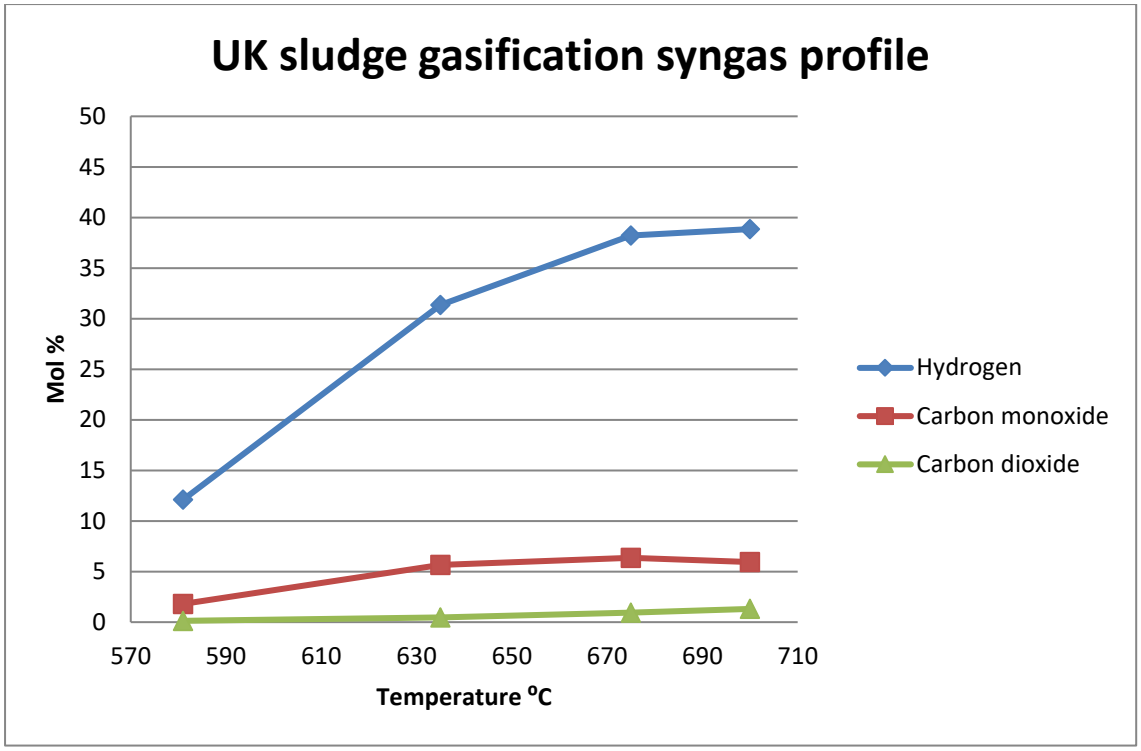

Figure 5.7. The figure above is a temperature profile (20 °C per minute) of sludge gasification shows major constituents of syngas; hydrogen and carbon monoxide content increase with temperature throughout the experiment.

However, unlike pyrolysis, gasification primarily generates syngas; pyrolysis generates other useful products such biochar and bi-oils. Which the typically have high CVs, where the combination CVs of biochar (7.75 MJ/m^3) and syngas (3.04 MJ/m^3) equates to 88.8 % of the original value of the feedstock. This is indicative of the pyrolysis process which has higher conversion efficiencies, storing energy in products, while for gasification, some of the energy is required in the partial combustion of the feedstock. This suggests that the process has the potential to be tailored to generate syngas only or a mixture of materials (including syngas) for re-use. Consideration may also be given to which technique is most appropriate in reducing the degree of chemical waste generated via the process to minimise the release of toxic (PAHs) materials to the environment.

5.3.4 Summary of syngas composition: GC-TCD and temperature profiles.

- Pyrolysis of pine wood shows a steady increase in hydrogen up to 730 °C and CO is liberated earlier (at lower temperatures) from the decomposition of side groups of carbon-oxygen containing molecules. CV of syngas from pyrolysis of pine wood was calculated based on the molar percentage of the gas mixture was found to be 6.34 MJ/m^3.
- Pyrolysis and gasification of pine wood show similarities, a steady increase in hydrogen with temperature, with a drop in CO and methane but unlike pyrolysis these appear to rise again at 700 °C. A potential cause for this increase is that at this temperature oxidation reactions occur. The gross calorific value of gasification syngas was higher than pyrolysis and calculated to be 10.46 MJ/m^3.
- Thermal treatment of brown field contaminated soil generates low amounts of hydrogen as the main simple gas. Unlike pinewood, brown filed soil contains compounds that are thermally stable with no reactive functional groups (comprised of PAHs) . The gross calorific value of the gas generated from brown field was determined to be CV of 0.725 MJ/m^3.
- UK sludge cake pyrolysis profile of shows an increase of hydrogen with a rise in temperature and CO occurs at a 'optimum' temperature range. CO arises from the cleavage of C-O bonds of oxygenated functional groups. The gross calorific value was determined to be 3.04 MJ/m^3,
- Ghana sludge cake appears very similar to the UK sample although the hydrogen and carbon monoxide levels are higher in Ghana sludge cake (48 % and 9 %) UK sludge cake (25 % and 2.2 %). This increase in carbon monoxide and hydrogen gives Ghana sludge cake syngas a significantly higher CV (12.24 MJ/m^3).

5.4 Tar characterisation from differing feedstocks.

5.4.1 Tars identified from the pyrolysis of pine wood.

For each feedstock that was thermochemically treated, the syngas was bubbled through three impingers containing 150 mL of acetone prior GC-TCD analysis. These scrubbers had a dual purpose, firstly to remove organic tars to clean the syngas and secondly to act as a trap so the tars could be identified using GC-MS. Both targeted and non targeted compounds were identified, via NIST database search and quantified (standard calibration) or semi-quantified (compared against an internal standard) respectively. The experiment was repeated on different occasions with good precision observed for compounds. An annotated total ion chromatogram (TIC) of scrubber one can be seen in appendix 1.0. The survey of tars originating from pinewood shows considerable breadth of chemistries with positive identifications made for both volatile aromatic, polyaromatic and phenolic compounds. Other non-targeted species include lignin break down products and cellulosic decomposition compounds.

Pine wood is comprised of mainly cellulose, a polymer of β-D-glucose units, hemicelluloses a mixed polymer of various hexose sugars and guaiacyl lignin (34,74–77) and is believed to be degraded during pyrolysis. Evidence of these degradation reactions are observed within the acetone scrubbers; furfuals and fural derivatives are derived from the decomposition of the hexose sugars such as xylan and glucose from hemicellulose and cellulose respectively (75). While the presence of andro D-mannosan is likely to be derived from the acetal reaction pathway of cellulose monomers and arabinose from hemicellulose breakdown (34,74–76). Phenolic compounds such as isoeugenol, phenol, cresol, ethyl guaiacol, salicyl alcohol and coniferyl alcohol are considered typical breakdown products of lignin (76,77). Other compounds present are terpenoids (minor constituent of biomass) and undesirable PAHs. The literature states that PAHs arise from tertiary reactions at temperatures in excess of 700 °C (34); however in this study, PAHs were observed at temperatures as low as 400 °C. Previous studies have indicated that these are formed due to charring process (34) or from thermal treatment of

terpens or terpenoids (78,99). For example, the PAH phenanthrene, may be generated from the thermochemical breakdown of the dehydroabeitic acid (99). The mechanism below (see Figure 5.8) details the break down products of dehydrobietic acid and these products were also identified the tar data further supporting that PAHs are produced at lower temperatures and from the generation of terpenoid compounds.

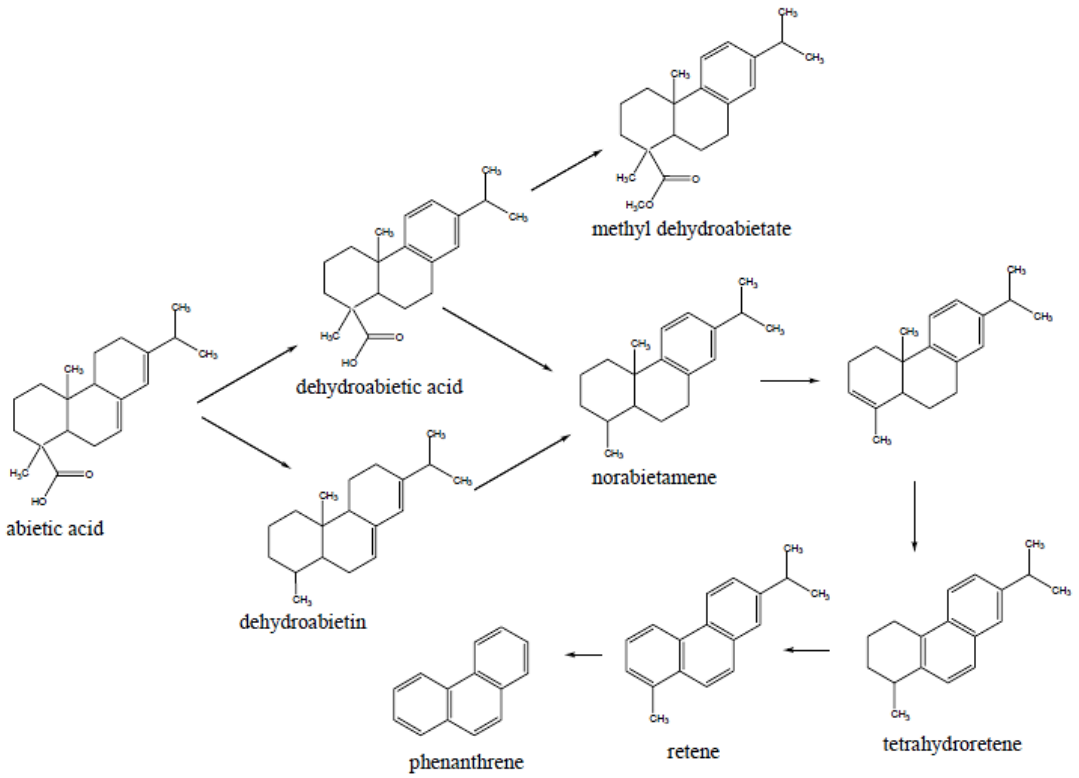

Figure 5.8 *A reaction scheme detailing the thermal degradation pathway of abietic acid to form phenanthrene and other PAHs proposed by Jerkovic et al 2011. This is a potential pathway for the generation of phenanthrene, retene, methyl dehydroabietate and dehydroabietic acid observed within the acetone scrubbers at lower pyrolytic temperatures of pine wood*

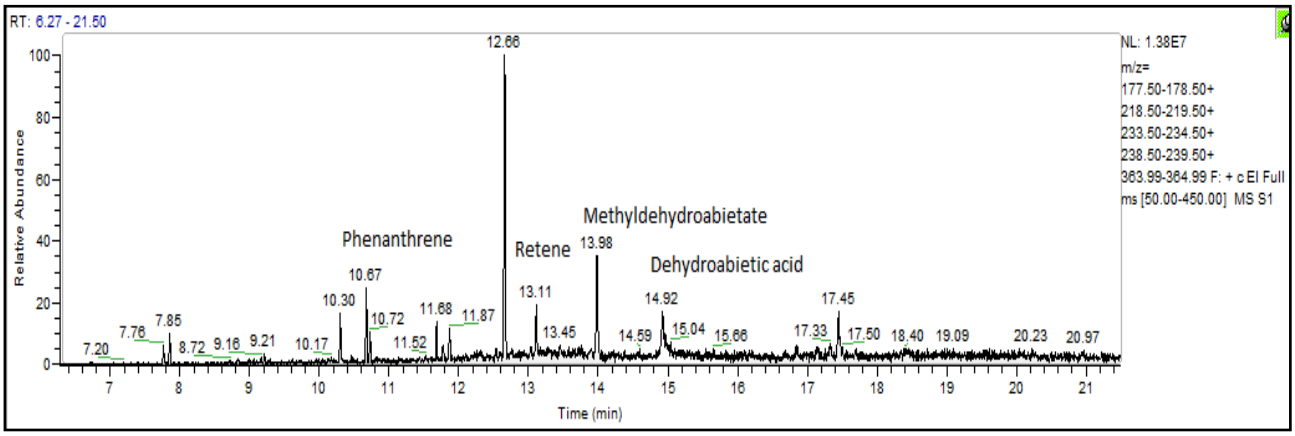

Figure 5.9 Figure illustrating an extracted ion chromatogram (XIC) from pine wood pyrolysis: annotated are dehydroalbietic acid (m/z 285), methyldehydroabietate (m/z 239) retene (m/z 219) and phenanthrene (m/z 178), which reflect the proposed pathway to form phenanthrene by Jerkovic et al. 2011

The overall pyrolysis process of pinewood was repeatable. Each batch produced similar compounds at similar concentrations. The overall concentration of tars, were similar for each batch that was analysed. The targeted compounds identified for VOT, SVOT for scrubbers 1 and 2 were totalled with the non-targeted compounds. The non-targeted compounds were identified by semi-quantitation. The total tar concentration for 10 g of pine wood was calculated to be on average 90.59 mg, this equates to 0.91 % of the mass of the original pinewood. However, these values only account for the tars that were volatile enough to make it to scrubber 1 and 2. Tars that were not compatible with GC-MS, non-volatile and highly polar compounds would not have been identified.

Pine wood	Compounds identified	Concentration (mg/L)		
		Scrubber 1	Scrubber 2	Scrubber 3
Volatile aromatic compounds (VOT)^	Benzene	31.71	ND	ND
	Toluene	25.60	0.16	ND
	Ethylbenzene	9.03	0.18	ND
	1, 3-Dimethylbenzene	5.50	ND	ND
	Styrene	3.00	ND	ND
	P-xylene	2.74	ND	ND
Polycyclic Aromatic (SVOT)^	Naphthalene	2.70	0.70	ND
	Acenaphthylene	0.46	0.13	ND
	Phenanthrene	0.41	ND	ND
	Anthracene	0.18	ND	ND
	Fluorene	0.21	0.15	ND
Phenolic compounds (SVOT)^	Phenol	10.98	1.90	ND
	4-Methylphenol	5.79	1.52	ND
	2-Methylphenol	6.84	1.01	ND
	2, 3-Dimethylphenol	7.40	1.00	ND
	4-Chloro-3-methylphenol	3.02	0.52	ND
Non-Targeted Other (LOD 0.05 mg/L)#	2-Furancarboxylic acid	5.70	2.05	ND
	2-Furanmethanol	7.30	2.79	ND
	2-Furanone	6.28	1.99	ND
	2-Cyclopenten-1-one	7.11	2.76	ND
	Carbanicacic-phenyl ester	9.23	4.11	ND
	3-Methylcyclopentane	10.06	3.43	ND
	Benzyl alcohol	4.47	1.98	ND
	2-Methoxyphenol	20.86	10.35	ND
	Cresol	31.06	27.57	ND
	6-Methyl-4-pyrimidinol	21.75	ND	ND
	4-Ethyl-2-hydroxy-Cyclopentene-1-one	5.21	5.29	ND
	Salicyl alcohol	6.32	3.65	ND
	p-Ethylguaicol	16.20	3.21	ND
	4-Ethenyl-2-methoxyphenol,	16.20	5.06	ND
	Isoeugenol	32.00	11.91	ND
	Anhydro-D-mannosan	150.12	5.74	ND
	Conifyl aldehyde	10.78	2.15	ND
	Arabinose	6.35	0.67	ND
	Dehydroabietic acid	0.10	ND	ND
	Methyldehydroabietate	0.060	ND	ND
	Retene	0.067	ND	ND
Estimated total Tar content in 1 mL aliquot of scrubber (150 mL acetone)		**482.80**	**101.98**	**<0.100 mg/L**
Total mass of tars mg Mass= conc/1000*volume of scrubber		**72.42 mg**	**15.30 mg**	**<0.015 mg**

Table 5.9 A table of compounds identified in scrubber 1 and 2 from a typical pyrolysis run of pine wood. Some of the compounds have been quantified by targeted analysis while some have been semi-quantified. Unknown peaks were elucidated by their mass spectrum from the NIST database and peak area was compared to an internal standard. ^targeted compounds, #non-targeted compounds.

A number of pyrolysis batches were run using pine wood. Variations were observed between batches for some of the compounds identified in both VOT and SVOT methods and is expected due to due to the heterogeneous structure of pine wood. However, despite this variation, the total extracted tars for pine wood remained repeatable with precision of the first <10 % for the first scrubber. Table below shows total concentration of the tars for pine wood.

	Run1		Run 2		Run3	Run 4	Average	% RSD
Total VOT S1 mg/L	76.43		77.54		94.78	91.52	85.07	9.61 %
Total VOT S2 mg/L	20.8		9.347		8.69		7.97	52.59 %
Total sVOT S1 mg/L	37.07	34.42	39.79	39.03	45.71	39.21	37.57	6.02 %
Total sVOT S2 mg/L	35.98		26.39		35.37		35.60	16.5 %
Total Non-targeted S1 +S2 mg/L	434.27		531.13		347.63	-	437.68	20.97 %

Table 5.10 Table showing the repeatability of the scrubber extraction for the tars identified by GC-MS for pine wood pyrolysis. The % RSD is below 25 % and is deemed repeatable.

To understand the effectivness and capacity of the scrubber the amount measured in each scrubber was weighted to total amount extracted. Therefore, the total average mass of tars generated by 10 g of sample that was captured by the scrubbers is approximately 90.58 mg (total average concentration x 0.15 L). The above example figure 5.10 was found to have a total of 93.04 mg of tars captured; this is within 3.65 % of the calculated average value for pine wood pyrolysis.

5.4.2 Tars identified in pine wood gasification.

To investigate the differences in tar production of pyrolysis over gasification 50 mL of compressed air was added to the laboratory pyrolyser rig and operated at 700 °C. As for pyrolysis the tars were captured and analysed with identification made using the NIST data

base. From initial screen of the data, the overall compound classes appeared to remain the same, however, there is a notable change in concentration.

For example, both volatile aromatics, polyaromatics and phenolic compounds were observed along with furfurals and fural derivatives and anhydro-D- mannosan. However, unlike pyrolysis volatile aromatics and phenols are observed at typically half the concentration. While gasification appears to generate slightly higher levels of of undesirable PAHs, possible as a result of incomplete combustion (129). Removal of these potentially harmful substances is imperative.

Overall, the level of tars is significantly reduced (~90 %) when air is added suggesting that these may be oxidised resulting in a higher production of carbon monoxide. The data presented within the syngas profile, suggests this oxidation zone is around 700 °C evidenced by a notable increase in carbon monoxide in the gasification profile for pine wood (see figure 5.3) absent during pyrolysis. During gasification, the char is also oxidised to form ash, and has no calorific value and due to low organic content.

Pine (gasification)	Compounds identified	Concentration (mg/L)	
		Scrubber 1	Scrubber 2
Targeted Volatile Aromatics (VOT) mg/L	Benzene Toluene Styrene	16.00 mg/L 8.00 mg/L 1.20 mg/L	ND ND ND
Targeted Polycyclic Aromatic (SVOT) mg/L	Naphthalene Acenaphthylene Phenanthrene Anthracene Fluroanthene Pyrene	5.0 mg/L 0.67 mg/L 1.25 mg/L 0.66 mg/L 0.50 mg/L 0.66 mg/L	ND ND ND ND ND ND
Phenolic Compounds SVOT	Phenol 4-Methyl-phenol 2-Methyl-phenol 2,3 Dimethyl-phenol Phenol 4 chloro 3 methyl	3.10 mg/L 2.09 mg/L 2.67 mg/L 2.59 mg/L 1.08 mg/L	ND ND ND ND ND
Non Targeted Other (LOD 0.1mg/L)	Furfural 2-Furanmethanol 2-Furanone 5-Hydroxy methylfurfural 4-Methyl catechol 1-Ethylidine 1 H indene Isoeugenol Anhydro-D-mannosan	2.51 mg/L 1.07 mg/L 1.34 mg/L 0.87 mg/L 2.11 mg/L 0.76 mg/L 1.04 mg/L 5.68 mg/L	ND ND ND ND ND ND ND ND
Estimated total tar content in impingers		**60.85 mg/L (~100%)**	**<0.10 mg/L**
Total mass of tars mg		**9.13 mg**	**<0.015 mg**

Table 5.11 Table of the compounds identified in scrubber 1 and 2 from gasification of pine wood. Some of the compounds have been quantified by targeted analysis while some have been semi-quantified. Unknown peaks were elucidated by their mass spectrum and peak area was compared to an internal standard.

5.4.3 Tars identified from the pyrolysis of brownfield soil.

A brown field soil sample contaminated with oily sludge derived from petroleum waste, was also characterised as a feedstock by pyrolysis. As expected, volatile aromatic and polyaromatic hydrocarbons were observed as major constituents, indicative of the degree of chemical contamination with very high amounts captured in the intial scrubber, particularly for benzene and naphthalene. It is important that these compounds are measured and characterised if generated given their harmful and mutagenic properties (8,34,90,128,129). Interestingly, the

compound profile observed in the scrubbers post-pyrolysis appear to be the same observed the solvent extraction pre-pyrolysis of the soil with no additional compounds detected. This suggests that perhaps thermal degradation has not occurred of these compounds but their release from within contaminants associated with the soil. Aliquots of the scrubbers were analysed at different pyrolysis temperatures and it was identified that the presence of these compounds was related to their volatility, with volatile aromatics and polyaromatics, such as naphthalene (218 °C), observed at temperatures up to 300 °C. As operating temperatures increased to 400 ^{o}C more mid-range PAHs, such as phenanthrene (339 °C), were observed with PAHs of boiling points below benz(a)anathracene (438 °C) present up to 500 °C. To observe larger PAHs (e.g. benzo(ghi)perylene, boiling point 550 °C) pyrolysis temperatures above 600 °C were required. This is important to understand particulary for oily sludge samples with high PAH content as this data suggests that the operating temperature of the pyrolysis process may be chosen to control the release of undesirable PAH and use a particular solvent scrubbers, to capture the maximum amount of these harmful pollutants. Given the low calorific value of this feedstock, it is unlikely that pyrolysis will be used to generate syngas for power generation, however, this data has shown the potential for soil remediation following contamination. Another upshot of pyrolysis is that the organic compounds generated during this process do have a high calorific value (>30 MJ/kg) and can be easily trapped (condensable) offering an alternative source of fuel.

Brown Field (10% contaminated with petroleum waste)	Compound name	Concentration (mg/L)		
		Scrubber 1	Scrubber 2	Scrubber 3
Targeted Volatile Aromatics (VOT)	Benzene	184.00	1.80	ND
	Toluene	73.28	0.36	ND
	Ethylbenzene	5.16	0.08	ND
	Styrene	24.92	0.03	ND
	p-Xylene	8.52	0.19	ND
	m-Xylene	5.92	0.09	ND
Targeted Phenols (SVOT)	Phenol	2.50	ND	ND
Targeted* and non-Targeted Polycyclic Aromatic (SVOT)	Napthalene*	169.61	4.13	ND
	2-Methylnapthalene	2.12	0.74	ND
	1-Methylnapthalene	11.71	0.42	ND
	Biphenyl	8.40	0.33	ND
	1, 6-Dimethylnaphthalene	5.79	0.22	ND
	1, 7-Dimethylnaphthalene	9.36	0.37	ND
	2-Ethenylnapthalene	4.24	0.02	ND
	Acenaphthylene*	27.6	1.02	ND
	Acenaphthylene derivatives	5.46	0.21	ND
	Phenalene	4.43	ND	ND
	Fluorene*	14.22	0.04	ND
	Dibenzothiophene	4.15	0.55	ND
	Phenanthrene*	67.6	0.23	ND
	2-Methylanthracene	11.2	2.39	ND
	8,9-dihydro-4-cyclopenta (def) - Phenanthrene	9.14	0.40	ND
	Anthracene*	16.23 *	0.43	ND
	2-Phenylnapthalene	4.92	0.64	ND
	Fluoranthene*	20.41 *	0.22	ND
	Pyrene*	27.62 *	0.73	ND
	Benz(a)anthracene*	8.00 *	0.94	ND
	Chrysene*	8.20 *	0.33	ND
	Benzo (a) pyrene*	3.54 *	0.32	ND
	Benz (b) fluoranthene*	5.47 *	0.32	ND
	Indeno (123-cd)pyrene*	1.20 *	0.26	ND
	Dibenza(ah)anthracene*	0.36 *	0.04	ND
	Benzo(ghi)perylene*	1.52 *	ND	ND
Estimated total Tar content in 1 mL aliquot of scrubber (150 mL acetone)		664.25	**17.85**	**<0.10 mg/L**
Mass of Tar		**114 mg**	**2.68 mg**	**0.015 mg**

Table 5.12 A table of the compounds identified in scrubber 1 and 2 from the pyrolysis of brown field soil. Some of the compounds have been quantified by targeted analysis while some have been semi-quantified. Unknown peaks were elucidated by their mass spectrum and peak area was compared to an internal standard.*

	Run1	Run 2	Run3	Run 4	Average	%RSD
Total VOT S1 mg/L	30.1.8 mg/L	410.06 mg/L	293.43 mg/L	232.92 mg/L	309.33 mg/L	20.52%
Total VOT S2	2.58 mg/L	0.80 mg/L	4.36 mg/L		2.58 mg/L	56.62 %
Total sVOT S1 mg/L	483.14 mg/L	346.4 mg/L	311.36 mg/L	330.0 mg/L	367.73 mg/L	21.28 %
Total SVOT S1+S2	494.8 mg/L	358.01 mg/L	318.3 mg/L	341.5 mg/L	378.18 mg/L	21.01 %
Total Non-targeted S1 +S2 mg/L	125.61 mg/L	98.2 mg/L	107.82 mg/L	111.96 mg/L	110.90 mg/L	10.26 %

Table 5.13 Table showing the repeatability of four batches of brownfield soil extraction; %RSD is below 25 %, the average for the individual scrubbers for SVOT, VOT and non- targeted were combined to give a final average value for the total tars identified. The repeatability of the results suggests that the sample analysed was somewhat homgenous and extraction was reproducible.

5.4.4 Tars identified from the pyrolysis of UK sludge cake.

To understand the potential risks involved in the tars generated during pyrolysis of sludge cake, the UK feedstock was also charcterised. This data proved particularly important as it highlighted the marked difference in tar composition with feedstock, revealing a high percentage of volatile aromatics and heterocyclic nitrogen containing aromatics (see table 5.15). This is consistent with what is known regarding sludge cake generated in the UK as it is often used as a fertiliser due to its perceived high nitrogen content. However, pine wood had a similar range of chemistries to sludge cake, of these compounds toluene was the most abundant, (33.15 mg/L) of the volatile aromatic group. However, the summation of benzene, toluene, ethyl benzene and xylene (BTEX) at 80.01 mg/L was determined to be similar value to pine wood (77.91 mg/L). Another significant component of the tar extract were the heterocyclic nitrogen aromatics, observed at a similar concentration to the BTEX (90.97 mg/L). These are primarly cyclohexylamine derivatives, piperidine analogues and triazoles and are important building

blocks of bioactive substances and various pharmaceuticals (135,136) potentially originating from the degradation of such materials. However, alternative sources of these compound could be the thermal decomposition and rearrangement of amino acids from microbes and dietary proteins (135,136) and this may be more likely due to the abundance of microbial remains from wastewater treatment. As with aromatic compounds it is key to capture these to limit their release into the environment as they are potential pollutants harmful to human health (with some being fatal) reducing the risks of sludge release and its recycling. From our data it is clear that acetone is capable of capturing complex 'real world' samples such as sludge cake with the majority of the compounds dissolved in the first scrubber and consequently removed from the syngas.

UK sludge cake	Compound name	Concentration (mg/L)		
		Scrubber 1	Scrubber 2	Scrubber 3
Volatile aromatic compounds (VOT)^	Benzene	6.50	0.38	ND
	Toluene	32.40	0.75	ND
	Ethylbenzene	6.50	0.22	ND
	o-Xylene	15.31	0.13	ND
	p-Xylene	2.00	ND	ND
	Styrene	11.40	0.15	ND
	1,3-Dimethylbenzene	1.72	ND	ND
	1-Methyl-2-ethylbenzene	0.66	ND	ND
Polycyclic Aromatic (SVOT)^	Naphthalene	5.00	0.36	ND
	Acenaphthylene	0.74	0.15	ND
	Phenanthrene	1.30	0.24	ND
	Anthracene	0.30	ND	ND
	Fluoranthene	0.21	0.01	ND
	Pyrene	0.30	ND	ND
	Benzo (b) fluoranthene	0.11	ND	ND
	Benzo (a) anthacene	0.11	ND	ND
Phenolic compounds (SVOT)^	Phenol	4.60	0.89	ND
	4-Methylphenol	2.40	0.43	ND
	2-Methylphenol	6.50	0.83	ND
	2,3-Dimethylphenol	6.50	0.60	ND
Nitrogen containing compounds (LOD <0.1 mg/L)[#]	n-Isopropyl cyclohexamine	3.93	ND	ND
	2-Ethylaminomethyl cyclohexanone	22.52	2.26	ND
	n-Cyclohexylpropanamide	18.31	1.73	ND
	n-Cyclohexylacrylamide	3.88	ND	ND
	2, 2, 6, 6-Tetramethy-4-piperidinone	19.09	0.54	ND
	1, 2, 2, 5-Tetramethyl-3-piperidinone	7.52	2.05	ND
	3-hydroxy-1-isopropyl-2-methyl-4(1H)-pyridinone	1.29	ND	ND
	5-Pentyl-1-h-1,2,4-triazol amine	0.83	ND	ND
	5-Hexyl-1-H-1,2,4-triazol	1.13	ND	ND
Estimated total Tar content in 1mL aliquot of scrubber (150 mL acetone)		**183.06 mg/L**	**11.72 mg/L**	**<0.100 mg/L**
Mass of Tars		**27.46 mg**	**1.76 mg**	**<0.015 mg**

Table 5.14 Table of the compounds identified in scrubber 1 and 2 from the pyrolysis of UK sludge cake. Some of the compounds have been quantified by targeted analysis while some have been semi-quantified. Unknown peaks were elucidated by their mass spectrum and peak area was compared to an internal standard.

	Run1		Run 2		Run3		Run 4	Average	%RSD
Total VOT S1 mg/L	20.54		28.07		16.31		19.55	21.12	10.85 %
Total VOT S2 mg/L	4.286	4.267	1.34	1.34	10.50	9.88	10.793	6.06mg/L	68.7 %
Total sVOT S1 mg/L	63.87	67.85	61.25		56.36		58.7	58.7	4.16 %
Total sVOT S2 mg/L	6.834		2.66		2.831			4.11mg/L	46.89 %
Total Non-targeted S1 mg/L	136.19		100.96		98.21		-	111.78	18.94 %
Total Non-targeted S2 mg/L	27.2		22.48		32.41		-	27.36	18.15%

5.156 Table showing the repeatability of four batches of UK sludge cake extraction; %RSD is below 25 %, the average for the individual scrubbers for SVOT, VOT and non-targeted were combined to give a final average value for the total tars identified. The repeatablity of these results suggests that the Sludge cake is a fairly uniform sample.

5.4.5 Tars identified in UK sludge cake gasification (addition of air).

The sludge cake sample from the UK was characterised following gasification. It was apparent from the data that addition of air had no alteration of the types tars generated, but it did influence the concentration of tars generated. For example the total tars quantified from pyrolysis of 10 g of sludge cake was 30.09 mg , this was reduced by 55.1 % to 13.52 mg during gasification and is likely to be a result of oxidation of the tars similar to what was seen in the air gasification of pine wood. Therefore, reducing the amount of potential harmful tars associated with the recycling of sludge cake and generating a higher CV gas (5.5 MJ/m^3) compared to pyrolysis (3.04 MJ/m^3). However, gasification does limit the production of other useful products (syngas only) and ash generated via this method has little use with a low CV.

UK Sludge cake gasification	Compound name	Concentration (mg/L)		
		Scrubber 1	Scrubber 2	Scrubber 3
Targeted Volatile Aromatics (VOT) mg/L	Benzene Toluene Ethyl benzene P-Xylene Styrene Benzene 1,3 dimethyl Benzene (1-methyl-2-ethyl)	8.0 mg/L 15.0 1.20 0.144 7.20 1.30 3.16	0.50 0.28 ND ND 0.10 ND ND	ND ND ND ND ND ND ND
Targeted Polycyclic Aromatic (SVOT) mg/L	Naphthalene	0.41	ND	ND
Targeted Phenolics SVOT mg/L	Phenol 4-Methyl phenol 2-Methyl Phenol 2,3-dimethyl phenol	2.67 1.53 3.16 1.0	0.356 0.534 1.035 1.00	ND ND ND ND
Non-targeted oxygenates and nitrogen containing compounds (LOD <0.1 mg/L)	N-ethyl 2-methyl cyclohexanamine Methyl cyclohexanone-2-ethylamino n-Cyclohexyl-Propanamide n-Cyclohexylacrylamide 2,2,6,6-Tetramethyl-4-piperidinone 1,2,2,5-Tetramethyl-3-piperidinone 5-Pentyl 1-h 1,2,4 triazol amine 5-hexyl 1-H-1,2,4 triazol	2.63 6.51 14.23 1.77 7.40 6.86 1.13 1.06	ND ND ND ND ND ND ND ND	ND ND ND ND ND ND ND ND
Estimated total tar content in scrubbers (150ml acetone)		**86.36**	**3.8**	**<0.10**
Mass of Tars mg		**12.95**	**0.57**	**<0.015**

Table 5.16 Table showing the compounds identified in scrubber 1 and 2 from the gasification of UK sludge cake. Some of the compounds have been quantified by targeted analysis while some have been semi-quantified. Unknown peaks were elucidated by their mass spectrum and peak area was compared to an internal standard

5.4.6 Organic tars derived from the pyrolysis of Ghana sludge cake.

To assess the tar content from an alternative plant (Ghana) operating with the same treatment process, samples were pyrolysed and compared to UK sludge cake. Both tars generated by UK and Ghana samples contained predominantly volatile aromatics, phenols and nitrogen containing heterocyclic compounds. However, Ghana sludge cake generated a greater amount of tar compounds indicative of a higher nitrogen (N=3.5 mg/Kg) and semi-volatile content (SVOC 3.5 g/Kg) contained within this feedstock prior to pyrolysis, compared to UK sludge (N = 2.5 mg/Kg and SVOC 230 mg/Kg). These initial feedstock values indicate that this sample is capable of generating a higher calorific syngas and biochar than UK sludge, although the pyrolysis of this

material has shown a greater proportion of undesirable toxic nitrogen aromatics, with over double the amount of potentially harmful nitrogen containing aromatics (188.1 mg/L) than UK sludge (85.08 mg/L). This data highlights the importance of feedstock and tar characterisation to ensure appropriate clean-up processes are in place to remove these harmful emissions from syngas to reduce the potential for environmental contamination.

These nitrogenous compounds were consistent with the UK sludge sample with one additional compound identified, 1-butyl-2,5 dimethyl-1 H pyrrol, but belongs in the same class of compounds as the nitrogen containing heterocycles. In this experiment one of the impingers was replaced for a condenser. It can be seen that close to half of the nitrogenous compounds (~58 %) can be removed by condensation in to an oil which may have an added advantage of prolonging the scrubber life time. These compounds as discussed earlier may be of some worth if purified (pharmaceutical building blocks) adding another potential valuable product.

Ghana sludge cake	Compound name	Concentration (mg/L)		
		Scrubber 1 (Condenser)	Scrubber 2	Scrubber 3
Volatile aromatic compounds (VOT)^	Benzene	8.00	19.47	ND
	Toluene	22.10	44.18	ND
	Ethylbenzene	4.91	2.13	ND
	p-Xylene	2.75	0.87	ND
	Styrene	4.49	0.80	ND
	1,3 Dimethylbenzene	2.95	0.60	ND
Phenolic compounds (SVOT)^	Phenol	5.20	ND	ND
	4-Methylphenol	2.27	ND	ND
	2-Methylphenol	22.49	ND	ND
	2,3-Dimethylphenol	3.13	ND	ND
Nitrogen containing compounds (LOD <0.1 mg/L)	n-Isopropyl cyclohexamine	5.47	2.07	ND
	Methyl-cyclohexanone-2-ethylamino	37.61	19.19	ND
	2,2,6,6 Tetramethyl-4-piperidinone	26.91	30.49	ND
	n-Cyclohexylacrylamide	1.53	1.47	ND
	n-Cyclohexyl-propanamide	13.62	13.73	ND
	1-Butyl-2,5 dimethyl-1 H-pyrrol	6.33	2.33	ND
	1,2,2,5-Tetramethyl-3-piperidinone	7.47	4.73	ND
	Indole	4.80	ND	ND
	Indolizine 7 methyl	4.87	ND	ND
	Glutamic acid dibutyl ester	5.53	ND	ND
Estimated total tar content in 1 mL aliquot of scrubber (150 mL acetone)		**192.43**	142.06	<0.100
Mass of Tars		28.86	21.31	<0.015

Table 5.18 A Table summarising the compounds identified in scrubber 1 and 2 from the pyrolysis of sludge filter cake from Ghana. Some of the compounds have been quantified by targeted analysis while some have been semi-quantified. Unknown peaks were elucidated by their mass spectrum and peak area was compared to an internal standard. There is a notable similarity in the compounds present between the UK and Ghana sludge cake.

5.4.7 Summary of tar results.

- Tars identified in the scrubbers for pine wood were synonymous with biomass thermal treatment. The presence of furfuals and fural derivatives are evidence for the decomposition of the hexose sugars such as xylan and glucose from hemicellulose and cellulose respectively. Phenolic compounds such as isoeugenol, phenol, cresol, ethyl guaiacol, salicyl alcohol and coniferyl alcohol are considered typical breakdown products of lignin. The identification of PAHs at low temperatures are suspected to originate from the decomposition of the extractive compounds.

- Gasification of pinewood generated similar tars to pyrolysis However, unlike pyrolysis the level of tars is significantly reduced (~90 %) when air is added suggesting that these may be oxidised resulting in a higher production of carbon monoxide.
- The tars identified in thermal treatment of Brownfield contaminated soil contained volatile aromatic and poly-aromatic hydrocarbons, typical compounds associated with petroleum 'oily' sludge. Interestingly, the compound profile observed in the scrubber post-pyrolysis appear to be the same observed the solvent extraction pre-pyrolysis of the soil with no additional compounds detected. This suggests that perhaps thermal degradation has not occurred of these compounds but their release from within contaminants associated with the soil. This data has shown the potential for soil remediation following contamination using thermal treatment processes.
- Both UK and Ghana sludge generated similar tar compounds, predominantly volatile aromatic compounds, phenolic compounds and a high percentage of nitrogen containing heterocyclic compounds. With the latter, likely originating from the thermal decomposition and rearrangement of amino acids from microbes and dietary proteins. However, Ghana sludge cake generated a greater amount of tar compounds indicative of a higher nitrogen (N=3.5 mg/Kg) and semi-volatile content (SVOC 3.5 g/Kg) contained within this feedstock prior to pyrolysis.

5.5 Conclusion.

After successful selection of solvent for the scrubber, the selected feedstocks were then characterised by solvent extraction to investigate the semi-volatile material associated with the material. It was found that the extracts contained a variety of semi-volatile compounds each indicative of its feedstock; pinewood consisted of terpenoid compounds common with softwood extractables, brown field contaminated soil containing high amounts of volatile aromatic and polyaromatic compounds, typical of contaminants of oily sludge waste, and the sludge from UK and Ghana contained high amounds of non-polar mixed hydrocarbons, cholesterol derivatives and phytosterols, respectively. Thermochemical treatment (pyrolysis and gasification) and capture of these tar compounds in acetone, was used as a preparation method for the identification of these tar compounds. The acetone also provided a means of syngas cleaning and simple gases could then be monitored using GC-TCD. To get a complete picture of the behaviour of the semi-volatiles, the remaining material from the thermochemical treatment was again solvent extracted and analysed via GC-TCD.

Analysis of the contaminated acetone impingers *via* GC-MS provided compound information of the breakdown products of the main constituents of the feedstocks. This could be used to understand the potential risks of recycling these uncharacterised feedstocks (brownfield soil and sludge cake). Using pine wood as a benchmark, it was likely that many of the compounds originated from the main constituents of the material; for biomass this included furfural derivatives derived from decomposition of cellulose and hemicellulose, while phenolic compounds such as isoeugenol and coniferyl acid arise indicative of lignin decomposition. However, it was suggested that some tars may arise from the extractable terpenoid compounds seen in the pre-pyrolysed extract. Phenanthrene has since been postulated to arise from alternative mechanism; the degradation of the dehydroalbetic acid (extractive). This was supported by the presence of retene (an intermediate in the dehydroalbetic acid mechanism)(99) and dehydroalbetic acid in the scrubber. The generation of PAHs is generally

considered to arise at high temperatures (excess of >700 °C) but this new evidence could explain why PAHs were identified at a lower temperature (table 4.9). However, the presence of these 'marker' compounds from pyrolysis of pine wood was sufficient to verifiy succesful operation of the pyrolysis rig and scrubber system.

Other uninvestigated problematic waste samples were also studied. For example brown field contaminated soil generated tars that were synonomous with oily sludge containing high amounts of harmful volatile aromatics and PAHs, whilst sludge cake contained a mixture of tars typical with biomass samples (phenols and some furfurals) and a high percentage of toxic nitrogenous compounds. Overall the capturing and analysing of the tars using solvent traps was a robust method. Typically repeat pyrolysis trials generated similar quantities of tars and RSD values of the total targeted tars were below 25 % indicating that the process was repeatable. Pine and UK sludge pyrolysis offered the most repeatable batches with % RSD below 10 % for pine wood and below 11 % for UK sludge cake on targeted compounds (SVOT and VOT methods). Brownfield soil however, had higher %RSD for targeted compounds (<25 %), suggesting these samples were more heterogenous than pine wood and UK sludge. Although quantitation is possible with this setup, the method does have its limitations; non GC compatible compounds, such as larger more polar molecules (disaccharides) could not be identifed in the scrubbers and would require confirmation by other means (LC-MS). Therefore, the 'true' concentration of tars is likely to be higher than the quoted values identified in the scrubbers and should be considered for further work in implementing this approach. This capture of these harmful substances enables the recycling of samples to be realised, de-risking the process and limiting waste that may be directed to landfill. However, an additional upshot is that this work has shown the need in assessing cleanliness of feedstocks, as an important evaluative tool for occupational health monitoring.

The success of the acetone scrubber provided a means cleaning the syngas, suitable in readiness for analysis by GC-TCD, to determine the suitablility of the syngas for other processes such as

FT. Results of the GC-TCD showed that pine wood gasification provided the most calorifc gas for energy production (10.46 MJ/m^3) and brownfield having the lowest CV gas (0.73 MJ/m^3) . It is therefore, unlikely to use pyrolysis of contaminated soil for energy use but results of the remaining 'char' suggests that pyrolysis could be used for soil remediation as there was evidence that ~80 % of contaminants were removed after thermal treatment of brownfield soil. The GC-TCD was used to compare the syngas production with feedstocks and understand which suitable for with FT. Pine wood which was air gasified generated a steady 1:6 ratio of CO: H_2 and highest amount of CO (max 17 %) and hydrogen (46 %) which would in theory generate more hydrocarbons if used in FT, this was closely followed by UK sludge gasification (max CO and H_2 9 % and 48 % respectively).

Chapter 6:

Re-use of waste materials of pyrolysis: biochar.

Biochar from pine wood, UK sludge cake and Ghana sludge cake, was activated using phosphoric acid and investigated into its potential as a sorbent for organic pollutants. Biochar is a highly graphitised material whith a large surface area that contains a variety of functional groups giving it a potential to act as a sorbent. This is a developing area of research (23,24) and the suitability of these feedstocks is unknown. However all char materials do require preparation, typically through 'activation', in addition to characterisation before use. The remaining material from brownfield pyrolysis was considered unsuitable for activation as it mainly consisted of silicate materials with little or no carbon content. Therefore, the biochar from pine wood, UK sludge cake and Ghana sludge cake, was activated using phosphoric acid and tested as a low cost sorbent for treating contaminated water containing a mixture of PAHs, phenols and diesel and gasoline. This involved passing contaminated water over a bed of biochar held within an empty solid phase extraction (SPE) cartridge, a more detailed method is decribed in chapter 2.5.2. Acativated biochars generated at different temperatures were tested for their recovery efficiency towards selected compounds; polyaromatic hydrocarbons and phenolic compounds. Standard mixtures representing PAHs, and phenols were prepared as quality control samples, 'spike before' and 'spike after' to determine recovery of specific analytes to the sorbent. The samples were run in triplicate and quantified against an internal standard calibration curve containing analytes present in the standard mixture.

To assess the viability of biochar for use with complex samples indicative of industrial contamination, these were investigated for the clean-up of a gasoline and diesel standards. Mixtures of diesel and gasoline were used to prepare QCs spiked before and after extraction to give a 2 mg/L solution. The SBE was prepared using 100 mL deionised water spiked with 10 µL

of the diesel and gasoline standards (20 mg/mL) and passed through biochar extraction cartridge. The SAE was prepared as an extracted 100 mL deionised water sample, collected, and spiked with 10 µL of diesel or gasoline standards. Due to the high hydrophobicity of these samples they would typically be eluted using pentane to ensure solubility. However, preliminary work involving direct elution using pentane showed the co-extraction of other highly abundant organic species from the biochar which compromised the selectivity of the analytical method. Therefore, the water collected after passing over the biochar was extracted using 10 mL of pentane of which 1 mL was analysed using GC-MS under full scan conditions as a survey scan.

To determine the recovery of diesel and gasoline, the extracted ion current chromatograms (EICCs) were integrated to generate a signal response as peak area (see equation 6.1) and compared to the area count of the QC SAE. For quantitation of PAHs and phenolic compounds the single ion monitoring (SIM) chromatogram for the relevant target ion was integrated to generate the signal response (equation 6.2).

$$\frac{Peak\ area\ spike\ before\ extraction}{Peak\ area\ spike\ after\ extraction} \times 100 = \%\ Recovery\ (adsorption) \qquad \text{Equation 6.1}$$

$$\frac{concentration\ spike\ before\ extraction}{concentration\ after\ extraction} \times 100 = \%\ Recovery\ (adsorption) \qquad \text{Equation 6.2}$$

The recovery or retention of these compounds was investigated on different feedstocks; sludge cake from two wastewater plants located in the UK and Ghana and a recognised biochar feedstock, pine wood. The UK sludge cake samples was also used to prepare biochar at two different processing temperatures (400 and 700 °C) to detect any change in selectivity of the biochar chemistry. The data collected for the biochar sorbent recovery generally show good precision with relative standard deviations (RSD) below 25 % for majority of PAHs and phenolic compounds (see tables 6-6.2). Interestingly, the lower temperature sludge biochar seemed to have more repeatable recovery for phenolic and PAH compounds (both volatile and semi-volatile) versus pine wood indicated by a lower % RSD. Typically, repeatable retention of

phenolic compounds (<25 % RSD) was observed for all biochars tested; this also appeared to be the case for volatile PAHs (boiling point range 218-404 °C) however, anthracene had poorer repeatability with 29.7 % RSD using pine wood biochar. Overall, semi-volatile PAHs (438-550 °C) appeared to be extracted with greater precision than volatile PAHs regardless of the origin of the biochar. For these compounds the sludge cake biochar showed improved repeatability *versus* pine wood with RSDs below 10 %. Pine wood biochar did show reasonable repeatability for this class of compounds with RSDs less than 25 % apart from benzo (b) fluoranthene, with an RSD of 27.6 %. In summary, this data suggests that biochar may have selectivity towards compound class as well as retention (recovery), with sludge cake biochar showing the best repeatability out of the two sample types. However, a larger sample size with more replicates (run in triplicate for this investigation) would provide more meaningful data on repeatability and reproducibity.

Volatile PAH compound (218-404 °C)	Boiling point	Log P	Pine wood biochar 400 °C		UK sludge cake biochar 400 °C		UK sludge cake biochar 700 °C		Ghana sludge cake biochar 400 °C	
			Mean % Recovery	Precision (% RSD)	Mean % recovery	Precision (% RSD)	Mean % Recovery	Precision (% RSD)	Mean % recovery	Precision (% RSD)
Naphthalene	218 °C	3.3	61.5	15.0	55.6	1.13	41.0	24.5	53.6	12.9
Acenaphthylene	280 °C	3.7	54.6	16.9	59.1	3.04	35.9	8.88	67.8	12.9
Acenaphthene	279 °C	3.9	70.3	8.57	61.5	3.18	65.4	12.2	88.8	20.2
Fluorene	294 °C	4.2	66.7	12.8	64.6	3.46	57.0	23.2	78.6	18.5
Phenanthrene	339 °C	4.5	77.1	12.7	68.2	4.00	65.0	7.61	52.0	5.44
Anthracene	340 °C	4.4	69.3	29.7	73.4	2.54	46.8	11.5	66.0	12.9
Fluoranthene	375 °C	5.2	81.0	19.2	70.6	3.00	54.5	6.62	39.0	7.25
Pyrene	404 °C	4.9	84.5	22.6	69.8	3.00	55.8	4.19	35.3	1.00

Table 6 A table summarising the removal of the target PAHs within boiling point range 218-404 °C from the 'scrubber' using biochar as an extraction sorbent, with extraction recoveries above 50% highlighted in blue. Pine wood biochar and that from UK sludge cake processed at 400 °C shows good mean recovery for PAHs within this range (54.6-84.5 % and 55.6-73.4 %, respectively). Ghana sludge cake biochar is effective at recovering PAH naphthalene to anthracene (52-88.8 %). UK sludge cake at

6.1 Characterisation of biochar selectivity.

6.1.1 Retention selectivity for PAH and phenols: compound class.

The results of the recovery experiment show that pine wood biochar prepared at 400 °C, has the most effective recovery for volatile PAHs with average % recovery of 70.6 %, ranging from (54.6-84.5 %) despite having higher %RSD (poorer precision). UK sludge cake biochar prepared at 400 °C showed similar recoveries to pine wood, with a range 55.6- 73.4 %, however, UK sludge biochar showed improved precision, indicating that both biochars may be suitable as sorbents with a selectivity towards volatile PAHs. However, the lower temperature biochar (400 °C) from UK sludge generally showed increasing recovery for volatile PAH compounds typically with a higher hydrophobicity (log P), indicating a potential selectivity of this material for specific compound classes.

It appears that UK sludge and pine wood biochar produced at 400 °C has a similar selectivity towards volatile and semi volatile PAH compounds. A statistical comparison using a t-test for these feedstocks indicate no significant difference and therefore, these materials both prepared at this temperature exhibit the same selectivity for the same compounds.

Semi-volatile PAH compound (438-550 °C)	Boiling point	Log P	Pine wood biochar 400 °C		UK sludge cake biochar 400 °C		UK sludge cake biochar 700 °C		Ghana sludge cake biochar 400 °C	
			Mean % Recovery	Precision (% RSD)	Mean % recovery	Precision (% RSD)	Mean % Recovery	Precision (% RSD)	Mean % recovery	Precision (% RSD)
Benzo (a) anthracene	438 °C	5.8	51.1	19.1	48.3	2.00	35.3	0.40	30.1	3.06
Chrysene	448 °C	5.7	41.1	6.72	41.5	2.29	30.1	5.88	25.3	1.40
Benzo (b) fluoranthene	481 °C	6.4	43.5	27.6	55.6	1.95	21.8	4.88	16.0	8.42
Benzo (a) pyrene	496 °C	6.0	44.7	24.7	49.7	1.70	24.0	8.84	18.9	5.99
Dibenzo (a) anthracene	524 °C	6.5	37.7	5.07	44.8	2.05	32.2	0.66	19.2	0.74
Indeno (123) cd pyrene	536 °C	7.0	41.1	24.3	39.6	5.35	29.8	4.04	17.3	4.90
Benzo (ghi) perylene	550 °C	6.6	38.8	8.02	45.2	2.34	26.7	4.51	15.4	2.30

Table 6.1. A table summarising the removal of the target PAHs within boiling point in the range 438-550 °C from the 'scrubber' using biochar as an extraction sorbent (recoveries >50% highlighted in blue). There is an overall reduction of PAH recoveries using all biochars for PAH within this range with similar recover data observed for pine wood and UK sludge cake. Note: boiling point and log P data were retrieved from PubChem compound database.

For semi-volatile PAHs all biochars showed reduced recovery; typically, retention (recovery) decreased with increasing boiling point of the compound regardless of biochar. It is therefore posssible that another mechanism other than hydrophobicity is involved in the selectivity for these compounds (23–26,28). It is unlikely that the elution capacity of acetone has been reached as all the compounds are soluble in acetone. Of the biochar, pine wood and UK sludge low temperature biochar showed the highest recovery for higher boiling point PAHs, with similar recoveries of 37.7-51.5 % and 39.6-55.6 %, respectively. Unlike data for volatile PAHs, retention appears to decrease with increasing boiling point and hydrophobicity. This data suggests that selectivity of retaining PAHs may not solely be dictated by chemical interaction but potentially molecular size (cross-section). For example, the higher the boiling point, the larger the physical size of the PAH, therefore PAHs greater in molecular weight than pyrene, recovery appears to reduce; possibly as they are unable to fit within molecular pore of the sorbent to interact by hydrophobicity (24,26,28,137). From studies on activated carbon materials, It is postulated that

adsorption of substrate molecules that are aromatic, such as PAHs and phenols are strongly influenced by dispersion forces over electrostatic. The mechanism of adsorption is contact time dependant, meaning the longer the material is immersed in the solution, the greater the uptake of the substrate (138,139). The initial mechanism of adsorption is surface driven by physisorption and surface pores, secondary mechanisms that occurs over a longer time scale intraparticle diffusion (140). Intraparticle diffusion mainly is influenced by pore filling (141,142). Due to the relative short residence time of this experiment, the modes of interaction will be surface mediated, through physisorption and surface pores (143). For phenolic compounds, pine wood and UK sludge low temperature biochar generally gave poorer recoveries than the remaining compounds tested (see table 6.2). The more polar chloro- and nitro-phenol species however, showed the greatest recovery, with trichloro compounds showing the highest retention (78.7-88.8 %) over the range, suggesting some affinity for more polar material at this synthesis temperature. For UK sludge biochar at 700 °C temperature, the phenolic compounds show similar recovery to the biochar prepared at 400 °C however, the more polar chloro- and nitro-phenol species showed a reduction in recovery with temperature and trichloro compounds showing recoveries of 53.9-64.9 %. The overall poorer recoveries for more volatile phenolic compounds suggests that the prepared biochars may be have reduced surface oxidisable groups which can interact with the with polar functional groups (–OH and chlorine) of phenolic compounds, such as hydrogen bonding, and it is secondary interactions such as non-polar, hydrophobic interactions that may be the cause of retention (23–26,28,29).

Phenolic compound	Boiling point	Log P	Pine wood biochar 400 °C		UK sludge cake biochar 400 °C		UK sludge cake biochar 700 °C		Ghana sludge cake biochar 400 °C	
			Mean % Recovery	Precision (% RSD)	Mean % Recovery	Precision (% RSD)	Mean % Recovery	Precision (% RSD)	Mean % recovery	Precision (% RSD)
Phenol	182 °C	1.5	18.6	24.3	19.7	2.87	16.1	18.4	17.8	10.8
2-Chlorophenol	175 °C	2.1	24.1	24.3	19.9	1.78	17.7	18.4	24.4	17.4
2-Methylphenol	191 °C	2.0	13.6	5.74	12.3	2.89	10.3	23.9	14.6	15.5
4-Methylphenol	202 °C	1.9	16.3	2.60	15.2	3.72	12.8	21.0	20.0	21.8
2-Nitrophenol	216 °C	1.8	35.8	14.1	25.4	3.90	17.4	8.56	30.8	22.8
2,3-Dimethylphenol	218 °C	2.6	22.7	23.9	19.0	4.85	20.3	23.8	30.9	18.5
2,5-Dichlorophenol	211 °C	3.1	38.0	1.32	34.3	3.71	31.7	13.9	31.7	17.0
2,6-Dichlorophenol	220 °C	2.7	36.5	4.41	33.5	1.90	30.8	23.8	30.5	12.9
4-Chloro-3-methylphenol	235 °C	3.1	31.8	10.9	24.0	1.17	26.6	22.0	29.8	17.4
2,3,5-Trichlorophenol	248-253 °C	3.6	60.5	24.5	78.7	1.52	64.9	20.2	49.1	13.6
2,3,6-Trichlorophenol	272 °C	3.8	62.0	24.8	88.8	5.81	53.9	18.6	38.5	21.3

Table 6.2. A table summarising the removal of the target phenols from the 'scrubber' using biochar as an extraction sorbent with recoveries greater than 50 % highlighted in blue. Pine wood biochar and UK sludge cake biochar appears to be effective at removing 2,3,5-trichlorophenol and 2,3,6-trichlorophenol, demonstrating the highest mean recoveries, 64.9 and 53.9 % for UK biochar and 60.5 and 62.0 % for pine wood biochar. Note: boiling point and log P data were retrieved from PubChem compound database.

6.1.2 Retention selectivity for PAH and phenols: biochar processing temperature.

For the UK sludge cake samples, the processing temperature of the biochar was investigated to determine if those obtained at higher temperatures (in this case 700 °C) offered more retention to hydrophobic analytes than those at lower temperatures (400 °C). It is was postulated that the higher temperature biochar would be less suited to retention of polar analytes as these would contain less oxidised groups on the surface and more non-polar groups suited to retain non-polar species via hydrophobic interations. In a similar experiment it was documented that higher processing temperatures of activated carbon (AC), showed enhanced in π-π dispersion forces with a decreased surface acidic groups (COOH), and a increased surface area and porosity. This enhanced the adsorption abilities of AC towards phenol substrates (139). It is apparent from

the recovery data that the lower temperature biochar showed greater precision in performance across all analyte tests with RSDs below 6 %. This gives greater confidence in the recovery result as the results are repeatable. However, a larger sample size with more replicates would be required to get a true reflection of repeatability and reproducibility. Unexpectedly, UK sludge biochar prepared at higher temperature showed reduced recovery of PAHs (21.8-65.4 %), particularly for less volatile hydrophobic species. The higher temperature biochar also showed poorer precision in recovery although this was still within reasonable levels (<25 %). This data may suggest that at higher temperatures the sorbent pore structure may become damaged causing the porous structure to collapse or coalesce reducing the surface area of the biochar and its sorptive ability (137).

In terms of sorptive performance it is thought that biochars prepared at a lower temperature (400 °C) should have a greater degree of polar functionality (23,29) offering greater retentive properties for more polar organic material. However, the data provided showed that despite a marginal increase at lower temperatures there is a (see tables 1-3) a lower than expected polar functionality, with often a greater affinity towards volatile PAHs observed.

From more detailed analysis of more polar compounds, the low temperature biochar showed higher levels of recovery for all compounds apart from 2-nitrophenol and 4-chloro-3-methylphenol. However, the results for these two compounds are very similar with recoveries of 19 and 24% (low) and 20.3 and 26.6 (high), respectively. To evaluate if these recoveries are significantly different, a t-test to compare the mean data was applied and proved particularly helpful for data that initially appeared similar. For example, of those tested, only phenol, 2-chlorophenol, 2-methylphenol, 4-methylphenol, 2,5-dichlorophenol and 4-chloro-3-methylphenol did not show a significant difference between the mean recoveries for low and high temperature biochars (see appedix 5 for details) and these showed similar recoveries to other compounds justifying the use of significance testing here. This again suggests that

production temperature may not be the sole determining factor for biochar chemistry. A possible mechanism for retaining organic compounds is through pore filling effects rather than surface interaction; here pores of limited size may contain some non-polar functionality (26,137) allowing the entrance of hydrophobic molecules of a certain cross sectional area and specific conformation. While larger semi-volatile PAH (greater than benzo (a) anthracene) do not enter the pores as they are too large or do not have the correct shape (137). There is evidence in the literature backing this claim, as studies have shown that activated carbon materials are more effective at adsorption, if the PAH substrate has a certain molecular size complementary to pore sizes of the material. (144). This data emphasises the need for sorbent testing to determine its application suitability as a sorbent.

6.1.3 Retention selectivity for PAH and phenols: sludge cake biochar location.

A comparative study was undertaken for sludge cake biochar taken from two different locations generated from the same treatment process to determine the potential variation in feedstock. Interestingly, our results indicate that sludge biochar derived from the Ghana wastewater plant showed reduced precision and more variation in recovery for PAHs and phenolic compounds compared with biochar from a UK sludge sample. Ghana sludge cake biochar demonstrated improved extraction recovery (52-88.8 %) for more volatile PAHs (napthalene to anthracene) while UK sludge biochar showed overall good recovery for volatile PAHs (napthalene to pyrene) including those with a higher boiling point >339 °C (70.6, 69.8 %). The sludge cake biochar sourced from Ghana showed lower recovery (15.4-30.1 %) of semi-volatile PAHs compared to UK sludge cake, potentially indicating that there may be smaller pore sizes within this sample limiting the retention of compounds with a larger cross-sectional area (23,28,29,137,145). The biochar generated from UK sludge cake showed greater retention for phenolic compounds compared to Ghana sample with recoveries of 15.2 – 88.8 % and 14.6-49.1 %, respectively. In particular, the largest difference in retention was observed for the tricholoro compounds with

increased recovery observed for UK biochar from 78.8-88.8% and 38.5-49.1 % for 2,3,5-trichlorophenol and 2,3,6-trichlorophenol, respectively, suggesting a stronger affinity towards the more hydrophobic phenol (high Log P) . In summary, this sludge cake data highlights the inherent differences in the feedstocks despite an apparent similar initial method of synthesis and that biochars produced from similar source material may have differing selectivity for certain pollutant classes, and should therefore be tested/selected accordingly prior to use. In a study by K. Jindo et al 2014 of biochar derived from agricultural waste, samples of hardwood (apple tree branch and oak tree branch), rice husks and rice straw, were treated at different temperatures to generate biochar. Each sample showed that with increasing pyrolytic temperature both pore size and its adsorption ability towards Iodine and methylene blue increased. Interestingly, although the wood samples were of similar type (hardwood) or from the same plant material, the variation in chemical composition was enough for the biochar to exhibit differences between samples, such as physical properties (pores sizes varied between samples) and adsorption. Apple tree branch biochar generated larger pore sizes and had increased absorbance of iodine and methylene blue over oak tree branch, while rice husk showed similar trend compared to rice straw (146). Therefore, akin to the sludge cakes trial from in this investigation, the differences in composition can account for differences in adsorption properties. It is well documented that ligin and cellulosic content on material can have an effect on the structure and chemistry of the biochar. With feedstocks of higher lignin generating biochar with higher hydrophobicity and increased pore sizes (28,147).

6.2 Application of biochar as a sorptive medium: clean-up for gasoline and diesel spills.

To evaluate the effectiveness of biochars for clean-up of complex samples, the biochars were tested with water contaminated with gasoline and diesel standards. This was used to determine a possible application of these sorbents for the treatment of industrial contaminated water.

Two methods were considered for measuring the retentive ability of the sorbent; [1] integrating target masses of the extracted ion chromatogram representing gasoline and diesel components and, [2] integrating the total ion chromatogram for the retention times typical of the gasoline and diesel components. To ensure that the retentive capability was consistent, the target mass approach was adopted, monitoring ions at *m/z* 77, 105, 119 and 128, representing light aromatic and naphthenic compounds within gasoline, and ions *m/z* 85, 131, 145, 155, 165 and 190 for hydrocarbons and larger polyaromatic compounds within diesel. The sum of the chromatographic peak areas for these extracted ions were used to determine the compound range and used to calculate recovery by comparing the area of the QC spiked before extraction and QC after extraction. These were replicated and analysed; results, summarised in figure 6, were compared to the second approach proposed which compared the total ion chromatogram as a check of the rationale applied using the extracted ion approach.

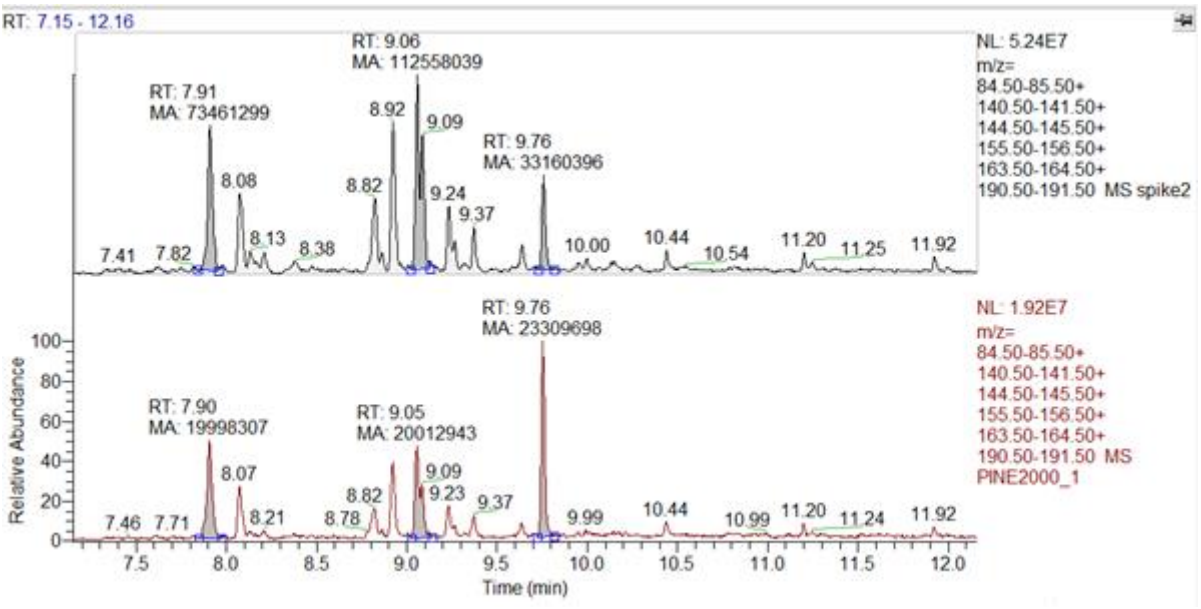

Figure 6 Figure of an extracted ion chromatogram (XIC) of the diesel contaminated water treated with pine biochar at 700 °C (red XIC) to the spike after quality control sample (XIC black) showing a notable decline in area count between the two samples. Extracted peaks integrated between 7.15-12.16 minutes are typical diesel range compounds; ions m/z 85, 131, 145, 155, 165 and 190 are associated with relevant hydrocarbons and larger polyaromatic compounds.

The recovery data shows a distinctive decline in area count of gasoline and diesel range compounds after application to activated biochar (see figure 6) for example data of biochar originating from pine wood). Upon closer inspection of the replicate data all biochar samples tested delivered good precision of extraction with RSDs <21 % for both gasoline and diesel (figure 6.1). In particular, greater precision was observed for biochars prepared at lower temperature of 400 °C, with those derived from sludge cake, having RSDs <3 % for gasoline and <13 % for diesel. It is apparent from the data set that pine wood biochar appeared to be the most successful at removal of gasoline and diesel compounds with recovery values >61 % and excellent precision (<7 %RSD), both for high and low preparation temperatures. For lower temperature prepared pine wood biochar recoveries were similar to the volatile and semi-volatile PAH data suggesting a similar mechanism for retention. The higher temperature biochar from pine wood appeared to be more effective at recovering gasoline and diesel compounds and showing significantly better precision. It was initially postulated that high temperature feedstock would be better suited at removal of hydrophobic compounds; the results for pinewood seem to agree with this statement as it appears to have improved recovery for gasoline and diesel compounds, suggesting a greater degree of hydrophobicity due to increased carbonisation (23,24,26,29).

The sludge cake generated from Ghana wastewater treatment plant, showed poorer recovery to that from the UK for PAHs compounds however, similar recoveries were observed in the gasoline and diesel recovery experiment, suggesting that the location of the biochar sludge cake may be less significant for complex sample clean-up. For UK sludge cake biochar, recoveries of volatile PAHs were lower than expected for the lighter, more volatile gasoline sample (mean 65.4 % with volatile PAH standards versus 49.22% for gasoline) however, comparable recoveries were observed for diesel samples (mean recovery 46.4 % for semi-volatile PAH standards versus 45.88% for diesel). These results indicate that other sample components within gasoline may

influence extraction and further characterisation using real-life samples are required. For complex samples, the sludge cake biochar samples from the UK and Ghana prepared at 400 °C appear to have comparable recoveries for gasoline and diesel compounds with good precison suggesting good reproduciblity between locations. This suggests that Ghana samples may also offer the potential for re-use.

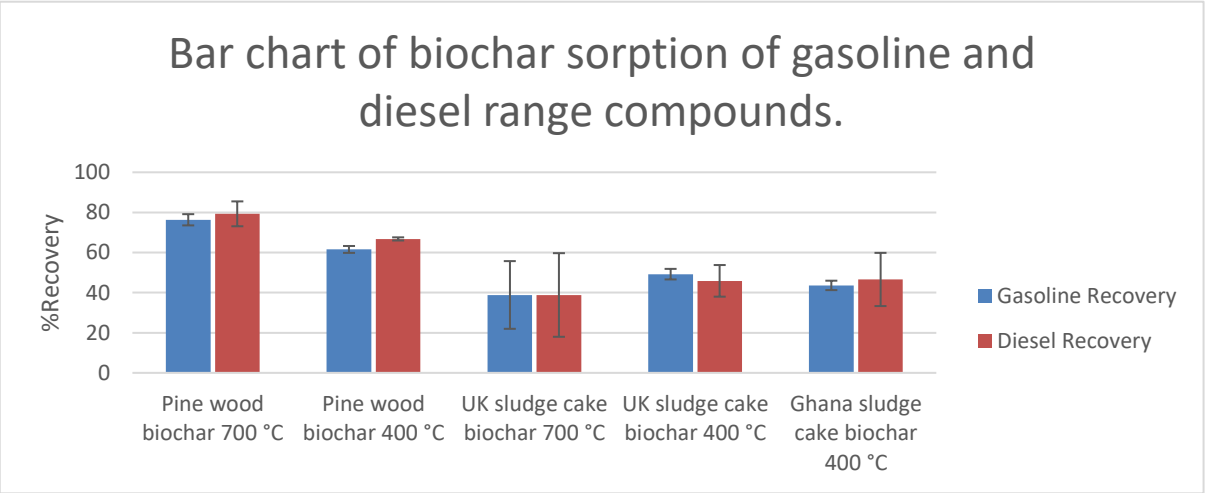

Figure 6.1. A graphical representation of gasoline and diesel recovery of various prepared biochars. Pinewood biochar prepared at 700 °C shows greates selectivity for gasoline and diesel range compounds.

6.3 Conclusion.

This investigation focused on the re-use of biochar derived from pyrolysis recycling of biomas, as a sorptive medium for waste water treatment, with particular focus on water scrubbers and industrial contaminated water. This work has assesed biochar synthesised from an uncharacterised feedstock derived from wastewater treatment of sludge using anaerobic digestion, termed sludge cake, this was sampled from two separate locations, a treatment works in the UK and treatment work in Ghana. The biochars in question were generated at different temperature, high and low (700 and 400 °C) as it was postulated that processing temperature would have an impact on the selectivity of the biochar towards specific chemistries, with higher processing temperatures favouring more hydrophobic compounds and lower temperture

biochars offering more selectilvity towards polar compounds (23,24). The results of this investigation was compared to a recognised feedstock, pine wood. The initial studies used specific compounds with known physical properties and which represented anticipated contaminants from the thermochemical process likely to be found in the scrubber system. Further to this a complex sample containing gasoline and diesel was analysed as a potential for treating petroleum spills. The data indicates that biochar is a promising sorbent it can reduce the level of petroleum contamination in water by up to 79 % for pine wood biochar and ~50 % for sludge cake.

It appears from the data that pine wood biochar is the most effective sorbent as the recovery was greatest for PAHs, gasoline and diesel compounds, pine wood also showed an improvement in performance performance when generated at higher temperature (700 °C), suggesting an increase in hydrophobic character possibly due to increased carbonisation reactions . However, of the uncharacterised feedstocks, UK sludge cake shows biochars processed at lower temperatures (400 °C) have improved selectivity and affinity for PAHs, gasoline and diesel suggesting physical and chemical differences of this initial feedstock to pine wood, requiring less energy to obtain a similar hydrophobicity. It was proposed that biochars generated at lower temperatures would be more selective at removing the more polar phenolic compounds, as lower temperature biochars typically have higher degree of oxidisable groups (23,24) associated with the material which have an affinity towards polar groups such as phenols through interactions such as hydrogen bonding. However, this was not the case as phenol recovery was poor for not only for sludge cake biochar, but for all the biochars prepared, suggesting a similar mechanism of affinity towards phenols, which is more reliant on the hydrophobic interaction rather than a polar interaction.

A possible explanation for the difference in behaviour of sludge cake and pine wood, could be linked to the differences in the composition of the starting material. Sludge cake typically has a

a lower lignin composition compared to that of pine wood and it is believed that lignin is required to create the porus structure of biochar (137). A reduction in lignin content will result in fewer pores which are believed to be the mechanism of interaction of the biochar and analyte At higher preparation temperatures, the pores can be damaged as they collapse or coalesce reducing the surface area of the biochar, and its sorptive ability (137). However, sludge cake has shown the potential as an effective and repeatable sorbent with a selectivity for hydrophobic compounds. The advantage of using sludge cake is it can be be generated at a lower preparation temperature and thus a more energy efficient and cost effective means of generating a sorbative product.

To conclude, biochars produced from pyrolysis of waste recycling can be used to selectively remove hydrophobic compounds such as PAHs, gasoline and diesel contamination in water. This may offer a cost effective means of treating contaminated water scrubbers used in the clean-up of thermochemical processes which are likely to contain volatile PAHs. In addition to the method of disposing contaminated water has the potential to be used in the prevention and onsite treatment of petroleum spills with the intention of localising and limiting the potential further contamination of ground water. The benefits associated with the application of biochar can have a wider purpose with regards to aiding wastewater management, providing a more environmentally friendlier alternative compared to disposal on landfill and agricultural land. Further investigation into the preparation of biochar may offer a more optimal processing temperature with a higher efficiency for recovering specific compounds. These activated biochars, will need further testing on 'real scenario' contaminated waters to acertain their behaviour with complex matrices.

Chapter 7

Fischer- Tropsch catalyst development and testing.

Current FT catalysts are generally expensive to synthesise and purchase and one prohibative factor for FT technology. Current approaches to catalyst preparation differ in the method at which the active ingredients are deposited on the support (148). These preparation stages have been well documented and common techniques such as incipient wetness (deposition of active salt solution on to support), co- precipitation (deposition of active ingredient with promoter on to support), 'sol-gel' method which is used in silica supported catalysts (formation of a gel to enhance binding affinity between support and active metal) (148,149) and some recent techniques such as microemulsion (150) and chemical vapour deposition (151) all require a high heat treatment stage (148,149) such as calcination (650 °C for up to 12 h) (47,152,153). Interest has now moved focus to low thermal preparation techniques such as plasma treatment, to make the process more feasible and environmentally friendly. Low thermal techniques (plasma) has generated successful catalysts with good dispersion of active sites and catalytic activity (154). This work investigated the preparation of a cobalt catalyst using a less energy and cost intensive approach to producing the desired transition state of an FT catalyst. Cobalt chloride (active metal) and manganese sulfate (promoter) solution was deposited on to the supported through incipient wetness, and dried at 300 ° C, before the deposited active ingredient was modified chemically. This modification was based on a simple oxidation reaction aimed at replacing the lengthy calcination approach. A number of tests were performed to characterise the catalyst synthesised using this approach, such as X-ray diffraction (XRD), scanning electron microscopy (SEM), inductively coupled plasma optical emision spectroscopy (ICP-OES) and Brunauer-Emmett-Teller (BET) analysis. The catalyst was prepared by addition of cobalt chloride (CoCl) solution (and some manganese sufide) to aluminium oxide (Al_2O_3) by incipent wetness. The CoCl was oxidized by titrating sodium hypochloride solution to the supported material to produce

cobalt (III) oxide (Co_2O_3). The modified catalyst was then heated (250 °C) for 2 hours to form a stable precursor catalyst. Prior to catalyst testing the precursor catalyst was reduced in hydrogen atmosphere at 400 °C for 4-6 hours (inside the FT reactor) to form the active catalyst. In order to generate hydrocarbons, the temperature of the reactor was lowered to 350 °C, while the addition of carbon monoxide and hydrogen under pressure provided the conditions for the reaction to commence.

7.1 Catalyst characterisation.

The elemental composition of the digested catalyst was determined by inductively coupled plasma optical emission spectroscopy (ICP-OES) using an argon plasma to atomise the sample and detect the characteristic wavelength of photons of excited elements as they return to ground state (121). For this technique, concentration is directly proportional to the intensity of the emitted photons and can be determined using a calibration graph. Using this approach the precursor (inactive) catalyst (CAT-1) was measured and found to contain 13 % cobalt, 80 % aluminium and 2 % manganese (promoter) by mass. These cobalt levels are within the typical range for FT catalysts of 10-15 % (152,155,156) (see table 7.1).

Elemental composition of CAT-1	Concentration mg/kg	% mass of element
Aluminium	77536	79.555
Cobalt	12798	13.131
Nickle	13.47	0.014
Antimony	9.14	0.009
Copper	4.09	0.004
Iron	246	0.252
Manganese	2490	2.555
Magnessium	0.98	0.001
Potassium	2451	2.515
Sodium	1913	1.963

Table 7 A table showing the elemental composition of the catalyst as determined by ICP-OES spectromety.

The surface composition and crystalline structure of the catalyst are key to the viability and efficiency of the catalyst and requires characterisation prior to further use. These were characterised using X-ray diffraction (XRD) by analysing the inactive and active material. The inactive precursor (CAT-1) contained a mixture of cobalt oxide starting materials, Co_2O_3 (green arrow, figure 7) and Co_3O_4 (brown arrow, figure 7) confirming the ICP-OES data that the oxidation reaction was succesful and Co had been immobilised on the support. After reduction of the inactive catalyst in hydrogen the XRD spectrum shows a slightly different signature, indicating that these Co species have been successfully reduced forming metallic hexagonal compact crystallite active sites of cobalt (blue arrow, figure 7.1). The minimum crystallite sizes required for FT reactions are 6-8 nm (157) with larger particles deemed more effective due to a larger surface area for coordination to occur (152,157). Although activity is not solely dependent on crystal size, selectivity of the catalyst for hydrocarbon production is size dependent (152,157). For example, larger cobalt particle sizes favour the formation of heavier

hydrocarbons, such as those desired for fuel production, as there is greater probability for chain growth (152). The crystallite size for the cobalt catalyst generated in-house was estimated via XRD through the calculation of the area at the full width half maximum (FWHM) for the relevant cobalt peaks. Using this approach the approximate crystallite sizes range between 9.2-14.2 nm indicating sufficient cross-sectional area for fuel production.

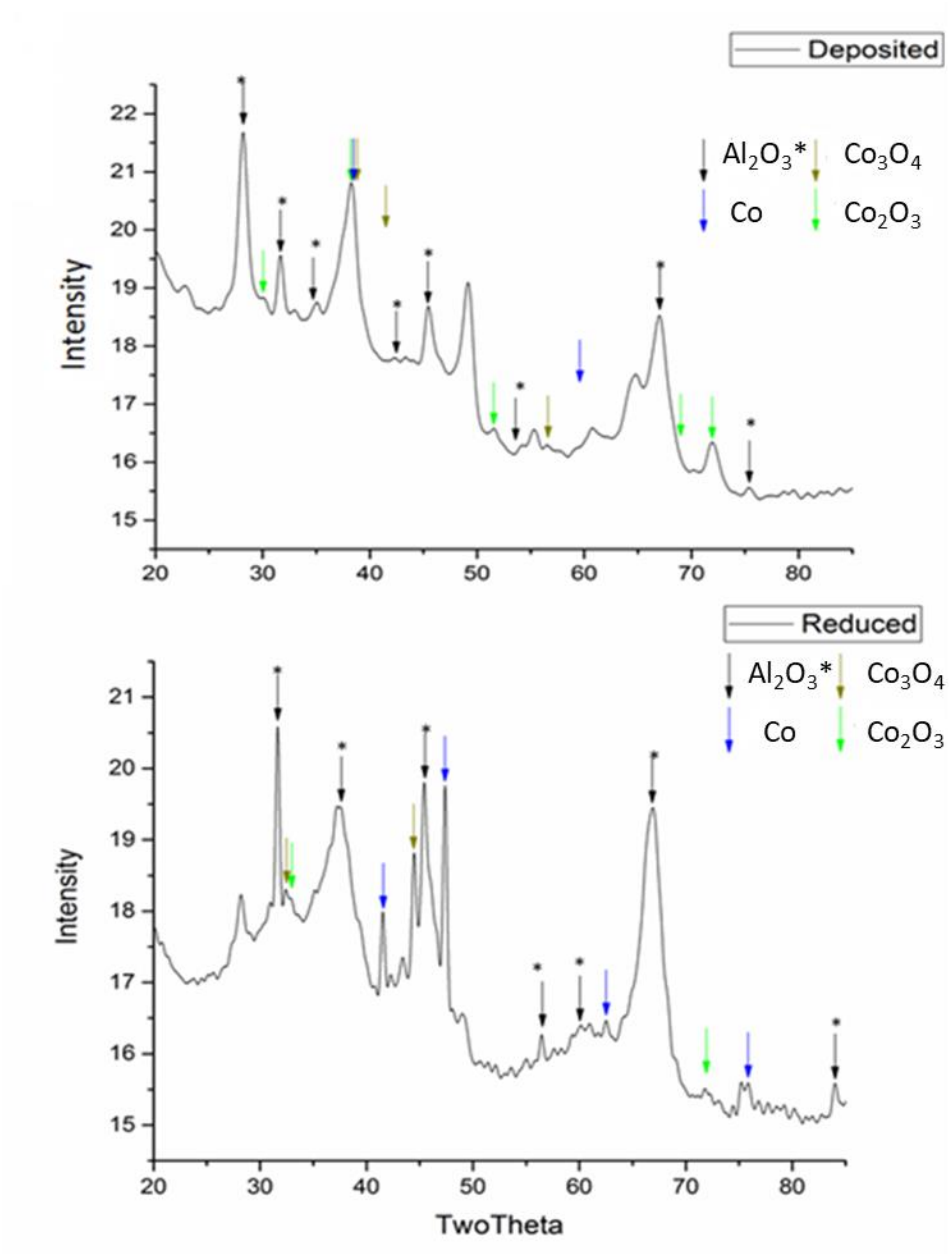

Figure 7 Figure of the XRD spectrum of non-reduced inactive catalyst (above) and the catalyst following the reduction process (bottom right). Oxides of cobalt (green and brown arrows) are predominant versus metallic cobalt hexagonal compact crystallite (blue) for the spectrum on the left indicating the inactive transition state of the catalyst has been formed. The reduced catalyst shows peaks indicative of metallic cobalt (blue arrow) and these are predominant over cobalt oxides. Aluminium oxide (black arrow) peaks indicative of the catalyst support may be used as a control showing little change in the peak intensity following the reduction process.

To extend the characterisation additional analysis using SEM was used to characterise particle size and surface topography. To assess the repeatability of the new synthesis process, an additional batch of catalyst was generated and analysed. Characterisation by SEM showed both catalysts had a very similar surface morphology (see figure 7.1), with particle sizes ranging between 0.3-16 µm, and evenly distrubuted over the surface, indicating that the novel production approach is also repeatable for routine use.

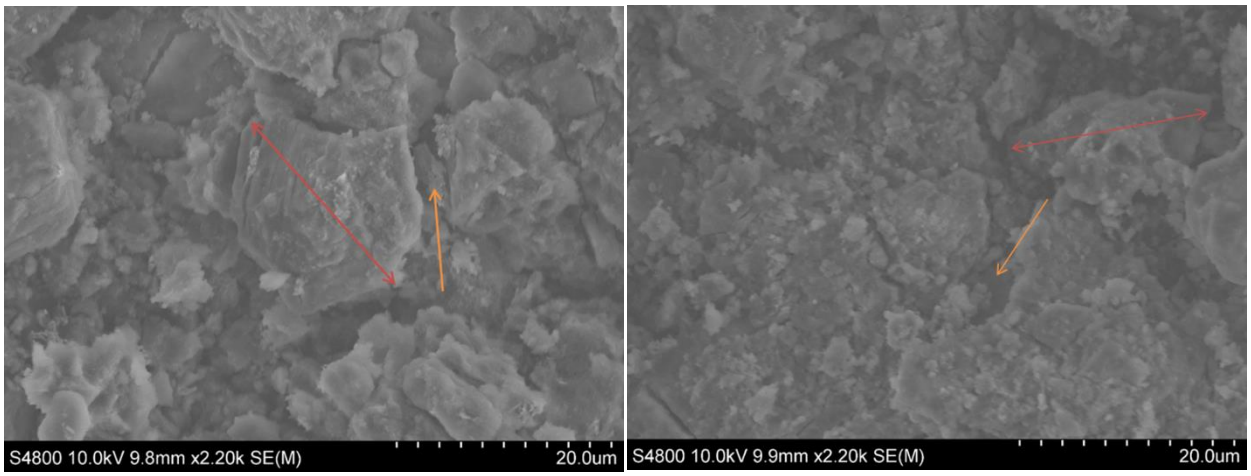

Figure 7.1 A scanning electron microscope image of the reduced catalyst at 10.0 kV at x2.20 k magnification; batch 1 (left) and batch 2 (right). The red and orange arrows on the images indicate the crystallite structure and catalyst pores, respectively.

A Brunauer- Emmett-Teller (BET) analysis was used to determine the catalyst pore size and surface area. Along with a minimum crystallite size of 6-8 nm (157), the pore size is key in determining overall catalytic activity, enabling increased activity by improving the accessibility of the catalyst surface area for the reactants. Ghampson et al. (2010) (152), demonstrated that the activity of cobalt catalysts increased with pore size up to 13 nm, after this pore size value it was ineffective. It is thought that increased activity of larger pores is linked to the greater number of metallic cobalt sites contained within the structures that can absorb CO, the larger pores allowing effective diffusion of reactants and product throughout the catalyst. Further to this a paper by Intarasiri et al. (2017) (158), showed that the selectivity of products generated is also linked to pore size They compared two cobalt catalyst termed 20 CS1 and 20 CS2 that had

a pore diamerer of 7.5 nm and 3.1 nm respectively, each had different selectivity towards petroleum range hydrocarbons. The larger pore size (7.5 nm) was more selective towards heavier hydrocarbons (gasoline and diesel) and ineffective at producing lighter LPG range hydrocarbons.

BET analysis determined an average pore size of 7.13 nm for active catalyst and pore volume of 0.24 cm^3 with total surface area of 125.6 m^2/g . In Jacobs, et al. 2002 (159), a number of cobalt catalysts have been described which can be used to benchmark CAT-1 and compare those prepared through calcination or oxidation (CAT-1). Interestingly, CAT-1 showed similarities to 11 % supported calcinated Co/Al_2O_3 catalyst, with pore sizes and volume of 6.4 nm and 0.317 cm^3 respectively, and surface area of 99.7 m^2/g. Our data suggests that this process may enable the synthesis of Co/Al_2O_3 catalysts with improved catalytic activity. Interestingly, a Co/SiO_2 with similar loading of 15 %, had similar pore size (7.7 nm) to CAT-1 however, the silicon supported catalyst had greater pore volume (0.840 cm^3) and surface area (217 m^2/g). Given the information in the literature and pore size of CAT-1 it is anticipated that that active CAT-1 will result in selectivity towards heavier hydrocarbons with reasonable activity.

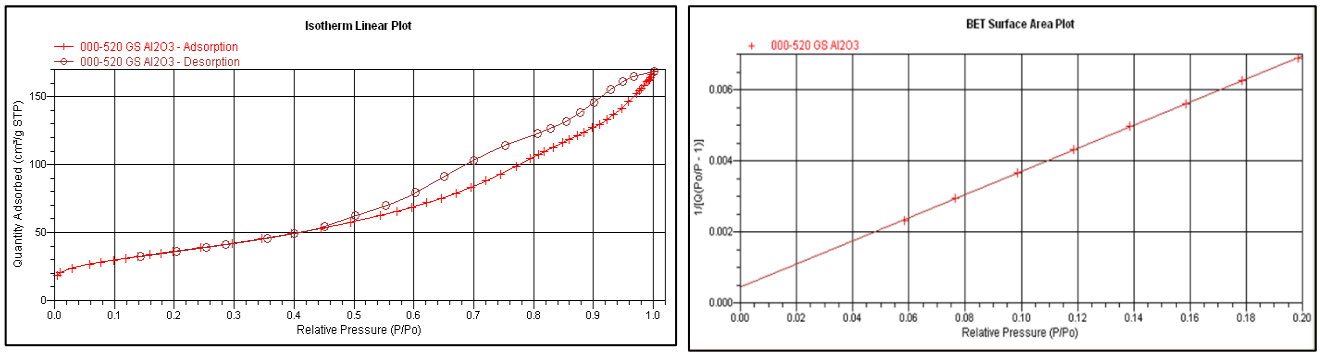

Figure 7.2 shows the results of BET analysis. Left is linear isotherm plot and right is the BET surface area plot, both are used to calculate pore size and surface area determined by the change in pressure by adsorbed nitrogen and the cross-sectional area of the adsorbate molecules.

7.2 Application of catalyst for hydrocarbon synthesis.

To determine the functionality of the catalyst for FT production of the desired linear chain alkanes, the catalyst was tested using the pilot FT reactor. During operation and testing the design of the reactant gas mixing valve of the FT rig was identified as delivering sub-optimal gas ratios within the rig. However, due to the large volumes of gas entering the rig, the reactants would be in plentiful supply and this would not be a limiting factor. It was therefore decided to keep the valve in place as a replacement would have been cost prohibitive. Once initiated, the rig was switched to an input gas flow of 75 mL/minute of hydrogen and carbon monoxide. The rig was pressurised to 4 bar and temperature lowered to 350 °C to mimic high temperature FT of 300 to 350 °C to form lighter distillates. The reaction was carried out for 30 minutes to ensure this went to completion. The output of the rig was connected to an acetone impinger to capture undesirable hydrocarbon material, while the condensed organic liquid in the rig (believed to contain desirable hydrocarbons) was diluted and cleaned using solid phase extraction. To ensure maximum recovery of target alkanes some of the active catalyst was extracted using pentane after the reaction and the extract was cleaned using SPE to remove potential metallic contaminants. The extracts were then spiked with internal standards (deuterated alkane markers) and then analysed using GC-MS optimised for the detection and quantitation of hydrocarbons. These results indicated hydrocarbon material was synthesised on the catalyst, typically between C20-C30 in chain length, and the most abundant species being C24 and C26. Using the internal standard approach to quantitation the hydrocarbons were determined to be within 0.07 to 0.50 mg/kg of the sample, totalling to 2.87 mg/kg of material shown in table 7.1.

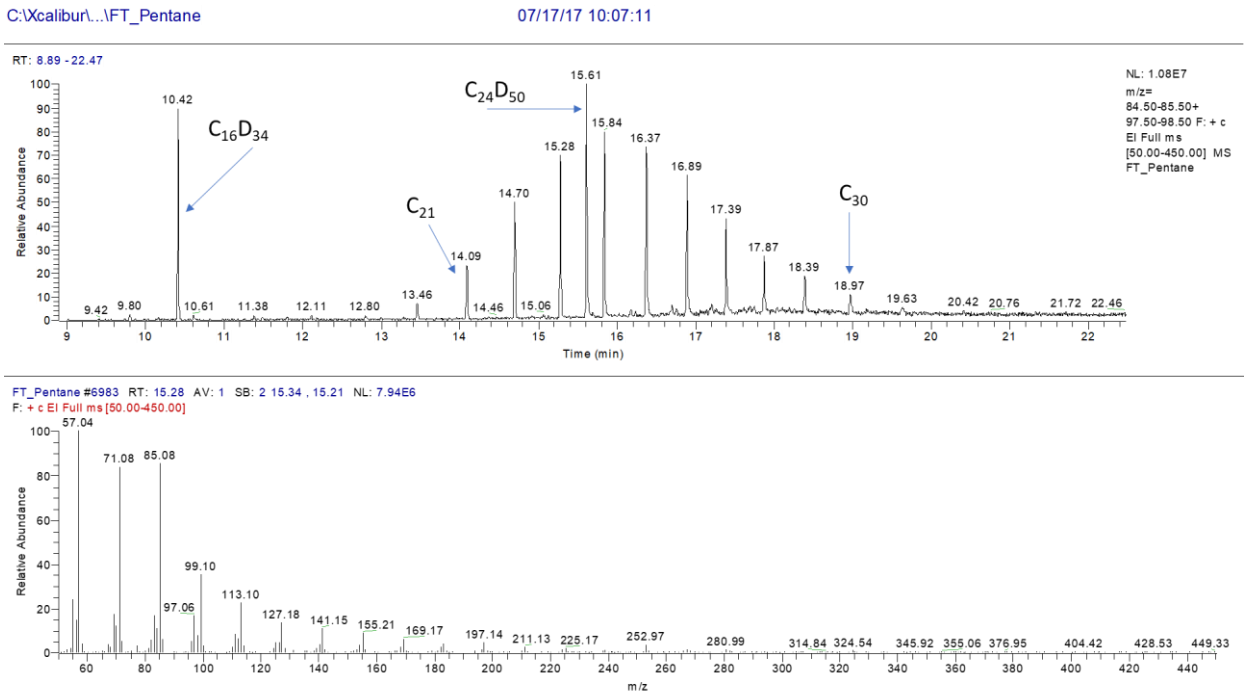

Figure 7.3 An extrcted ion chromatogram (above) of the hydrocarbons identified in the hydrocarbon synthesis experiment. Some peaks have been identified using C number for reference and hydrocarbon distrubution ranges from C20-C30. Below this is a mass spectrum of C23

Alkane Number	Concetration In extract mg/kg	Mass of hydrocarbon µg in 1 mL	No of mMoles of hydrocarbon (1 mL pentane)
C20	0.101	0.101	0.00015
C21	0.106	0.106	0.00036
C22	0.293	0.293	0.00068
C23	0.326	0.326	0.00100
C24	0.499	0.499	0.00118
C25	0.367	0.367	0.00104
C26	0.472	0.472	0.00099
C27	0.248	0.248	0.00065
C28	0.301	0.301	0.00043
C29	0.097	0.097	0.00024
C30	0.066	0.066	0.00016
Total	2.876	2.876	0.00688

Table 7.1 A table of the quantatative results of the hydrocarbons identified in the hydrocarbon synthesis experiment

To assess the performance of the catalyst the turn over frequency (TOF) was used following the method by Stowell and Korgel (160). This is a measurement of the reaction kinetics (rate) of catalytic systems and can be determined using the equation below. It is deemed a good initial indicator of catalyst performance and can be used as a comparative tool for similar catalysts.

$$TOF = \frac{\frac{N° \ of \ moles \ of \ HC \ generated}{N° \ of \ cobalt \ active \ sites}}{Time} \qquad \text{Equation 7.1}$$

Equation 7.1. Equation adapted from Stowell and Korgel (2005); TOF was defined as number of molecules of hydrocarbons generated per active site over the duration of the reaction.

$$Nact = \frac{Ap}{(Auc \times n)} \qquad \text{Equation 7.2}$$

Equation 7.2. Equation showing how the active site was calculated by assuming that all surface atoms are active. Where Ap is the surface area of the catalyst determined by BET analysis, Auc is the average surface area of an Co unit cell face, and n is the number of Co particles found in a unit cell face (XRD suggests hexagonal compact crystalllite of cobalt) .

The TOF for the active catalyst was estimated to be 0.003 S^{-1}; disappointingly this is lower than typical cobalt Fischer-Tropsch catalysts (0.014-0.026) S^{-1} (152,160) however, unlike the in-house rig, these are typically operated at higher pressures of 10-20 bar (152,160). The operating partial pressure is known to influence the catalyst performance, with higher operating partial pressure increasing the TOF of the catalytic reaction. To compare the TOF of other cobalt catalysts at equivalent low pressure of the in-house rig, a paper by Jalama, (156) using cobalt catalyst on titanium support was used to estimate comparative performance. This paper showed data of the TOF at a range of operating pressures; 0.0002 S^{-1} at 1 bar, 0.0099 S^{-1} at 10 bar and 0.0270 S^{-1} at 20 bar, enabling an estimation of equivalent TOF to be determined by establishing the relationship between these parameters. These TOF values were plotted versus operating

pressure, with the TOF at 4 bar estimated by substitution into the equation of the trendline of the graph. This indicated that the cobalt catalyst on a TiO_2 support would have an equivalent TOF of 0.003 S^{-1} and is comparable to that synthesised in-house (0.003 S^{-1})(47,159). A further encouraging point from this data is that TiO_2 supports encourage higher TOF than Al_2O_3 (47). Therefore, the result for CAT-1 is actually better than expected.

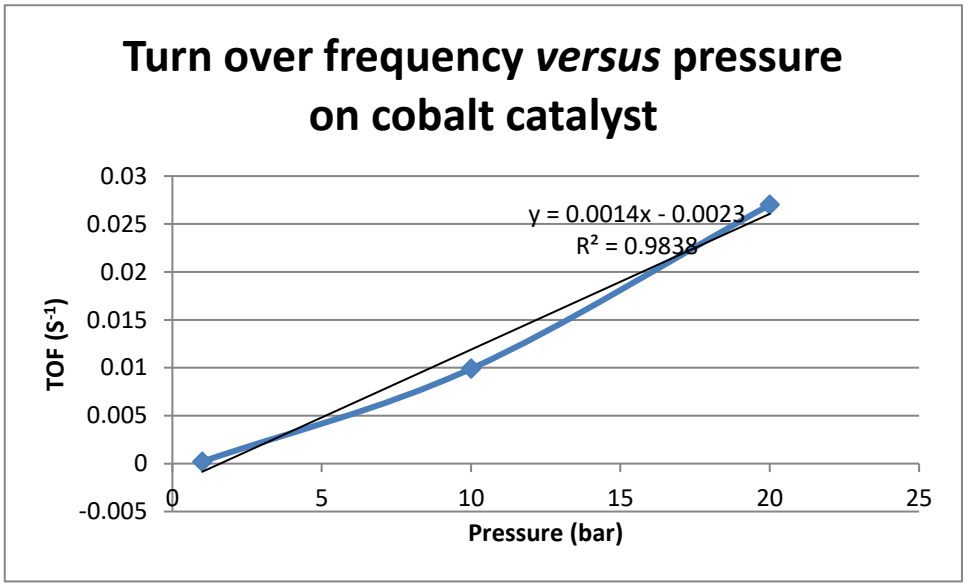

Figure 7.4 . A graph plotted using data plotted from Jalama, 2015, to determine whether CAT-1 had comparable TOF at low pressures FT cobalt catalyst.

7.3 Interfacing pyrolysis/gasification rig to Fischer-Tropsch.

For the combined thermal-chemical treatment (pyrolysis or gasification) to Fischer-Tropsch (FT); there are key practical considerations that must be overcome for wide spread use. Specifically, the syngas generated must be in sufficient quantity to produce adequate amounts of hydrocarbons from the FT reaction and the syngas needs to be free of volatile impurities to maintain the catalyst integrity. To do this with our rig storage of the syngas was neccasary for sufficient quantity of gas at pressure to pass over the the Fischer-Tropsch catalyst. This required modifications to the original rig including a motorised screw to allow for an unlimited amount

of feedstock to be thermochemically treated and a fan to draw air through the feedstock to cause gasification of the material. The syngas was forced through two impingers containing 300 mL of acetone and the scrubbed gases were then collected in an inverted barrel, housed in a water tank where the syngas would displace the water until it was filled. This was the storage vessel for the syngas and the volume of gas collected was approximately 100 L. Once the collection vessel was full, the syngas was then diverted to the Fischer-Tropsch reactor and an in-line compressor generated a pressure of 2 bar before entering the FT rig. Unfortunately, the pressure was less than desired pressure of 10 bar but was what could be achieved with with limited resources and budget. To test the performance of the rig, 100 g of catalyst was packed into the FT reactor reduced in pure hydrogen for 4 hours at 400 °C. The FT reaction commenced at 350 °C until the syngas storage was empty. Figure 7.6 is a schematic of the combined pyrolysis/gasification – FT process:

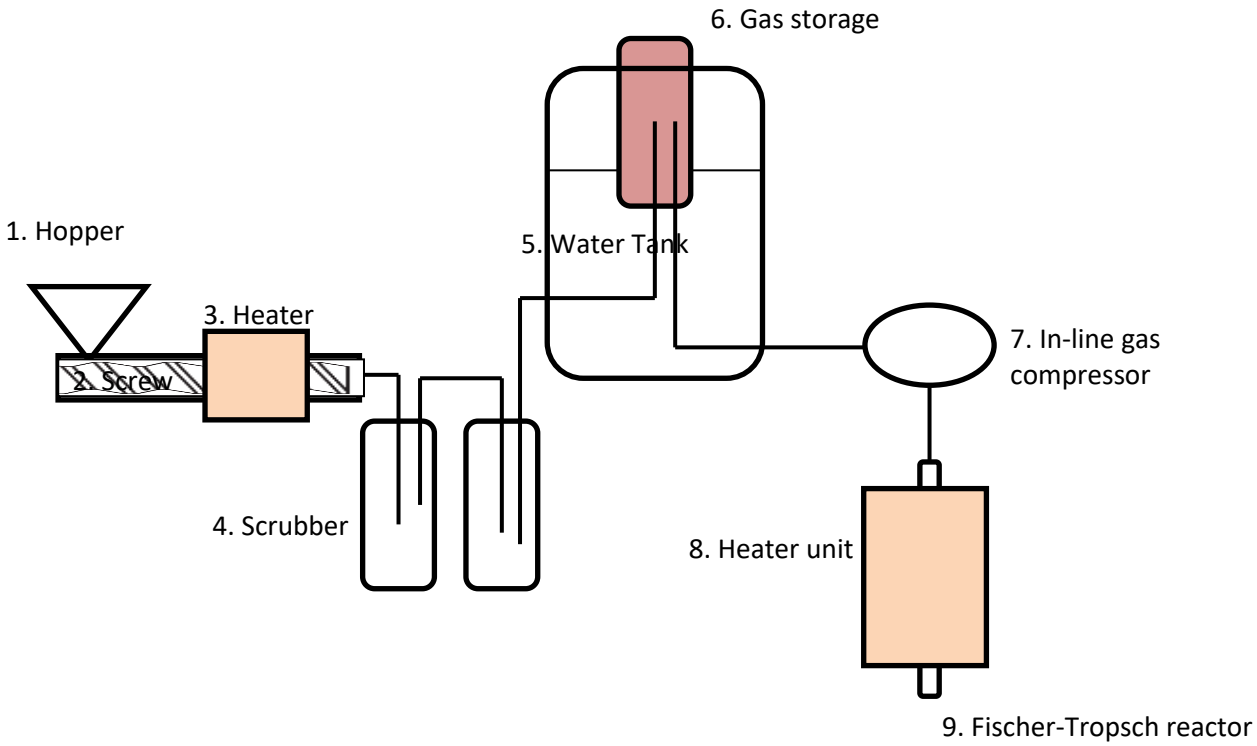

Figure 7.5. A schematic of the combined pyrolyser/gasifier- Fischer-Tropsch reactor desinged in house by Phil Knight and Geraint Sullivan. Feedstock is feed in to the (2) screw pyrolyser through the (1) hopper. The (3) heater unit provides the thermal energy to the pyrolyser, the generated syngas is then passed through a number of (4) acetone scrubbers and stored in the (6) gas storage vessel. The syngas is then diverted to the (9) Fischer-Tropsch reactor under pressure; pressure is generated by the (7) in-line compressor. A second (8) heater unit is used to maintain the temperature of the FT reactor.

Gas samples were taken at two points, one at the storage vessel and secondly post Fisher-Tropsch reactor. Gas analysis of the stored syngas showed that levels of hydrogen to carbon monoxide were approximately 1: 1.2, lower than the experiments in chapter 5. The level of carbon monoxide (CO) was found to be 0.08% entering the FT which is equivalent to 800 ppm or 916 mg/m^3. The gas leaving the FT bubbled through an acetone impinger to capture any volatile hydrocarbons and was also tested for carbon monoxide. The level of CO was reduced to 0.015% or 150 ppm, equivalent to 171 mg/m^3 post FT. This puts the reduction of CO to 81.33%. In order to determine the conversion of CO to hydrocarbons the surface of the catalyst

and impinger was tested for hydrocarbons generated by the FT process. These were dissolved in pentane, passed through SPE clean-up and analysed by the relevant GC-MS method. If generated, hydrocarbon material would then be compared to the mass of CO to determine the % conversion of CO.

$$\%\ CO\ conversion = 100\ \times \frac{Total\ mass\ of\ hydrocarbons\ generated}{Mass\ of\ CO\ \ per\ 100\ L\ of\ syngas} \qquad \text{Equation 8.3}$$

Hydrocarbon C number	Concentration hydrocarbons mL	Mass of hydrocarbons mL
C22	50 µg/L	50 ng
C23	30 µg/L	30 ng
C24	91 µg/L	91 ng
C25	191 µg/L	191 ng
C26	142 µg/L	142 ng
C27	133 µg/L	133 ng
C28	75 µg/L	75 ng
Total hydrocarbon content	712 µg/L	712 ng

Table 7.2 A table of results from the combined pyrolysis/gasification-FT experiment. The concentration of hydrocarbons was determined via GC-MS and converted to mass of hydrocarbon contained in 1 mL of pentane.

It was apparent that the hydrocarbons resided with the catalyst as the catalyst extract proved positive for hydrocarbons, see table 7.2 for results. The results show that the majority of hydrocarbons generated from the combined pyrolysis/ gasification-FT rig were within, the C22-C28 range similar to the hydrocarbons identified in the initial catalyst study. However, the concentration of hydrocarbons on this occasion was significantly less (≈75 %) in the combined pyrolysis/ gasification-FT experiment and the CO conversion to hydrocarbon was calculated to be low at 7.7 x 10^{-4} % (up to 50 to 90 % conversion efficiency (20)), and is likely to be due to the low partial pressure of hydrogen in the syngas and low operational pressures of the FT rig.

7.4 Conclusion.

The catalyst generated using this novel lower temperature process has shown evidence of the desired cobalt transition state and formation of crystallite active sites for FT activity. Initial characterisation data using XRD and SEM showed that the catalyst had a crystalline structure, with the desired cobalt oxide transitions. This was important for generating an immobilised pre-catalyst which was reduced in hydrogen to activate the catalyst forming metallic cobalt sites. The use of XRD to confirm the presence of metallic cobalt crystallites and were above the minimum crystallite size of 6 nm (estimated size 8-14 nm) deemed necessary for activity. When tested within an FT rig, the catalyst was capable of synthesising waxy hydrocarbons, ranging between C20-C31, targeted for fuel production. This proved to be a relatively efficient process with no evidence of smaller hydrocarbons detected in the process, suggesting hydrocarbon selectivity is likely to be in favour of the formation of preferred heavier hydrocarbons. Data obtained on the porosity and surface area using BET analysis, was then used to establish turn over frequency of the catalyst, to benchmark the catalyst activity versus other cobalt catalysts. The turn over frequency (TOF) for the active catalyst was determined at 0.003 S^{-1} and found to be comparable to other cobalt Fischer-Tropsch catalysts when operated at lower pressures used in this experiment (156). These results suggest this new synthesis has the potential to offer a low energy approach of generating a successful Fischer-Tropsch catalyst, to produce target hydrocarbons for fuel production without significant optimisation of the FT rig.

Finally, we investigated combining the FT process with gasification; these included the generation and storage of sufficient quantities of syngas, syngas cleaning before use and the pressurising of the syngas within a limited budget before entering the FT reactor. Despite modifications to the design, a major issue still remained such as the lower than anticipated gas ratio and the operating pressure of the syngas. However, despite these challenges the rig was still tested and some hydrocarbons were identified albeit at low concentrations. A gas sample

on the pre and post FT reaction showed an 81% reduction in CO. Although the percentage conversion of CO to hydrocarbon was calculated to be very low, it is possible that the CO was adsorbed to the catalyst but not converted. The low operational pressures (< 2 bar) of the rig and low partial pressure of hydrogen of the syngas is likely reason for a low CO conversion as the thermodynamic equillibrium of the reaction requires high partial pressures. Positively, there was no apparent contamination of the catalyst from the tars or in acetone impinger post FT, demonstrating the effectiveness of the syngas cleaning.

However, further work is required to optimise the process and mitigate some of the issues with the pilot rig. For example, alterations such as introducing a high pressure gas pump and steam reformation could be used to increase the hydrogen: carbon monoxide ratio and increase the overal pressure needed for a high functioning FT reaction (37). Further to this, the could be enhanced to include alternative promoters such as rare earth (palladium and rhodium) (46,159) to increase catalytic activity and turnover rate and other supports (TiO_2) to enhance the surface area and porosity of the catalyst, which will influence activity, product yield and distribution. However, this needs to be balanced versus the cost benefits given that alternative promoters and supports will increase the cost of production of the catalyst and possibly compromise the research aim of generating a cheaper alternative.

Chapter 8:

Conclusion.

The interest of using thermal conversion techniques such as gasification and pyrolysis, to treat waste is becoming more popular. These alternative technologies have lowered CO_2, NOx and SOx emissions which contributes less to release of greenhouse gases to the environment. In addition to this, the generation of value-added products (syngas, bio-oil and biochar) allows more manageable redistribution of energy, as the products are easily transportable for use a different locations. Additionally, the products from alternative recycling technology having the potential to be used as petroleum replacements, such as bio-oil (pyrolysis of biomass) and FT hydrocarbons.

An increased effort to recycle more waste can only be advantageous, as it will effectively reduce the amount of space used for landfill, that could be better served as agricultural land, together reducing the potential problems associated waste disposal, such as ground water contamination and methane emission (another greenhouse gas). Finally, there is a vast potential store of energy in waste which is an underutilised which could be used to subsidise some of the current global demands.

This project investigated the thermal treatment of three potential waste feedstocks, and characterise the products generated using GC-MS and GC-TCD, to see if these were potential candidates for waste recycling. The main theme throughout the investigation was to do this as cost effectively and environmentally friendly as possible. A solvent trap method was used for syngas cleaning, this also doubled up as a GC-MS preparation stage for organic tar analysis. Acetone was deemed a worthy trapping solvent was as it was cheap, dissolved a wide range of organic compounds, it was suitable for GC and its recapture by distillation offered a simple recycling technique. The use of solvent traps, saved on analysis cost as there was no

requirement for instrument modification to accommodate gas samples, and specialised sampling devices (Gresham tubes). Solvent traps provide a cheap method of syngas cleaning compared to alternative techniques that may use reforming catalysts and hot gas filters. To further enhance economic feasibility of the process waste carbon from pyrolysis was recycled to produce activated biochar a useful product that could be used to mitigated waste water polluted with organic pollutants. This had potential to be used to remove organics from scrubbers saturated with tars. Finally, a low temperature FT catalyst was synthesised using a novel chemical oxidation which reduced the costs associated with high temperature catalyst preparation. Although it was not fully optimized, due to time restrain and limited funding of the project. Evidence of hydrocarbons associated with the catalyst confirmed that it was possible to produce a functioning catalyst using this low-cost method.

Prior to the experimental procedure, GC methods were developed and validated to assess their suitability to characterise the organic material generated during pyrolysis/gasification and FT recycling process. Two GC-MS methods were succesfully validated for the characterisation of volatile and semi-volatile organic impurities (VOT and SVOT) generated from the thermochemically treatment of waste. A third GC-MS method, aimed at analysing hydrocarbon material from the FT process (FT monitoring method) was also developed and validated. All GC-MS methods surpassed the figure of merits deemed necessary for validation (accuracy and precision < 20 %) and showed excellent precision, accuracy, and retention time stability with low sensitivity. Therefore, deemed reliable for the quantitation (targeted) and identification of tar impurities. Further to this, a fourth GC method was developed to analyse simple molecular gases. This used a non-selective detector GC-TCD to identify the gases. This provided excellent retention reproducibility and was deemed fit for purpose and used for identifying the composition of syngas.

The capture of tars and effective clean up of syngas using acetone proved to be more effective than common solvent scrubbers (water and methanol), this was evidenced by higher recoveries of target impurities (SVOT and VOT standards). It also shown that tar levels (including problematic small unsaturated tars) could be reduced by up to 90 % using sequential scrubbers, providing a suitably clean syngas. Acetone capture of impurities also provided a cheap means of sample preparation which could be used with standard liquid injection GC-MS (no need for costly preparation and instrument modifications). It was also noted the vast variety of tars that were soluble in acetone, as a number of different compound classes were identified in the scrubbers. Typical compounds oberved, were non polar, light volatile aromatic and poly aromatic compounds, polar cellulosic and lignlosic breakdown products and heterocyclic compounds. Although thermochemical treatment provides an alternative approach to disposal of difficult wastes, the captured tars and char still needs further processing. A method remediating the scrubbers to generate bio-oil proved successful and this could potentially have applications as a fuel or re-processed for value-added products. However, more research is required in this area to make it feasible. For biochar, (biomass) its re-use as a sorbent to treat contaminated water was investigated. Pinewood and sludge cake biochar after activation all showed selective adsorption towards different classes of organic compounds (PAHs, phenols, gasoline and diesel range organics), with preparation temperature of the biochar having an effect on compound selectivity. It evident from the results that activated biochar may be selective towards compound size, as it was shown that larger PAHs had reduced recovery, this could suggest that biochar may be only affective to particular size range of organic pollutant. For the biochar generated, good precision (<25 %) data for recovery was seen for the different compound classes which may suggest a reproducible sample preparation (clean-up) method. However, a larger trial with more replicates and different sampling loactions may give a wider understanding on the apparent heterogenoicity of the samples and will give better understanding of repeatability and reproducibility of the adsorbents. It is therefore important

that biochar characterisation is necessary prior to re-use, perhaps through surface characterisation techniques, such as SEM, surface chemistry analysis and BET, which could be an indicator of potential suitability as an adsorbent i.e pore size, and surface functionality.

Finally, to enhance to cost effectiveness of biomass recycling, especially in the generation of hydrocarbons *via* the FT process; a low energy catalyst was prepared using an alternative approach. Chemical oxidation of over calcination was the preferred method. This provided both an energy and time-saving approach for generating a pre-catalyst with the correct cobalt oxide transition state. Characterisation of the catalyst suggested that the catalyst had been successfully reduced to form the active species, with crystallite size (9-14 nm) within range (> 6nm) and a comparable surface area and porosity to other Co catalysts. The final evidence for its success was the identification of hydrocarbons immobilised on the catalyst after testing (C20-C31). Although catalyst preparation appears to be successful, there are many more parameters that could be investigated to make the catalyst more functional, such as investigating how different supports and promoters can affect activity and selectivity, providing the initial aim of keeping the cost low is not compromised. Prior to this, the difficulties with the lab-scale FT reactor design and operation (low pressure and regulation of gas mixtures) needs resolving, so the rig can be fully optomised and the full potential of the catalyst can be investigated. By having increased regulation on FT conditions will allow for deeper insight into catalyst activity at different pressures and better understanding of conversion efficiencies of syngas to hydrocarbons; it is understood that higher pressures with ideal gas rations have improved productivity on hydrocarbon yield.

References.

1. Zou C, Zhao Q, Zhang G, Xiong B. Energy revolution: From a fossil energy era to a new energy era. Nat Gas Ind [Internet]. 2016;36(1):1–10. Available from: http://dx.doi.org/10.1016/j.ngib.2016.02.001
2. Abas N, Kalair A, Khan N. Review of fossil fuels and future energy technologies. Futures [Internet]. 2015;69(March):31–49. Available from: http://dx.doi.org/10.1016/j.futures.2015.03.003
3. Jeswani HK, Azapagic A. Assessing the environmental sustainability of energy recovery from municipal solid waste in the UK. Waste Manag. 2016;50:346–63. Available from: http://dx.doi.org/10.1016/j.wasman.2016.02.010
4. Perera N, Boyd Gill Wilkins E, Phillips Itty R. Literature Review on Energy Access and Adaptation to Climate Change. 2015;(May). Available from: https://assets.publishing.service.gov.uk/media/57a0896b40f0b652dd0001fe/LitRev-EnergyAccessandAdaptation-Final-2.pdf
5. Berndes G, Hoogwijk M, Van Den Broek R. The contribution of biomass in the future global energy supply: A review of 17 studies. Biomass and Bioenergy. 2003;25(1):1–28.
6. Hopewell J, Dvorak R, Kosior E. Plastics recycling: challenges and opportunities. Philos Trans R Soc B Biol Sci [Internet]. 2009;364(1526):2115–26. Available from: http://rstb.royalsocietypublishing.org/cgi/doi/10.1098/rstb.2008.0311
7. Arena U. Process and technological aspects of municipal solid waste gasification. A review. Waste Manag [Internet]. 2012;32(4):625–39. Available from: http://dx.doi.org/10.1016/j.wasman.2011.09.025
8. DEFRA. Review of Environmental and Health Effects of Waste Management: Municipal Solid Waste and Similar Wastes. Univ Birmingham [Internet]. 2004;420. Available from: https://www.gov.uk/government/uploads/system/uploads/attachment_data/file/69391/pb9052a-health-report-040325.pdf
9. Matsakas L, Gao Q, Jansson S, Rova U, Christakopoulos P. Green conversion of municipal solid wastes into fuels and chemicals. Electron J Biotechnol. 2017;26:69–83. Available from: http://dx.doi.org/10.1016/j.ejbt.2017.01.004
10. World Energy C. World Energy Resources Waste to Energy | 2016. Waste-To-Energy [Internet]. 2016;1–76. Available from: https://www.worldenergy.org/wp-content/uploads/2017/03/WEResources_Waste_to_Energy_2016.pdf
11. Defra. Advanced Thermal Treatment of Municipal Solid Waste. Dep Environ Food Rural Aff [Internet]. 2013;(February). Available from: https://www.gov.uk/government/uploads/system/uploads/attachment_data/file/221035/pb13888-thermal-treatment-waste.pdf
12. Wijekoon KC, Hai FI, Kang J, Price WE, Guo W, Ngo HH, et al. The fate of pharmaceuticals, steroid hormones, phytoestrogens, UV-filters and pesticides during MBR treatment. Bioresour Technol [Internet]. 2013;144:247–54. Available from: http://dx.doi.org/10.1016/j.biortech.2013.06.097
13. Defra. UK Implementation of the EC Urban Waste Water Treatment Directive. Water Serv [Internet]. 2002;20. Available from: http://www.defra.gov.uk/publications/files/pb6655-uk-sewage-treatment-020424.pdf
14. Krylova AY. Products of the Fischer-Tropsch synthesis (A Review). Solid Fuel Chem [Internet]. 2014;48(1):22–35. Available from: http://link.springer.com/10.3103/S0361521914010030
15. Mohan D, Pittman CU, Steele PH. Pyrolysis of wood/biomass for bio-oil: A critical review. Energy and Fuels. 2006;20(3):848–89.
16. Rabou LPLM, Drift A Van Der. Benzene and ethylene in Bio-SNG production : nuisance , fuel or valuable products? Proc Int Conf Polygeneration Strateg 11. 2011;11(October):157–62. Available from: https://www.ecn.nl/publications/PdfFetch.aspx?nr=ECN-M--11-092
17. Sector VP. Renewable Energy Technologies: Cost Analysis Series. IRENA Work Pap [Internet]. 2012;1(4/5). Available from: https://hub.globalccsinstitute.com/sites/default/files/publications/138178/hydropower.pdf
18. Fichtner_Consulting_Engineers Ltd. The Viability of Advanced Thermal Treatment of MSW in the

UK. Estet. 2004;98(7):1–91.
19. Brownsort PA. Biomass Pyrolysis Processes: Review of Scope, Control and Variability. Biomass. 2009;38.
20. E4tech. Review of Technologies for Gasification of Biomass and Wastes. Biomass [Internet]. 2009;(June):125. Available from: http://www.nnfcc.co.uk/tools/review-of-technologies-for-gasification-of-biomass-and-wastes-nnfcc-09-008
21. Thapa S, Bhoi PR, Kumar A, Huhnke RL. Effects of syngas cooling and biomass filter medium on tar removal. Energies. 2017;10(3):1–12.
22. Demirbas A. Progress and recent trends in biofuels. Prog Energy Combust Sci. 2007;33(1):1–18.
23. Ok Y. Biochar: production, characterisation and application. CRC press; 2015.
24. Tan X, Liu Y, Zeng G, Wang X, Hu X, Gu Y, et al. Application of biochar for the removal of pollutants from aqueous solutions. Chemosphere. 2015;125:70–85. Available from: http://dx.doi.org/10.1016/j.chemosphere.2014.12.058
25. Silvani L, Vrchotova B, Kastanek P, Demnerova K, Pettiti I, Papini MP. Characterizing Biochar as Alternative Sorbent for Oil Spill Remediation. Sci Rep. 2017;7:1–10. Available from: http://dx.doi.org/10.1038/srep43912
26. Li H, Qu R, Li C, Guo W, Han X, He F, et al. Selective removal of polycyclic aromatic hydrocarbons (PAHs) from soil washing effluents using biochars produced at different pyrolytic temperatures. Bioresour Technol [Internet]. 2014;163:193–8. Available from: http://dx.doi.org/10.1016/j.biortech.2014.04.042
27. Ogbonnaya U, Semple K. Impact of Biochar on Organic Contaminants in Soil: A Tool for Mitigating Risk? Agronomy [Internet]. 2013;3(2):349–75. Available from: http://www.mdpi.com/2073-4395/3/2/349/
28. Nartey OD, Zhao B. Biochar preparation, characterization, and adsorptive capacity and its effect on bioavailability of contaminants: An overview. Adv Mater Sci Eng. 2014;2014.
29. Chen B, Zhou D. Transitional Adsorption and Partition of Nonpolar and Polar Aromatic Contaminants by Biochars of Pine Needles with Different Pyrolytic Temperatures. 2008;42(14):5137–43.
30. Marshall AJ, Wu PF, Mun SH, Lalonde C. Commercial application of pyrolysis technology in agriculture. Am Soc Agric Biol Eng Annu Int Meet 2014, ASABE 2014. 2014;5:3868–86. Available from: http://www.scopus.com/inward/record.url?eid=2-s2.0-84911480172&partnerID=40&md5=5fa9fe3e5653107da3d2af7d28d6d7a7
31. Al Arni S. Comparison of slow and fast pyrolysis for converting biomass into fuel. Renew Energy [Internet]. 2018;124:197–201. Available from: https://doi.org/10.1016/j.renene.2017.04.060
32. Rajvanshi AK. Biomass Gasification. Encycl Energy. 2004;1(4):213–21.
33. Boerrigter H, Rauch R. Review of applications of gases from biomass gasification. ECN Biomass, Coal Environ …. 2006;(June):33.
34. Garcia-Perez M. The Formation of Polyaromatic Hydrocarbons and Dioxins During Pyrolysis:A Review of the Literature with Descriptions of Biomass Composition, Fast Pyrolysis Technologies and Thermochemical Reactions. Energy. 2008;(June):63.
35. Basu P. Combustion and gasification in fluidized beds. J Chem Inf Model. 2013;53(9):1689–99.
36. Lohitharn N, Goodwin JG, Lotero E. Fe-based Fischer-Tropsch synthesis catalysts containing carbide-forming transition metal promoters. J Catal. 2008;255(1):104–13.
37. Jager B. Development of Fischer Tropsch Reactors. American Institute of Chemical. 2003. p. 1–9. Available from: http://www.fischer-tropsch.org/primary_documents/presentations/AIChE 2003 Spring National Meeting/BJager-DvlpFTReactor.pdf
38. Inderwildi OR, Jenkins SJ, King DA. Fischer-Tropsch mechanism revisited: Alternative pathways for the production of higher hydrocarbons from synthesis gas. J Phys Chem C. 2008;112(5):1305–7.
39. Diehl, F. Khodakov AY. Promotion of Cobalt Fischer-Tropsch catalysts with nobel metals: a review. Oil Gas Sci Tecnol. 2008;64(1):11–24.
40. Davis BH. Fischer-Tropsch Synthesis: Reaction mechanisms for iron catalysts. Catal Today. 2009;141(1–2):25–33.
41. Ojeda M, Nabar R, Nilekar AU, Ishikawa A, Mavrikakis M, Iglesia E. CO activation pathways and the mechanism of Fischer-Tropsch synthesis. J Catal [Internet]. 2010;272(2):287–97. Available from: http://dx.doi.org/10.1016/j.jcat.2010.04.012

42. Davis BH. Fischer-Tropsch synthesis: Current mechanism and futuristic needs. Fuel Process Technol. 2001;71(1–3):157–66.
43. Farnetti E, Monte R Di, Kašpar J. M ES PL C E O – PL C E O –. 1999;II.
44. Davis ME, Davis RJ. Heterogeneous catalysts: Fundamentals of chemical reaction engineering. McGraw-Hill. Boston; 2003. 133-183 p.
45. Matthias, B. Saten, R. Renken A. Catalysis: From principles to applications. Verlang: Wiley; 2012.
46. Deutschmann, O. Knozinger, H. Kochloefl, K. Turek T. Heterogeneous catalysts and soild catalysts,. Verlang: Wiley-VCH; 2003.
47. Jahangiri H, Bennett J, Mahjoubi P, Wilson K, Gu S. A review of advanced catalyst development for Fischer–Tropsch synthesis of hydrocarbons from biomass derived syn-gas. Catal Sci Technol [Internet]. 2014;4(8):2210–29. Available from: http://xlink.rsc.org/?DOI=C4CY00327F
48. Espinoza RL, Steynberg AP, Jager B, Vosloo AC. Low temperature Fischer-Tropsch synthesis from a Sasol perspective. Appl Catal A Gen. 1999;186(1–2):13–26.
49. Jager B, Espinoza R. Advances in low temperature Fischer-Tropsch synthesis. Catal Today. 1995;23(1):17–28.
50. Belgiorno V, De Feo G, Della Rocca C, Napoli RMA. Energy from gasification of solid wastes. Waste Manag. 2003;23(1):1–15.
51. Chang CY, Shie JL, Lin JP, Wu CH, Lee DJ, Chang CF. Major Products Obtained from the Pyrolysis of Oil Sludge. Energy and Fuels. 2000;14(6):1176–83.
52. Simell P, Hannula I, Tuomi S, Nieminen M, Kurkela E, Hiltunen I, et al. Clean syngas from biomass—process development and concept assessment. Biomass Convers Biorefinery. 2014;4(4):357–70.
53. Kumar A, Jones DD, Hanna MA. Thermochemical biomass gasification: A review of the current status of the technology. Energies. 2009;2(3):556–81.
54. Werther J, Ogada T. Sewage sludge combustion. Prog Energy Combust Sci. 1999;25(1):55–116.
55. Werner K, Pommer L, Broström M. Thermal decomposition of hemicelluloses. J Anal Appl Pyrolysis . 2014;110(1):130–7. Available from: http://dx.doi.org/10.1016/j.jaap.2014.08.013
56. Devi L, Ptasinski KJ, Janssen FJJG. A review of the primary measures for tar elimination in biomass gasification processes. Biomass and Bioenergy. 2002;24(2):125–40.
57. Font Palma C. Modelling of tar formation and evolution for biomass gasification: A review. Appl Energy [Internet]. 2013;111:129–41. Available from: http://dx.doi.org/10.1016/j.apenergy.2013.04.082
58. Al-Dury SS. Removal of Tar in Biomass Gasification Process Using Carbon Materials. Vol. 18, CHemical Engineering Transactions. 2009. p. 1–6.
59. Boerrigter H, van Paasen SVB, Bergman PC a, Könemann JW, Emmen R, Wijnands a. “Olga” Tar Removal Technology. Energy. 2005. 58 p.
60. Hansen C. The three dimensional solubility parameters and solvent diffusion coefficient: Their importance in surface coating formulation. COPENHAGEN: Danish Technical press; 1967.
61. Balas M, Lisy M, Kubicek J, Pospisil J. Syngas cleaning by wet scrubber. WSEAS Trans Heat Mass Transf. 2014;9(1):195–204.
62. Burr B, Lyddon L. A COMPARISON OF PHYSICAL SOLVENTS FOR ACID GAS REMOVAL. Water. Texas; 1998.
63. Jamali SH, Ramdin M, Becker TM, Torres-Knoop A, Dubbeldam D, Buijs W, et al. Solubility of sulfur compounds in commercial physical solvents and an ionic liquid from Monte Carlo simulations. Fluid Phase Equilib. 2016;433:50–5. Available from: http://linkinghub.elsevier.com/retrieve/pii/S0378381216305684
64. Unyaphan S, Tarnpradab T, Takahashi F, Yoshikawa K. An Investigation of Low Cost and Effective Tar Removal Techniques by Venturi Scrubber Producing Syngas Microbubbles and Absorbent Regeneration for Biomass Gasification. Energy Procedia. 2017;105:406–12. Available from: http://dx.doi.org/10.1016/j.egypro.2017.03.333
65. Nakamura S, Siriwat U, Yoshikawa K, Kitano S. Development of Tar Removal Technologies for Biomass Gasification using the By-products. Energy Procedia. 2015;75:208–13. Available from: http://dx.doi.org/10.1016/j.egypro.2015.07.305
66. Carpenter DL, Deutch SP, French RJ. Quantitative measurement of biomass gasifier tars using a molecular-beam mass spectrometer: Comparison with traditional impinger sampling. Energy and Fuels. 2007;21(5):3036–43.

67. WŁÓKA, Daiusz. Smol M. Evaluation of extraction methods of polycyclic aromatic hydrocarbons (PAHs) from soil and sewage sludge matrix Evaluation of extraction methods of polycyclic aromatic hydrocarbons (PAHs) from soil and sewage sludge matrix. Inżynieria i Ochr Środowiska. 2014;4(2015):683–96.
68. Diem Q, Elisa A, Tran-nguyen PL. Effect of extraction solvent on total phenol content , total flavonoid content , and antioxidant activity of Limnophila aromatica. J Food Drug Anal [Internet]. 2013;22(3):296–302. Available from: http://dx.doi.org/10.1016/j.jfda.2013.11.001
69. Huang X, Li S. Solubility of Acetylene in Alcohols and Ketones. J Chem Eng Data. 2018;63(6):2127–34. Available from: http://pubs.acs.org/doi/10.1021/acs.jced.8b00126
70. Dayton D. Review of the Literature on Catalytic Biomass Tar Destruction: Milestone Completion Report. 2002;(December). Available from: http://www.osti.gov/servlets/purl/15002876-cI4XbH/native/
71. Simell PA, Hirvensalo EK, Smolander VT, Krause AOI. Steam reforming of gasification gas tar over dolomite with benzene as a model compound. Ind Eng Chem Res. 1999;38(4):1250–7.
72. Di Felice L, Courson C, Niznansky D, Foscolo PU, Kiennemann A. Biomass gasification with catalytic tar reforming: A model study into activity enhancement of calcium- and magnesium-oxide-based catalytic materials by incorporation of iron. Energy and Fuels. 2010;24(7):4034–45.
73. Krajnc N. Wood and Fuels handbook. Food and agricultural organization; 2015.
74. Shen DK, Gu S. The mechanism for thermal decomposition of cellulose and its main products. Bioresour Technol [Internet]. 2009;100(24):6496–504. Available from: http://dx.doi.org/10.1016/j.biortech.2009.06.095
75. Shen DK, Gu S, Bridgwater A V. Study on the pyrolytic behaviour of xylan-based hemicellulose using TG-FTIR and Py-GC-FTIR. J Anal Appl Pyrolysis [Internet]. 2010;87(2):199–206. Available from: http://dx.doi.org/10.1016/j.jaap.2009.12.001
76. Brebu M, Vasile C. Thermal degradation of lignin—a review. Cellul Chem Technol . 2010;44(9):353–63. Available from: http://www.cellulosechemtechnol.ro/pdf/CCT9(2010)/P.353-363.pdf
77. Kibet J, Khachatryan L, Dellinger B. Molecular products and radicals from pyrolysis of lignin. Environ Sci Technol. 2012;46(23):12994–3001.
78. Britt PF, Buchanan a. C, and Owens C V. Mechanistic investigation into the formation of polycyclic aromatic hydrocarbons from the pyrolysis hydrocarbons from the pyrolysis of terpenes. Prepr, Pap,-Am ChemSoc,DivFuel Chem,. 2004;49(2001):868–71.
79. Gu Y, Li Y, Li X, Luo P, Wang H, Wang X, et al. Energy Self-sufficient Wastewater Treatment Plants: Feasibilities and Challenges. Energy Procedia [Internet]. 2017;105:3741–51. Available from: http://dx.doi.org/10.1016/j.egypro.2017.03.868
80. Rulkens W. Sewage sludge as a biomass resource for the production of energy: Overview and assessment of the various options. Energy and Fuels. 2008;22(1):9–15.
81. Gavala HN, Yenal U, Skiadas I V., Westermann P, Ahring BK. Mesophilic and thermophilic anaerobic digestion of primary and secondary sludge. Effect of pre-treatment at elevated temperature. Water Res. 2003;37(19):4561–72.
82. Oliver B. Cardiff and Afan advanced digestion plants. Waste water Treat sewerage. :45–51.
83. Rosa AP, Chernicharo CAL, Lobato LCS, Silva R V., Padilha RF, Borges JM. Assessing the potential of renewable energy sources (biogas and sludge) in a full-scale UASB-based treatment plant. Renew Energy. 2018;124:21–6. Available from: https://doi.org/10.1016/j.renene.2017.09.025
84. Werle S. Gasification of a Dried Sewage Sludge in a Laboratory Scale Fixed Bed Reactor. Phys Procedia. 2015;66:253–6.
85. Pokorna E, Postelmans N, Jenicek P, Schreurs S, Carleer R, Yperman J. Study of bio-oils and solids from flash pyrolysis of sewage sludges. Fuel. 2009;88(8):1344–50. Available from: http://dx.doi.org/10.1016/j.fuel.2009.02.020
86. UNICEF Ghana. Assessment of Waste Water Treatment Plants in Ghana. 2016;18. Available from: https://www.unicef.org/ghana/assessment_of_waste_water_plant_report.pdf
87. Callegari A, Capodaglio AG. Properties and Beneficial Uses of (Bio)Chars, with Special Attention to Products from Sewage Sludge Pyrolysis. Resources [Internet]. 2018;7(1):20. Available from: http://www.mdpi.com/2079-9276/7/1/20
88. Tian K, Liu WJ, Qian TT, Jiang H, Yu HQ. Investigation on the evolution of N-containing organic compounds during pyrolysis of sewage sludge. Environ Sci Technol. 2014;48(18):10888–96.

89. Chen H, Namioka T, Yoshikawa K. Characteristics of tar, NOx precursors and their absorption performance with different scrubbing solvents during the pyrolysis of sewage sludge. Appl Energy [Internet]. 2011;88(12):5032–41. Available from: http://dx.doi.org/10.1016/j.apenergy.2011.07.007
90. American petroleum institute. Reclaimed petroleum hydrocarbons: residual waste from petroleum refining. 2010;
91. Qin L, Han J, He X, Zhan Y, Yu F. Recovery of energy and iron from oily sludge pyrolysis in a fluidized bed reactor. J Environ Manage [Internet]. 2015;154:177–82. Available from: http://dx.doi.org/10.1016/j.jenvman.2015.02.030
92. Hu G, Li J, Zeng G. Recent development in the treatment of oily sludge from petroleum industry: A review. J Hazard Mater [Internet]. 2013;261:470–90. Available from: http://dx.doi.org/10.1016/j.jhazmat.2013.07.069
93. DEFRA, Espinoza RL, Steynberg AP, Jager B, Vosloo AC, Farnetti E, et al. Enhanced oil recovery-an overview. Inorg Bio-Inorganic Chem [Internet]. 2004;98(1):9–19. Available from: https://www.gov.uk/government/uploads/system/uploads/attachment_data/file/69391/pb9052a-health-report-040325.pdf
94. Khan Z, Troquet J, Vachelard C. Sample preparation and analytical techniques for determination of polyaromatic hydrocarbons in soils. Int J Environ Sci Tech © Autumn. 2005;2(3):275–86.
95. Dean JR. Solid Phase Extraction. 2009;49–84.
96. Agilent. Fundamentals. Agil Present [Internet]. 2014;42(11):2555–68. Available from: http://dx.doi.org/10.1016/B978-0-12-381373-2.10061-4%0Ahttp://linkinghub.elsevier.com/retrieve/pii/B9780123813732000612%0Ahttps://www.degruyter.com/view/books/9783110289169/9783110289169/9783110289169.xml
97. Koning S, Janssen H-G, Brinkman UAT. Modern Methods of Sample Preparation for GC Analysis. Chromatographia [Internet]. 2009;69(S1):33–78. Available from: http://www.springerlink.com/index/10.1365/s10337-008-0937-3
98. Lomond JS, Tong AZ. Rapid analysis of dissolved methane, ethylene, acetylene and ethane using partition coefficients and headspace-gas chromatography. J Chromatogr Sci. 2011;49(6):469–75.
99. Jerković I, Marijanović Z, Gugić M, Roje M. Chemical profile of the organic residue from ancient amphora found in the adriatic sea determined by direct GC and GC-MS analysis. Molecules. 2011;16(9):7936–48.
100. Engewald W, Dettmer-wilde K. Practical Gas Chromatography. 2014. Available from: http://link.springer.com/10.1007/978-3-642-54640-2
101. Jennings W, Mittlefehldt E, Stremple P. Analytical Gas Chromatography. Analytical Gas Chromatography. 1997. p. 285–355. Available from: http://www.sciencedirect.com/science/article/pii/B9780123843579500106
102. Harold M. Mcnair JMM. Basic Gas Chromatography. Vol. 53, Journal of Chemical Information and Modeling. 1997. 3-27 p.
103. Restek. Guide to GC Column Selection and Optimizing Separations. 2013;1–16. Available from: http://www.restek.com/pdfs/GNBR1724-UNV.pdf
104. Gallego E, Roca FJ, Perales JF, Guardino X. Experimental evaluation of VOC removal efficiency of a coconut shell activated carbon filter for indoor air quality enhancement. Build Environ [Internet]. 2013;67:14–25. Available from: http://dx.doi.org/10.1016/j.buildenv.2013.05.003
105. Barry EF. Columns : Packed and Capillary ; Chromatography. Control. 2004. 65-191 p.
106. Zhou Y, Wang C, Free W, Zone T, Firor R, Technologies A. Analysis of Permanent Gases and Methane with the Agilent 6820 Gas Chromatograph Application. 2003;
107. Zeng H, Zou F, Lehne E, Zuo JY, Zhang D. Gas Chromatograph Applications in Petroleum Hydrocarbon Fluids. Adv Gas Chromatogr Prog Agric Biomed Ind Appl. 2012;363–88.
108. Vazquez-Roig P, Pico Y. Gas chromatography and mass spectroscopy techniques for the detection of chemical contaminants and residues in foods [Internet]. Chemical Contaminants and Residues in Food. Woodhead Publishing Limited; 2012. 17-61 p. Available from: http://dx.doi.org/10.1533/9780857095794.1.17
109. Zeeuw J de, de Zeeuw J. Impact of GC Parameters on The Separation, Part 3: Choice of Column Length. Sep Sci. 2014;6(4):8–13.
110. Chladek P, Coleman LJI, Croiset E, Hudgins RR. Gas chromatography method for the characterization of ethanol steam reforming products. J Chromatogr Sci. 2007;45(3):153–7.

111. Budiman H, Nuryatini, Zuas O. Comparison between GC-TCD and GC-FID for the determination of propane in gas mixture. Procedia Chem [Internet]. 2015;16:465–72. Available from: http://linkinghub.elsevier.com/retrieve/pii/S1876619615002284
112. Isobe K, Koba K, Ueda S, Senoo K, Harayama S, Suwa Y. A simple and rapid GC/MS method for the simultaneous determination of gaseous metabolites. J Microbiol Methods . 2011;84(1):46–51. Available from: http://dx.doi.org/10.1016/j.mimet.2010.10.009
113. de Hoffmann, E. Stroobant V. Mass Spectrometry principles and applications. 3rd ed. Wiley; 2007. 502 p.
114. Watson J. T, Sparkman OD. Electron Ionization. Introduction to Mass Spectrometry: Instrumentation, Applications, and Strategies for Data Interpretation. 2007. 315-448 p.
115. Gross JH. Mass Spectrometry . 2nd editio. Berlin, Heidelberg: Springer Berlin Heidelberg; 2011. Available from: http://link.springer.com/10.1007/978-3-642-10711-5
116. Gross JH. Mass Spectrometry [Internet]. Berlin, Heidelberg: Springer Berlin Heidelberg; 2004. Available from: http://link.springer.com/10.1007/3-540-36756-X
117. Maštovská K, Lehotay SJ. Evaluation of common organic solvents for gas chromatographic analysis and stability of multiclass pesticide residues. J Chromatogr A. 2004;1040(2):259–72.
118. Azargohar, R., Dalai AK. Activated carbon from Eucalyptus camaldulensis Dehn bark using phosphoric acid activation. Microporous Mesoporous Mater. 2008;110(17):413–21.
119. Feng, S., Hom BJ. Sensitive and Reproducible detection of PAHs Using the Agilent 5977A Series GC / MSD. Appl note . 2013;1–8. Available from: 5991-1811EN
120. Zhao, L. Zheng, W. Masek, O. Chen, X. Gu, B. Sharma, B. Cao X. Roles of phosphoric acid in biochar formation: synchronously improving carbon retention and sorbtion capacity. J Env Qual. 2017;46(2).
121. Olesik JW. Fundemental research in ICP-OES and ICPMS. Anal Chem News Featur. 1996;469–74.
122. Brame J, Griggs C. Surface Area Analysis Using the Brunauer- Emmett-Teller (BET) Method Scientific Operating Procedure Series : SOP-C Environmental Laboratory. Eng Res Dev Cent. 2016;(September).
123. Vladimir Z, Sparkman J. NIST 2008 User Guide. Natl Inst Stand Technol NIST. 2004;(June 2008):1–49. Available from: http://www.nist.gov/srd/
124. Thermo Scientific ISQ Series Single Quadrupole GC-MS Systems. Thermo Scientific; 2013. p. 1–2. Available from: https://assets.thermofisher.com/TFS-Assets/CMD/Specification-Sheets/PS-51872-ISQ-Single-Quadrupole-GC-MS-PS51872-EN.pdf
125. ISO. ISO 17025. General requirements for the competence of testing and calibration laboratories. Technical corrigendum 1. 2006;1–55.
126. Seo, M.W., Yun, Y.M., Cho, W.C., Ra, H.W., Yoon, S.J., Lee, J.G., Kim, Y.K., Lee, S.H., Eom, W.H, Lee, U.D, Lee SB. Methanol absorption characteristics for removal of H2S (hydrogen sulfide), COS (Carbonyl sulfide) and CO2 (Carbondioxide) on pilot scale biomass to liquid process. Energy. 2014;66:56–62.
127. Tan GHCM-K. Sample Preparation in the Analysis of Pesticides Residue in Food by Chromatographic Techniques. Pestic - Strateg Pestic Anal. 2011;29–58.
128. Jain A, Ramanathan V, Sankararamakrishnan R. Lone pair ⋯ π interactions between water oxygens and aromatic residues: Quantum chemical studies based on high-resolution protein structures and model compounds. Protein Sci. 2009;18(3):595–605.
129. Abdel-Shafy HI, Mansour MSM. A review on polycyclic aromatic hydrocarbons: Source, environmental impact, effect on human health and remediation. Egypt J Pet. 2016 Mar;25(1):107–23. Available from: http://dx.doi.org/10.1016/j.ejpe.2015.03.011
130. America LN, Hill M. Dissolved acetylene. 2016;1–4.
131. Ooi LG, Liong MT. Cholesterol-lowering effects of probiotics and prebiotics: A review of in Vivo and in Vitro Findings. Int J Mol Sci. 2010;11(6):2499–522.
132. Eyssen HJ, De Pauw G, Van Eldere J. Formation of hyodeoxycholic acid from muricholic acid and hyocholic acid by an unidentified gram-positive rod termed HDCA-1 isolated from rat intestinal microflora. Appl Environ Microbiol. 1999;65(7):3158–63.
133. Soupas L, Juntunen L, Lampi AM, Piironen V. Effects of sterol structure, temperature, and lipid medium on phytosterol oxidation. J Agric Food Chem. 2004;52(21):6485–91.
134. Lara-gonzalo A, Kruge MA, Lores I, Gutiérrez B, Gallego JR. Organic Geochemistry Pyrolysis GC – MS for the rapid environmental forensic screening of contaminated brownfield soil. Org

Geochem [Internet]. 2015;87:9–20. Available from: http://dx.doi.org/10.1016/j.orggeochem.2015.06.012
135. Shneine JK, Alaraji YH. Chemistry of 1, 2, 4-Triazole: A Review Article. Int J Sci Res ISSN (Online Index Copernicus Value Impact Factor. 2013;14611(3):2319–7064. Available from: www.ijsr.net
136. Velghe I, Carleer R, Yperman J, Schreurs S. Study of the pyrolysis of sludge and sludge/disposal filter cake mix for the production of value added products. Bioresour Technol [Internet]. 2013;134:1–9. Available from: http://dx.doi.org/10.1016/j.biortech.2013.02.030
137. Paethanom A, Yoshikawa K. Influence of pyrolysis temperature on rice husk char characteristics and its tar adsorption capability. Energies. 2012;5(12):4941–51.
138. Ania CO, Cabal B, Pevida C, Arenillas A, Parra JBÃ, Rubiera F, et al. Removal of naphthalene from aqueous solution on chemically modified activated carbons. 2007;41:333–40.
139. Lin JQ, Yang SE, Duan JM, Wu JJ, Jin LY, Lin JM. The Adsorption Mechanism Activated Carbon on Phenol of. 2016;03040.
140. Ding L, Zou B, Gao W, Liu Q, Wang Z, Guo Y, et al. Adsorption of Rhodamine-B from aqueous solution using treated rice husk-based activated carbon. Colloids Surfaces A Physicochem Eng Asp [Internet]. 2014;446:1–7. Available from: http://dx.doi.org/10.1016/j.colsurfa.2014.01.030
141. Hema M, Arivoli S. Rhodamine B adsorption by activated carbon: Kinetic and equilibrium studies. Indian J Chem Technol. 2009;16(1):38–45.
142. Yuan M, Tong S, Zhao S, Jia CQ. Adsorption of polycyclic aromatic hydrocarbons from water using petroleum coke-derived porous carbon. J Hazard Mater [Internet]. 2010;181(1–3):1115–20. Available from: http://dx.doi.org/10.1016/j.jhazmat.2010.05.130
143. Sullivan GL, Holliman PJ. Bioresource Technology Reports Thermal treatment of Himalayan balsam : Tar and biochar analysis. Bioresour Technol Reports. 2019;5(November 2018):164–9. Available from: https://doi.org/10.1016/j.biteb.2019.01.007
144. Yang, Kun., Zhu, Lizhong., Xing B. Adsorption of Polycyclic Aromatic Hydrocarbons by Carbon Nanomaterials. Environ Sci Technol. 2006;40(6):1855–61.
145. Taylor PJ. Matrix effects: The Achilles heel of quantitative high-performance liquid chromatography-electrospray-tandem mass spectrometry. Clin Biochem. 2005;38(4):328–34.
146. Jindo K, Mizumoto H, Sawada Y, Sonoki T. Physical and chemical characterization of biochars derived from. Biogeosciences. 2014;6613–21.
147. Chiou CT, Xing B. Compositions and Sorptive Properties of Crop Residue-Derived Chars. Environ Sci Technol. 2004;38(17):4649–55.
148. Khodakov AY, Chu W, Fongarland P. Advances in the Development of Novel Cobalt Fischer − Tropsch Catalysts for Synthesis of Long-Chain Hydrocarbons and Clean Fuels. 2007;1692–744.
149. Sarkari M, Fazlollahi F, Atashi H, Mirzaei AA, Hecker WC. Using Different Preparation Methods to Enhance Fischer-Tropsch Products over Iron-based Catalyst. 2013;27(3):259–66.
150. Akbari M, Akbar A, Atashi H, Arsalanfar M. Journal of the Taiwan Institute of Chemical Engineers Effect of microemulsion parameters on product selectivity of MgO-supported iron – cobalt – manganese – potassium nanocatalyst for Fischer – Tropsch synthesis using response surface methodology. J Taiwan Inst Chem Eng. 2018;91:396–404. Available from: https://doi.org/10.1016/j.jtice.2018.06.004
151. Xiong H, Moyo M, Motchelaho MA, Tetana ZN, Dube SMA, Jewell LL, et al. Fischer – Tropsch synthesis : Iron catalysts supported on N-doped carbon spheres prepared by chemical vapor deposition and hydrothermal approaches. J Catal. 2014;311:80–7. Available from: http://dx.doi.org/10.1016/j.jcat.2013.11.007
152. Ghampson IT, Newman C, Kong L, Pier E, Hurley KD, Pollock RA, et al. Effects of pore diameter on particle size, phase, and turnover frequency in mesoporous silica supported cobalt Fischer-Tropsch catalysts. Appl Catal A Gen. 2010;388(1–2):57–67. Available from: http://dx.doi.org/10.1016/j.apcata.2010.08.028
153. Kababji AH, Joseph B, Wolan JT. Silica-supported cobalt catalysts for fischer-tropsch synthesis: Effects of calcination temperature and support surface area on cobalt silicate formation. Catal Letters. 2009;130(1–2):72–8.
154. Govender BB, Iwarere SA, Ramjugernath D. The Application of Non-thermal Plasma- Catalysis in Fischer-Tropsch Synthesis at Very High Pressure : the Effect of Cobalt Loading. 2017;II:25–8.
155. Yan Z, Wang Z, Bukur DB, Goodman DW. Fischer-Tropsch synthesis on a model Co/SiO2catalyst. J Catal [Internet]. 2009;268(2):196–200. Available from:

http://dx.doi.org/10.1016/j.jcat.2009.09.015
156. Jalama K. Fischer-Tropsch Synthesis Over Titania- supported Cobalt Catalyst: Optimum Pressure for C5+ Hydrocarbons Production. 2015;II:22–4.
157. Bezemer GL, Bitter JH, Kuipers HPCE, Oosterbeek H, Holewijn JE, Xu X, et al. Cobalt particle size effects in the Fischer-Tropsch reaction studied with carbon nanofiber supported catalysts. J Am Chem Soc. 2006;128(12):3956–64.
158. Intarasiri, S., Ratana, T., Somchamni, T., Phonjaksorn, M., Tungkamani S. Effect of pore size diameter of cobalt supported catalyst on gasoline – diesel selectivity. Energy Procedia. 2017;138:1035–40.
159. Jacobs G, Das TK, Zhang Y, Li J, Racoillet G, Davis BH. Fischer-Tropsch synthesis: Support, loading, and promoter effects on the reducibility of cobalt catalysts. Appl Catal A Gen. 2002;233(1–2):263–81.
160. Stowell CA, Korgel BA. Iridium nanocrystal synthesis and surface coating-dependent catalytic activity. Nano Lett. 2005;5(7):1203–7.

Appendix 1.0 examples of total ion chromatograms (TIC) and mass spectra.

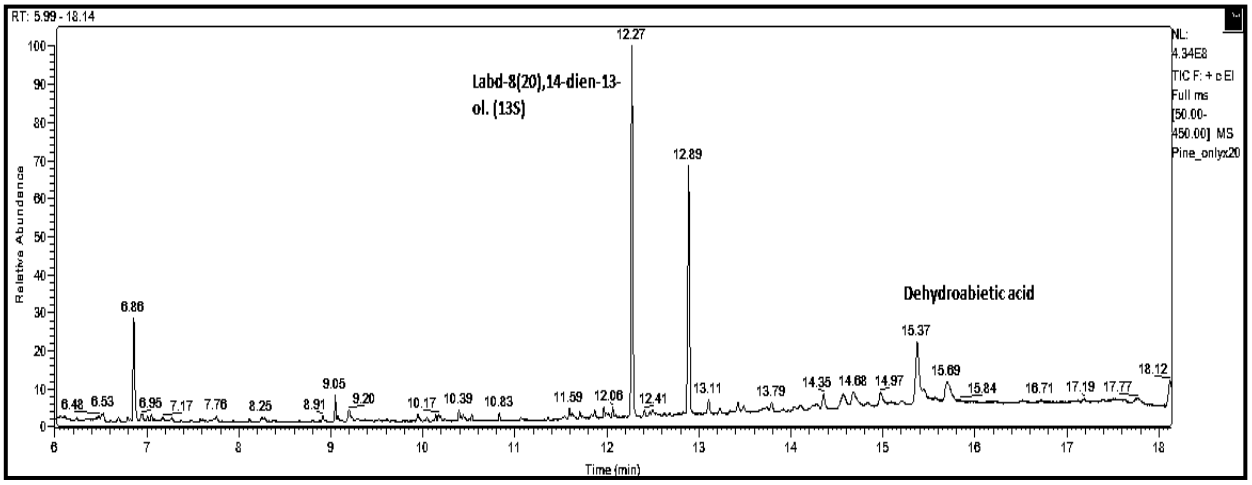

Appendix 1.1 shows a total ion chromatogram (TIC) of the pentane extract for 0.5g of pine wood, Main components are Labd-8(20),14-dien-13-ol, (13S) and dehydroabietic acid.

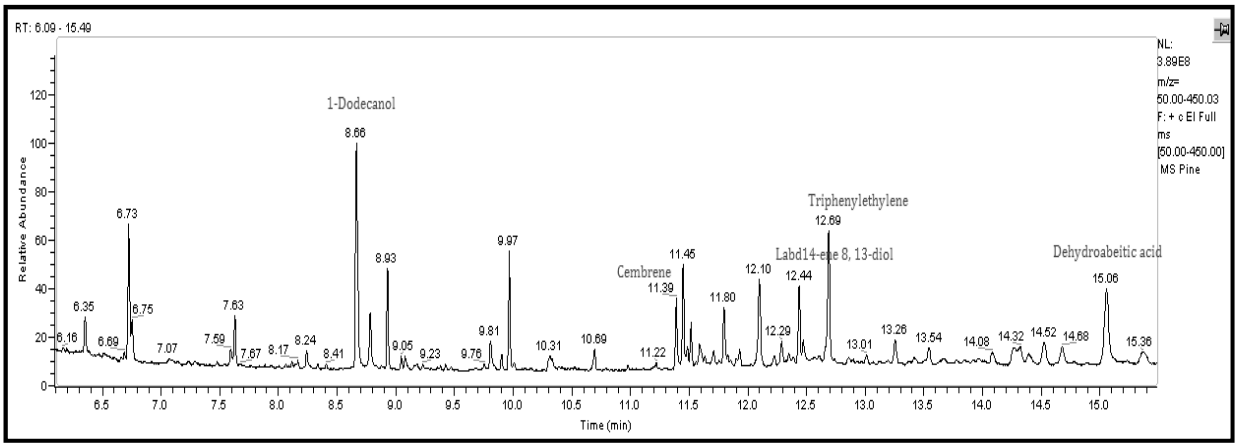

Appendix 1.2 shows a total ion chromatogram (TIC) of the acetone extract for 0.5g of pine wood, There are more peaks present and represent more extractives.

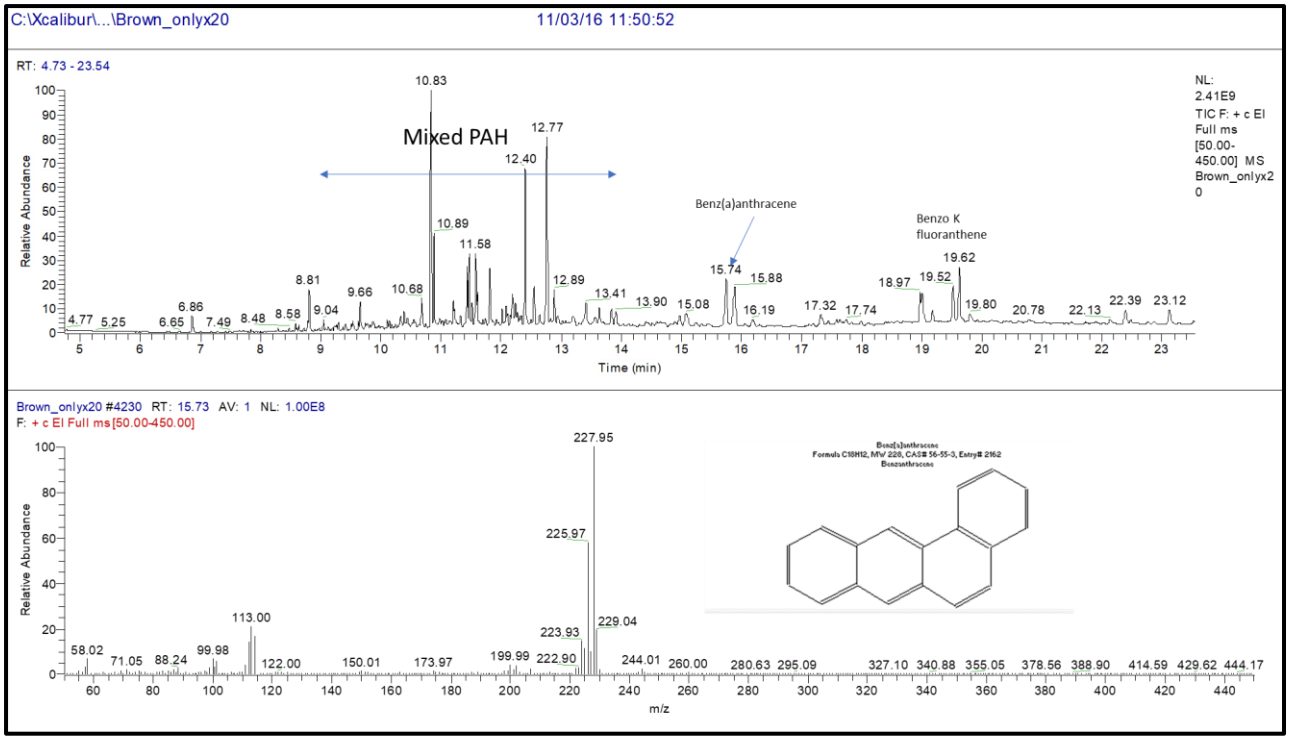

Appendix 1.3 shows a total ion chromatogram (TIC) of the solvent extract for 0.5g of brown field soil (10% contaminated), the majority of compounds are polyaromatic hydrocarbons (PAHs).

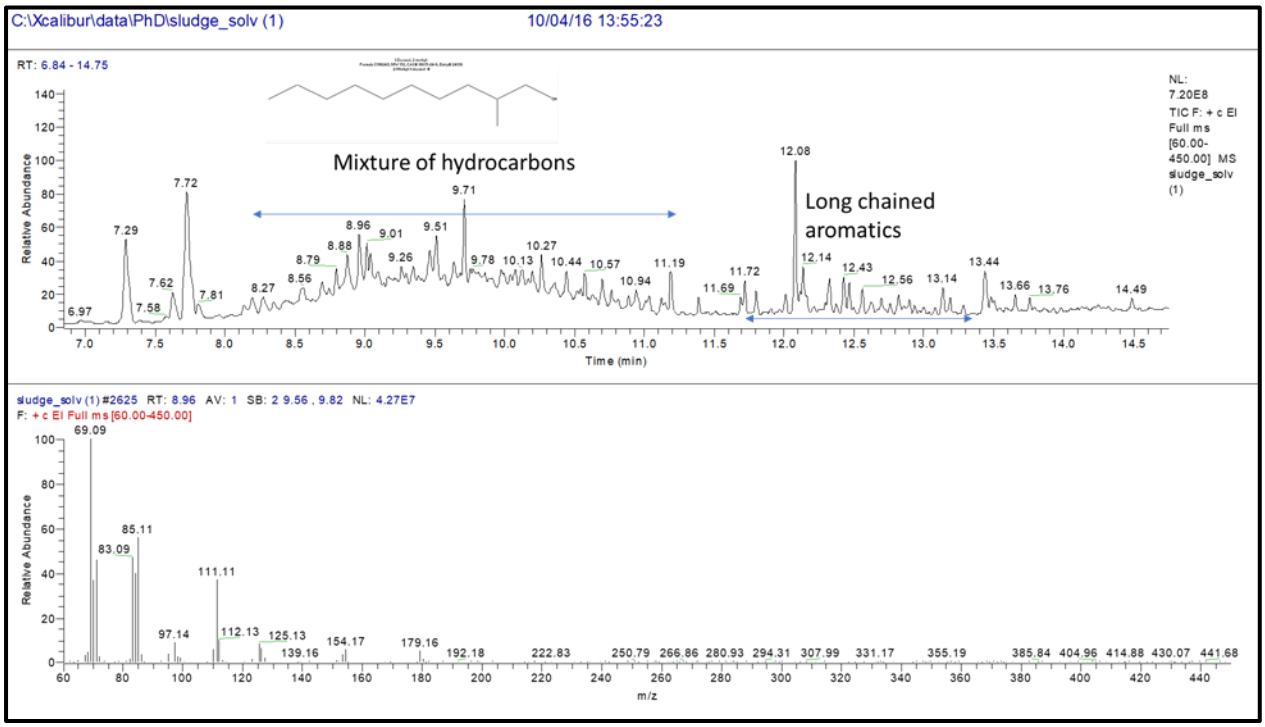

Appendix 1.4 shows a total ion chromatogram (TIC) of the solvent extract for 0.5g of sludge filter cake, the extract comprises of mainly fatty acids and lipid soluble molecules.

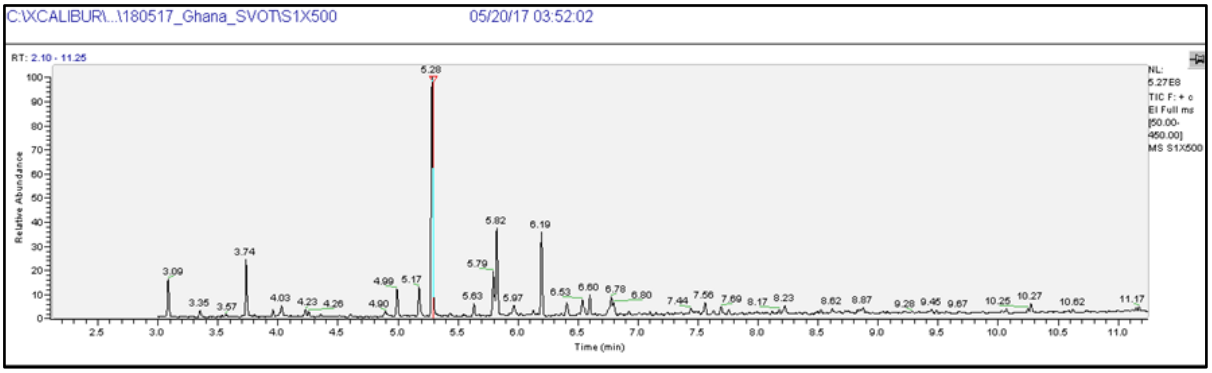

Appendix 1.5 shows the TIC of the tars captured in the pyrolysis of Ghana sludge cake. The compounds identified where very simular to UK sludge cake.

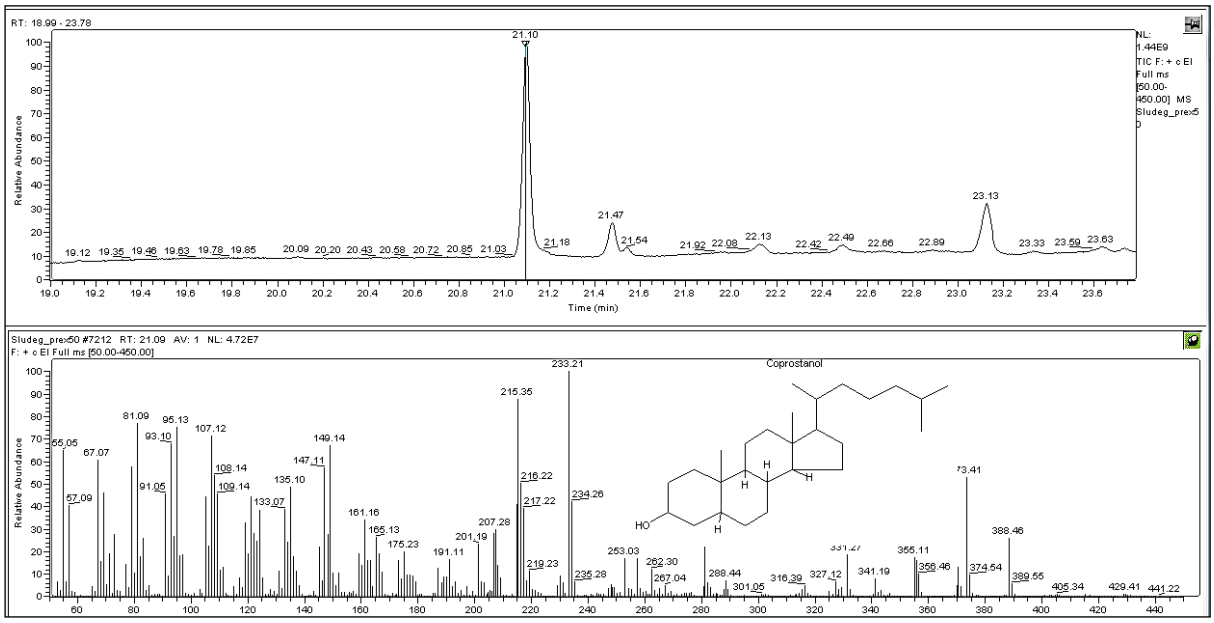

Appendix 1.6 is the TIC of the major compounds extracted from Ghana sludge cake. These were identified by their mass spectra (Below) to be sterol compounds.

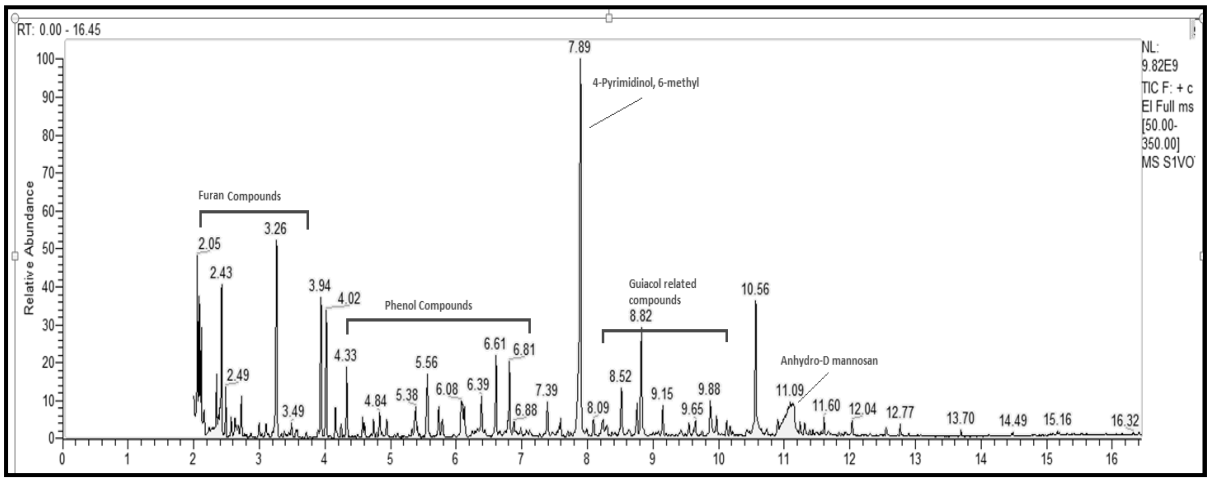

Appendix 1.7 is a TIC of the compounds captured in scrubber 1 from the pyrolysis of pine wood. This was run for semi-volatile organic tars (SVOT). The compounds identified are typical of soft wood pyrolysis.

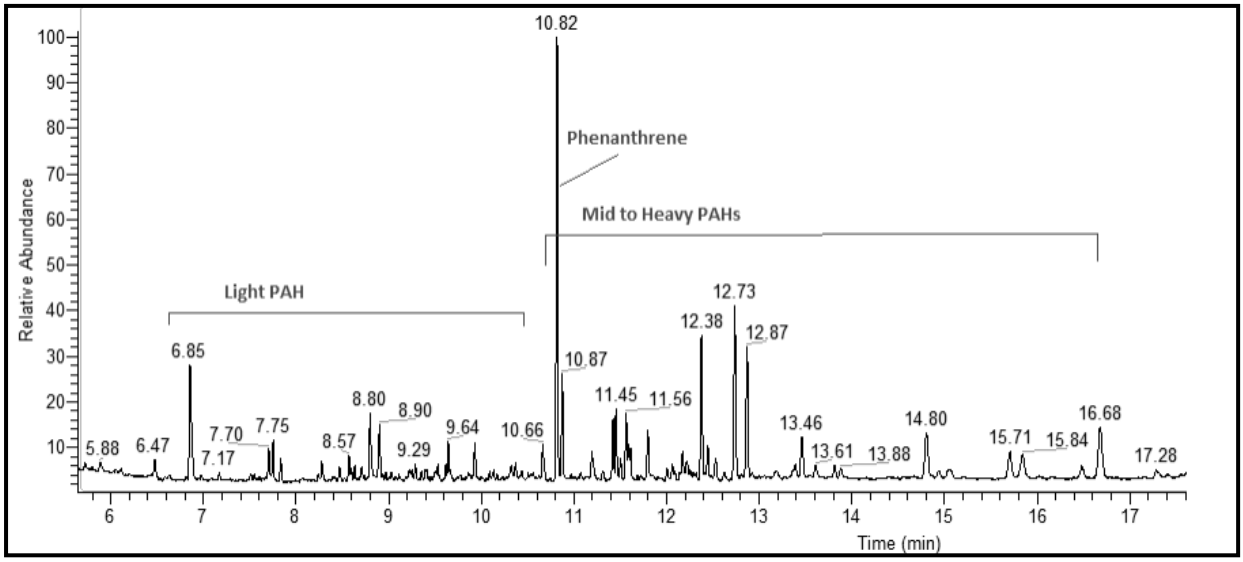

Appendix 1.8 is TIC of the compounds captured in scrubber 1 from the pyrolysis of brown field soil. This was run for semi-Volatile organic tars (SVOT). The tars identified are mainly polyaromatic hydrocarbons

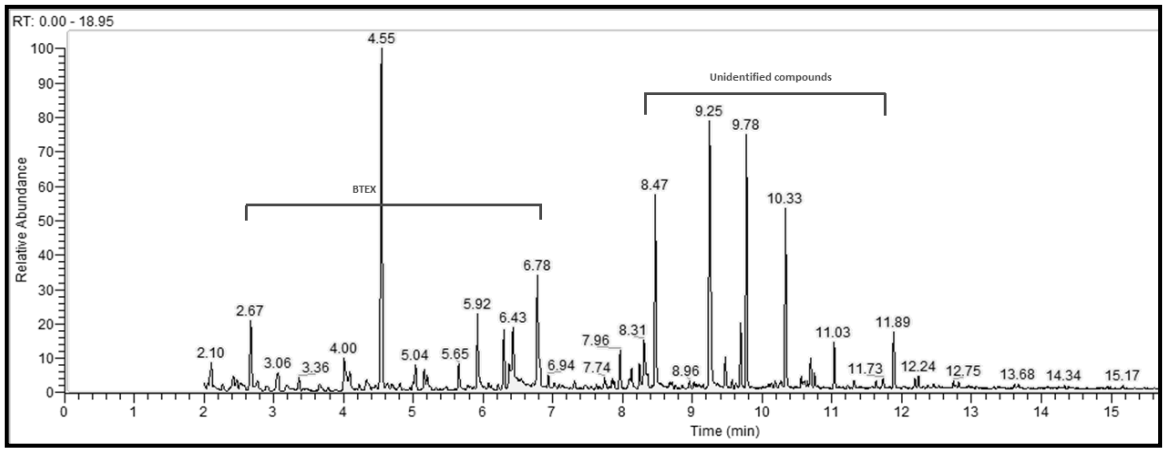

Appendix 1.9 is a TIC of the volatile compounds captured in scrubber 1 from the pyrolysis of sludge filter cake. This was run for Volatile organic tars (VOT) and the main composition of tars derived from sludge filter cake are small volatiles aromatics C6-C10.

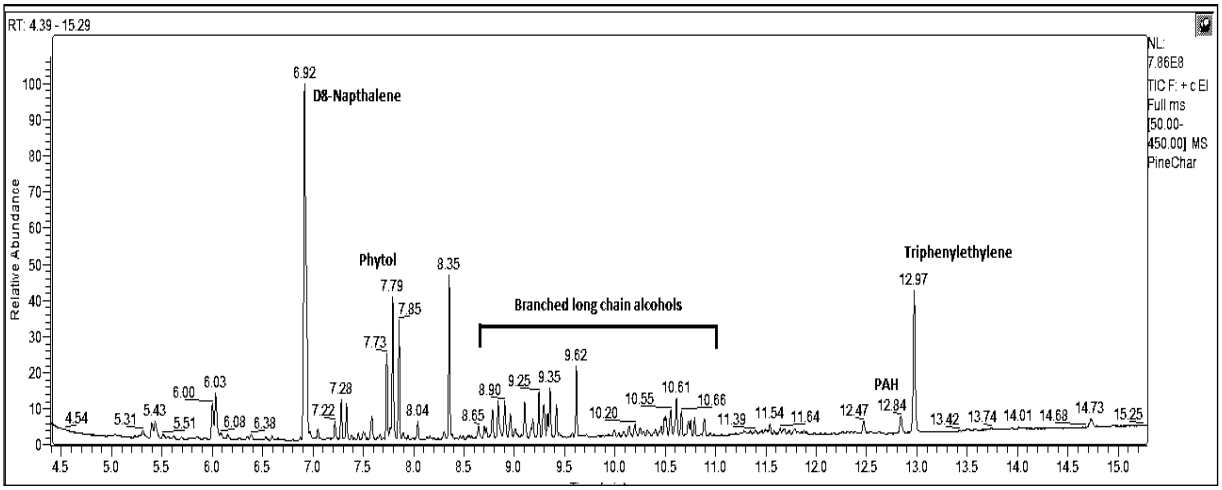

Appendix 1.10 shows a total ion chromatogram (TIC) of the solvent extract for 0.5 g of pine wood char after pyrolysis, majority of the compounds identified are branched alcohols and phytols.

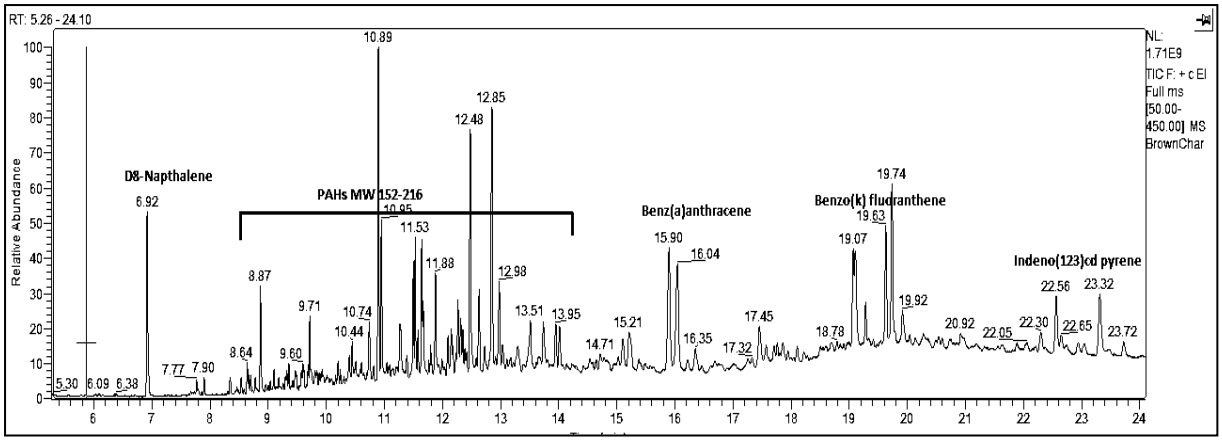

Appendix 1.11 shows a total ion chromatogram (TIC) of the solvent extract for 0.5 g of Brown field char after pyrolysis, majority of the compounds identified are PAHs.

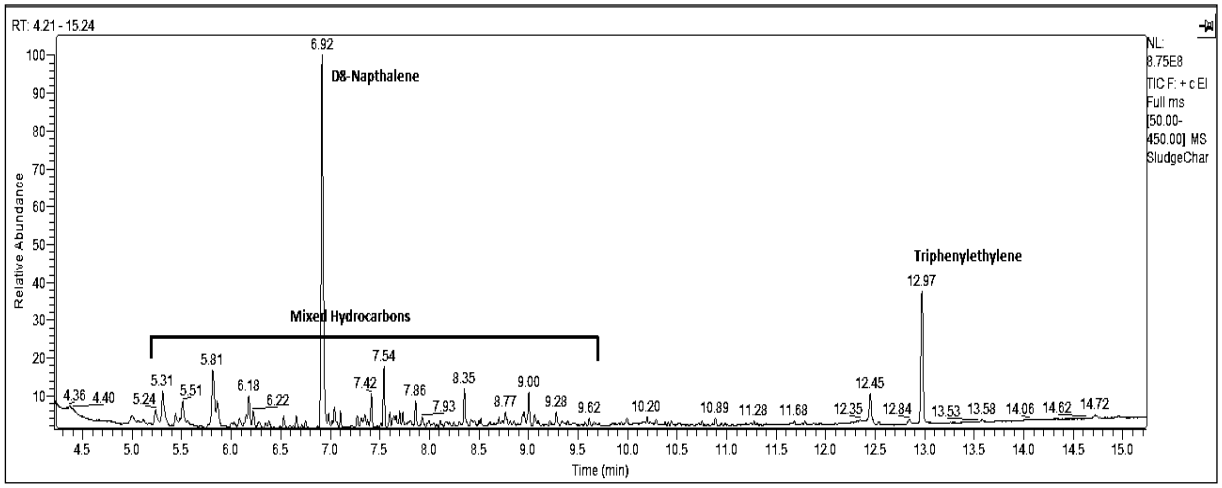

Appendix 1.12 shows a total ion chromatogram (TIC) of the solvent extract for 0.5 g of UK sludge cake after pyrolysis. Majority of the compounds are hydrocarbons.

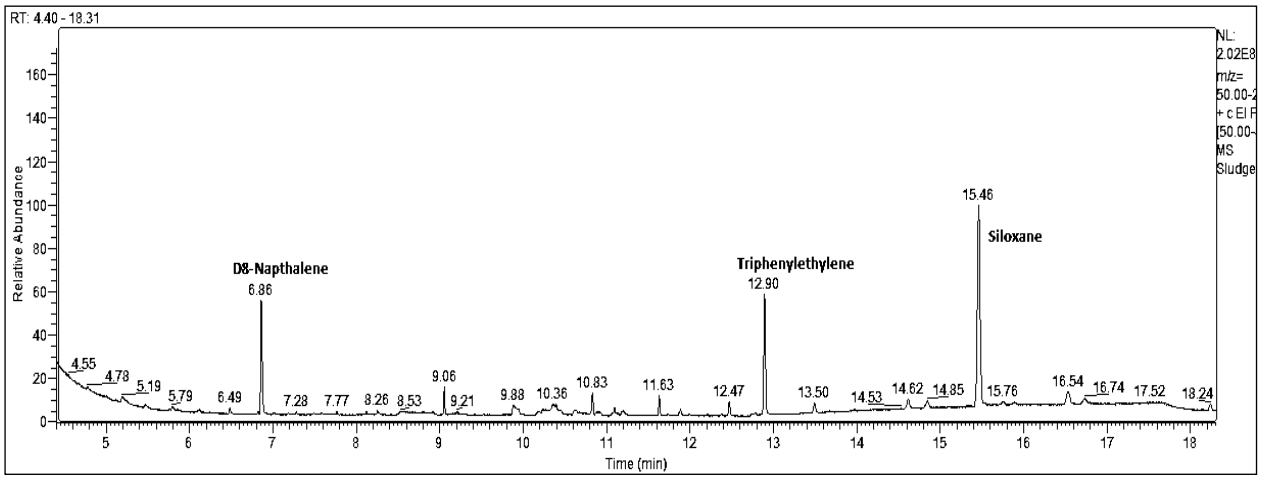

Appendix 1.13 shows a total ion chromatogram (TIC) of the solvent extract for 0.5 g UK sludge cake ash after gasification.

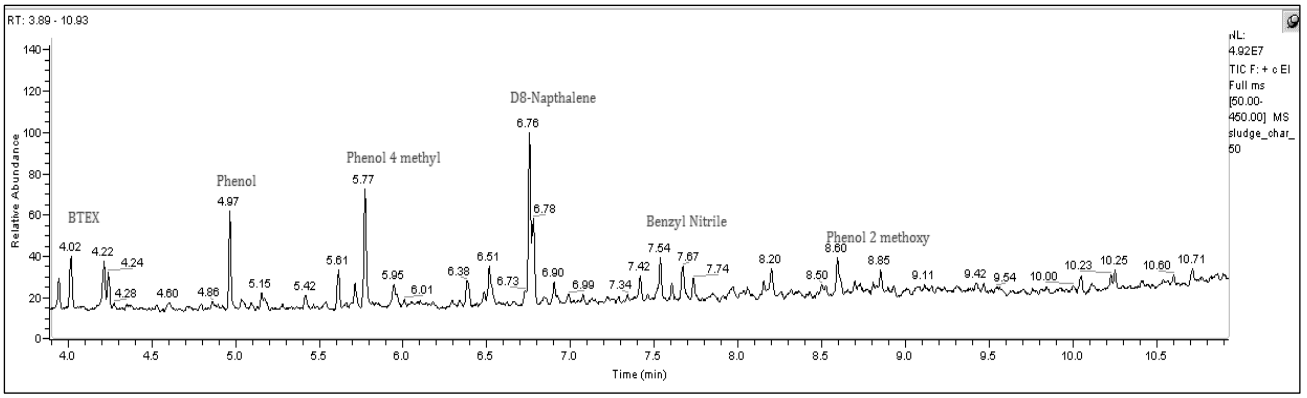

Appendix 1.14 shows a total ion chromatogram (TIC) of the solvent extract for 0.5g Ghana sludge cake char after pyrolysis. Consists of Phenols and BTEX.

Appendix 2.0 Addition analysis.

Appendix 2.1 Total Fatty acid compounds in sludge: (Gravimetric analysis)

Method:

5 g of sludge was added to glass tube and 25 mL of 2: 1 water : methanol was added and the sample sonicated for 15mins. This causes the break up of the sludge material and precipitation of proteins out.

The sample was then centrifuged for 15 mins at 2000 rpm. The eluent was decanted and was extracted and acidyfied with 0.5 ml conc HNO_3 with 5 mL pentane. The pentane layer was carefully removed and placed into a clean glass tube (weighed prior). This extraction was done three times to ensure maximum recovery of lipophilic compounds.

The pentane layer was air dried and the glass ware re-weighed. Below is the resultsof the total lipophilic compounds.

Sample (5g)	Bottle before (g)	Bottle after (g)	Total lipophilic compounds (mg)	% lipophilic compounds
Ghana Sludge	24.2821 g	24.2861 g	4.0 mg	0.04%
UK sludge	24.3955 g	24.4013 g	5.8 mg	0.12%

Appendix 2.2 Total Nitrogen content (Kjeldahl method)

1 g of sample was added to a 250 ml round bottom flask, to this 2.5 g potassium sulfate, 0.3 g copper sulfate and 0.3 g titanium oxide was added, which acted as a catalyst.

20 ml of concentrated sulfuric acid was then added to the mixture and 100ml deionised water was added using a dropping funnel; the contents were heated to 200^{o}C for 2 hours.

The dissolved mixture was then diluted to 1:100 in deionised water and neutralised by adding 1ml of 1M sodium hydroxide solution (pH 7.0) .

This diluted sample was then tested for ammonia using palintest ammonia kit. This a colourmetric test run on a palintest metre. Please see https://www.palintest.com/en for further details. Ammonia is determined in terms of N mg/kg and is equivalent to the nitrogen content of the sample.

Sample	Total Nitrogen N mg/kg
Ghana sludge	3.5 mg/kg
UK sludge	2.5 mg/kg

Table appendix 4.2 shows total nitrogen content of UK and Ghana sludge cake.

Appendix 3.0 T-test results

Appemdix 3.1 T-test data for comparison of solvents methanol and acetone on recovery of standard compounds.

Volatile aromatic	Boiling point	Methanol mean recovery	Aceton mean recovery	Methanol SD	Acetone SD	T-test result (P=0.05) n=4 Critical Value 2.78
Benzene	80 °C	117.29	126.24	16.99	11.09	-0.76
Toluene	111 °C	90.00	84.23	6.86	10.05	0.82
Chloro benzene	131 °C	72.78	68.92	2.04	13.11	0.50
Ethyl benzene	136 °C	79.16	94.32	3.97	12.59	-1.99
p,o-xylene	140 °C	75.65	99.13	8.06	13.24	-2.48
Styrene	145 °C	79.45	94.90	4.55	14.27	-1.17
Benzene (1-methyl-2 ethyl)	165 °C	63.16	117.58	2.13	9.27	-5.09

Table appendix 3.1 Shows the t-test comparison of acetone and methanol for volatile aromatic compounds; the critical value was 2.78 for 3 degrees of freedom.

Volatile PAH compound	Boiling point	Acetone mean recovery	Methanol mean recovery	Acetone SD	Methanol SD	T-test result (P=0.05) n=4 Critical Value 2.78
Naphthalene	218 °C	93.43	44.90	3.98	2.69	17.50
Acenaphthylene	280 °C	68.84	66.35	6.50	2.53	0.62
Acenaphthene	279 °C	67.25	64.10	3.03	5.70	0.85
Fluorene	294 °C	63.58	64.82	3.91	2.16	-0.48
Phenanthrene	339 °C	56.41	62.45	1.95	5.07	-1.93
Anthracene	340 °C	60.70	59.90	2.11	3.15	0.37
Fluoranthene	375 °C	54.52	47.32	2.55	0.45	4.82
Pyrene	404 ° C	54.52	45.71	3.00	2.61	3.84
Benzo (a) anthracene	438 °C	56.07	29.23	3.21	0.94	13.90
Chrysene	448 °C	54.87	34.53	2.86	0.73	11.95
Benzo (a) pyrene	496 °C	55.00	33.20	3.01	0.93	11.97
Benzo (b) fluoranthene	481 °C	52.80	31.67	3.11	1.34	10.79
Dibenzo (a) anthracene	524 °C	49.18	29.80	1.35	0.81	21.34
Indeno (123) cd pyrene	536 °C	49.63	32.16	2.28	0.56	12.90
Benzo (ghi) perylene	550 °C	47.66	28.13	1.83	0.80	16.91

Table appendix 3.1.1 Shows the t-test comparison of acetone and methanol for polyaromatic aromatic hydrocarbons; the critical value was 2.78 for 3 degrees of freedom.

Phenolic compounds	Boiling point	Acetone mean recovery	Methanol mean recovery	Acetone SD	Methanol SD	T-test result (P=0.05) n=4 Critical Value 2.78
Phenol	182 °C	82.47	68.36	0.65	3.45	6.97
2-chlorophenol	175 °C	84.31	68.19	5.25	1.31	5.16
2-methylphenol	191 °C	81.86	69.22	2.14	4.11	4.72
4-methylphenol	202 °C	77.14	69.47	6.19	4.37	1.75
2-nitrophenol	216 °C	86.52	73.82	5.92	6.21	2.57
2,3-dimethylphenol	218 °C	79.33	74.00	2.63	2.59	2.50
2,5-dichlorophenol	211 °C	80.33	69.47	3.21	4.36	3.47
2,6-dichlorophenol	220 °C	84.89	70.67	5.00	2.86	-4.27
4 chloro 3 methyl phenol	235 °C	72.20	71.75	3.68	6.35	0.11
2,3,5 trichloro phenol	248-253 °C	72.92	76.57	1.29	10.30	-0.61
2,3,6 trichlorophenol	272 °C	73.76	76.39	3.08	1.04	-1.40

Table appendix 3.1.2 Shows the t-test comparison of acetone and methanol for phenolic compounds; the critical value was 2.78 for 3 degrees of freedom.

Appendix 3.2 T-test data for comparison of UK sludge biochar recovery of standard compounds prepared at different temperatures.

Volatile PAH compound	Boiling point	Afan biochar 400° C mean recovery	Afan biochar 700° C mean recovery	Afan biochar 400° C SD	Afan biochar 700° C SD	Afan 400° C and 700° C T-test result (P=0.05) n=4 Critical Value 2.78
Naphthalene	218 °C	55.6	35.2	1.13	5.30	6.53
Acenaphthylene	280 °C	103.5	35.9	3.04	3.18	26.60
Acenaphthene	279 °C	106.5	65.4	3.18	7.99	8.28
Fluorene	294 °C	116.5	57.0	3.46	13.22	7.54
Phenanthrene	339 °C	118.9	65.0	3.96	4.95	14.73
Anthracene	340 °C	130.3	46.8	2.55	5.37	24.32
Fluoranthene	375 °C	106.3	54.5	2.97	3.61	19.22
Pyrene	404 ° C	106.2	55.7	2.97	2.26	23.43
Semi volatile PAH compound	**Boiling point**	**Afan biochar 400° C mean recovery**	**Afan biochar 700° C mean recovery**	**Afan biochar 400° C SD**	**Afan biochar 700° C SD**	**Afan 400° C and 700° C T-test result (P=0.05) n=4 Critical Value 2.78**
Benzo (a) anthracene	438 °C	48.3	35.3	0.97	0.14	22.97
Chrysene	448 °C	41.5	30.1	0.95	1.77	9.88
Benzo (a) pyrene	496 °C	55.6	25.3	1.09	0.28	46.69
Benzo (b) fluoranthene	481 °C	49.7	22.5	0.85	0.32	51.95
Dibenzo (a) anthracene	524 °C	44.8	28.9	0.92	0.49	26.35
Indeno (123) cd pyrene	536 °C	39.6	32.2	2.12	0.21	6.05
Benzo (ghi) perylene	550 °C	45.2	26.7	1.06	1.13	20.61

Table appendix 3.2 Shows the t-test comparison of UK sludge biochar prepared at 700 and 400 °C for Poly aromatic compounds; the critical value was 2.78 for 3 degrees of freedom.

Phenolic compounds	Boiling point	Afan biochar 400° C mean recovery	Afan biochar 700° C mean recovery	Afan biochar 400° C SD	Afan biochar 700° C SD	Afan 400° C and 700° C T-test result (P=0.05) n=4 Critical Value 2.78
Phenol	182 °C	19.7	19.1	0.57	4.24	0.24
2-chlorophenol	175 °C	19.9	18.5	0.35	4.38	0.53
2-methylphenol	191 °C	12.3	13.4	0.35	2.62	0.72
4-methylphenol	202 °C	15.2	15.9	0.57	3.39	0.35
2-nitrophenol	216 °C	25.4	17.4	0.92	1.49	7.98
2,3-dimethylphenol	218 °C	19.0	25.6	0.92	0.07	0.09
2,5-dichlorophenol	211 °C	34.3	34.4	1.27	1.41	6.53
2,6-dichlorophenol	220 °C	33.5	35.9	0.64	0.14	6.51
4 chloro 3 methyl phenol	235 °C	24.0	28.2	0.28	6.79	1.07
2,3,5 trichloro phenol	248-253 °C	78.7	58.3	1.20	9.19	3.80
2,3,6 trichlorophenol	272 °C	88.8	54.2	5.16	10.47	5.13

Table appendix 3.2.1 Shows the t-test comparison of UK sludge biochar prepared at 700 and 400 °C for Poly aromatic compounds; the critical value was 2.78 for 3 degrees of freedom.

Appendix 4.0: Example 1 of processed data for hydrocarbon identification method validation

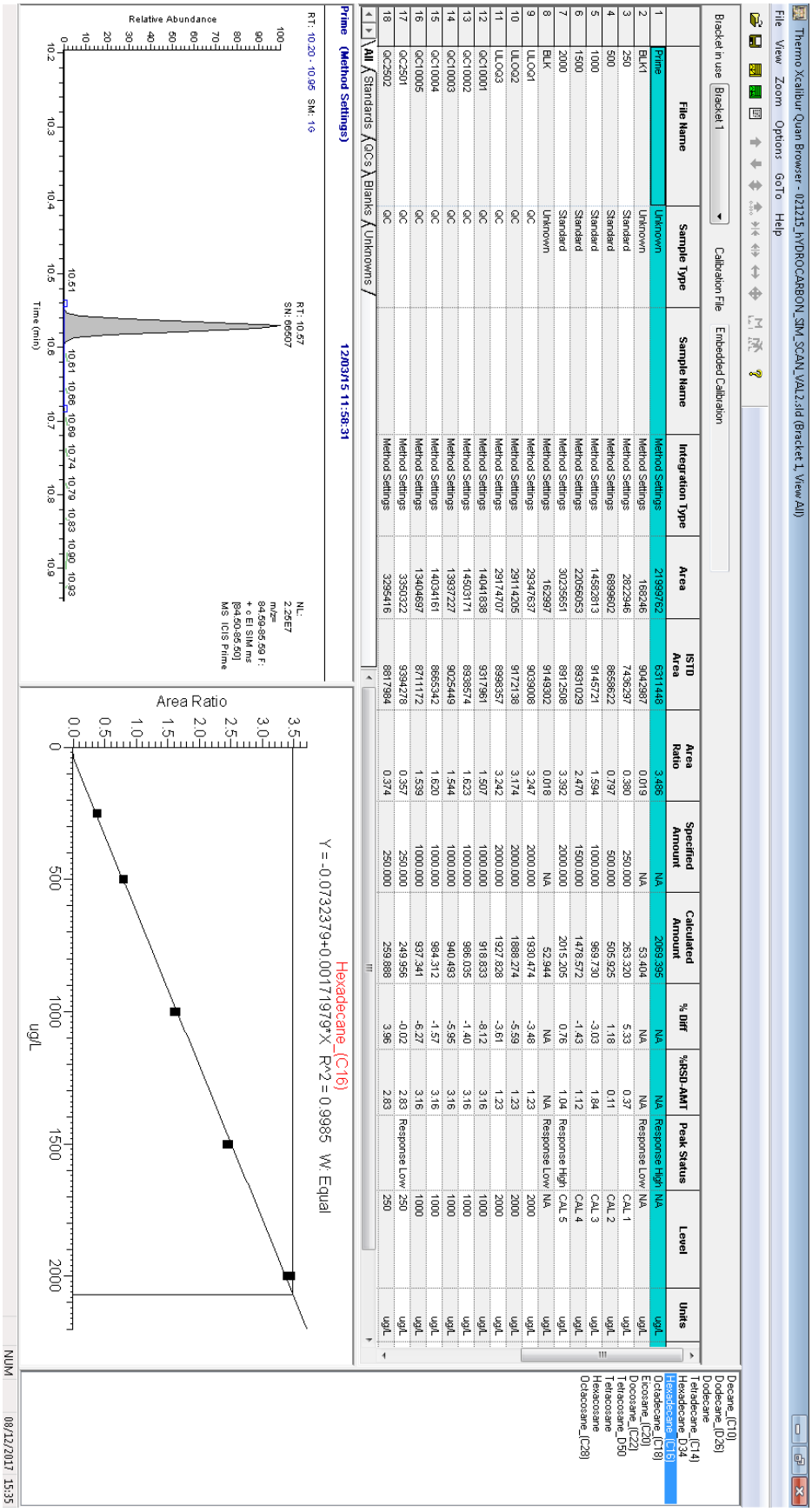

	File Name	Sample Type	Sample Name	Integration Type	Area	ISTD Area	Area Ratio	Specified Amount	Calculated Amount	% Diff	%RSD-AMT	Peak Status	Level	Units
1	Prime	Unknown	Method Settings	Method Settings	2199762	6311448	3.486	NA	2069.395	NA	NA	Response High	NA	ug/L
2	BLK1	Unknown	Method Settings		168246	9042987	0.019	NA	53.404	NA	NA	Response Low	NA	ug/L
3	250	Standard	Method Settings	Method Settings	2822946	7436297	0.380	250.000	263.320	5.33	0.37		CAL 1	ug/L
4	500	Standard	Method Settings	Method Settings	6089602	8658622	0.797	500.000	505.925	1.18	0.11		CAL 2	ug/L
5	1000	Standard	Method Settings	Method Settings	14582813	9145721	1.594	1000.000	969.730	-3.03	1.84		CAL 3	ug/L
6	1500	Standard	Method Settings	Method Settings	22056053	8931029	2.470	1500.000	1478.572	-1.43	1.12		CAL 4	ug/L
7	2000	Standard	Method Settings	Method Settings	30235651	8912508	3.392	2000.000	2015.205	0.76	1.04	Response High	CAL 5	ug/L
8	BLK	Unknown	Method Settings		162997	9149302	0.018	NA	52.944	NA	NA	Response Low	NA	ug/L
9	ULOQ1	QC	Method Settings	Method Settings	29347637	9039008	3.247	2000.000	1930.474	-3.48	1.23		2000	ug/L
10	ULOQ2	QC	Method Settings	Method Settings	29114205	9172138	3.174	2000.000	1888.274	-5.59	1.23		2000	ug/L
11	ULOQ3	QC	Method Settings	Method Settings	29174707	8998357	3.242	2000.000	1927.828	-3.61	1.23		2000	ug/L
12	QC10001	QC	Method Settings	Method Settings	14041838	9317961	1.507	1000.000	918.833	-8.12	3.16		1000	ug/L
13	QC10002	QC	Method Settings	Method Settings	14503171	8938574	1.623	1000.000	986.035	-1.40	3.16		1000	ug/L
14	QC10003	QC	Method Settings	Method Settings	13937227	9025449	1.544	1000.000	940.493	-5.95	3.16		1000	ug/L
15	QC10004	QC	Method Settings	Method Settings	14034161	8665342	1.620	1000.000	984.312	-1.57	3.16		1000	ug/L
16	QC10005	QC	Method Settings	Method Settings	13404697	8711172	1.539	1000.000	937.341	-6.27	3.16		1000	ug/L
17	QC2501	QC	Method Settings	Method Settings	3350322	9394278	0.357	250.000	249.956	-0.02	2.83	Response Low	250	ug/L
18	QC2502	QC	Method Settings	Method Settings	3295416	8817984	0.374	250.000	259.888	3.96	2.83		250	ug/L

Decane_(C10)
Dodecane_[D26]
Dodecane
Tetradecane_(C14)
Hexadecane_D34
Hexadecane_(C16)
Octadecane_(C18)
Eicosane_(C20)
Docosane_(C22)
Tetracosane_D50
Tetracosane
Hexacosane
Octacosane_(C28)

Example 2 of processed data for Tetracosane from the Fisher-Tropsch catalyst testing.

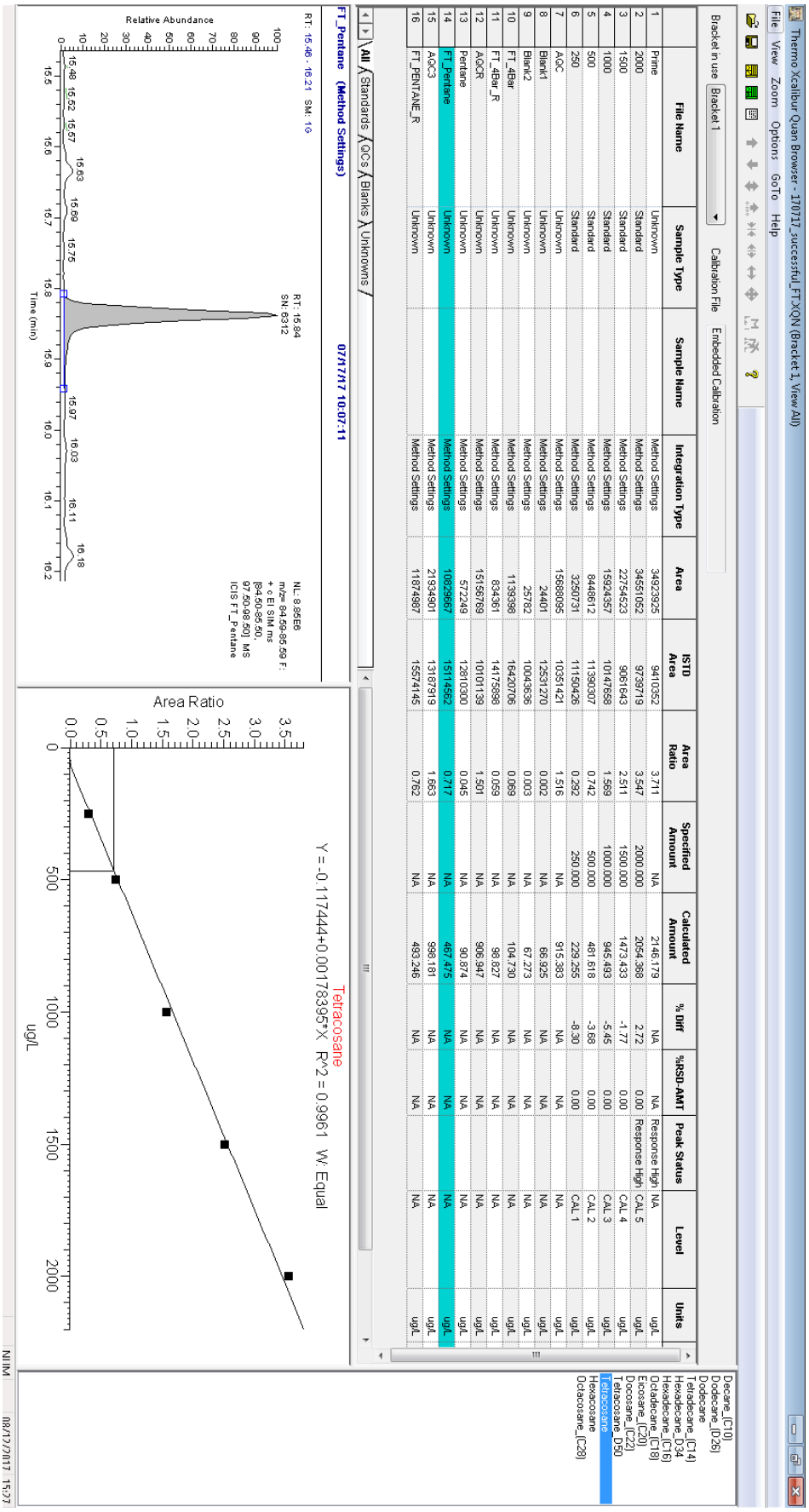

	File Name	Sample Type	Sample Name	Integration Type	Area	ISTD Area	Area Ratio	Specified Amount	Calculated Amount	% Diff	%RSD-AMT	Peak Status	Level	Units
1	Prime	Unknown		Method Settings	34923925	9410352	3.711	NA	2146.179	NA	NA	Response High	NA	ug/L
2	2000	Standard		Method Settings	34551052	9739719	3.547	2000.000	2054.368	2.72	0.00	Response High	CAL 5	ug/L
3	1500	Standard		Method Settings	22754523	9061643	2.511	1500.000	1473.433	-1.77	0.00		CAL 4	ug/L
4	1000	Standard		Method Settings	15924357	10147658	1.569	1000.000	945.493	-5.45	0.00		CAL 3	ug/L
5	500	Standard		Method Settings	8448612	11390307	0.742	500.000	481.618	-3.68	0.00		CAL 2	ug/L
6	250	Standard		Method Settings	3250731	11150426	0.292	250.000	229.255	-8.30	0.00		CAL 1	ug/L
7	AQC	Unknown		Method Settings	15688085	10351421	1.516	NA	915.383	NA	NA		NA	ug/L
8	Blank1	Unknown		Method Settings	24401	12531270	0.002	NA	66.925	NA	NA		NA	ug/L
9	Blank2	Unknown		Method Settings	25782	10043636	0.003	NA	67.273	NA	NA		NA	ug/L
10	FT_4Bar	Unknown		Method Settings	1139398	16420706	0.069	NA	104.730	NA	NA		NA	ug/L
11	FT_4Bar_R	Unknown		Method Settings	834361	14175898	0.059	NA	98.827	NA	NA		NA	ug/L
12	AQCR	Unknown		Method Settings	15156769	10101139	1.501	NA	906.947	NA	NA		NA	ug/L
13	Pentane	Unknown		Method Settings	572249	12810300	0.045	NA	90.874	NA	NA		NA	ug/L
14	FT_Pentane	Unknown		Method Settings	10829667	15114552	0.717	NA	487.475	NA	NA		NA	ug/L
15	AQC3	Unknown		Method Settings	21934901	13187919	1.663	NA	998.181	NA	NA		NA	ug/L
16	FT_PENTANE_R	Unknown		Method Settings	11874987	15574145	0.762	NA	493.246	NA	NA		NA	ug/L

Example 3 of VOT validation run: processed data for ethyl benzene.

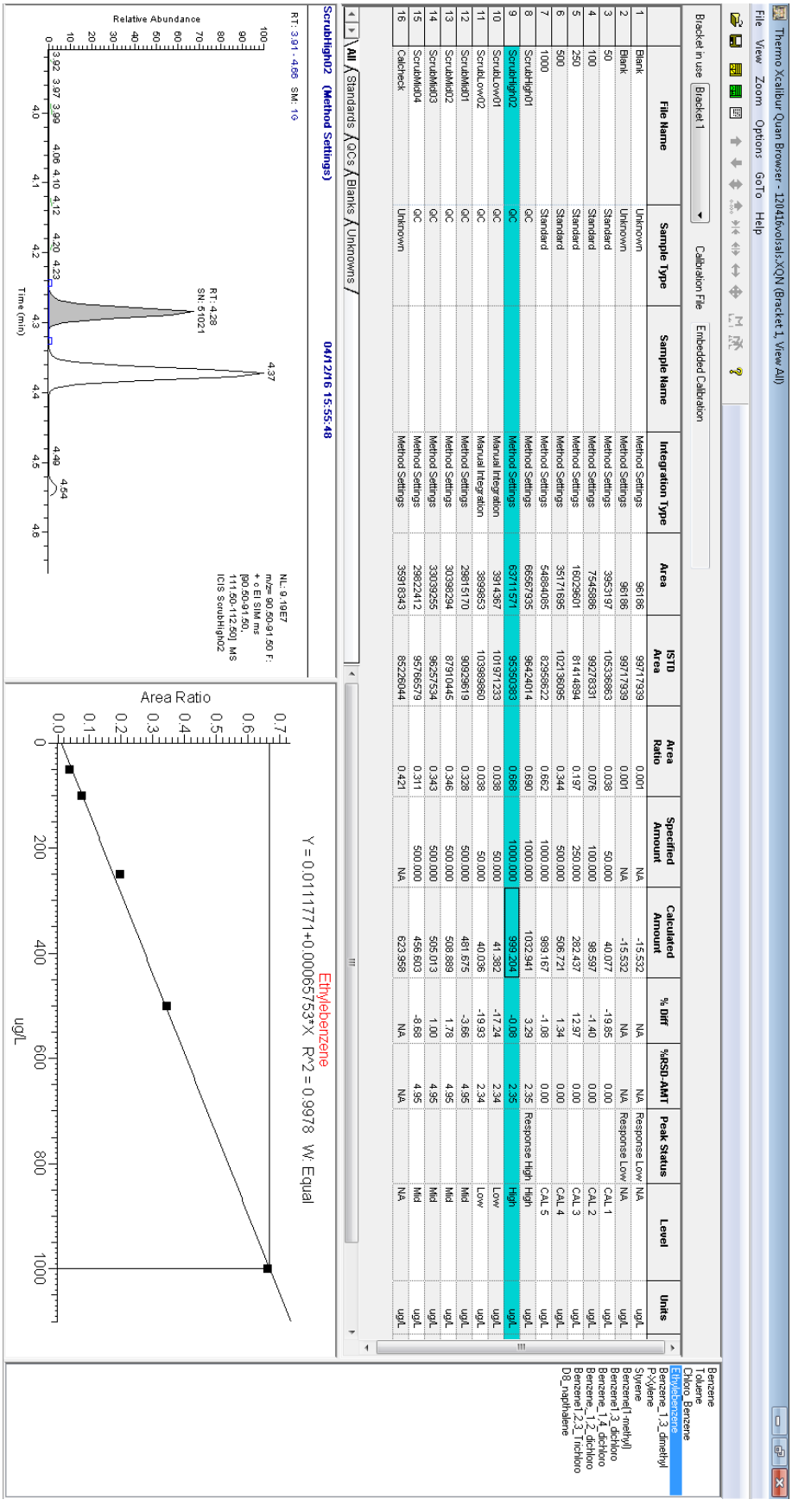

	File Name	Sample Type	Sample Name	Integration Type	Area	ISTD Area	Area Ratio	Specified Amount	Calculated Amount	% Diff	%RSD-AMT	Peak Status	Level	Units
1	Blank	Unknown		Method Settings	96186	99717939	0.001	NA	-15.532	NA	NA	Response Low	NA	ug/L
2	Blank	Unknown		Method Settings	96186	99717939	0.001	NA	-15.532	NA	NA	Response Low	NA	ug/L
3	50	Standard		Method Settings	3953197	105338883	0.038	50.000	40.077	-19.85	0.00		CAL 1	ug/L
4	100	Standard		Method Settings	7545886	99278331	0.076	100.000	98.597	-1.40	0.00		CAL 2	ug/L
5	250	Standard		Method Settings	16029801	81414894	0.197	250.000	282.437	12.97	0.00		CAL 3	ug/L
6	500	Standard		Method Settings	35171685	102136095	0.344	500.000	506.721	1.34	0.00		CAL 4	ug/L
7	1000	Standard		Method Settings	54894085	82956822	0.662	1000.000	989.167	-1.08	0.00		CAL 5	ug/L
8	ScrubHigh01	QC		Method Settings	66567935	96424014	0.690	1000.000	1032.941	3.29	2.35	Response High	High	ug/L
9	ScrubHigh02	QC		Method Settings	63711571	95560383	0.666	1000.000	999.204	-0.08	2.35		High	ug/L
10	ScrubLow01	QC		Manual Integration	3914367	101971233	0.038	50.000	41.382	-17.24	2.34		Low	ug/L
11	ScrubLow02	QC		Manual Integration	3898653	103988860	0.038	50.000	40.036	-19.93	2.34		Low	ug/L
12	ScrubMid01	QC		Method Settings	23815170	90929619	0.328	500.000	481.675	-3.66	4.95		Mid	ug/L
13	ScrubMid02	QC		Method Settings	30398294	87910445	0.345	500.000	508.889	1.78	4.95		Mid	ug/L
14	ScrubMid03	QC		Method Settings	33039255	96257534	0.343	500.000	505.013	1.00	4.95		Mid	ug/L
15	ScrubMid04	QC		Method Settings	29822412	95765579	0.311	500.000	456.603	-8.88	4.95		Mid	ug/L
16	Calcheck	Unknown		Method Settings	35918343	85226044	0.421	NA	623.958	NA	NA		NA	ug/L

Example 4 of processed VOT data for Styrene from the Gasification of UK sludge cake.

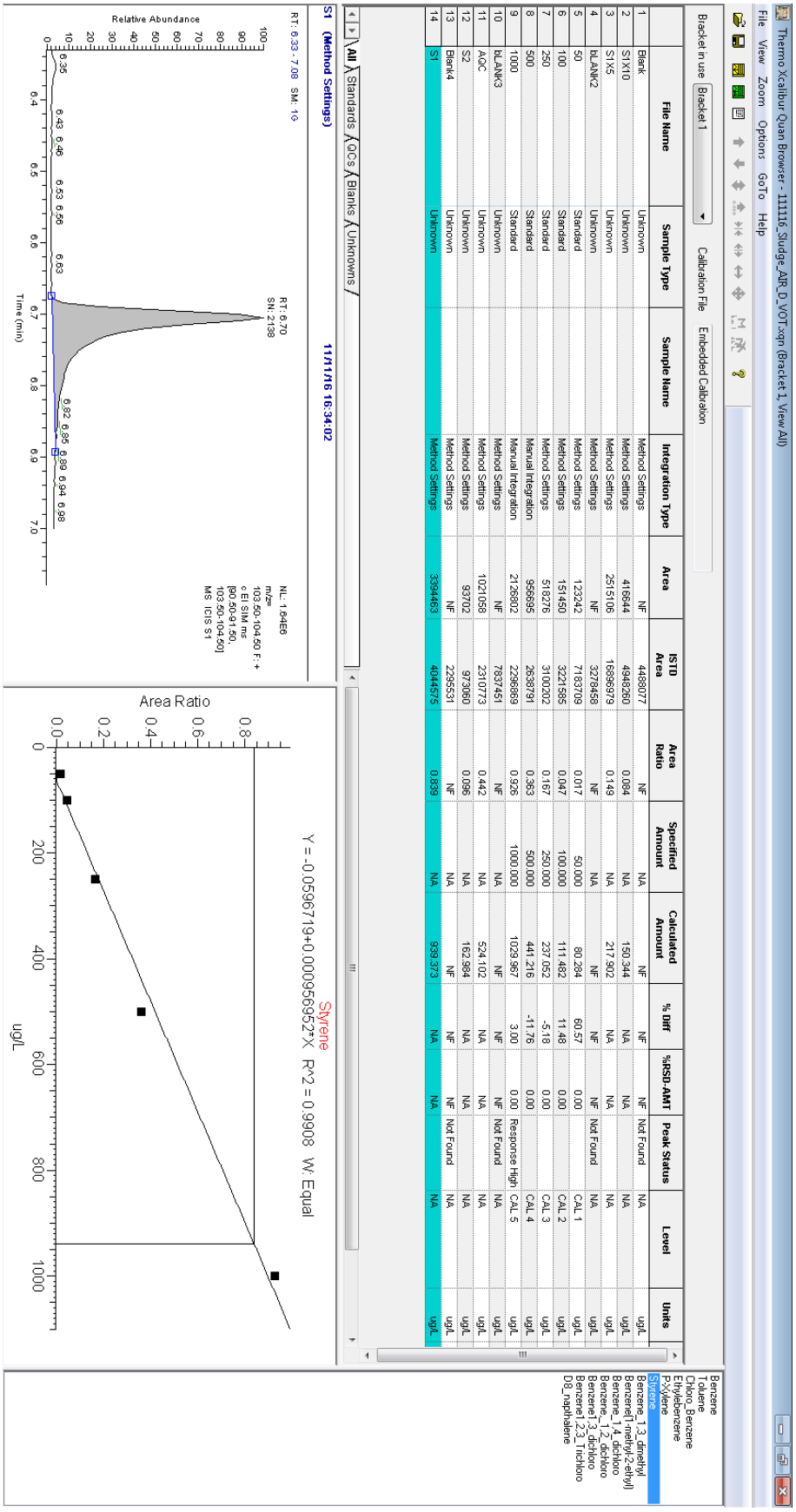

	File Name	Sample Type	Sample Name	Integration Type	Area	ISTD Area	Area Ratio	Specified Amount	Calculated Amount	% Diff	%RSD-AMT	Peak Status	Level	Units
1	Blank	Unknown	Method Settings	Method Settings	NF	4438077	NF	NA	NF	NF	NF	Not Found	NA	ug/L
2	S1X10	Unknown	Method Settings	Method Settings	416644	4946260	0.084	NA	150.344	NA	NA	NA	NA	ug/L
3	S1X5	Unknown	Method Settings	Method Settings	2515106	16898979	0.149	NA	217.902	NA	NA		NA	ug/L
4	bLANK2	Unknown	Method Settings	Method Settings	NF	3278458	NF	NA	NF	NF	NF	Not Found	NA	ug/L
5	50	Standard	Method Settings	Method Settings	123242	7183709	0.017	50.000	80.284	60.57	0.00		CAL 1	ug/L
6	100	Standard	Method Settings	Method Settings	151450	3221585	0.047	100.000	111.482	11.48	0.00		CAL 2	ug/L
7	250	Standard	Method Settings	Method Settings	518276	3100202	0.167	250.000	237.052	-5.18	0.00		CAL 3	ug/L
8	500	Standard	Method Settings	Manual Integration	956695	2638791	0.363	500.000	441.216	-11.76	0.00		CAL 4	ug/L
9	1000	Standard	Method Settings	Manual Integration	2126802	2298689	0.926	1000.000	1029.967	3.00	0.00	Response High	CAL 5	ug/L
10	bLANK3	Unknown	Method Settings	Method Settings	NF	7837451	NF	NA	NF	NF	NF	Not Found	NA	ug/L
11	AQC	Unknown	Method Settings	Method Settings	1021058	2310773	0.442	NA	524.102	NA	NA		NA	ug/L
12	S2	Unknown	Method Settings	Method Settings	93702	973060	0.096	NA	162.964	NA	NA		NA	ug/L
13	Blank4	Unknown	Method Settings	Method Settings	NF	2295531	NF	NA	NF	NF	NF	Not Found	NA	ug/L
14	S1	Unknown	Method Settings	Method Settings	3394463	4044575	0.839	NA	939.373	NA	NA		NA	ug/L

Example 5 of SVOT validation run: processed data for Anthracene.

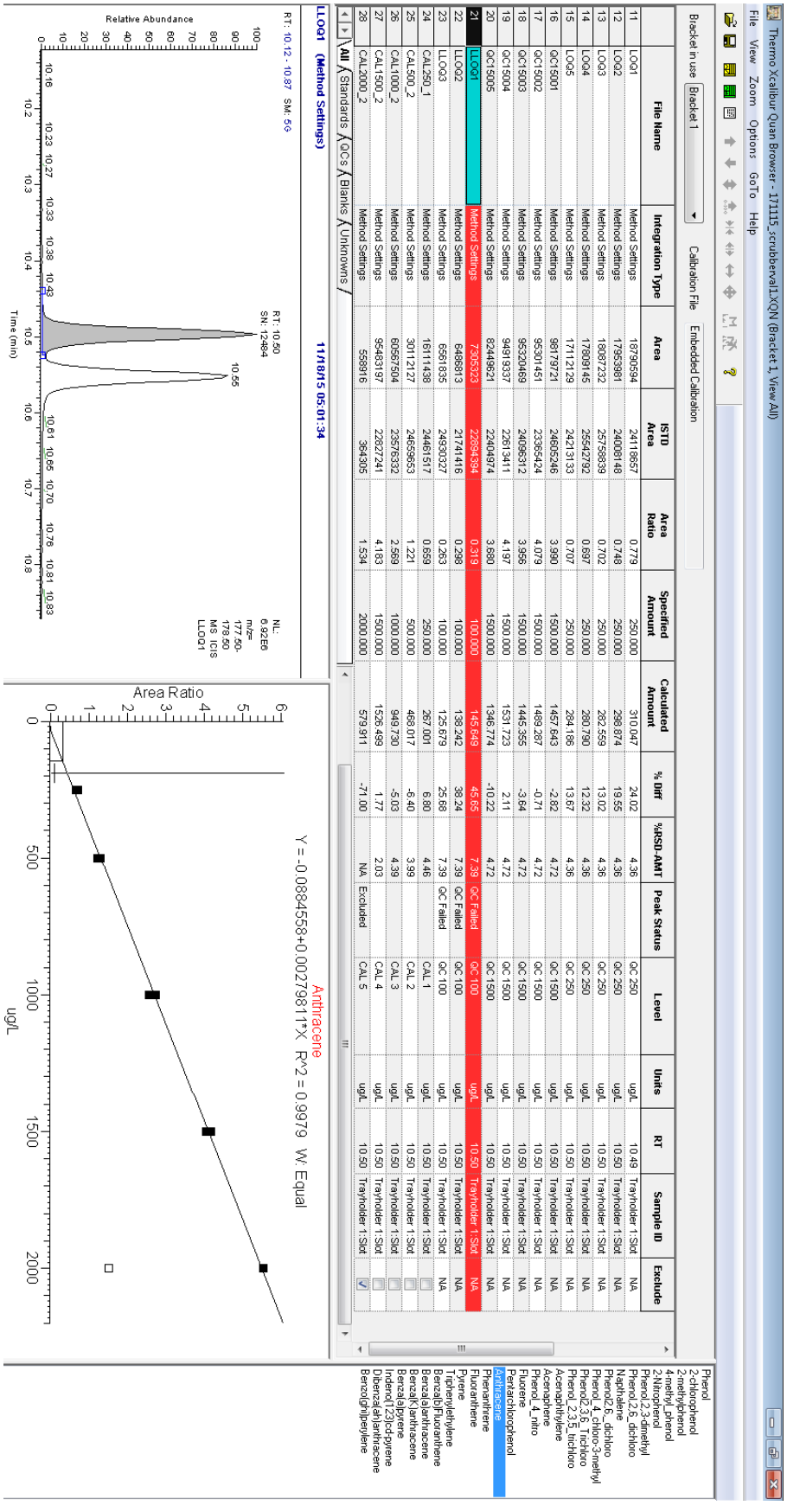

	File Name	Integration Type	Area	ISTD Area	Area Ratio	Specified Amount	Calculated Amount	% Diff	%RSD-AMT	Peak Status	Level	Units	RT	Sample ID	Exclude
11	LOQ1	Method Settings	16790594	24116657	0.779	250.000	310.047	24.02	4.36		QC 250	ug/L	10.49	Trayholder 1:Slot	NA
12	LOQ2	Method Settings	17953981	24008148	0.748	250.000	298.874	19.55	4.36		QC 250	ug/L	10.50	Trayholder 1:Slot	NA
13	LOQ3	Method Settings	18087232	25758839	0.702	250.000	282.559	13.02	4.36		QC 250	ug/L	10.50	Trayholder 1:Slot	NA
14	LOQ4	Method Settings	17809145	25542792	0.697	250.000	280.790	12.32	4.36		QC 250	ug/L	10.50	Trayholder 1:Slot	NA
15	LOQ5	Method Settings	17112129	24213133	0.707	250.000	284.186	13.67	4.36		QC 250	ug/L	10.50	Trayholder 1:Slot	NA
16	QC15001	Method Settings	98179721	24605246	3.990	1500.000	1457.643	-2.82	4.72		QC 1500	ug/L	10.50	Trayholder 1:Slot	NA
17	QC15002	Method Settings	95301451	23365424	4.079	1500.000	1489.287	-0.71	4.72		QC 1500	ug/L	10.50	Trayholder 1:Slot	NA
18	QC15003	Method Settings	95320469	24096312	3.956	1500.000	1445.355	-3.64	4.72		QC 1500	ug/L	10.50	Trayholder 1:Slot	NA
19	QC15004	Method Settings	94919337	22613411	4.197	1500.000	1531.723	2.11	4.72		QC 1500	ug/L	10.50	Trayholder 1:Slot	NA
20	QC15005	Method Settings	82449621	22404974	3.680	1500.000	1346.774	-10.22	4.72		QC 1500	ug/L	10.50	Trayholder 1:Slot	NA
21	LLOQ1	Method Settings	7305323	22894394	0.319	100.000	145.649	45.65	7.39	QC Failed	QC 100	ug/L	10.50	Trayholder 1:Slot	NA
22	LLOQ2	Method Settings	6486813	21741416	0.298	100.000	138.242	38.24	7.39	QC Failed	QC 100	ug/L	10.50	Trayholder 1:Slot	NA
23	LLOQ3	Method Settings	6561835	24930327	0.263	100.000	125.679	25.68	7.39	QC Failed	QC 100	ug/L	10.50	Trayholder 1:Slot	NA
24	CAL250_1	Method Settings	16111438	24461517	0.659	250.000	267.001	6.80	4.46		CAL 1	ug/L	10.50	Trayholder 1:Slot	
25	CAL500_2	Method Settings	30112127	24659653	1.221	500.000	468.017	-6.40	3.99		CAL 2	ug/L	10.50	Trayholder 1:Slot	
26	CAL1000_2	Method Settings	60567504	23576332	2.569	1000.000	949.730	-5.03	4.39		CAL 3	ug/L	10.50	Trayholder 1:Slot	
27	CAL1500_2	Method Settings	95463197	22827241	4.183	1500.000	1526.499	1.77	2.03		CAL 4	ug/L	10.50	Trayholder 1:Slot	
28	CAL2000_2	Method Settings	558916	364305	1.534	2000.000	579.911	-71.00	NA	Excluded	CAL 5	ug/L	10.50	Trayholder 1:Slot	

Example 6 of processed SVOT data for 2-methyl phenol from the pyrolysis of pine wood .

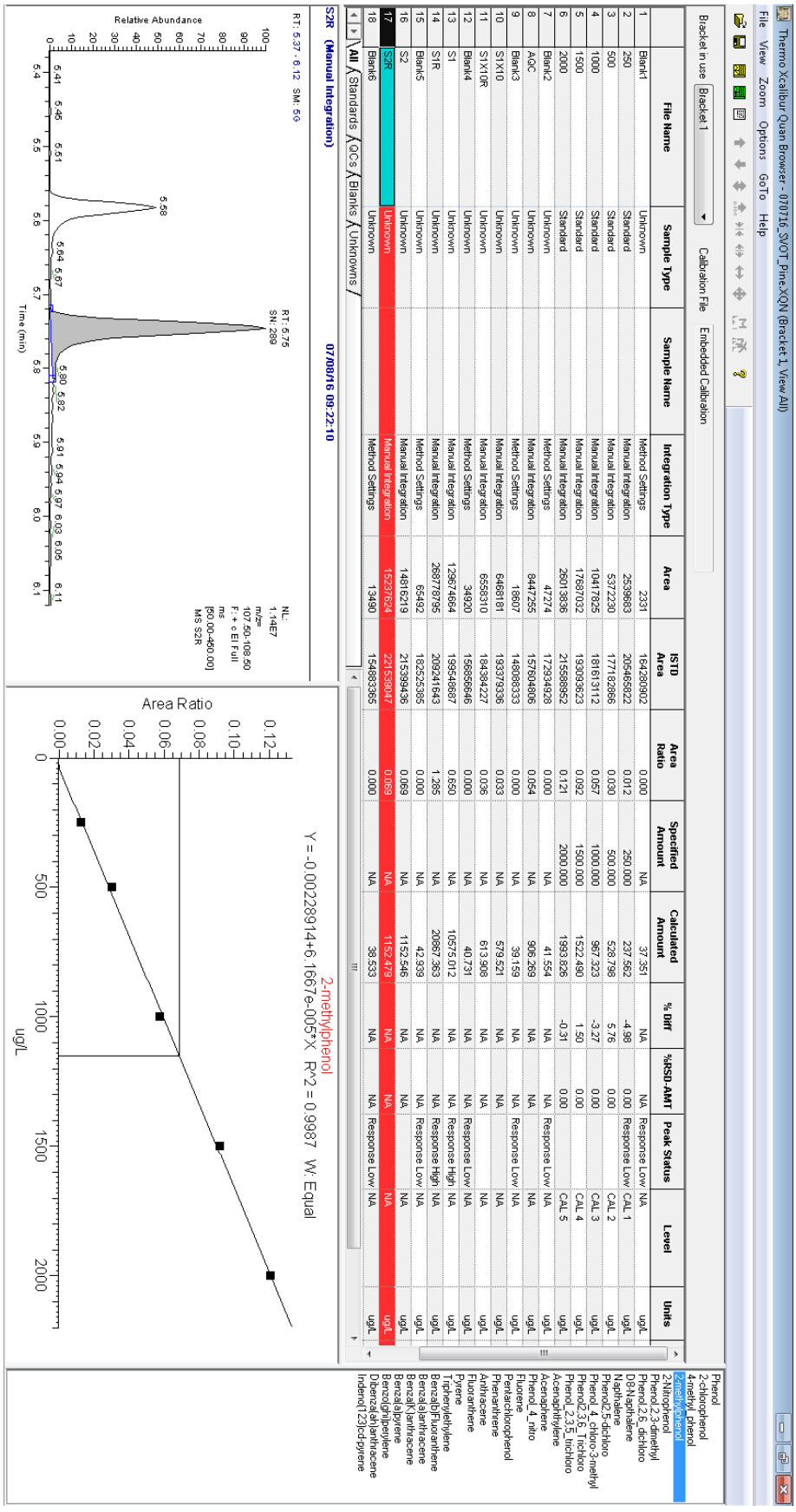

	File Name	Sample Type	Sample Name	Integration Type	Area	ISTD Area	Area Ratio	Specified Amount	Calculated Amount	% Diff	%RSD-AMT	Peak Status	Level	Units
1	Blank1	Unknown		Method Settings	2331	16428902	0.000	NA	37.351	NA	NA	Response Low	NA	ug/L
2	250	Standard		Manual Integration	2539683	20546822	0.012	250.000	237.562	-4.98	0.00	Response Low	CAL 1	ug/L
3	500	Standard		Manual Integration	5372230	17716286	0.030	500.000	528.798	5.76	0.00		CAL 2	ug/L
4	1000	Standard		Manual Integration	10417825	18161312	0.057	1000.000	967.323	-3.27	0.00		CAL 3	ug/L
5	1500	Standard		Manual Integration	17687032	19309623	0.092	1500.000	1522.490	1.50	0.00		CAL 4	ug/L
6	2000	Standard		Manual Integration	26013836	21558952	0.121	2000.000	1993.826	-0.31	0.00		CAL 5	ug/L
7	Blank2	Unknown		Method Settings	47274	17293928	0.000	NA	41.554	NA	NA	Response Low	NA	ug/L
8	AQC	Unknown		Manual Integration	8447255	15760806	0.054	NA	906.269	NA	NA		NA	ug/L
9	Blank3	Unknown		Method Settings	18607	14808333	0.000	NA	39.159	NA	NA	Response Low	NA	ug/L
10	S1X10	Unknown		Manual Integration	6468181	19337936	0.033	NA	579.521	NA	NA		NA	ug/L
11	S1X10R	Unknown		Manual Integration	6556310	18438227	0.036	NA	613.908	NA	NA		NA	ug/L
12	Blank4	Unknown		Method Settings	34920	15865646	0.000	NA	40.731	NA	NA	Response Low	NA	ug/L
13	S1	Unknown		Manual Integration	12967464	19954687	0.650	NA	10575.012	NA	NA	Response High	NA	ug/L
14	S1R	Unknown		Manual Integration	26877875	20924643	1.285	NA	20867.363	NA	NA	Response High	NA	ug/L
15	Blank5	Unknown		Method Settings	85492	18252385	0.000	NA	42.939	NA	NA	Response Low	NA	ug/L
16	S2	Unknown		Manual Integration	14816219	21539436	0.069	NA	1152.546	NA	NA		NA	ug/L
17	S2R	Unknown		Manual Integration	15237624	22153947	0.069	NA	1152.479	NA	NA		NA	ug/L
18	Blank6	Unknown		Method Settings	13490	15488385	0.000	NA	38.533	NA	NA	Response Low	NA	ug/L

Glossary of Terms

1. **Biochar: Black, highly porus, carbonaceous material derived from carbonisation process.**
2. **Bio-oil: Condensible gases produce a free flowing liquid, high in organic compounds.**
3. **Calibration curve: A linear graph generated from the response factor of calibration standards over concentration. Generated over a specific concentration range.**
4. **Calibration Standards: Certified reference materials of target analytes used to generate calibration curves.**
5. **Carbonisation: Takes place at high temperatures, when volatile material is driven off leaving behind a rich carbon residue, also reffered to as tertary reactions.**
6. **Catalyts: A substance that speeds up both forward and reverse reactions without taking part in the reaction itsself, (does not effect equilibrium) but lowers the activation energy.**
7. **Feedstock: Starting material used in a process.**
8. **Fischer-Tropsch reaction: Process by converting carbonmonoxide and hydrogen into liquid fuels using a transition metal catalyst**
9. **Full scan: Operational mode of scanning mass spectrometers, whereby the mass spectrometer scans the whole mass range determined by the instrument parameters.**
10. **Gas Chromatography: The separation of mixture of analytes based on the partion coefficient (retention time) of the individual analytes towards a soild stationary phase and a gaseous mobile phase.**
11. **Gasification: The intense heating of material with a controlled amount of oxidant, typically above 700 °C, to generate syngas and inert ash**
12. **Hydrocarbon: A compound that empirically contains carbon and hydrogen.**
13. **Internal standard: a deuterated analougue or isomer of target analyte, used to correct for losses of analyte in the procedure.**
14. **Ionisation: Process whereby a compound is bombarded by a high energy electron, to generate a positive species, typically this species may undergo fragmentation to generate secondary fragment ions.**
15. **Limit of quantitation (LOQ): The lowest concentration that can be accuratley determined from a calibration curve, typically the lowest standard.**
16. **Limt of detection (LOD): The lowest concentration that can be identified, typically with S/N greater > 3.**

17. **Lower limit of Quantitation (LLOQ): The lowest concentration that can be accuratley determined below the LOQ.**
18. **Mass spectrometry: Separation of ions based on their mass: charge ratio. The ions are detected to generate a respose.**
19. **Pyrolysis: The intense heating of material in an inert atmosphere, typical range 300-700 °C. Generates, syngas, biochar and bio-oil.**
20. **Scrubber: A vessel containing a solvent used to remove impurities in syngas.**
21. **Signal to noise: The ratio of peak height to a given noise region. Typically the minimum ratio of a peak is set at >3.**
22. **Single ion monitoring: Operational mode of mass spectrometers, whereby the mass spectrometer, focuses on a single mass unit.**
23. **Syngas: Gas mixture containing, hydrogen, carbon monoxide, methane and tars.**
24. **Tars: Organic compounds with a molecular mass greater than benzene, generated typically in the pyrolysis reactions.**
25. **Upper limit of Quantitation (UPLOQ): The maximum concentration that can be accurately determined from a calibration curve, typically the highest standard.**